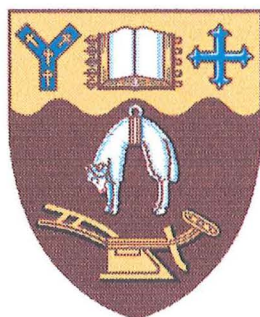


AUSTRALASIAN FUNGI: A NATURAL PRODUCT STUDY

A thesis
submitted in partial fulfilment
of the requirements for the degree
of
Doctor of Philosophy in Chemistry
in the
University of Canterbury
by
Gillian M. Nicholas



University of Canterbury

1998

ABSTRACT

A number of Australasian fungi were investigated in a search for novel biologically active natural products.

Extracts of the fungus *Favolaschia calocera* were investigated, and resulted in the isolation of four compounds. These compounds were structurally assigned using mass spectrometry and NMR spectroscopy as the 5-stearate (**30a**) and 5-palmitate (**30b**) esters of (2*E*,6*E*)-1-(2-hydroxy-4-methoxyphenyl)-5-hydroxy-3,7,11-trimethyldodeca-2,6,10-triene, (*E*)-6-phenylhex-5-en-2-ol (**32**) and as methyl (4*E*,6*E*)-3-hydroxy-7-phenylhepta-4,6-dienoate (**28b**). The absolute stereochemistry of the previously isolated and characterised methyl (4*E*,6*E*)-3-benzoyloxy-7-phenylhepta-4,6-dienoate (**28a**) was determined using Mosher's method.

To unambiguously assign the structure of the *Favolaschia calocera* metabolite 9-methoxystrobilurin K as structure **16**, appropriate model compounds (**33-40**) were synthesised. The previously reported epoxyprenyl structure for 9-methoxystrobilurin K (**17**) and the dioxan structure for 9-methoxystrobilurin L (**20**) are now both revised to the prenyldioxepin structure **16**.

A blue-violet compound was isolated from an extract of *Entoloma hochstetteri*. This compound was identified as 7-acetyl-1,4-dimethylazulene (**56**) and is thought to be an artefact of the extraction and isolation process.

The chemistry of a *Cortinarius* species collected from the Catlins (New Zealand) was investigated because crude extracts showed significant biological activity. Three disulfide compounds (**59-61**) were isolated and identified using a combination of NMR spectroscopy, mass spectrometry and synthesis. Two of these compounds (**59** and **61**) were assigned as symmetrical disulfides that arise from the third unsymmetrical

disulfide, cortamidine oxide (**61**), through disulfide exchange. All three compounds were assigned as also containing *N*-oxide functionality.

Extracts of the Australian mushroom *Cortinarius rotundisporus* were investigated due to the cytotoxicity observed against the P388 murine leukaemia cell line during a screening programme. Two triterpenes of the malabaricane class were isolated and identified, using NMR techniques and mass spectrometry, as rotundisine A (**94**) and B (**95**).

ACKNOWLEDGMENTS

I would like to express my gratitude to my supervisors, Dr John Blunt and Dr Murray Munro, for their encouragement and guidance throughout my time in the natural product group at Canterbury and to my associate supervisor Dr Anthony Cole (Department of Plant and Microbial Sciences).

Access to the Australian collection of fungi held by Dr Melvyn Gill (University of Melbourne) was very much appreciated and to whom I am grateful for the supply of *Cortinarius rotundisporus*.

I would like to thank the technical staff of the Chemistry Department that contributed to this work, including Gill Ellis for the biological assays and Bruce Clark for mass spectrometry analysis and assistance with spectral interpretation. I am also grateful to Dr Lewis Pannell (National Institute of Health, U.S.A) and Professor Rodney Rickards (Australian National University, Australia) for additional mass spectrometry analysis.

Many people have made my time at Canterbury a thoroughly enjoyable experience. These include Rachel Lill, Sarah Hickford, David Stirling, Michael Stewart, Jo Hart and Kate Fulton of the natural product group and other students in the Chemistry Department especially Stuart Black, Stuart Simpson, Fiona Buchanan, Susie Meade and Alisa Roddick. Dr Jonathan Morris - a relatively new addition to the Chemistry Department - has been a valuable source of advice.

A special thank you goes to Andy Phillips who has been a wonderful source of inspiration and support. My parents and sister have also been supportive and full of encouragement over my many years at University.

TABLE OF CONTENTS

ABBREVIATIONS.....	1
--------------------	---

CHAPTER ONE

INTRODUCTION	3
--------------------	---

1.1	NATURAL PRODUCTS	3
1.2	THE SEARCH FOR BIOLOGICALLY ACTIVE NATURAL PRODUCTS.....	4
1.2.1	<i>The need for new modes of biological activity</i>	4
1.2.2	<i>Detection of bioactive natural products</i>	5
1.3	FUNGAL NATURAL PRODUCTS	9
1.3.1	<i>General</i>	9
1.3.2	<i>Basidiomycetes natural products</i>	11
1.3.3	<i>Biologically active natural products from basidiomycetes</i>	11
1.4	Work done at the University of Canterbury	15
1.4.1	<i>General</i>	15
1.4.2	<i>Aims of this research</i>	16

CHAPTER TWO

FAVOLASCHIA CALOCERA	17
-----------------------------------	-----------

2.1	INTRODUCTION	17
2.1.1	<i>The genus Favolaschia</i>	17
2.1.2	<i>History of the strobilurins</i>	20
2.1.3	<i>Further investigation of Favolaschia calocera</i>	21
2.2	CHROMATOGRAPHY OF <i>F. CALOCERA</i> EXTRACT AND STRUCTURAL ELUCIDATION OF 30A-B , 32 AND 28B	23
2.2.1	<i>Chromatography of F. calocera extract</i>	23
2.2.2	<i>Structural elucidation of compounds 30a-b, 32 and 28b</i>	24
2.3	ABSOLUTE STEREOCHEMISTRY OF METHYL (4 <i>E</i> ,6 <i>E</i>)-3- BENZOYLOXY-7-PHENYLHEPTA-4,6-DIENOATE (28A)	30

2.4	SYNTHESIS OF MODEL COMPOUNDS TO CONFIRM STRUCTURE OF	
	9-METHOXYSTROBILURIN K AS 16	32
2.4.1	<i>Introduction</i>	32
2.4.2	<i>Synthesis of compounds 33-40</i>	33
2.4.3	<i>Conclusions</i>	43
2.5	CULTURING OF <i>F. CALOCERA</i>	45
2.5.1	<i>Introduction</i>	45
2.5.2	<i>General techniques and procedures</i>	45
2.5.3	<i>Culturing of F. calocera</i>	45

CHAPTER THREE

COLLECTION, EXTRACTION AND

	SCREENING PROGRAMME.....	49
3.1	INTRODUCTION	49
3.2	COLLECTIONS AND EXTRACTIONS	50
3.3	BIOLOGICAL ASSAYS	51
3.4	RESULTS	52
3.4.1	<i>General observations</i>	52
3.4.2	<i>Tables of Results</i>	53
3.4.3	<i>Specimens targeted for further investigation</i>	56
3.5	DISCUSSION	57

CHAPTER FOUR

	<i>ENTOLOMA HOCHSTETTERI</i>	58
4.1	INTRODUCTION	58
4.1.1	<i>Entoloma hochstetteri</i> (Reich.)Stevenson.....	58
4.1.2	<i>Natural products isolated from the Entoloma genus</i>	59
4.1.3	<i>Guaiane pigments from Lactarius species</i>	60
4.1.4	<i>Guaiane pigments from marine sources</i>	61

4.1.5	<i>Biological activity of guaiane pigments</i>	62
4.2	EXTRACTION OF <i>E. HOCHSTETTERI</i>	63
4.3	CHROMATOGRAPHY OF THE <i>E. HOCHSTETTERI</i> EXTRACT.....	64
4.3.1	<i>General</i>	64
4.3.2	<i>Isolation of compound 56</i>	64
4.3.3	<i>Other Pigments</i>	65
4.4	STRUCTURE ELUCIDATION	66
4.4.1	<i>Compound 56</i>	66
4.4.2	<i>Other Pigments</i>	71
4.5	DISCUSSION	72

CHAPTER FIVE

CORTINARIUS SPECIES (CATLINS).....74

5.1	INTRODUCTION	74
5.1.1	<i>Chemistry of the Cortinarius genus</i>	75
5.1.2	<i>N-Oxide and N-hydroxy containing natural products</i>	77
5.1.3	<i>Disulfide natural products</i>	80
5.2	EXTRACTION OF <i>CORTINARIUS</i> SP.	81
5.2.1	<i>Original Biological Screening results</i>	81
5.2.2	<i>Recollection</i>	82
5.3	CHROMATOGRAPHY OF <i>CORTINARIUS</i> SP. EXTRACTS.....	83
5.3.1	<i>Chromatography of the first extract</i>	83
5.3.2	<i>Second collection, extraction and chromatography of Cortinarius sp.</i>	87
5.4	STRUCTURE ELUCIDATION	90
5.4.1	<i>Structure elucidation of 2,2'-dithiobis(pyridine N-oxide) (59)</i>	90
5.4.2	<i>Structure elucidation of cortamidine oxide (60)</i>	92
5.4.3	<i>Structural assignment of 61</i>	104
5.5	BIOLOGICAL ACTIVITY OF 2,2'-DITHIOBIS(PYRIDINE N-OXIDE) (59), CORTAMIDINE OXIDE (60) AND 61.....	107

5.5.1	2,2'-Dithiobis(pyridine N-oxide) (59)	107
5.5.2	Cortamidine oxide (60) and compound 61	108
5.6	CONCLUSIONS	109

CHAPTER SIX

CORTINARIUS ROTUNDISPORUS.....110

6.1	INTRODUCTION	110
6.1.1	Natural products isolated from the Cortinarius genus.....	111
6.1.2	Malabaricane triterpenes isolated from plants	111
6.1.3	Malabaricane/Isomalabaricane triterpenes from marine sources.....	113
6.2	EXTRACTION OF CORTINARIUS ROTUNDISPORUS	115
6.3	CHROMATOGRAPHY OF CORTINARIUS ROTUNDISPORUS	
	EXTRACT	117
6.4	STRUCTURAL ELUCIDATION OF COMPOUNDS 94 AND 95	119
6.4.1	Structural elucidation of compound 94	119
6.4.2	Structural elucidation of compound 95	133
6.4.3	Isomerisation of the C14-C15 olefin	137
6.5	BIOSYNTHESIS OF ROTUNDISINE A (94) AND B (95)	137
6.6	BIOLOGICAL ACTIVITY OF ROTUNDISINE A (94) AND B (95).....	137
6.7	DISCUSSION	138

CHAPTER SEVEN

EXPERIMENTAL.....139

7.1	GENERAL METHODS	139
7.2	WORK DESCRIBED IN CHAPTER TWO	145
7.3	WORK DESCRIBED IN CHAPTER THREE	160
7.4	WORK DESCRIBED IN CHAPTER FOUR	161
7.5	WORK DESCRIBED IN CHAPTER FIVE	162
7.6	WORK DESCRIBED IN CHAPTER SIX	172

Abbreviations

$[\alpha]_{\text{D}}^{25}$	specific rotation (at 589nm at 25°C)
APT	attached proton test
Ar	aryl
AT	acquisition time (in NMR)
Bn	benzyl
b.p.	boiling point
br	broad (spectral)
C18	octadecyl-phase (in HPLC)
°C	degrees Celsius
calcd	calculated
CI	chemical ionization (mass spectrometry)
cm	centimetre(s)
CN	cyano-phase (in HPLC)
COSY	correlation spectroscopy (in NMR)
δ	chemical shift in parts per million downfield from tetramethylsilane
d	doublet (spectral)
DIOL	dialcohol-phase (in HPLC)
DMAP	4-(dimethylamino)pyridine
DMF	dimethylformamide
DMSO	dimethyl sulfoxide
EI	electron impact (in mass spectrometry)
ESI	electrospray ionisation (in mass spectrometry)
Et	ethyl
FAB	fast atom bombardment (in mass spectrometry)
g	gram(s)
GC	gas chromatography
GC/MS	gas chromatography linked to a mass spectrometer
hr	hour(s)
HMBC	heteronuclear multiple bond coherence (in NMR)
HPLC	high-performance liquid chromatography
HRMS	high-resolution mass spectrum
HSMQC	heteronuclear single and multiple quantum coherence (in NMR)
HSQC	heteronuclear single quantum coherence (in NMR)

HSQC-TOCSY	heteronuclear single quantum coherence - total correlation spectroscopy (in NMR)
Hz	hertz
IR	infrared
IPA	isopropyl alcohol
<i>J</i>	coupling constant (in NMR)
L	litre(s)
μ	micro
m	multiplet (spectral), metre(s), milli
M	moles per litre
<i>m</i> -CPBA	<i>m</i> -chloroperoxybenzoic acid
Me	methyl
MHz	megahertz
min	minute(s)
mol	mole(s)
MS	mass spectrometry
<i>m/z</i>	mass to charge ratio (in mass spectrometry)
NMR	nuclear magnetic resonance
NOBA	<i>m</i> -nitrobenzyl alcohol (in mass spectrometry)
NOE	nuclear Overhauser effect
NOESY	nuclear Overhauser effect spectroscopy
Ph	phenyl
ppm	parts per million (in NMR)
q	quartet (spectral)
rt	room temperature
RT	retention time
s	singlet (NMR); second(s)
t	triplet (spectra)
TFA	trifluoroacetic acid
THF	tetrahydrofuran
TLC	thin layer chromatography
TMS	trimethylsilyl, tetramethylsilane
TOCSY	total correlation spectroscopy
UV	ultraviolet

CHAPTER ONE

INTRODUCTION

1.1 Natural Products

Natural products are compounds of natural origin that are usually unique to an organism or group of closely related organisms. In many instances, natural products would appear to be non-essential components of the producing organism. Undoubtedly, part of the explanation for their existence must be to give a competitive advantage to the organisms that produce them. Typically, organisms that lack an immune system commonly contain natural products. Conversely, natural products are sparse in organisms that have an immune system. In general, vertebrates lack the array of natural products found in plants and micro-organisms, but there are exceptions. For example, a number of frogs from South America produce a variety of alkaloids, which are highly toxic.¹

Natural product resources provide excellent raw material for the discovery and development of novel biologically active compounds because of nature's seemingly limitless ability to synthesise a diverse range of them. Along with the discovery of new and active molecular entities, new mechanisms of action can be found enabling the development of innovative approaches for fighting diseases. The action of biologically active natural products can also help in understanding the cell cycle. Traditionally, proteins involved in the cell cycle have been investigated using a molecular biological approach. This involved the production of mutations in the genes encoding for these proteins causing either a loss or a gain of function. An alternative approach is to directly alter the function of the protein by introducing a ligand that binds to the protein. Many natural products can act as this type of ligand and by binding to proteins involved in cell-cycle regulation can cause disruption of the cell cycle. Identification of such proteins can increase our understanding of both the cell-cycle and the mechanism of action of many cell-cycle inhibitors.²

1.2 The search for biologically active natural products

1.2.1 The need for new modes of biological activity

The discovery of a new biologically active natural product is only the first step in a long process in the development of a potential pharmaceutical. The natural product is generally only valuable if the biological activity exhibited is selective. This selectivity enables the natural product to influence specific cells or processes within these cells without affecting surrounding ones.³

Resistance of bacteria and fungi to antibiotics is a continuing problem in the fight against infectious disease. The last antibiotic in our armoury against a number of

bacteria is vancomycin, a compound that inhibits bacterial cell wall biosynthesis by binding to the C-terminal peptide sequence in bacterial cell wall precursors. Some bacteria are now resistant even to this antibiotic. Fortunately, these bacteria are still susceptible to other antibiotics but transfer of genetic material from resistant bacteria to other strains is inevitable. The improper use and over prescription of antibiotics for medicinal purposes, and their use in the agriculture industry as food additives to promote growth in farm animals, has increased the speed with which resistance has developed.⁴

Resistance is not only a problem in the medical arena but also in the agricultural industry. Pathogenic micro-organisms quickly become resistant to new antifungal and antibacterial agents and overcome cultivars that have been bred to have resistance.

1.2.2 Detection of bioactive natural products

Over the last twenty years there has been a move away from isolating every possible natural product from a particular organism to bio-assay guided isolation to obtain any biologically active components. The assays used during the isolation procedure can either be sensitive to an array of activity, for example the brine shrimp lethality test (BLT),⁵ or very specific as for example in an enzyme inhibition assay. The bio-assay guided isolation allows the discovery of components that make up a very small percentage of the extract that might not have been noticed otherwise. Of course, compounds can still be overlooked if they do not possess the activity being assayed. There have also been problems with using rapidly dividing tumour cell lines as primary screens because this does not distinguish between cytotoxicity and antitumour activity. Although many antitumour compounds have been isolated, few have been clinically effective against slow-growing tumours. Unfortunately, *in vivo* assays that would screen for this type of activity are time consuming and expensive to run. A common

approach is therefore to use a sensitive assay such as the P388 murine leukaemia cell line, which assays for general cytotoxicity, is relatively inexpensive to run, and has a quick turn around time.

Initiation of a screening programme

A screening programme involves the collection and extraction of a large number of organisms and then the testing of these extracts for biological activity using the appropriate assay for the type of activity that is of interest. The system needs to be as efficient as possible so large numbers of extracts can be screened quickly. The collections need to be thoroughly documented so recollection of any particular organism is possible. The solvent used for the extraction is also important because natural products have a large range in polarity. A recommended approach involves two extractions for each organism so both an aqueous and organic extraction is carried out. An organic solvent system found to be useful in extracting a good range of natural products is MeOH and CH₂Cl₂. The only disadvantage is that CH₂Cl₂ shows activity in many assays, but by using a 3:1 mixture of MeOH/CH₂Cl₂ this problem can be alleviated. This solvent system is in fact more polar because of the water that is contained in the sample. In comparison, when marine sponges (2 g) are extracted with 3:1 MeOH/CH₂Cl₂ (20 mL) the solvent ends up being closer to 1:10:3 in H₂O/MeOH/CH₂Cl₂.

Extraction and isolation

Once an organism is known to contain a component(s) that exhibit biological activity a strategy then needs to be developed to isolate that component(s) in high purity and (hopefully) yield. The isolation and separation of natural products can be a relatively haphazard ordeal unless some time is taken at the start to carry out a number of preliminary investigations. In our hands, these initial investigations have been termed “chemical screening.” This involves the separation of a small amount of the crude

extract using a variety of chromatography phases in cartridge form. The solvents used to elute these cartridges are very steep stepped gradients. The fractions that elute from these cartridges are then tested in the appropriate assay. The results then give an indication of the polarity of the biologically active component(s) and depending on the phases used can indicate the size and the existence of acidic or basic functionality. The active fractions from each of the phases screened can be examined by High Performance Liquid Chromatography (HPLC) to look for common peaks between the samples. Common peaks could correspond to the active component. The large-scale extract can then be separated in the most efficient manner as indicated by the “chemical screening.”

Chromatography of the full extract can be done in a variety of ways. Partitioning the extract between two immiscible phases can remove large amounts of unwanted material. Polar salts or non-polar fatty material can be removed depending on the chosen solvent.

Traditional column chromatography using a gravity-driven approach has been surpassed by columns being eluted under pressure using either compressed air or nitrogen (so called “flash chromatography”). These columns can be packed with either reverse-phase (e.g. C18) or normal phase packing (e.g. DIOL or silica). The fractions that elute from these columns can then be examined by Thin Layer Chromatography (TLC) or HPLC and tested in the appropriate assay. Further purification of the active fraction can then be attempted using either more column chromatography or HPLC.

Structure elucidation of the biologically active natural product

A number of techniques are used in combination to determine the structure of the natural products once they are purified. These include mass spectrometry that allows

the determination of a molecular formula when used at high resolution. Fragmentation patterns in the mass spectrum also allows the identification of possible fragments.

Infra-red (IR) spectroscopy is useful for the identification of functional groups. The carbonyl stretching frequencies (ca 1650-1900 cm^{-1}) are characteristic for aldehydes, carboxylic acids or esters. Alcohols and amines can be suggested by broad bands around 3000 cm^{-1} .

^1H and ^{13}C NMR spectroscopies allow the identification of unique carbon and proton nuclei in the natural product. Protons on adjacent carbons can sometimes be assigned directly from the ^1H NMR spectrum from the observed spin-spin coupling. The number of protons attached to each carbon can be determined by running an Attached Proton Test (APT) experiment. To obtain further structural information and connectivity through the molecule 2-D NMR experiments are required. These include the COSY experiment (homonuclear CORrelation SpectroscopY) which allows protons on adjacent carbons to be assigned. However, confusion can arise when proton signals overlap. The TOCSY (Total Correlation SpectroscopY) experiment in 2-D or 1-D allows the assignment of a spin system by increasing the mixing time in the experiment. A third important experiment is the HSQC (Heteronuclear Single Quantum Coherence) experiment, which is used to assign which protons are attached to which carbons. A useful extension of this experiment is the HSQC-TOCSY, where a mixing time is added into the pulse sequence. The correlations observed for a particular proton will firstly be to the carbon to which it is attached, and then to any carbons that have protons that are coupled to the original proton. By extending the mixing time in this experiment, spin systems can be assigned. This experiment is particularly useful for assigning spin systems where the protons overlap but the carbons do not. The final experiment commonly used to determine connectivity is the HMBC (Heteronuclear Multiple Bond

Coherence) experiment. This experiment allows the assignment of quaternary centres and can traverse heteroatoms.

1.3 Fungal natural products

1.3.1 General

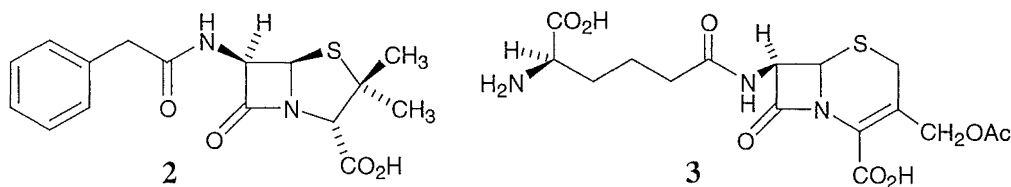
Fungi are a large and diverse group of organisms, presently estimated at around 100,000 species.⁶ This diversity not only includes their morphology, from the unicellular yeasts e.g. *Saccharomyces cerevisiae* to the fungi that form large solid fruiting bodies typified by the conspicuous red mushroom *Amanita muscaria* (Fig. 1.1), but also their biochemical machinery. This machinery has been exploited by humans for centuries in the brewing of wine, beer and the bread-making industries.



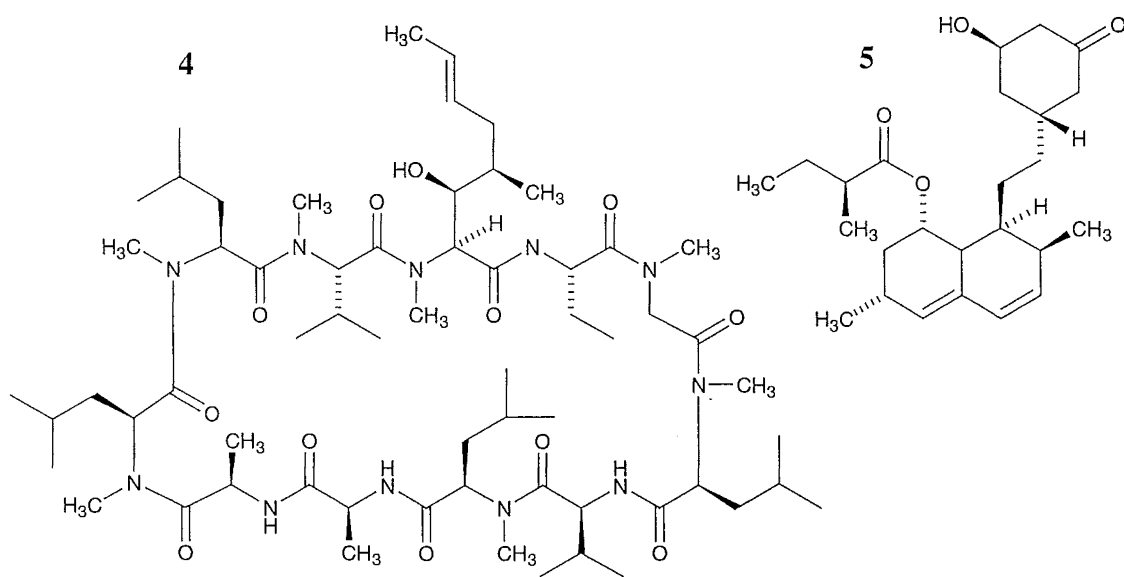
Figure 1.1 *Amanita muscaria* (L. ex Fr.) Hooker

Within this century, we have found other uses for the diverse biochemical properties of fungi by investigating the immense array of natural products or secondary metabolites that are produced by these organisms.⁷ The first of the β -lactam antibiotics, e.g. penicillin G (2), were discovered in the early 1940's, isolated from the mould *Penicillium notatum*. This was followed by cephalosporin C (3), first described in 1956 and isolated from *Cephalosporium acremonium*.⁸ In the four decades since the first

clinical trials of these antibiotics, they (and others since discovered from microbial sources) have been the basis of major advancement in the practice of medicine.



Furthermore, natural products from micro-organisms are now not only seen in the realm of the control of infectious diseases, but also as therapeutic agents for a wide range of human and animal disorders. Two well-known examples that illustrate the diverse applications of fungal natural products are firstly cyclosporin A (Sandimmune®) (4), which was isolated from the filamentous fungus *Trichoderma polysporum*. Cyclosporin A (4) exhibits antifungal activity, but more importantly is an immunosuppressant that prevents the rejection of transplanted organs. Mevinolin (Lovastatin®) (5) is another well known fungal natural product that inhibits the enzyme HMG CoA reductase (3-hydroxy-3-methyl glutaryl coenzyme A reductase) and can be used to control cholesterol biosynthesis in humans and therefore hypercholesterolemia. Mevinolin (5) was originally isolated from *Aspergillus terreus*.⁹



1.3.2 Basidiomycetes natural products

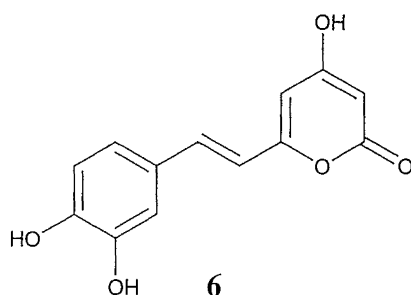
An enormous array of natural products have been isolated from fungi in the basidiomycetes subdivision. These include compounds from all the main biosynthetic pathways namely polyketide, shikimate, isoprenoid and also nitrogen containing non-proteinaceous amino acids and heterocycles. Two comprehensive overviews of fungal metabolites by Turner have been published.^{7,10} Mushroom derived natural products of terpenoid biosynthetic origin have been reviewed by Ayer and Browne encompassing the literature up to 1981, but they only covered di- and sesquiterpene compounds.¹¹ The distribution and biosynthesis of sterol triterpenes in fungi was reviewed by Weete in 1973¹² and a screen for sterol constituents in wood-rotting basidiomycetes was reported by Yokoyama *et al* in 1975.¹³ Plant and mushroom γ -glutamyl derivatives of amino acids and amines were reviewed by Kasai *et al* in 1978¹⁴ and then amino acids from mushrooms by Hatanaka in 1992.¹⁵ The area of pigments isolated from macromycetes has been extensively reviewed by Gill and Steglich up to 1987¹⁶ and then by Gill in 1992¹⁷ and 1995.¹⁸ These reviews relate predominantly to those pigments isolated from the basidiomycete subdivision. A short selection of 'chemical phenomena' of mushroom and toadstools was reported by Anke and Steglich in 1981¹⁹ and then by Steglich in 1989.²⁰ Natural products with antiinsectan activity isolated from the sclerotia produced by a number of fungi were reviewed by Gloer in 1995.²¹

1.3.3 Biologically active natural products from basidiomycetes

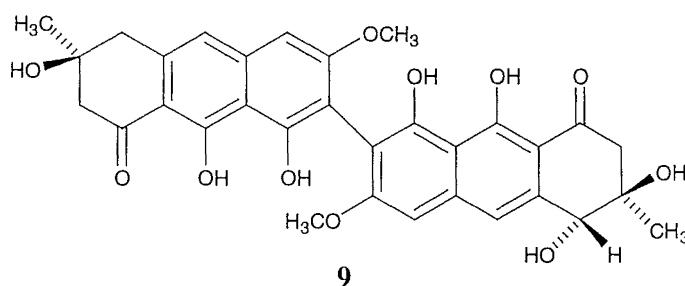
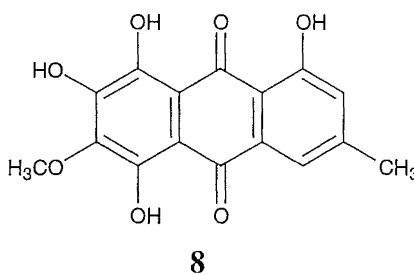
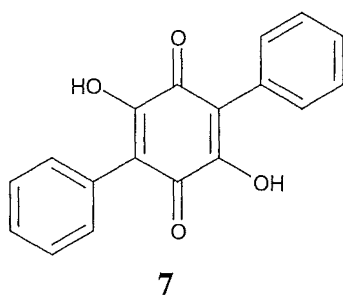
Pigments

A substantial amount of research has been conducted in the area of mushroom pigments and compounds that produce colour changes after either damage to the mushroom or with chemicals such as acid or alkali solutions. Many of these pigments are

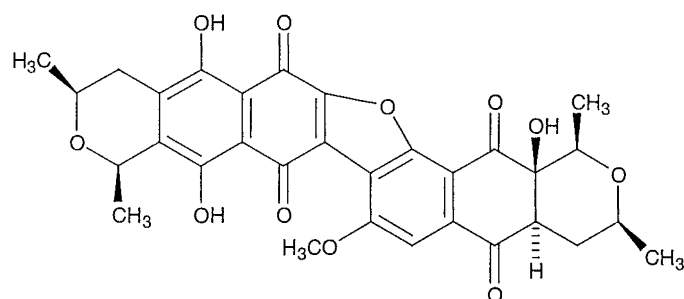
biologically active including the styrylpyrone hispidin (**6**), which exhibits *in vitro* antimicrobial activity.²²



Many biologically active mushroom pigments contain quinone functionality including terphenylquinones such as polyporic acid (**7**) and the anthraquinones and pre-anthraquinones, which are particularly abundant in the *Cortinarius* and *Dermocybe* genera. These include such pigments as dermocybin (**8**), first isolated from *Dermocybe sanguinea*, through to the more elaborate flavomannin derivative **9** from *Cortinarius splendens*. *trans*-4-Hydroxyflavomannin-6,6'-di-*O*-methyl ether (**9**) exhibits significant antibacterial activity but also causes pulmonary congestion and hepatic necrosis in mice.^{16,17}

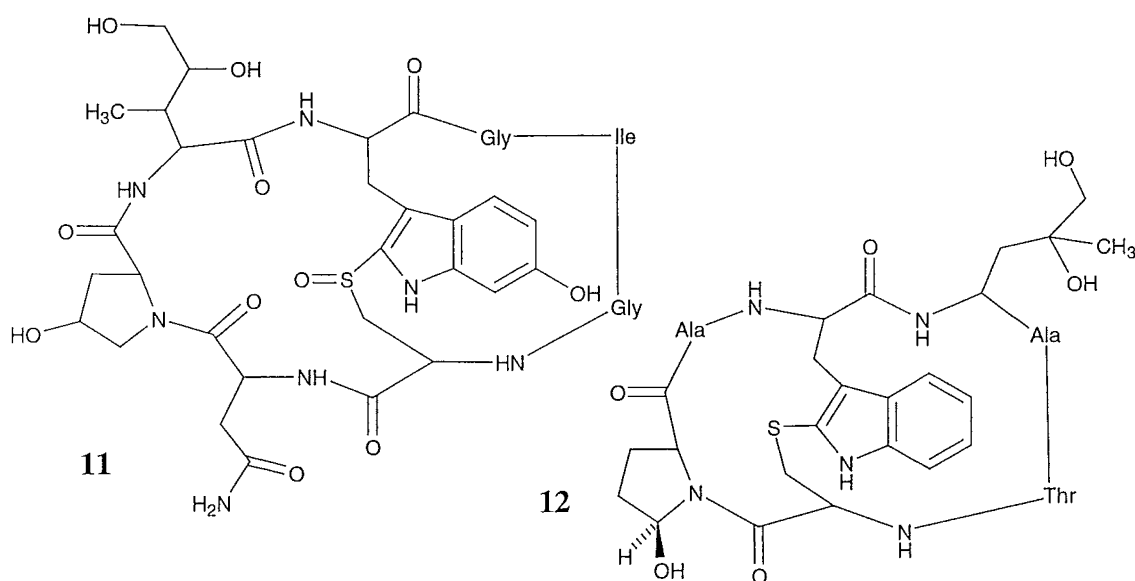


Other dimeric quinones, for example cardinalin 4 (**10**), have been isolated from the New Zealand mushroom *Dermocybe cardinalis*. This dimeric naphthoquinone exhibits cytotoxicity against the P388 cell line with an IC_{50} value of $0.28 \mu\text{g/mL}$.¹⁸

**10**

Peptide Toxins

Many fungi produce fruiting bodies that contain extremely toxic peptide natural products. The genus *Amanita* contains many species that produce these types of toxins. There are three classes of *Amanita* toxins: amatoxins, phallotoxins, and virotoxins. These toxins were first isolated from the “death cap” mushroom or *Amanita phalloidies*. They were later identified as including α -amanitin (**11**), a bicyclic octapeptide with an indole sulfoxide bridge, and phalloidin (**12**) a bicyclic heptapeptide with an indole thioether bridge. These toxins have LD_{50} values of 0.3 and 2.0 mg/kg respectively against mice.^{15,23}



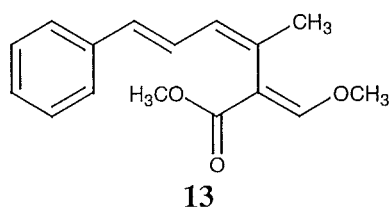
There are also a number of cyclic peptides that have been isolated from *Cortinarius speciosissimus*, which are discussed in the **Introduction** to **Chapter Five**.

Pharmaceuticals

The Shiitake mushroom or *Lentinus edodes* has probably been gathered in Asia for thousands of years, although its pharmaceutical effects were first recorded in the 15th century. One of the main biologically active components is lentinan, a β -1,4-glucan with β -1,6 branches, which can be extracted from the fruiting body or the cell wall of the vegetative hyphae. This polysaccharide (average MW 4×10^5 - 8×10^5 Da) is known to stimulate the immune system and has been investigated as both an anticancer and antiviral chemotherapeutic agent with great success.^{24,25}

Agrochemicals

An excellent example of a fungal natural product leading to the development of a commercial agrochemical is strobilurin A (**13**). The strobilurin story highlights a number of important issues that arise during the development of a natural product into a commercial product. The first is the length of time that is required for such a development with the first strobilurin discovered in the 1960's and the commercial products reaching the market in 1995. The second important issue was that strobilurin A displayed a novel mechanism of antifungal action by way of the β -methoxyacrylate functionality. The final important issue was that the natural product itself was too unstable for a commercial fungicide. Chemical variants were therefore developed that had the same mechanism of action but were more stable. The early development of the β -methoxyacrylate fungicides was reviewed by Anke and Steglich²⁶ and then later by Clough.²⁷

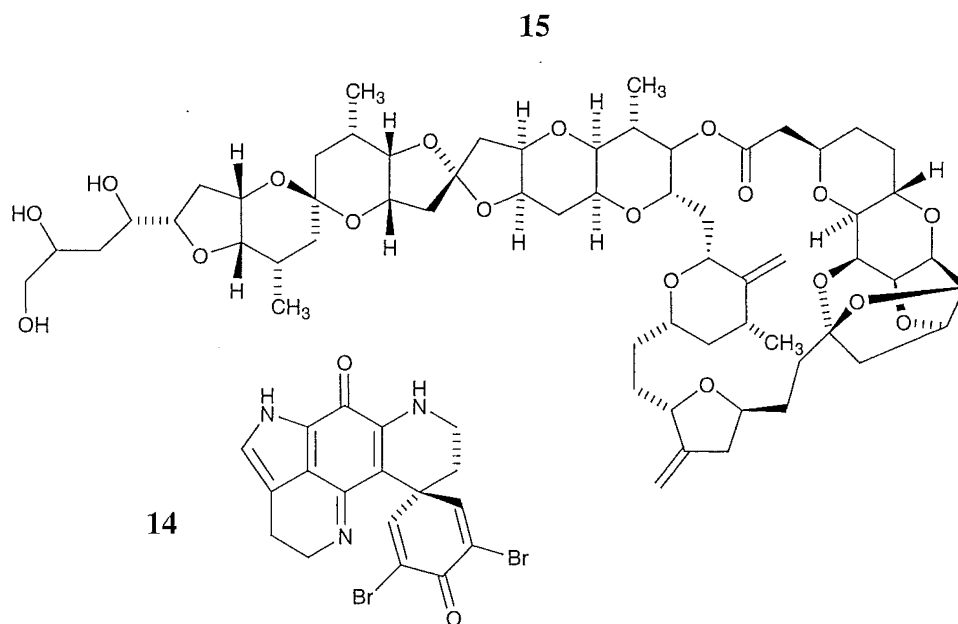


1.4 Work done at the University of Canterbury

1.4.1 General

In the past, the natural product chemistry group at the University of Canterbury has concentrated predominantly on the isolation and structure elucidation of marine natural products with antitumour or antiviral activity.

To date the most significant discoveries are a series of compounds called the discorhabdins and a sponge of the *Lissodendoryx* genus, which is a high yielding source of the series of compounds called the halichondrins. The discorhabdins were isolated from various *Latrunculia* species of sponge with some, for example discorhabdin C (**14**), showing potent cytotoxicity. The halichondrin of particular interest to the National Cancer Institute is halichondrin B (**15**), which is currently the subject of pre-clinical assessment.²⁸



1.4.2 Aims of this research

Even though the marine environment represents perhaps the largest unexplored area with respect to natural product chemistry, there are still organisms in the terrestrial environment that have yet to be explored, or may warrant re-exploration using a different approach.

The initial aim of research towards this PhD was to set up a screening programme using the approach described earlier in this chapter (**Section 1.2.2**). The programme would consist of the collection, extraction and screening of New Zealand and Australian fungi to look for biological activity. The biological assays used in this programme would include the P388 murine leukaemia cell line, antimicrobial zone of inhibition assays and antiviral assays as described in detail in **Chapter Three**.

A selection of these fungi would then be investigated further with the aim of isolating the component(s) responsible for the biological activity. The structural elucidation of any purified component(s) would be attempted using a combination of mass spectrometry, NMR spectroscopy techniques and synthesis.

CHAPTER TWO

FAVOLASCHIA CALOCERA

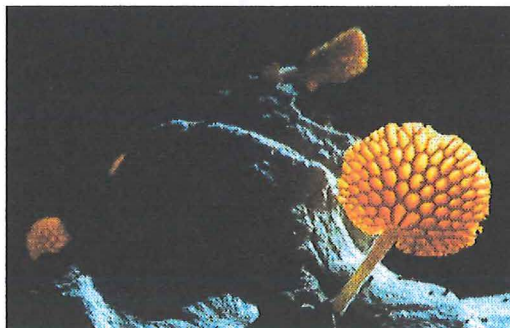
2.1 Introduction

2.1.1 The genus *Favolaschia*

Favolaschia calocera Heim.⁵⁹

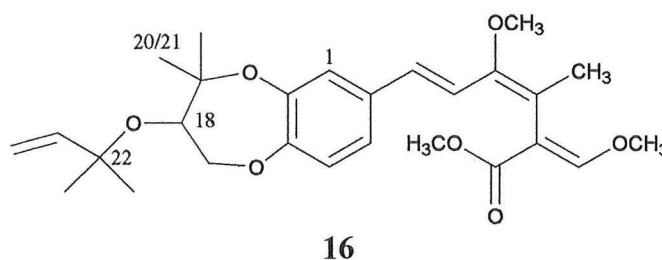
Dr Anthony Cole (Department of Plant and Microbial Sciences, University of Canterbury) initiated a programme for the collection of fungi that produce pigmented fruiting bodies, and the screening of their extracts for antifungal activity. During this programme the bright orange fruiting bodies of *Favolaschia calocera* were collected and extracted. This extract showed significant antifungal activity in their assay and was submitted for the full range of in-house assays in the Department of Chemistry, University of Canterbury. In these assays, this extract showed both significant antifungal activity and cytotoxicity against the P388 cell line. Extracts of this fungus

were investigated during research toward a Masters degree²⁹ and were then studied further during research towards this PhD.



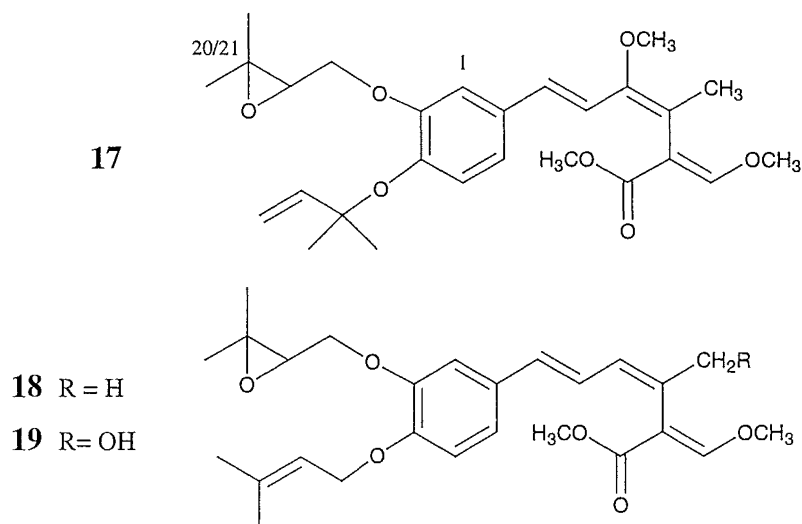
Picture 2.1 *Favolaschia calocera*

The research completed for a Masters degree included the isolation and structural assignment of 9-methoxystrobilurin K (**16**), the cytotoxic and antifungal component of *Favolaschia calocera* fruiting bodies. Two crucial pieces of NMR data that enabled the structural determination were an HMBC correlation from the C18 methine to the C22 quaternary carbon and an NOE between the methyl protons of C20/C21 and the aromatic H1 proton.^{29,30}



Favolaschia species (Ethiopia)

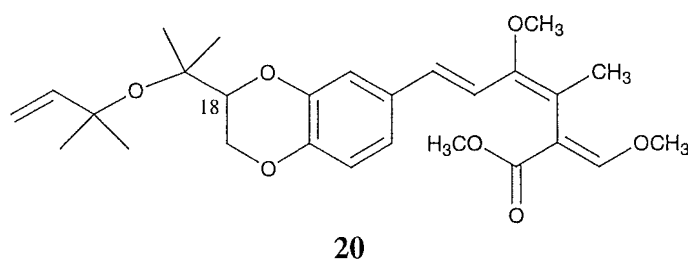
Six months after compound **16** was fully characterised, Steglich *et al* reported the isolation and structural elucidation of compound **17**, 9-methoxystrobilurin K, from an extract of the liquid culture of a *Favolaschia* species from Ethiopia.³¹ The ¹H and ¹³C NMR data that were reported for this compound were identical with those obtained for compound **16**. Structure **17** was assigned using HMBC, HMQC and NOE NMR experiments, and by comparison of ¹H and ¹³C data with those obtained for strobilurin D (**18**)³² and hydroxystrobilurin D (**19**).³³



The HMBC correlation from H18 to C22 would not be possible in structure **17**. An NOE was reported between the C20/C21 methyl protons and the aromatic H1 proton, but modelling studies suggested this would be unlikely for structure **17**.

Favolaschia pustulosa

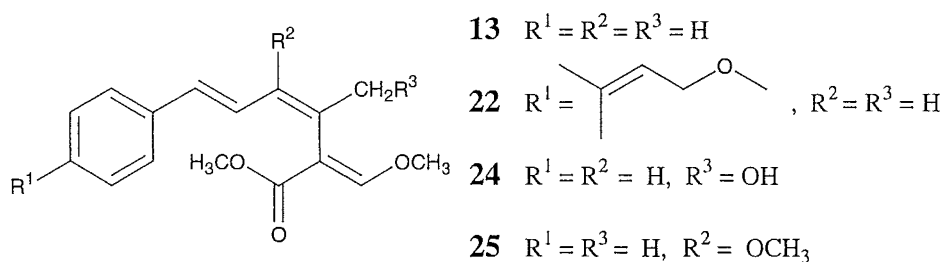
A reported investigation into the chemical components of *Favolaschia pustulosa* yielded another strobilurin compound assigned as structure **20**, which was called 9-methoxystobilurin L.³⁴ The ¹H and ¹³C NMR data for this compound were reported in CD₃OD. When the sample of 9-methoxystobilurin K (**16**) was run in CD₃OD the data were identical with those reported for compound **20**. Again, the HMBC correlation from H18 to the quaternary carbon would not be possible in structure **20**. The comparison of NMR data and the conclusions drawn are discussed in **Section 2.4.3**.

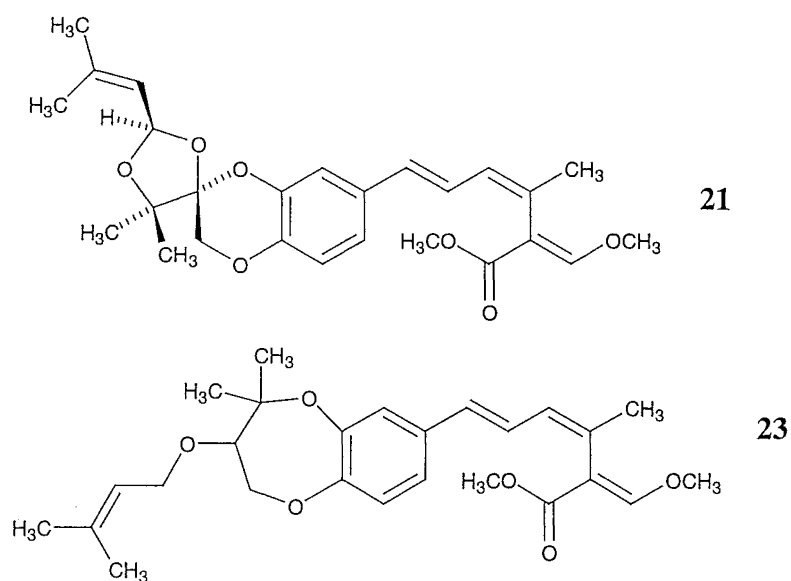


2.1.2 History of the strobilurins

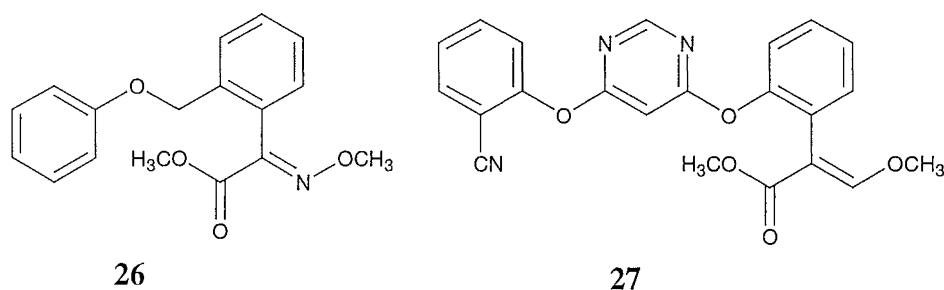
The strobilurins are a class of compounds that show significant antifungal activity, with some also exhibiting cytostatic properties. Both of these properties are attributed to inhibition of cellular respiration by the (β)-methoxyacrylate moiety. This inhibition is due to binding to a specific site on cytochrome *b* in mitochondria.²⁷

A large number of strobilurins have been isolated and characterised. While the β -methoxyacrylate functionality remains constant, there is substantial structural diversity with the substituents on the benzene ring. The first strobilurin reported was strobilurin A (**13**) in 1977, which was isolated from *Strobilurus tenacellus*,³⁵ but not structurally assigned until 1978.³⁶ The stereochemistry of the C9-C10 olefin was originally assigned as *E*. After synthesis of strobilurin A and re-examination of the spectroscopic data, the stereochemistry was revised to *Z*.³⁷ Since then eight new strobilurins, two hydroxystrobilurins and four 9-methoxystrobilurins have been reported. These include strobilurins D (**18**),³² E (**21**),³⁸ F (**22**)⁴⁸ and G (**23**),⁴⁸ hydroxystrobilurins A (**24**)³⁹ and D (**19**)³³ and 9-methoxystrobilurins A (**25**)³¹ and L (**20**)³⁴ from a variety of fungi mostly in the basidiomycetes subdivision but





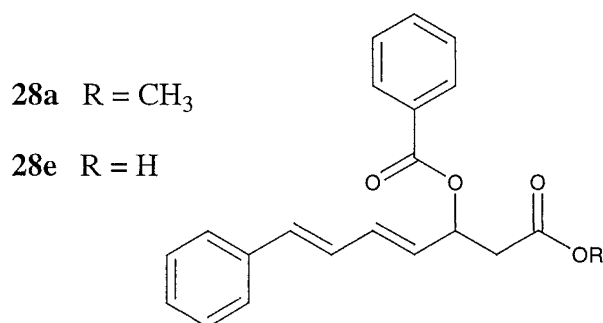
The significance of this class of compounds is evident, with some twenty companies having published over 200 patents in this area. BASF and Zeneca have developed the commercial fungicides, kresoxime (**26**) and azoxystrobin (**27**), respectively, which are both variants of the strobilurin natural products.⁴⁰



2.1.3 Further investigation of *Favolaschia calocera*

Favolaschia calocera is obviously an interesting organism that warranted further investigation. The revision of 9-methoxystrobilurin K from structure **17** to that of **16** was thought to be sound, based on NMR arguments, but to unambiguously assign this as the structure, synthesis of the appropriate model compounds was required. Therefore, a series of model compounds were synthesised, which are discussed in Section 2.4 of this chapter.

During the initial investigation of the extracts of *F. calocera*, a number of metabolites other than 9-methoxystrobilurin K (**16**) were isolated and characterised, including methyl (4*E*,6*E*)-3-benzoyloxy-7-phenylhepta-4,6-dienoate (**28a**) and the carboxylic acid of **28a** (**28e**).⁴¹ The absolute stereochemistry of compound **28a** was determined using Mosher's method and is discussed in **Section 2.3** of this chapter.



During further investigation of the CH₂Cl₂ extract of *F. calocera*, two compounds related to compound **28a** were isolated and characterised as methyl (4*E*,6*E*)-3-hydroxy-7-phenylhepta-4,6-dienoate (**28b**) and (*E*)-6-phenyl-5-hexen-2-ol (**32**). Two further unrelated compounds were also purified and characterised as 5-stearate (**30a**) and 5-palmitate (**30b**) esters of (2*E*,6*E*)-1-(2-hydroxy-4-methoxyphenyl)-5-hydroxy-3,7,11-trimethyldodeca-2,6,10-triene. The isolation and structure elucidation of these three compounds is discussed in **Section 2.2** of this chapter.

F. calocera was grown in liquid broth culture, and was shown to produce 9-methoxystrobilurin K and a number of other strobilurins in such cultures. This work is discussed in **Section 2.5** of this chapter.

2.2 Chromatography of *F. calocera* extract and structural elucidation of 30a-b, 32 and 28b

2.2.1 Chromatography of *F. calocera* extract

Work done during a Masters degree involved the purification of a CH₂Cl₂ extract of *F. calocera* fruiting bodies.^{29,30} After extensive chromatography of this extract, 9-methoxystrobilurin K (**16**) was isolated and characterised. The ¹H NMR spectra of a number of side fractions from the first column appeared to contain structurally related compounds to those already identified. Several of these fractions were investigated as research towards this PhD thesis.

Chromatography of fraction GN2-117.22

Work during this thesis included further chromatography of fraction GN2-117.22 (103 mg) by normal phase (DIOL) column chromatography, to give twenty-eight fractions (GN2-118.1-28). Combinations were made by TLC. Fractions GN2-118.17-25 (50.1 mg) were loaded onto a reverse-phase column and eluted with a stepped gradient system from H₂O through to MeOH and then to CH₂Cl₂. This gave fraction GN2-15.20 that was identified by NMR spectroscopy and mass spectrometry as a mixture of two derivatives of (2*E*,6*E*)-1-(2-hydroxy-4-methoxyphenyl)-5-hydroxy-3,7,11-trimethyldodeca-2,6,10-triene (**30a-b**) that were esterified with fatty acids at the 5-position.

Chromatography of fraction GN2-117.25

Fraction GN2-117.25 (182 mg) was further purified by DIOL column chromatography, to give twenty-one fractions. Combinations were made by TLC. The ¹H NMR spectrum of the fractions that eluted with 80% petroleum ether/CH₂Cl₂ (GN2-2.7-8, 69 mg) indicated the presence of a compound which was possibly structurally related to the

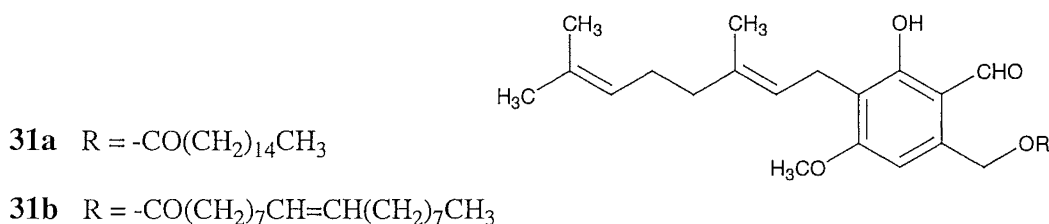
major component (**28a**) of the CH_2Cl_2 extract. Further purification using Lobar chromatography on normal phase CN (2% IPA/Hexane) followed by semi-preparative HPLC on CN (4% IPA/Hexane, 2.5 mL/min) yielded (*E*)-1-phenylhex-5-en-2-ol (**32**, 3.0 mg).

The fraction that eluted with 20% petroleum ether/ CH_2Cl_2 (GN2-2.9, 18.3 mg) was further purified by reverse-phase (C18) column chromatography using a gradient solvent system from H_2O through to MeOH. The fraction that eluted in 80% MeOH/ H_2O (GN2-11.17, 3.0 mg) contained methyl (4*E*,6*E*)-3-hydroxy-7-phenylhepta-4,6-dienoate (**28b**).⁴²

2.2.2 Structural elucidation of compounds 30a-b, 32 and 28b

Structural elucidation of 30a-b

The ^1H NMR spectrum of **30a-b** (Fig. 2.1) showed similarities to the NMR data for a series of compounds previously reported as hericene A (**31a**) and B (**31b**). These compounds contain a common core structure of a substituted phenolic ring, a geranyl chain and are esterified with a series of fatty acids.⁴³



High-resolution electron impact mass spectrometry gave two ions that could be assigned as the fatty acids stearic acid ($\text{C}_{18}\text{H}_{36}\text{O}_2$) and palmitic acid ($\text{C}_{16}\text{H}_{32}\text{O}_2$). The third ion was found to have the molecular formula of $\text{C}_{22}\text{H}_{30}\text{O}_2$. The IR spectrum contained a peak at 1720 cm^{-1} consistent with an aliphatic ester, a sharp band at 3590 cm^{-1} and a broad band between 3400 and 3550 cm^{-1} indicating an hydroxyl group.

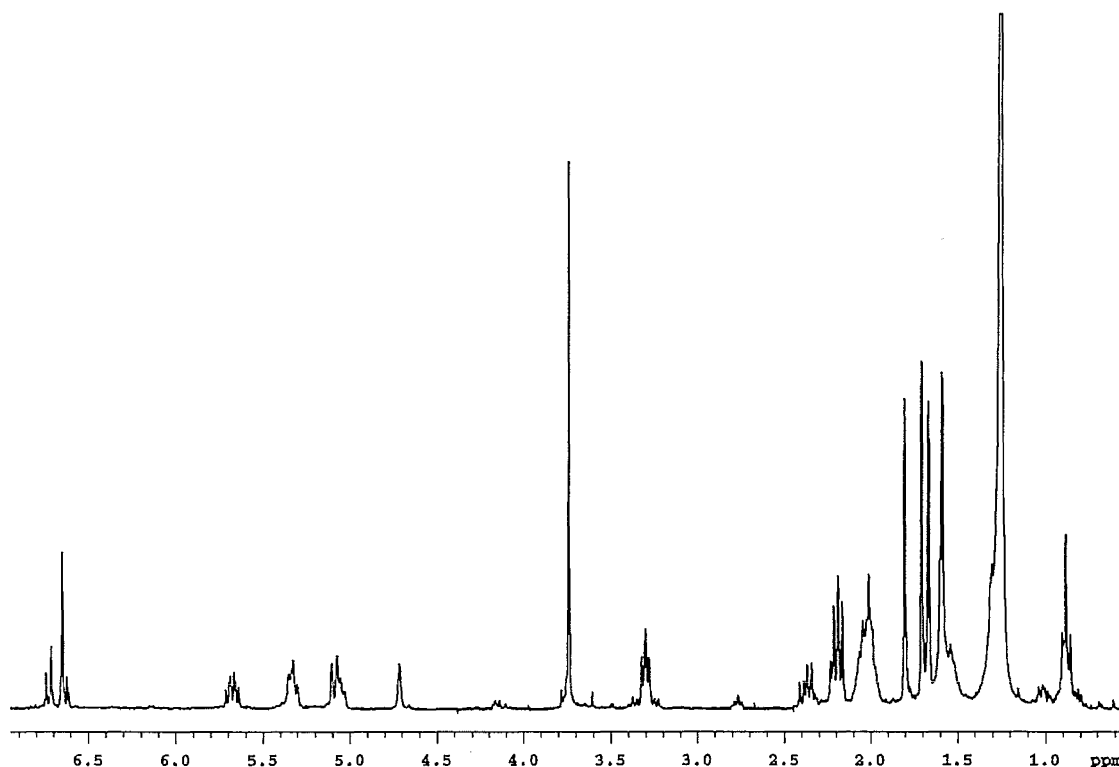


Figure 2.1 ^1H NMR spectrum of **30a-b** (in CDCl_3)

The common core of **30a-b** contained a substituted phenolic ring, different to that of the hericenens. The aromatic ring was assigned using a combination of COSY, HMBC and HMQC correlations as illustrated in **Fig. 2.2**.

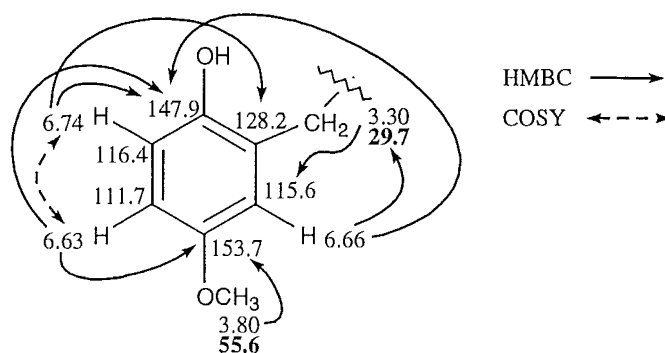


Figure 2.2 HMBC and COSY correlations for **30a-b**

Connectivity from the phenol ring along a farnesyl chain was achieved with further COSY and HMBC correlations as illustrated in **Fig. 2.3** and **Fig 2.4**. A feature of this farnesyl chain was the oxygenation at C5 (δ_{H} 5.68, δ_{C} 69.4). An HMBC correlation

was observed from the methine at δ_{H} 5.68 to the carbonyl (δ_{C} 173.8) of the fatty acids. This position was therefore the site of esterification.

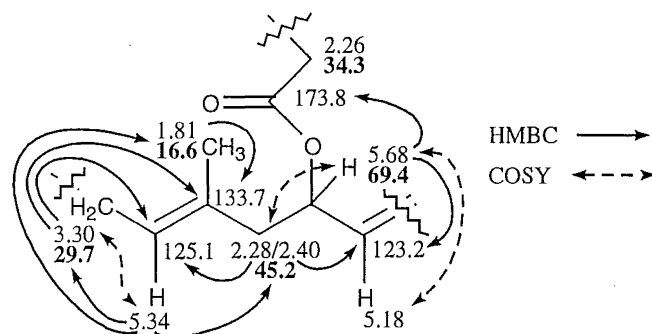


Figure 2.3 HMBC and COSY correlations for **30a-b**

Connectivity through the remainder of the farnesyl chain was achieved with a series of COSY and HMBC correlations. A selection of these correlations is illustrated in **Fig. 2.4**.

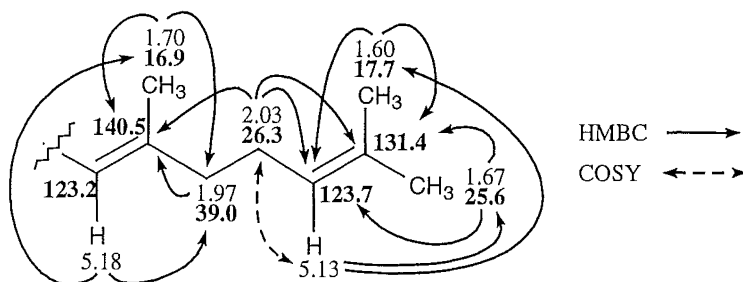


Figure 2.4 HMBC and COSY correlations for **30a-b**

The terminal methyl group of the fatty acids was confirmed by comparison of chemical shift data for an alkane chain and the HMBC and COSY correlations shown in **Fig. 2.5**. The ^1H and ^{13}C NMR data were consistent with the fatty acids being straight chain and fully saturated.

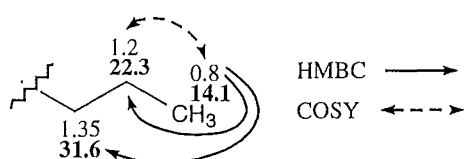


Figure 2.5 HMBC and COSY correlations for **30a-b**

The stereochemistry of the C2-C3 and C6-C7 olefins was determined using NOE experiments (**Fig. 2.6**). When the methyl at δ_{H} 1.81 (Me21) was irradiated, an NOE was observed for the methylene at δ_{H} 3.30 (H1), allowing the assignment of the C2-C3 olefin as *E*. An NOE observed for the C5 methine when Me20 (δ_{H} 1.70) was irradiated requires the C6-C7 olefin to also have *E* stereochemistry.

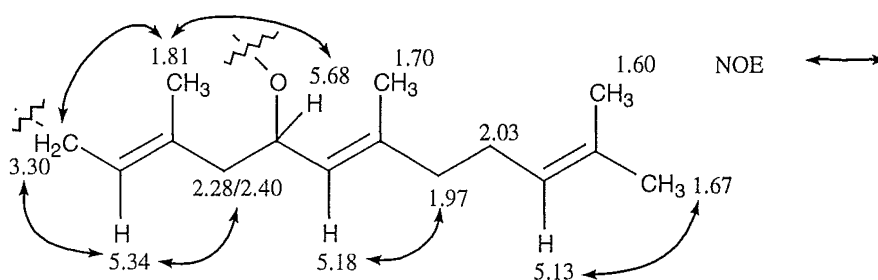
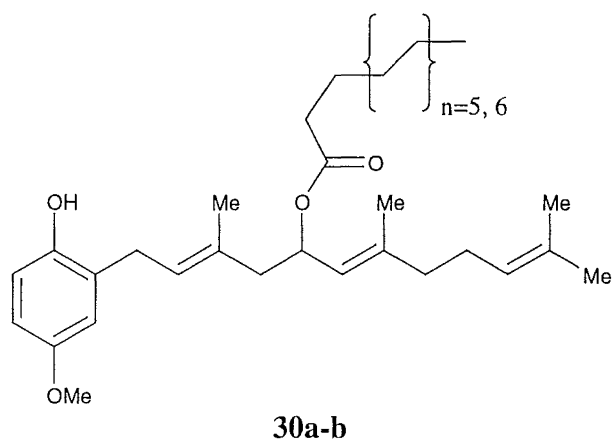


Figure 2.6 NOE effects observed for **30a-b**

Methanolysis of compounds **30a-b**

To confirm the identity of the fatty acids constituting the C5 esters of compounds **30a-b**, a small amount was subjected to methanolysis. Compounds **30a-b** were treated with sodium methoxide in MeOH to yield a mixture of fatty acid methyl esters that were analysed by GCMS. Two peaks were observed by GCMS. These peaks were identified as the methyl esters of stearic and palmitic fatty acids. This confirmed the identity of the fatty acids that were suggested in the fragmentation pattern of the original EI mass spectrum. Compounds **30a** to **30b** were therefore assigned as the 5-stearate (**30a**, 18:0, octadecanoate) and 5-palmitate (**30b**, 16:0, hexadecanoate) esters of (2*E*,6*E*)-1-(2-hydroxy-4-methoxyphenyl)-5-hydroxy-3,7,11-trimethyldodeca-2,6,10-triene.



Structural elucidation of 32 and 28b

(*E*)-6-Phenylhex-5-en-2-ol (**32**) was fully characterised by the ^1H NMR spectrum (**Fig. 2.7**), HMBC and HSMQC experiments. The ^1H NMR data were consistent with those previously reported.⁴⁴

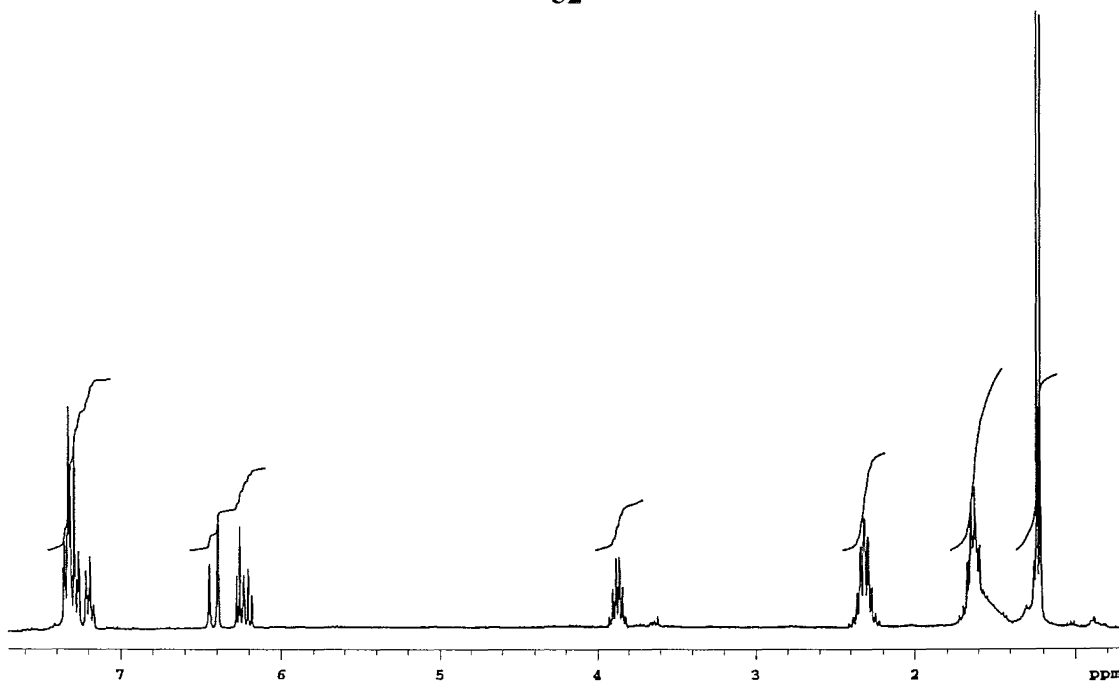
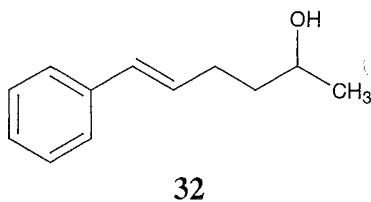


Figure 2.7 ^1H NMR spectrum of **32** (in CDCl_3)

The ^1H NMR spectrum (Fig. 2.8) of compound **28b** contained signals similar to those of the major component of the *F. calocera* extract, compound **28a**. The major differences were the disappearance of the signals corresponding to the benzoyl group, the change in appearance of the methylene α to the methyl ester and the movement of the methine at the site of the benzoyl substituent upfield by $\Delta\delta_{\text{H}}$ 1.2. Full assignment of compound **28b** as methyl (4*E*,6*E*)-3-hydroxy-7-phenylhepta-4,6-dienoate was achieved through HMBC and HSMQC correlations. The ^1H and ^{13}C NMR data were consistent with those previously reported.⁴²

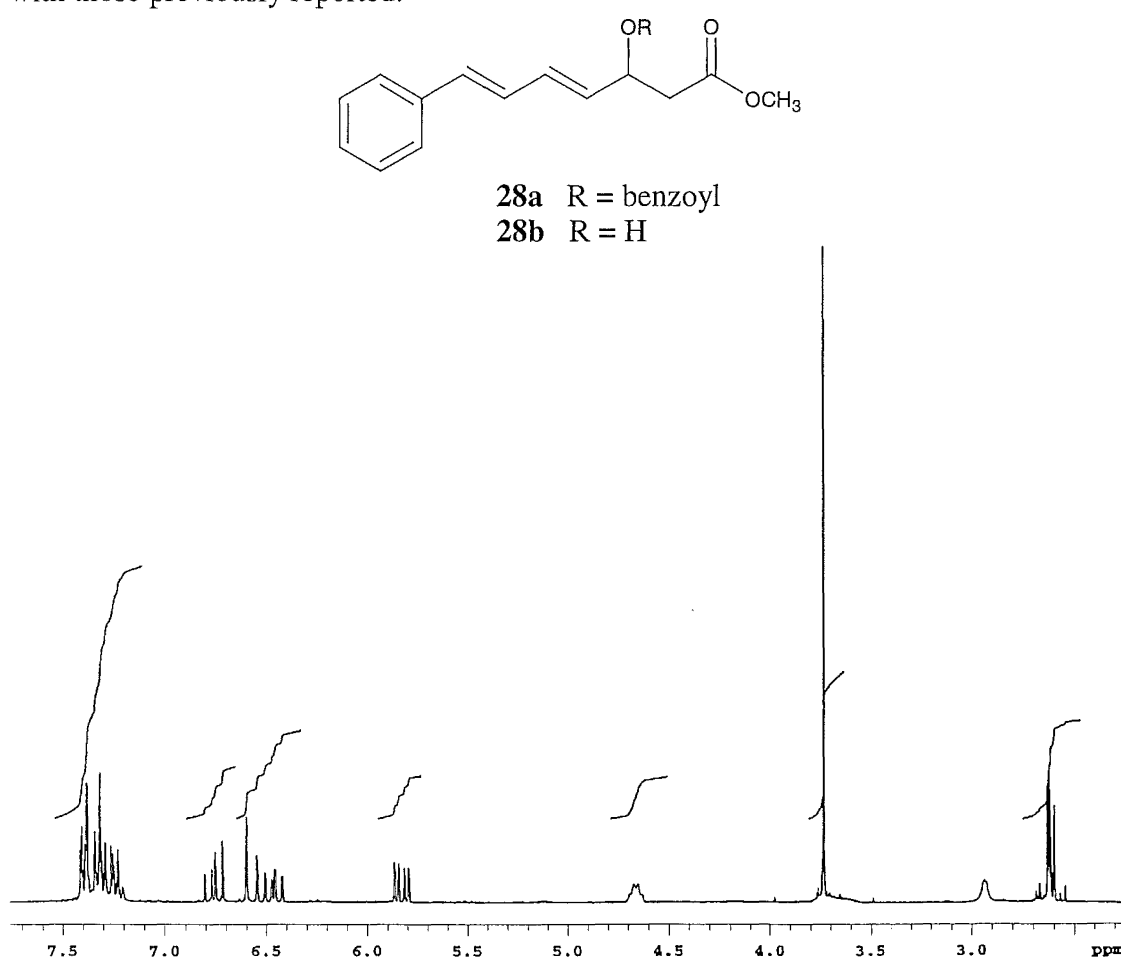


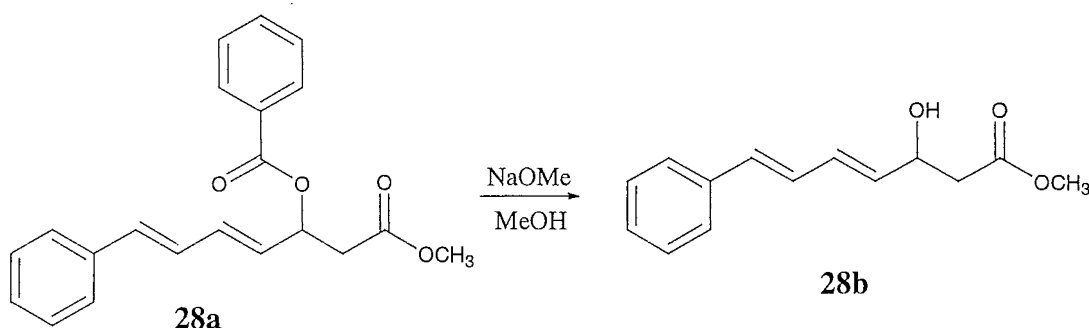
Figure 2.8 ^1H NMR spectrum of **28b** (in CDCl_3)

Biological activity of 30a-b, 32 and 28b

Compounds **30a-b**, **32** and **28b** did not show any biological activity in the assays in which they were screened. These included the P388 cell line, antimicrobial assays and antiviral assays as described in Chapter Three.

2.3 Absolute stereochemistry of methyl (4*E*,6*E*)-3-benzoyloxy-7-phenylhepta-4,6-dienoate (**28a**)

Methyl (4*E*,6*E*)-3-benzoyloxy-7-phenylhepta-4,6-dienoate (**28a**) was originally isolated as the major component of the CH₂Cl₂ extract of *F. calocera*. The stereochemistry at C3 was determined by Mosher's method on **28b** (obtained from **28a** by treatment with NaOMe/MeOH). The alcohol **28b** was also isolated from the extract, and the structure confirmed by comparison of ¹H NMR data with those previously reported.⁴²



Both the (*R*)- (**28c**) and (*S*)- α -methoxy- α -trifluoromethylphenylacetic acid (MTPA) (**28d**) ester derivatives of alcohol **28b** were made, and analysed by ¹H NMR spectroscopy.⁴⁵ The proton chemical shifts of H2-H6 in compounds **28c** and **28d** were assigned from selective 1D-TOCSY NMR experiments. The two carbon substituents of the stereocentre then needed to be assigned as either L₂ or L₃ as illustrated in (Fig. 2.9). Therefore, if $\Delta\delta[(R)-(S)]$ was positive, the substituent was assigned as being L₃, and if it was negative then the substituent was assigned as L₂.⁴⁶

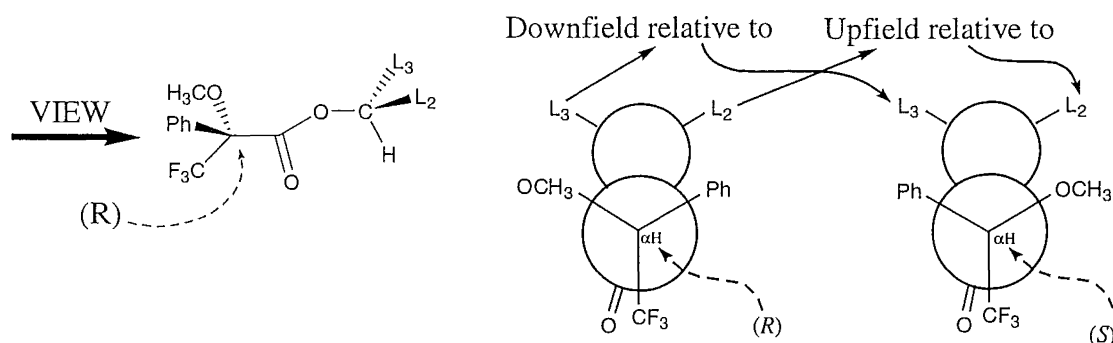


Figure 2.9 The assignment of L₂ and L₃

The downfield shift of the H2a/H2b and OCH₃ proton resonances for the (*R*)-MTPA ester compared to the (*S*)-MTPA ester (i.e. $\Delta\delta[(R)-(S)]$ positive) led to their assignment as L₃. In comparison, the upfield shift of the H4 and H5 resonances (i.e. $\Delta\delta[(R)-(S)]$ negative) led to their assignment as L₂ (**Fig. 2.10**).⁴⁶

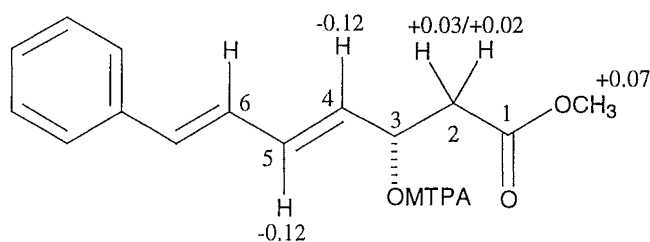
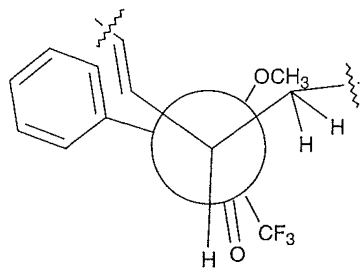


Figure 2.10 Chemical shifts differences ($\Delta\delta[(R)-(S)]$) between **28c** and **28d**

The configurations shown in **Fig. 2.11** are consistent with the observed chemical shift differences. The absolute stereochemistry at C3 was therefore assigned as *S* for **28b**, and by implication as *S* for **28a**.⁴⁶

(*R*)-MTPA



(*S*)-MTPA

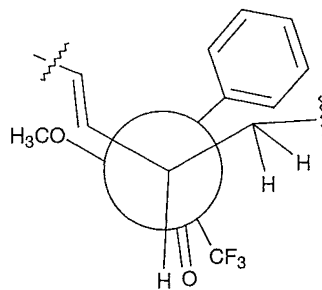


Fig. 2.11 Configurational correlation model for (*R*)-MTPA (**28c**) and (*S*)-MTPA (**28d**) ester derivatives of **28b**

2.4 Synthesis of model compounds to confirm structure of 9-methoxystrobilurin K as 16

2.4.1 Introduction

To support the NMR based reassignment of 9-methoxystrobilurin K as structure **16** and to provide support for structures in the strobilurin series, a number of model compounds were synthesised. Compound **33** corresponded to the isoprenoid fragment in strobilurin F (**22**), while compounds **35** and **38** corresponded to that reported for 9-methoxystrobilurin K (**17**) and that proposed for the revised structure **16**, respectively. Compound **39** corresponded to the isoprenoid fragment in both strobilurin D (**18**) and hydroxystrobilurin D (**19**), while compound **40** corresponded to that reported for strobilurin G (**23**).

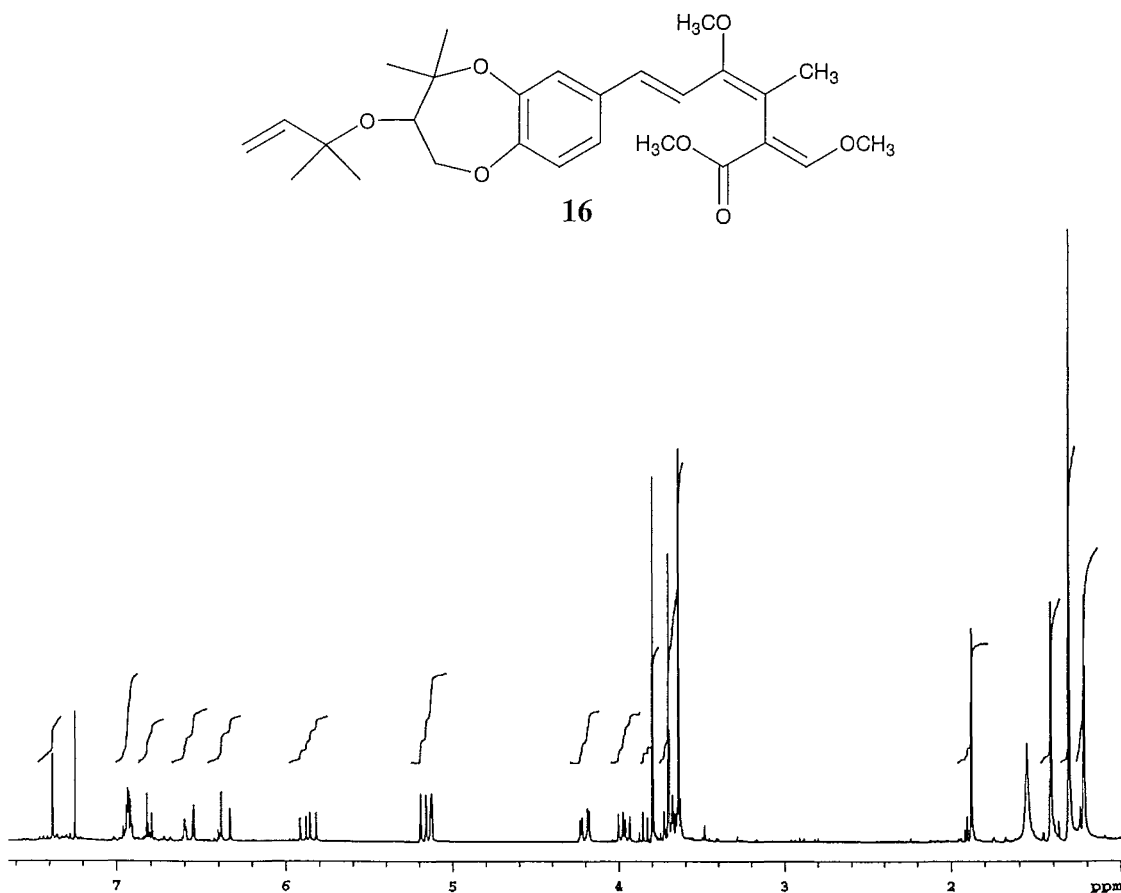
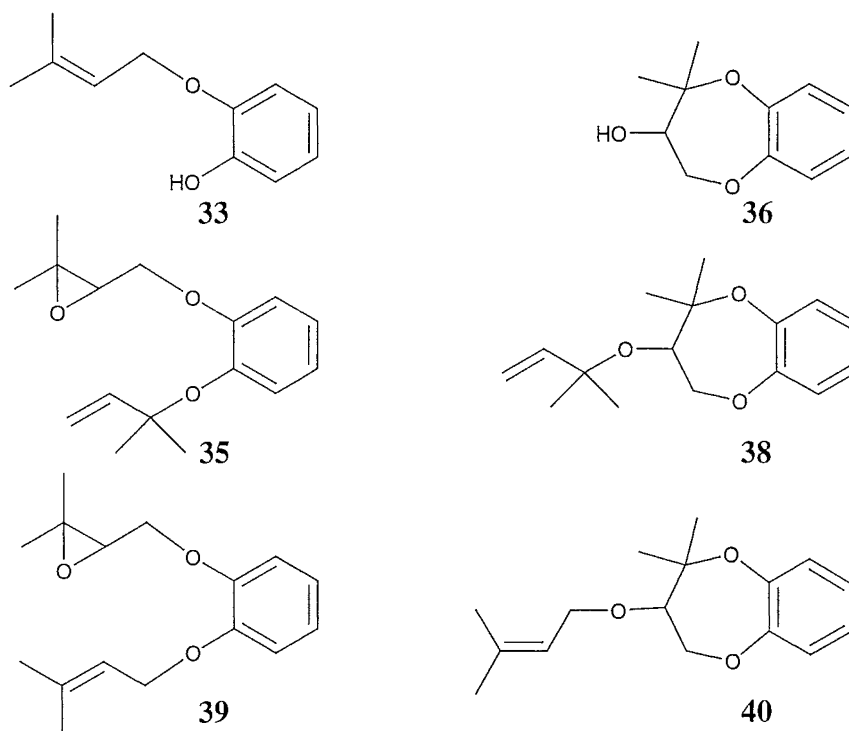


Figure 2.12 ¹H NMR spectrum of compound **16** (in CDCl₃)

The synthetic approach for the synthesis of these compounds was based around manipulations of unsaturated mono- and di- ethers of catechol. It was noted that all of the four desired compounds (**35**, **38**, **39** and **40**) could be obtained from compound **33**. With compounds **35** and **39**, this was possible through further alkylation, and with compounds **38** and **40** through an intramolecular epoxide opening reaction to form the dioxepin **36** followed by alkylation. A precedent for this intermolecular epoxide opening was found in the literature, with the synthesis of **36** by Williams *et al.*⁴⁷



2.4.2 Synthesis of compounds 33-40

Synthesis of compounds 33 and 35

Alkylation of catechol with 1-bromo-3-methylbut-2-ene gave the separable ethers **33** and **34** (89%, 16:1). Compound **33** displayed ^1H and ^{13}C NMR data (Fig. 2.13) consistent with those published for the relevant fragment of strobilurin F (**22**).⁴⁸ This result provided validation for this system as an appropriate model for comparison between the appropriate synthetic compounds and the corresponding fragment in the natural products.

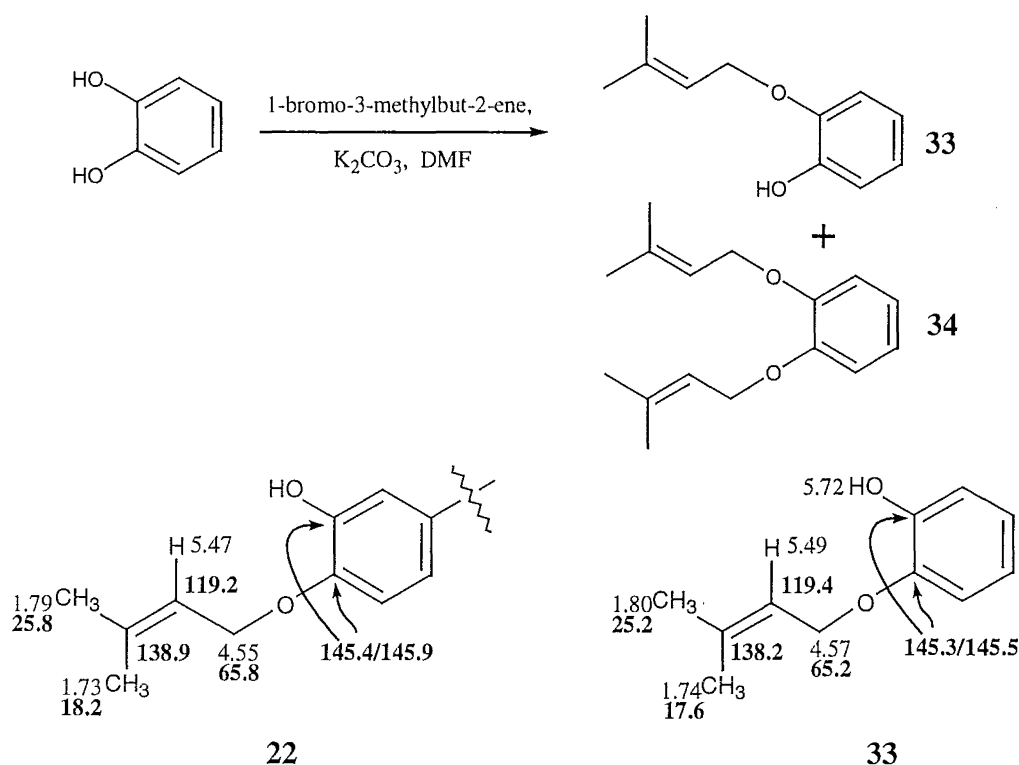
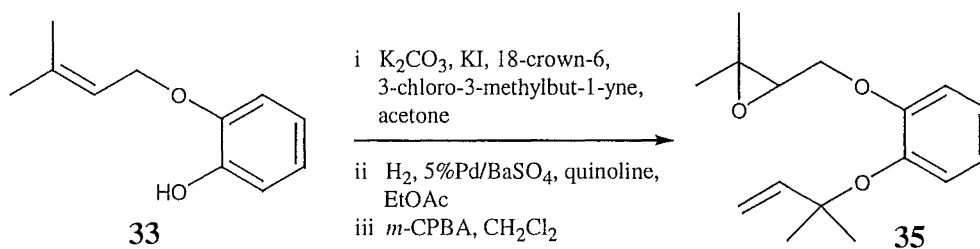


Figure 2.13 NMR chemical shift data for strobilurin F (**22**) and compound **33**

Alkylation of the ether **33** with 3-chloro-3-methylbut-1-yne^{49,50} gave an alkyne that was partially reduced with 5% palladium on barium sulphate (33% w/w with the alkyne), with quinoline (33% w/w with the alkyne) as a poison. Regioselective epoxidation of the trisubstituted alkene gave compound **35**, corresponding to the isoprenoid fragment claimed as part of the structure of 9-methoxystrobilurin K (**17**).



The 1H and ^{13}C NMR chemical shift data for compound **35** were inconsistent with those published for the natural product claimed as structure **17** (Fig. 2.14 and 1H NMR spectrum of **35** - Fig. 2.15).³¹ In particular, the chemical shifts of the epoxide carbons C18 and C19 were δ_C 14.0 and 23.5 respectively upfield from those of the natural product **17**. The NOEs observed for compound **35** were also inconsistent with those

reported, especially the absence of an NOE between the epoxide methine proton (δ_{H} 3.17) and the methyl protons (δ_{H} 1.44) of the 2-methylbut-3-en-2-oxy group reported for the natural product **17**. However, these methyl groups (δ_{H} 1.44) showed an NOE to an aromatic proton at δ_{H} 7.03, confirming their proximity to the aromatic ring. Observation of these NOEs, supported by molecular modelling,⁵¹ and the unacceptably large chemical shift differences for the epoxide carbons led to the conclusion that 9-methoxystrobilurin K could not have the epoxyprenyl structure (**17**) previously assigned.

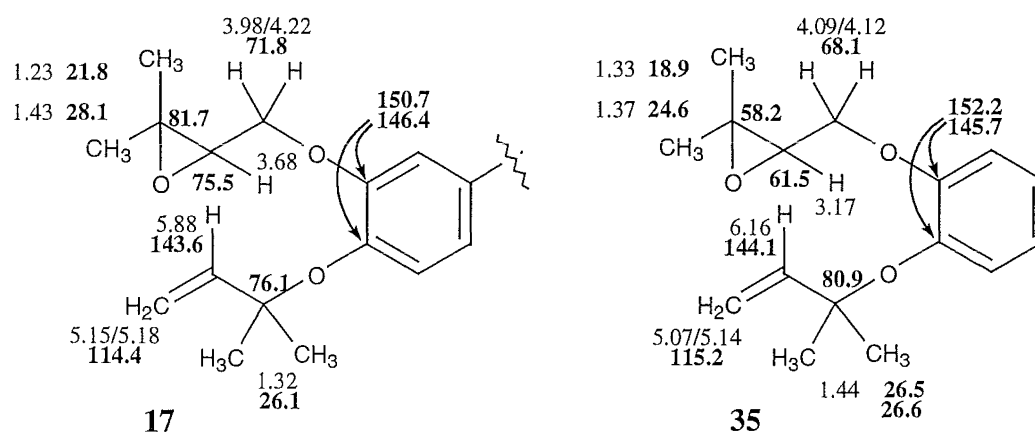


Figure 2.14 NMR data reported for strobilurin K (**17**) and compound **35**

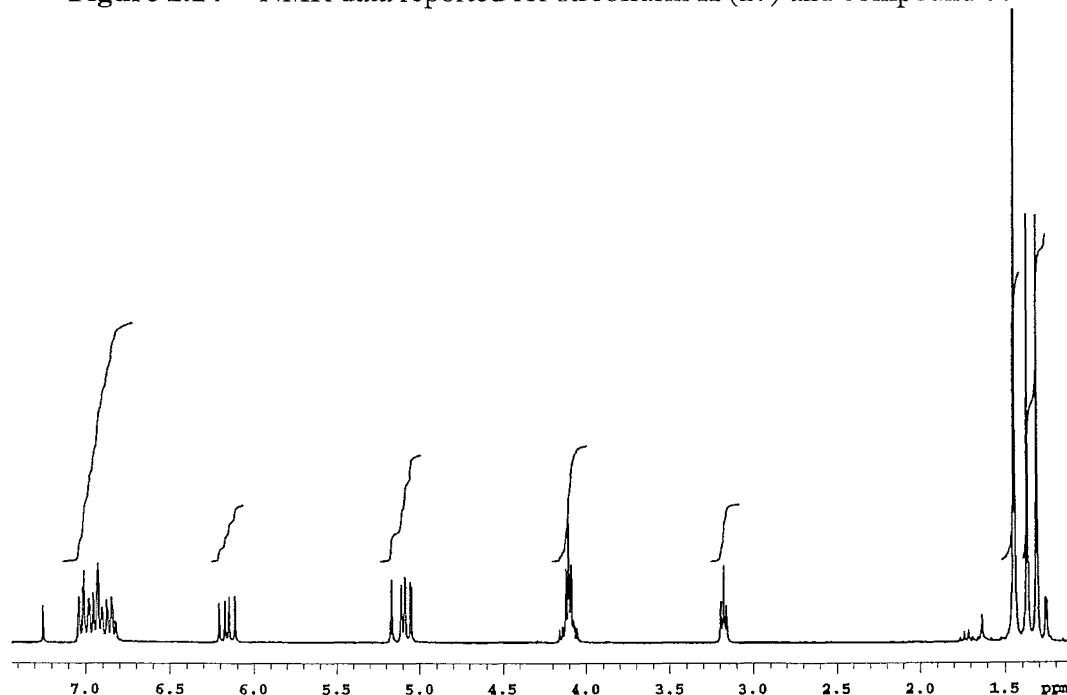
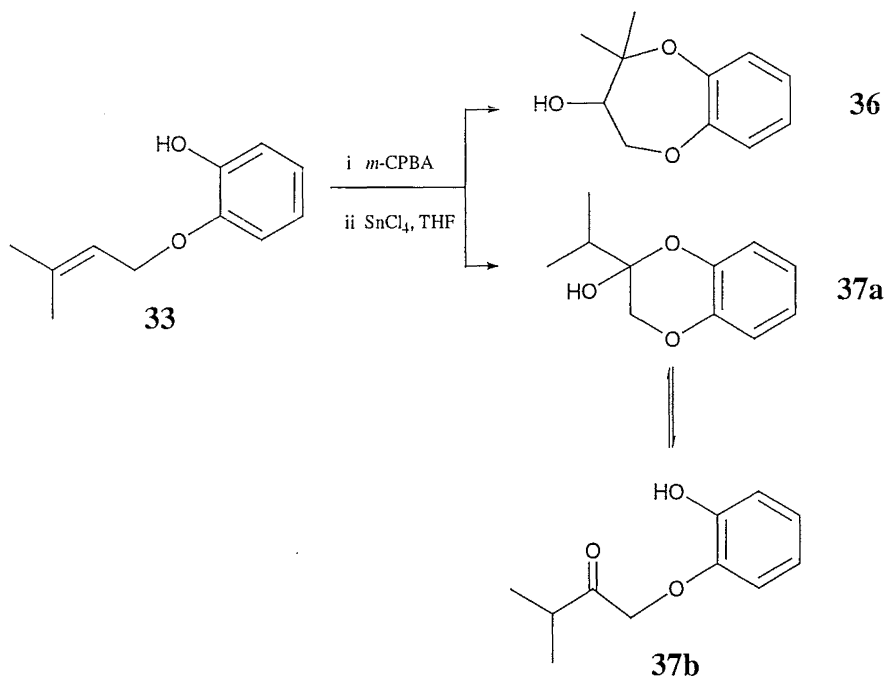


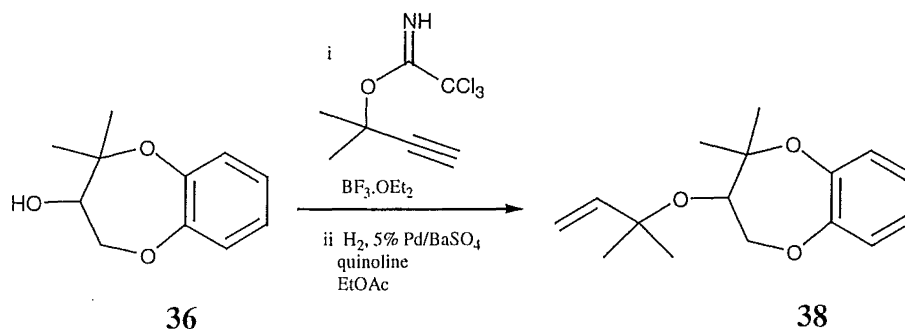
Figure 2.15 ^1H NMR spectrum of **35** (in CDCl_3)

Synthesis of **36** and **38**

The model compound **38**, corresponding to the isoprenoid fragment in the revised structure of 9-methoxystrobilurin K (**16**), was synthesised as shown below. Dioxepin **36** was prepared by slight modification of the procedure reported by Williams *et al.*⁴⁷ Epoxidation of ether **33** gave the substrate for an intramolecular epoxide opening, which upon treatment with SnCl_4 gave the desired dioxepin **36** and a major side product. This side product was assigned as the six-membered ring hemiacetal **37a** in equilibrium with the ketone **37b**. It presumably arises via a 1,2-hydride migration process.



Subsequent reaction of the dioxepin alcohol **36** with the trichloroacetimidate derivative⁵² of 2-methylbut-3-yn-2-ol gave an alkyne that, upon partial reduction to the alkene, yielded compound **38**. The trichloroacetimidate approach was investigated primarily because of indications that it would be a suitable method for generating tertiary alkylating agents under mild conditions.^{53,54}



Compound **38** corresponds to the isoprene fragment of the revised structure of 9-methoxystrobilurin K (**16**). The ¹H and ¹³C NMR data for **38** (in CDCl₃ and CD₃OD) were consistent with those for 9-methoxystrobilurin K (in CDCl₃, ¹H NMR spectrum - **Fig. 2.12**) and 9-methoxystrobilurin L (in CD₃OD). Comparison of the ¹H and ¹³C NMR data is detailed in **Fig. 2.17**. The ¹H NMR spectrum of compound **38** is shown in **Fig. 2.18**. The crucial HMBC correlation (from H18 to C22) in the structural elucidation of 9-methoxystrobilurin K as **16** was observed for compound **38**. The NOE between the protons of the two methyls at δ 1.32 and an aromatic proton (H1) of **38** was also observed, as in the natural product (**Fig. 2.16**). The synthesis of model compounds **35** and **38** supports the structural revision of 9-methoxystrobilurin K to **16**.

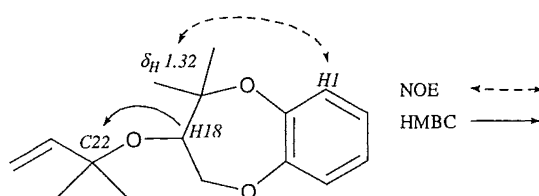


Figure 2.16 HMBC correlation and NOE for **38**

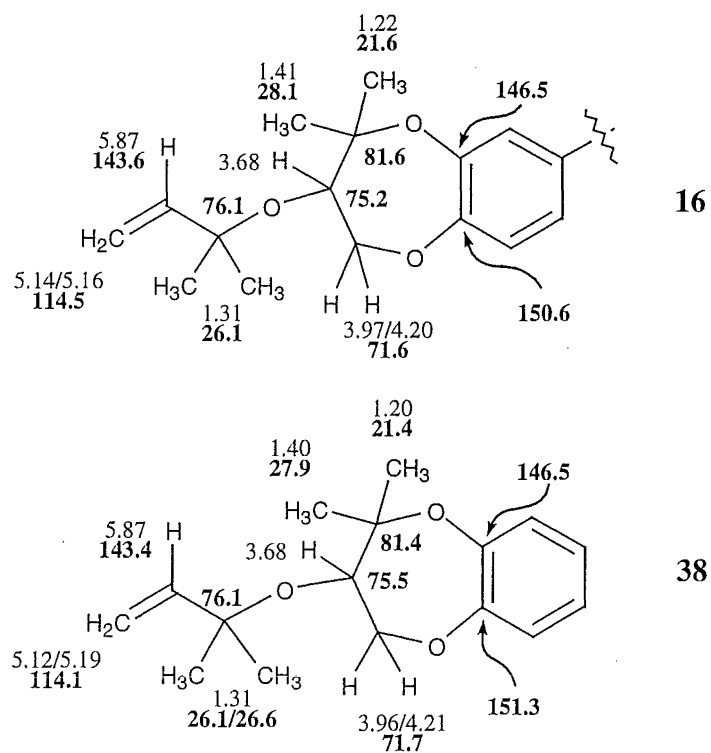


Figure 2.17 NMR data for 9-methoxystrobilurin K (**16**) and compound **38**

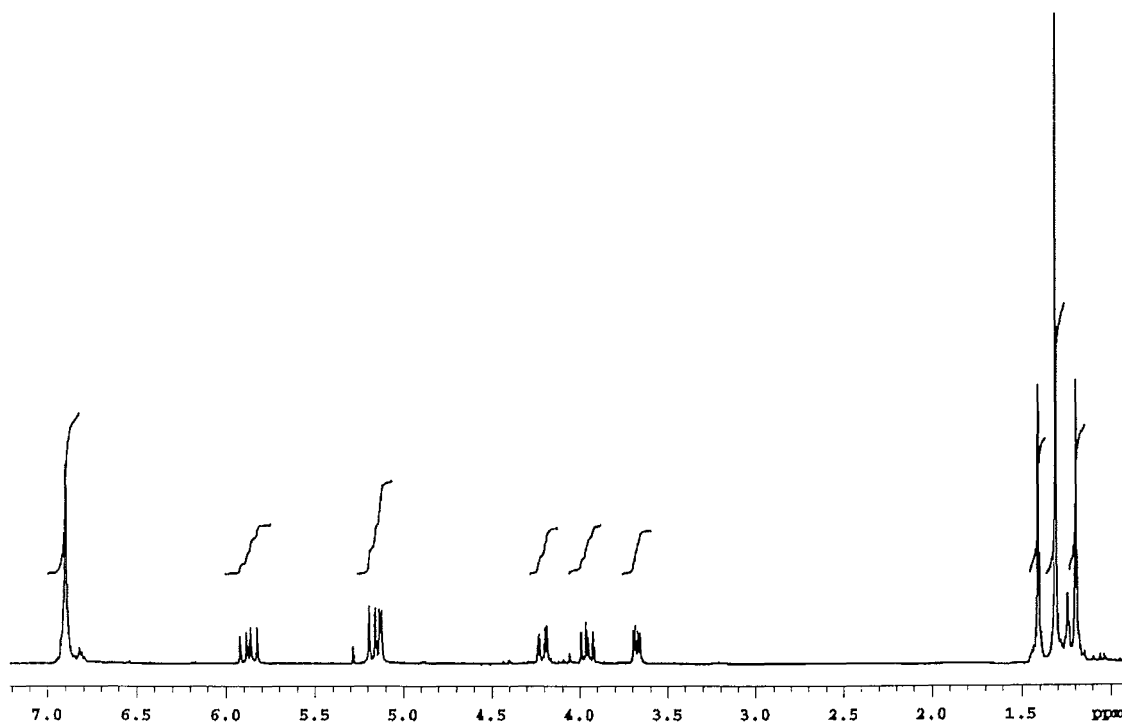


Figure 2.18 ^1H NMR spectrum of **38** (in CDCl_3)

Synthesis of compounds 39 and 40

The model compound **39**, which corresponds to strobilurin D (**18**)³² and hydroxystrobilurin D (**19**),³³ was synthesised as shown below. Reaction of the previously prepared diether **34** with 1.0 equivalent of *m*-CPBA yielded the epoxide **39**. Strobilurin D (**18**) and hydroxystrobilurin D (**19**) had also been assigned as containing the epoxyprenyl structure, as later assigned to 9-methoxystrobilurin K (**17**). The same significant differences in the chemical shifts of the epoxide carbons (**Fig. 2.19**) were observed (¹H NMR spectrum – **Fig. 2.20**). This suggested that the epoxyprenyl structures assigned to strobilurin D (**18**)³² and hydroxystrobilurin D (**19**)³³ were also incorrect.

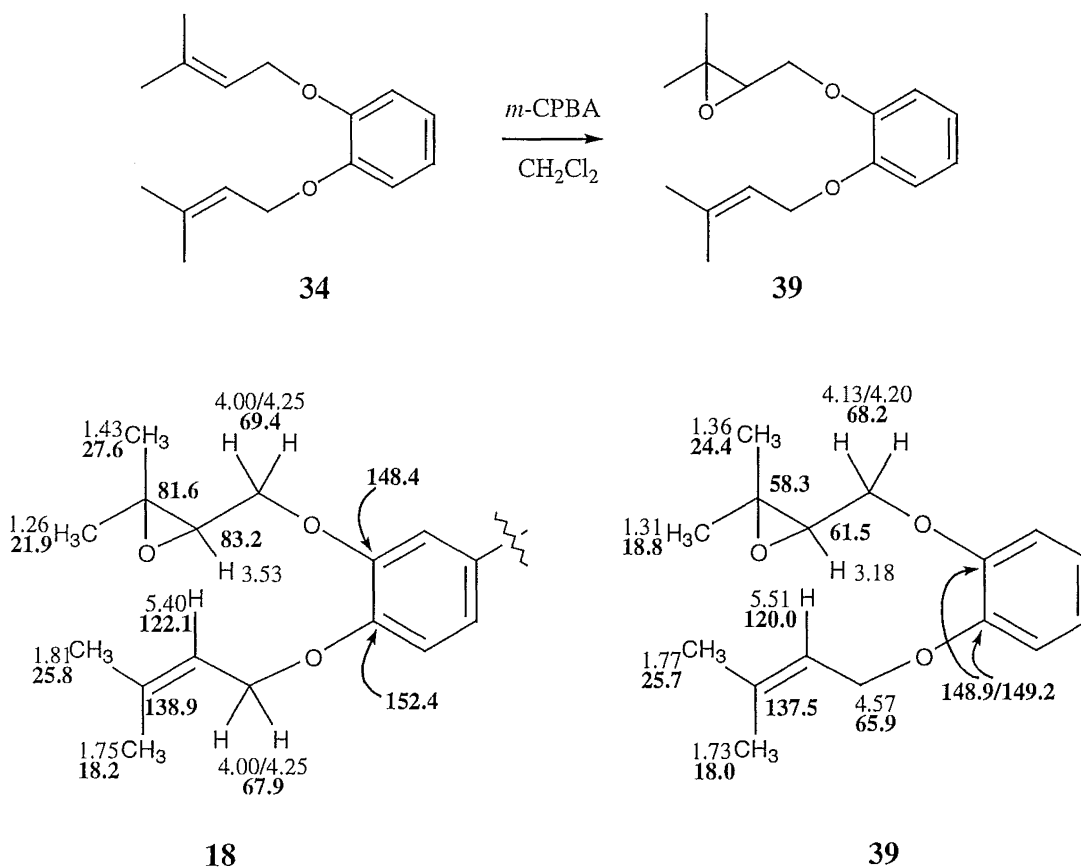


Figure 2.19 NMR data for strobilurin D (**18**) and compound **39**

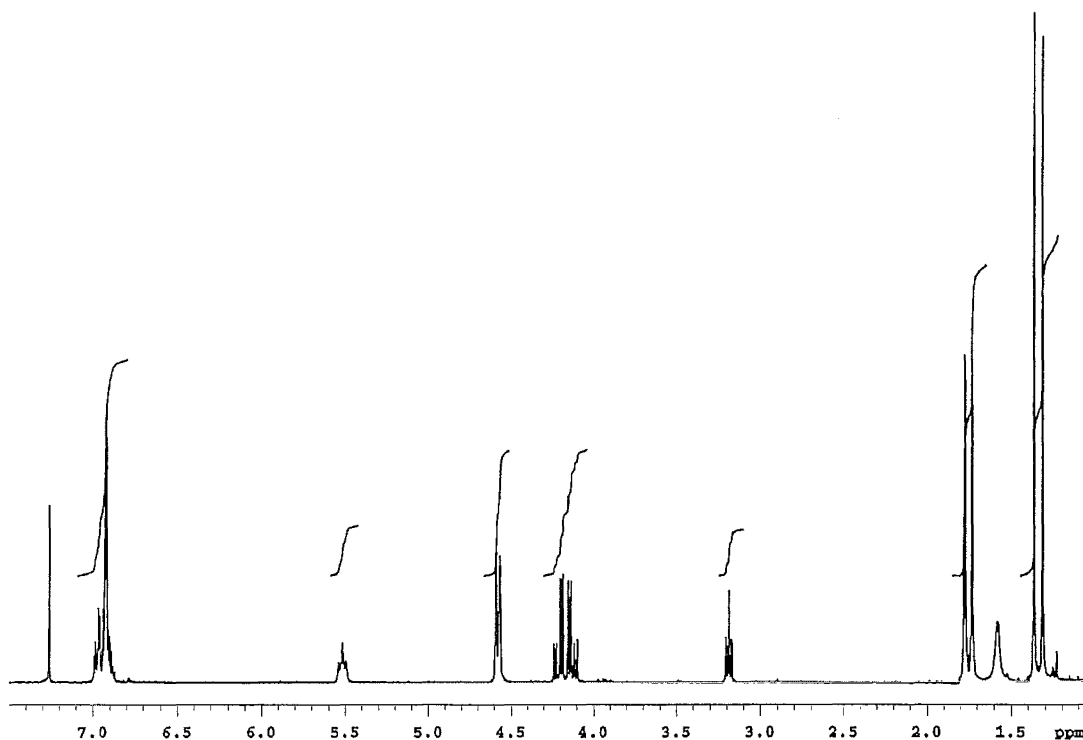
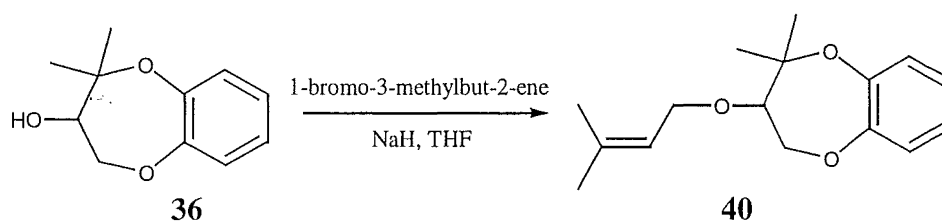


Figure 2.20 ^1H NMR spectrum of compound **39** (in CDCl_3)

Finally, the model compound **40**, corresponding to the prenyl substituted 1,5-dioxepin fragment of strobilurin G (**23**), was synthesised as shown below. Alkylation of **36** with 1-bromo-3-methylbut-2-ene yielded compound **40**.



All NMR data (in CDCl_3) for **40** were consistent with the appropriate fragment in strobilurin G (**23**) (in CDCl_3) (**Fig. 2.21**).⁴⁸ The ^1H NMR spectrum of compound **40** is shown in **Fig. 2.22**.

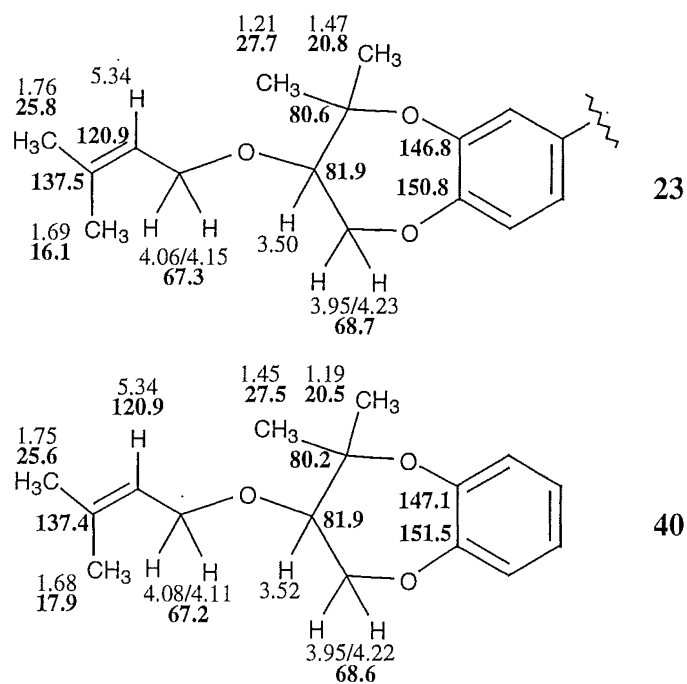


Figure 2.21 NMR chemical shift data for strobilurin G (23) and compound 40

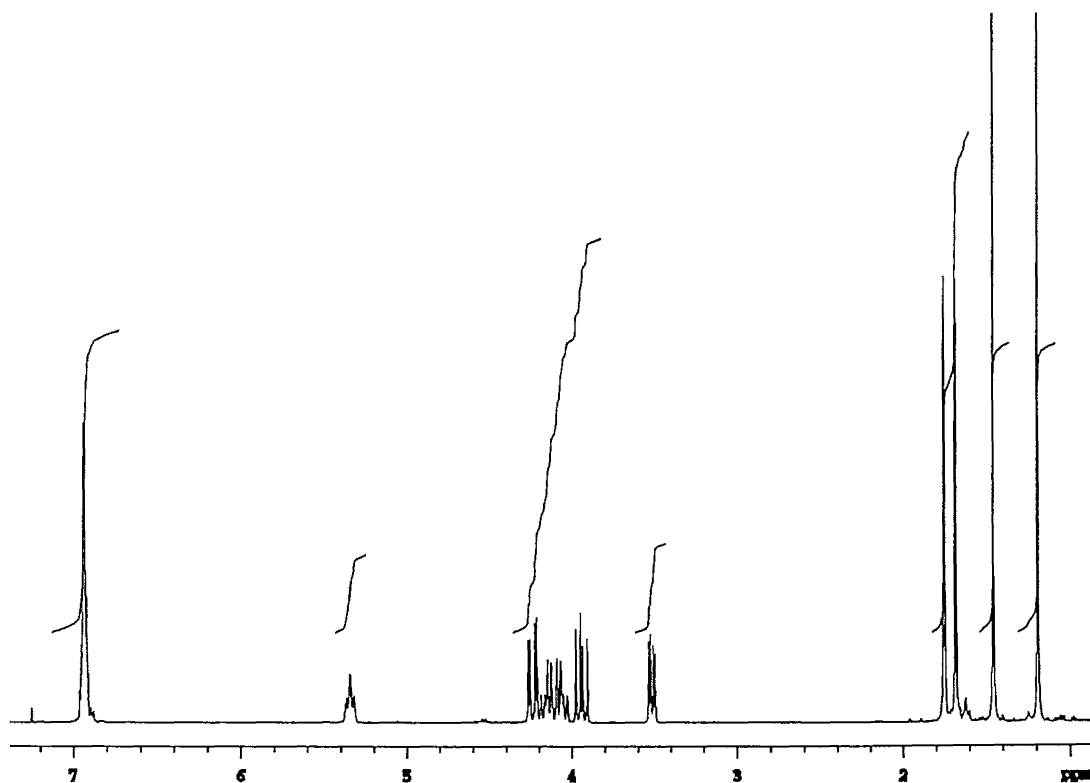
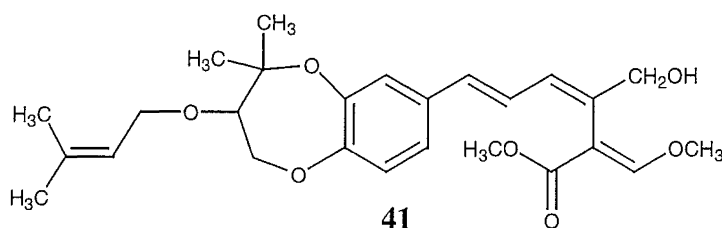


Figure 2.22 ^1H NMR spectrum of compound 40 (in CDCl_3)

The ^1H and ^{13}C NMR data (in CDCl_3 or CD_3OD) associated with the 1,5-benzodioxepin ring for compound **40** were also consistent with the appropriate fragment in both strobilurin D (**18**) (in CD_3OD)³² and hydroxystrobilurin D (**19**) (in CDCl_3).³³ However, chemical shifts reported for C23 in **19** and C24 in both **18** and **19** were inconsistent with compound **40** and strobilurin G (**23**). Due to the close correlation of the remainder of the ^1H and ^{13}C data, it is possible C24 was originally misassigned with C10 in **18** and **19**, and C23 with C8 in **19**. Such a reinterpretation is more consistent with the NMR data obtained from the series of synthesised model compounds **33**, **34**, **39** and **40**, which all contain this prenyl unit, and with the chemical shift data for other strobilurins, even though hydroxystrobilurin D (**19**) has a different substituent at C10. Therefore, this would suggest that strobilurin D and hydroxystrobilurin D should be revised as 1,5-benzodioxepin structures (e.g. **23** (previously reported as strobilurin G) and **41**, respectively).



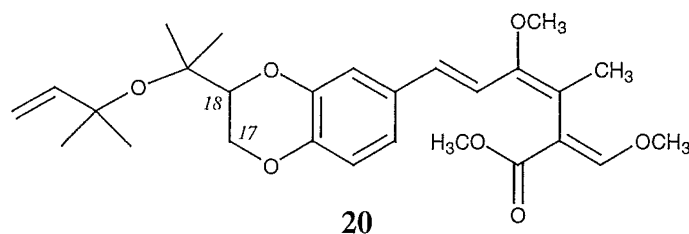
Biological activity of model compounds 33-40

Biological testing of 9-methoxystrobilurin K (**16**) showed it to be significantly cytotoxic (IC_{50} 0.5 ng/mL) against the P388 cell line and antifungal at 10 $\mu\text{g}/\text{disk}$ against *Candida albicans* (10 mm), *Trichophyton mentagrophytes* (5 mm), and *Cladosporium resinae* (5 mm), in a zone of inhibition assay. No antibacterial activity was observed, which is consistent with other strobilurins. The model compounds **33-40** were tested against the P388 cell line and in the antimicrobial assays. Mild cytotoxicity was observed for compound **35** (IC_{50} 37 $\mu\text{g}/\text{mL}$), **38** (IC_{50} 34 $\mu\text{g}/\text{mL}$), **39** (IC_{50} 34 $\mu\text{g}/\text{mL}$) and **40** (IC_{50} 24 $\mu\text{g}/\text{mL}$), while compound **36** showed mild antifungal activity at 0.3 mg/disk against *Candida albicans* (3mm) and *Trichophyton mentagrophytes* (10 mm).

2.4.3 Conclusions

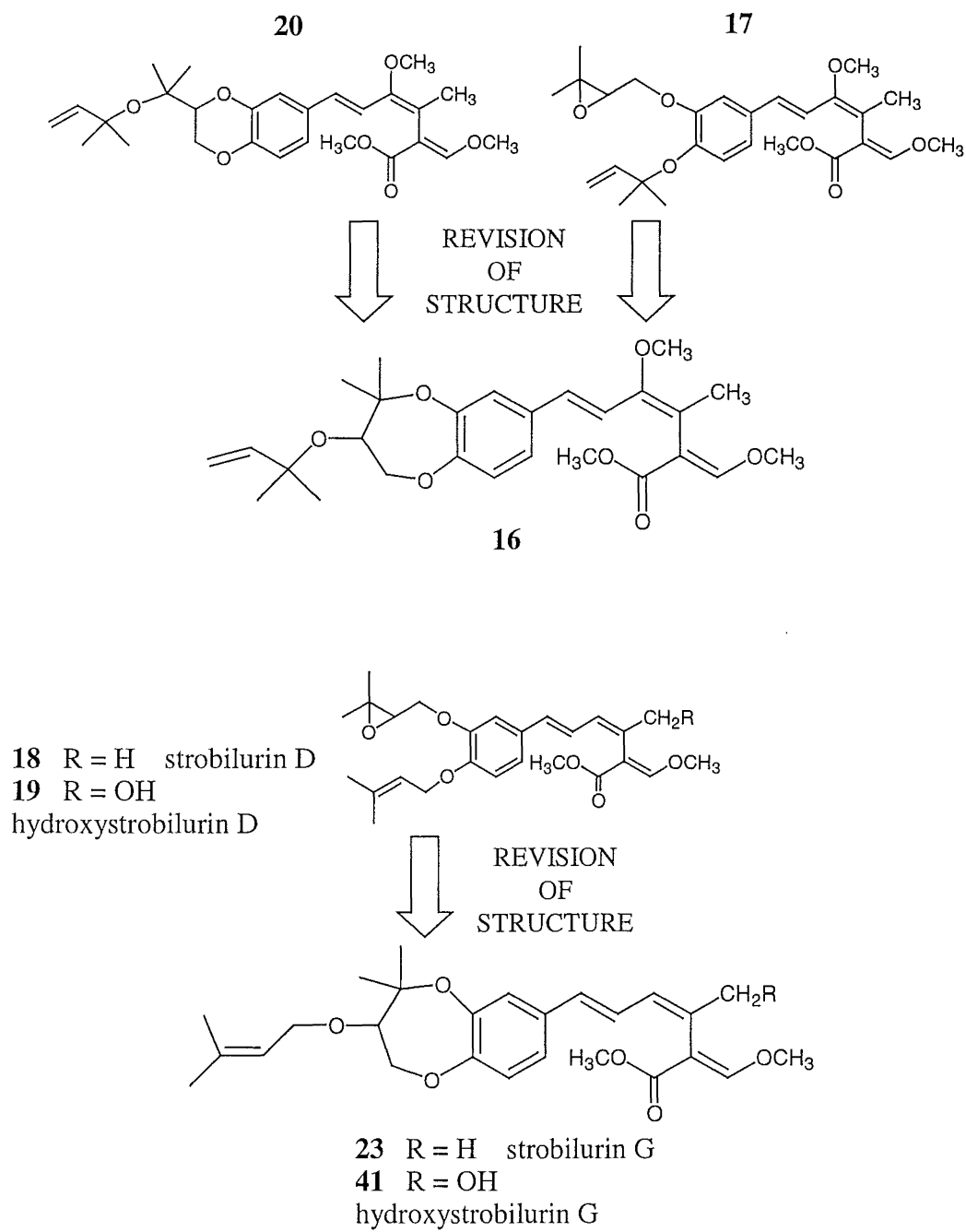
9-Methoxystrobilurin L (20)

The ^1H and ^{13}C NMR data (in CD_3OD) published for 9-methoxystrobilurin L (20) are indistinguishable from those obtained for 9-methoxystrobilurin K (16).³⁴ Moreover, the dioxan proposed for 9-methoxystrobilurin L (20) does not contain the ether linkage between C18 and C22, and so is not consistent with the HMBC correlation observed between H18 and C22 in this present work. In addition, during the structure determination of strobilurin G (23)⁴⁸ several model compounds were prepared including one consisting of a dioxan ring with a dimethylcarbinol side chain, as is found in 9-methoxystrobilurin L (20). The ^1H and ^{13}C NMR data (in CD_3OD) for this dioxan model compound were compared with those assigned to 9-methoxystrobilurin L (20). Significant differences were observed in chemical shifts for C17 and C18 ($\Delta\delta_{\text{C}}$ 7.3 and 2.3 respectively) suggesting the dioxan structure was incorrect.



9-Methoxystrobilurin K, strobilurin D and G and hydroxystrobilurin D

On the basis of this information, especially the significant HMBC correlation and the chemical shift data obtained from the synthetic model compounds 35-40, the structures of both 9-methoxystrobilurin K (17) and 9-methoxystrobilurin L (20) have been revised to 16 (Fig. 2.23). Furthermore, based on the synthetic model compounds 39 and 40, the structure for strobilurin D (18) should be revised to the dioxepin structure 23 (previously assigned as strobilurin G) and that of hydroxystrobilurin D (19) to 41 (Fig. 2.23).⁵⁵

Figure 2.23 Structure revision

2.5 Culturing of *F. calocera*

2.5.1 Introduction

The strobilurin natural products have usually been isolated from the liquid culture of the organism being investigated. From the original investigation of *F. calocera*, it was known that the organism produced components in culture that exhibited biological activity consistent with the extract of the fruiting bodies.⁵⁶ To determine if 9-methoxystrobilurin K (**16**) was the component responsible for the observed biological activity, a series of liquid cultures were grown.

2.5.2 General techniques and procedures

All culturing work was done in a laminar flow cabinet using standard aseptic techniques. Solid phase cultures of *F. calocera* were grown on Potato Dextrose Agar (PDA) plates. The agar was made up to one-fifth the normal strength (5 g/L) with distilled H₂O, autoclaved, cooled, then poured into sterile petrie dishes that were allowed to set and then stored at -4 °C until required.

2.5.3 Culturing of *F. calocera*

The original culture of *F. calocera* was obtained from Dr Anthony Cole (Department of Plant and Microbial Sciences, University of Canterbury). A plug from the outer regions of an old plate was placed upside down on a fresh plate. These plates were incubated for 2 weeks at 25 °C, and then left at room temperature. Subcultures were taken approximately every six weeks. Liquid broth cultures of *F. calocera* were grown using Potato Dextrose Broth (PDB), also at one-fifth the normal strength (5 g/L). Distilled H₂O (2 L) was added to PDB powder (10 g) and allowed to stir until all the material

had dissolved. PDB (approx. 150 mL) was poured into Fernback flasks (3 x 300 mL), autoclaved, cooled, then inoculated with 40-50 plugs of *F. calocera* grown on PDA plates. These cultures were incubated for 21 days at 25°C. The broth was combined and filtered through a bed of Celite to remove the mycelial mat. Five batches were grown up in this way, with each chromatographed separately.

Initial chromatography of the liquid broth of *F. calocera*

Each of the combined liquid cultures was chromatographed by reverse-phase (C18) column chromatography, eluting with a stepped gradient from H₂O through to MeOH and then 1:1 MeOH/CH₂Cl₂. Seven fractions were collected for each of the batches. Only the fractions that eluted in MeOH showed significant cytotoxicity (IC₅₀ 18.5 ng/mL) against the P388 cell line. The five active fractions from the five batches were analysed by analytical reverse-phase (C18) HPLC and by ¹H NMR spectroscopy. A number of peaks in the chromatograph had UV spectra consistent with those of a strobilurin skeleton. Characteristic signals in the ¹H NMR were also visible, including a cluster of methoxy signals (δ_{H} 3.6-3.8).

Chromatography of all biologically active fractions from the five batches

At this point, the total mass of active material was 51.0 mg. This sample was chromatographed by normal-phase (DIOL) column chromatography, with a stepped gradient from petroleum ether through CH₂Cl₂, EtOAc and a final MeOH strip. Analysis of all the combined fractions from this column by both analytical reverse-phase (C18) HPLC and ¹H NMR spectroscopy revealed that each sample contained a number of components. The biological assay results for each of these samples revealed a spread of antifungal activity, while the cytotoxicity against the P388 cell line was centred on one sample. Only the combined sample GN2-23.7-8 (1.3 mg, IC₅₀ 10 ng/mL) showed significant cytotoxicity, while fractions from GN2-23.5 through to 23.15 showed significant antifungal (but no antibacterial) activity at 2 µg/disk.

Biologically active components of *F. calocera* grown in liquid culture

The ^1H NMR spectrum (Fig. 2.24) of sample GN2-23.7-8 showed it to be a mixture. However, the characteristic signals for 9-methoxystrobilurin K (**16**) (^1H NMR spectrum Fig. 2.25) were visible. These signals included olefinic protons between δ_{H} 6.4-7.0, the vinyl protons at δ_{H} 5.14-5.16 and the adjacent methine at δ_{H} 5.87. The HPLC chromatograph of sample GN2-23.7-8 contained a number of peaks that had UV spectra consistent with that of the strobilurin skeleton, and one peak at a retention time consistent with that of 9-methoxystrobilurin K (**16**). The mixture was too complex to assign the other peaks as belonging to specific strobilurins, and with a mass of just 0.5 mg, so further purification was not undertaken.

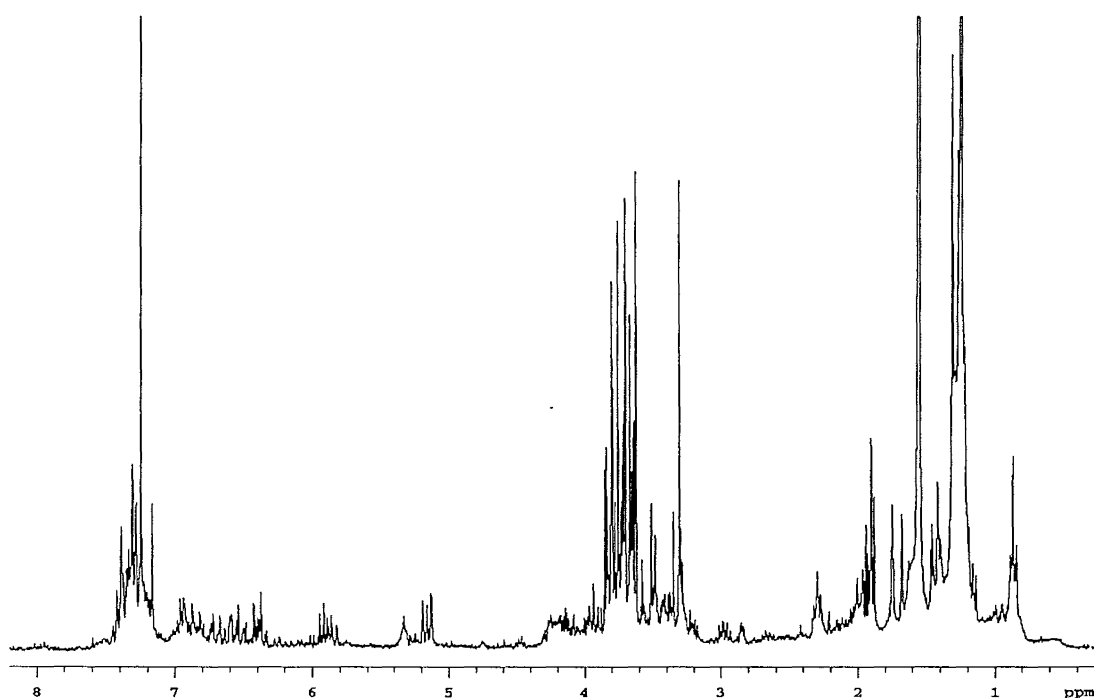


Figure 2.24 ^1H NMR spectrum of sample GN2-23.7-8 (in CDCl_3)

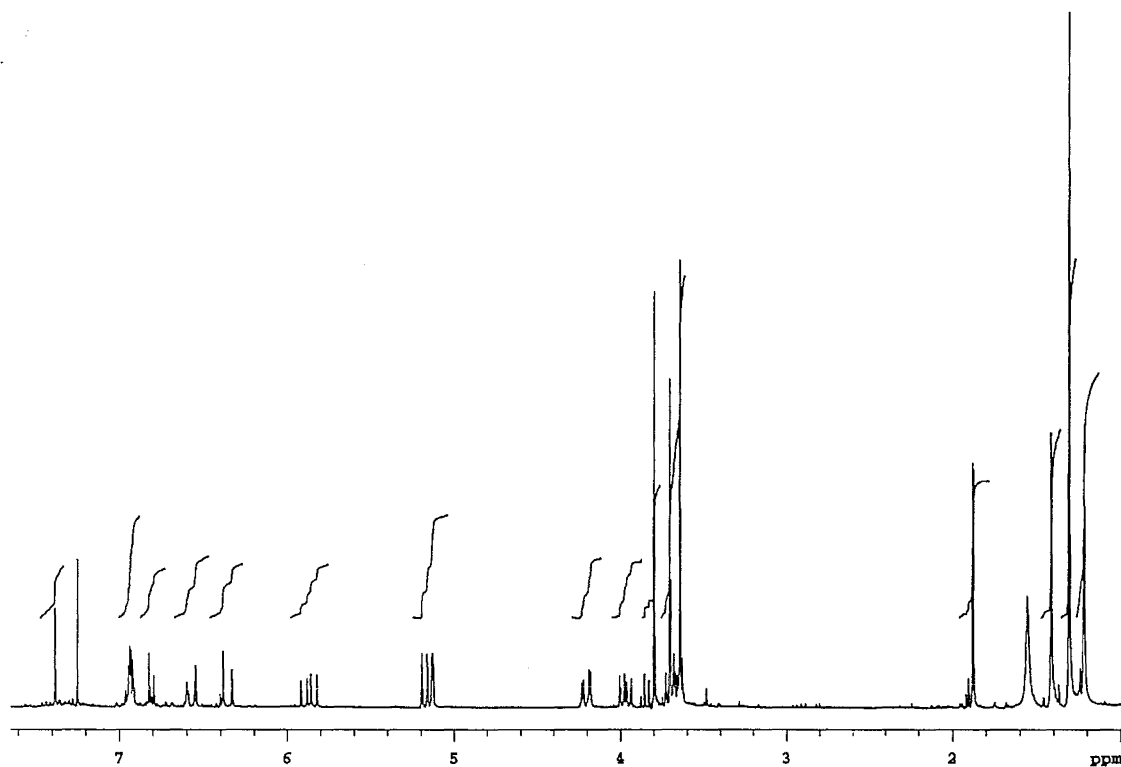


Figure 2.24 ^1H NMR spectrum of **16** (in CDCl_3)

The ^1H NMR spectra of the surrounding fractions also showed the characteristic methoxy and methyl signals of the strobilurin class of compounds. The mixtures were again very complex, and the lack of material hindered further purification, and therefore identification of the specific strobilurins in the liquid broth of *F. calocera*. The lack of large scale culturing facilities hindered the advancement of this area of research.

CHAPTER THREE

COLLECTION, EXTRACTION AND SCREENING PROGRAMME

3.1 Introduction

One of the primary aims of this research was to collect a large number of New Zealand fungi, carry out a small-scale extraction on each specimen and screen these extracts for biological activity. Interest in this area of research developed from a screening programme initiated by Dr Anthony Cole, Department of Plant and Microbial Sciences, University of Canterbury. In this programme, a number of fungi with pigmented fruiting bodies were collected and extracted. These extracts were tested for antifungal activity against a sensitive test fungus.⁵⁶ An extract obtained from *Favolaschia calocera* fruiting bodies that showed significant antifungal activity in their assay was also submitted for the full range of in-house assays in the Department of Chemistry, University of Canterbury. In these assays, this extract showed both significant

antifungal activity and cytotoxicity against the P388 cell line. Extracts of this fungus were then investigated during research toward a Masters degree and were then studied further during research towards this PhD (see **Chapter Two**).²⁹

3.2 Collections and Extractions

Collection trips were conducted in beech forests in the Craigieburn/Arthur's Pass area (Canterbury), in the Catlins Forest Park (Southland) and around Hunua Falls (Auckland). Each sample was given a specific code to denote the year, site of collection and a specimen number for that collection. Aqueous and organic (3:1 MeOH/CH₂Cl₂) extracts were made from small samples (2 g) of each specimen. These extracts were submitted for the in-house assays in the Department of Chemistry, University of Canterbury. These assays included testing for cytotoxicity against the P388 cell line, antiviral activity against *Herpes simplex* and *Polio* viruses and antimicrobial activity against a selection of bacteria and fungi (zone of inhibition assays) (see **Section 7.1.7, Chapter Seven**).

A large collection of Australian fungi, held by Dr Melvyn Gill (University of Melbourne, Melbourne) were extracted during a visit to Australia. These extracts were brought back to New Zealand and submitted for the in-house assays in the Department of Chemistry, University of Canterbury.

An aliquot of each extract that showed biological activity was removed and the solvent evaporated to determine the concentration of those active extracts. Many of the extracts that were originally thought to be cytotoxic were relatively concentrated. Once an IC₅₀ value was calculated, the cytotoxicity was found not to be significant.

3.3 Biological Assays⁵⁷

Antimicrobial Assay

Antimicrobial activity was detected using a zone of inhibition assay with activity expressed in millimetres (mass/disk). The organisms tested against were *Escherichia coli* (ATCC 25922), *Bacillus subtilis* (ATCC 19659), *Pseudomonas aeruginosa* (ATCC 27853), *Candida albicans* (ATCC 14053), *Trichophyton mentagrophytes* (ATCC 28185), and *Cladosporium resinae* (*Clf avellaneum* PAMS Dept. University of Canterbury). Antibiotic controls were run with each batch: Gentamycin (10 µg/disk) was used from *E. coli* and *P. aeruginosa*; Chloramphenicol (30 mg/disk) was used for *B. subtilis*; Nystatin (100 units/disk) was used for *C. albicans*, *C. resinae* and *T. mentagrophytes*. Suitable solvent controls were also used in every assay run.

Antitumour Assay (P388)

The P388 murine leukaemia cell line (ATCC CCL 46, P388D₁) was used to assay for cytotoxicity, with activities expressed as an IC₅₀. MTT tetrazolium (a yellow colour) is reduced to MTT formazan (a purple colour) by healthy cells so this can be used to determine the concentration of a sample required to reduce the P388 cell growth by 50%. Media, solvent, cell and positive controls were included with each assay run.

Antiviral Assay

Two viruses were used to detect antiviral activity. *Herpes simplex* virus type 1 (Strain F, ATCC VR 733) is a non-enveloped virus with a single standard RNA genome and a site of replication in the host cytoplasm. *Polio* virus type 1 (Pfiser Vaccine Strain (Sabin)) is an enveloped virus with a double standard DNA genome and a site of replication in the host nucleus. The cell line used as the host for these viruses is the African Green Monkey (*Cercopithecus aethiops*) kidney cell line (BSC-1, ATCC CCL 26). A well of the host cells infected with one of the two viruses is incubated with a

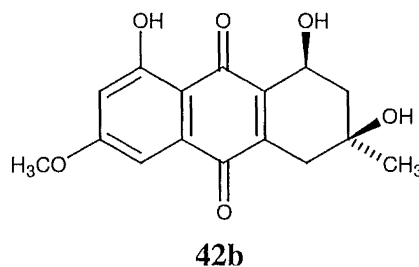
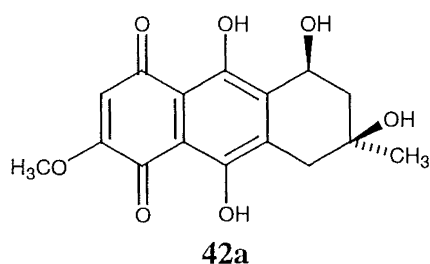
disk containing the sample being tested. The host cells are then examined for the presence of the virus and also if the sample being tested exhibited any cytotoxicity against the cell line.

3.4 Results

3.4.1 General observations

Collections undertaken in the forests in the Craigieburn and Arthur's Pass area were the largest carried out. Unfortunately, these collections showed the lowest proportion of biologically active extracts. From the New Zealand collections, the most fruitful were those conducted in the beech forests in the Catlins Forest Park, Southland. Those collections gave the highest proportion of biologically active extracts. However, even the collections from the Catlins did not compare well with the high proportion of biologically active extracts obtained from the Australian collection.

Most of Dr Melvyn Gill's Australian collection was originally assembled because the fruiting bodies were pigmented. Many of these specimens in this collection have since been chemically investigated in order to isolate and identify their pigments. These pigments do account for the biological activity observed in the extracts. The red mushroom *Dermocybe splendida* is one such example. This mushroom contains the antibacterial and antifungal tetrahydroanthraquinone pigments austrocortirubin (**42a**) and austrocortilutein (**42b**).¹⁶



3.4.2 Tables of Results

Table 3.1. The biological activity of significantly active extracts of fungi collected in Craigieburn, Arthur's Pass and Auckland, New Zealand

Sample No.	P388 IC ₅₀ ng/mL	Antimicrobial mm inhibition	Species, comments and known chemistry
95BRS1-11		5Cr	?
96CC1-1		5Tm	<i>Entoloma hochstetteri</i>
95CV1-16		5Tm	?
95CV1-38A	11302		<i>Hypholoma</i> , sulphur tuft, dipyrones
95CV1-59A	10865		<i>Dermocybe carnaria</i> , anthraquinones ¹⁶
95DF1-3		6Pa	<i>Cortinarius</i> species
95DR1-1	2668		<i>Pycnoporus</i> sp., orange bracket phenoxazin-3-ones ¹⁶
96HF1-6	<48.7		<i>Favolaschia pustulosa</i>
96HF1-6A	<68.2		strobilurins ³⁴
95LS1-20A	7046		?

BRS Broken River Skifield Road (Canterbury)

CC Charming Creek Walkway (Westland)

DF Dracophyllum Flats Walkway (Craigieburn, Canterbury)

CV Craigieburn Visitors Centre (Canterbury)

DR Dingle Dell Reserve (Auckland)

HF Hunua Falls (Auckland)

LS Lydon Saddle Walkway (Craigieburn, Canterbury)

A = Aqueous extract

Tm = *Trichophyton mentagrophytes*

Cr = *Cladosporium resinae*

Pa = *Pseudomonas aeruginosa*

Table 3.2. The biological activity of significantly active extracts of fungi collected in Catlins, New Zealand

Sample code	P388 IC ₅₀ ng/mL	Antimicrobial mm of inhibition (mg/disk)	Species
95CA1-6A	3219		
95CA1-12	1463		<i>Myxaciium</i> sp.
95CA1-18	2577		<i>Cortinarius</i> (MG138)
95CA1-20A		E4 Ca3 Cr6 (360)	<i>Tricholomopsis rutilans</i>
95CA1-26	1948	E8 B8 Ca10 Tm10 Cr22 (190)	<i>Cortinarius</i> sp.
95CA1-26A	144	E10 B10 Ca10 Tm12 Cr20 (5)	
95CA1-29	9180	B5 Ca10 Tm5 Cr15 (300)	
95CA1-29A	429	E10 Ca15 Tm12 Cr22 (60)	

CA Catlins Forest Park A = Aqueous extract

B = *Bacillus subtilis*

Ca = *Candida albicans*

Tm = *Tricophyton mentagrophytes*

E = *Escherichia coli*

Cr = *Cladosporium resinae*

Pa = *Pseudomonas aeruginosa*

Table 3.3. The biological activity of significantly antiviral and cytotoxic extracts of fungi collected in Australia

Sample code	P388 IC ₅₀ ng/mL	Antiviral mm inhibition		Species, comments and known chemistry ¹¹⁹
		HSV	PV	
95MG1-48		4/cyt1	4/cyt1	no chemistry
95MG1-69		4/cyt1	3/cyt1	<i>Cortinarius abnormis?</i> styrylpyrones
95MG1-100	3456	3/cyt1	-	flavomannin 6,6'-methyl ether
95MG1-101		4/cyt1	4/cyt1	no chemistry
95MG1-101A		4/cyt1	4/cyt1	no chemistry
95MG1-125		4/cyt1	4/cyt1	no chemistry
95MG1-220'		4/cyt1	4/cyt1	Old <i>Dermocybe violaceous</i> no chemistry

MG Melvyn Gill, University of Melbourne, Australia

A = Aqueous extract

HSV = *Herpes Simplex Virus*

PV = *Polio Virus*

cyt = cytotoxicity

Table 3.4. The biological activity of significantly antimicrobial and cytotoxic extracts from fungi collected in Australia

Sample code	P388 IC ₅₀ (ng/mL)	Antimicrobial (mm of inhibition)	Species, comments and known chemistry ¹¹⁹
95MG1-2 95MG1-2A	8274	B8 Ca1 Tm10 Cr12 B8 Ca10 Tm10 Cr12	<i>Boetus</i> sp. purple capskin no chemistry
95MG1-29 95MG1-29A		B8 Ca10 Tm12 Cr10 B8 Ca10 Tm13 Cr13	<i>D. splendida</i> tetrahydroanthraquinones & gentiobiosides
95MG1-74 95MG1-74A	6780	B9 Ca15 Tm15 Cr22 B8 Ca8 Tm9 Cr15	MG33? torosachrysone & austrocortilutein
95MG1-80 95MG1-80A	8928	E10 Ca15 Tm13 Cr22 E8 Ca12 Tm11 Cr15	austrocortilutein & austrocortirubin
95MG1-82A		E3 Bs3 Pa5 Cr1	no chemistry
95MG1-109	4374		austrocortilutein & torachrysone
95MG1-112 95MG1-112A	2835 2001		no chemistry
95MG1-138	2912		xanthorin & hydroxyxanthorin ethers
95MG1-222	4752		<i>Cortinarius rotundisporus</i> no chemistry
95MG1-240A	1955		<i>Rozites tricolor</i> no chemistry
95MG1-244 95MG1-244A	7842 209		<i>Boletus</i> sp. no chemistry <i>Boletus</i> sp. no chemistry
95MG1-252	2012		<i>Pycoporus</i> sp. - orange bracket phenoxazin-3-ones

MG Melvyn Gill, University of Melbourne, Australia

A = Aqueous extract

B = *Bacillus subtilis*

Ca = *Candida albicans*

Tm = *Tricophyton mentagrophytes*

E = *Escherichia coli*

Cr = *Cladosporium resinae*

Pa = *Pseudomonas aeruginosa*

3.4.3 Specimens targeted for further investigation

In total, one hundred and sixty specimens from New Zealand and one hundred and thirty specimens from Australia were screened. Three species were targeted for further investigation during research towards this PhD.

The bright blue mushroom *Entoloma hochstetteri* gave a MeOH extract that exhibited mild antifungal activity. The blue pigmentation of the fruiting bodies increased the degree of interest in this mushroom. No chemical examination of this mushroom for either the pigments or biologically active component(s) was found in the literature. The extraction and investigation of the pigments and biologically active component(s) of *E. hochstetteri* is described in **Chapter Four**.

A New Zealand species of *Cortinarius* was collected in the Catlins Forest Park, Southland. Extracts of this species exhibited significant antimicrobial activity and cytotoxicity against the P388 cell line (IC₅₀ 1948 ng/mL (organic) and 144 ng/mL (aqueous)). It is also a relatively large species and recollection of a reasonable amount meant that isolation of the biologically active component(s) was feasible. The extraction, isolation and structural elucidation of the biologically active components of this *Cortinarius* species is described in **Chapter Five**.

Of the Australian specimens that exhibited biological activity, *Cortinarius rotundisporus* was chosen for further study as no chemistry on this species had been reported and an ample supply was available. The organic extract of *C. rotundisporus* exhibited cytotoxicity against the P388 cell line, with an IC₅₀ value of 4752 ng/mL. The extraction, isolation and structural elucidation of the biologically active components of *C. rotundisporus* is described in **Chapter Six**.

3.5 Discussion

Almost three hundred fungal specimens were screened for biological activity during the course of this programme. In total, forty-four extracts from thirty-four specimens exhibited significant biological activity (ten specimens showed activity in both the organic and aqueous extracts). This amounted to approximately ten percent of specimens giving biologically active extracts.

The proportion of biologically active extracts observed in this programme was only marginally lower than that obtained for screening programmes of marine organisms conducted by the Marine Group over the last ten years (Department of Chemistry, University of Canterbury). There was however, a difference in the level of biological activity found in the fungal extracts, which was lower than that found in the collections of marine organisms.⁵⁸

As can be seen from the work described in **Chapters Four – Six** both novel and biologically active compounds can be isolated from the fruiting bodies of New Zealand and Australia fungi. The future of this resource is limited by the difficulties involved in recollection of large amounts of material. A possible solution to this problem is to culture the organisms of interest. However, this can also produce problems such as whether the fungus will grow in culture, and if it does, whether it will produce the desired biologically active metabolite.

CHAPTER FOUR

ENTOLOMA HOCHSTETTERI

4.1 Introduction

4.1.1 *Entoloma hochstetteri* (Reich.)Stevenson

Entoloma hochstetteri is a bright blue mushroom found in beech forests, predominantly on the West Coast of the South Island and in the North Island of New Zealand. This species is almost certainly the same as the Japanese species *E. virescens* (Berk. & Curt.) Horak.^{59,60} Screening of a MeOH extract of *E. hochstetteri* fruiting bodies revealed mild antifungal activity. The blue pigmentation of the fruiting bodies increased the degree of interest in this mushroom. No chemical examination of this mushroom was found in the literature.

A blue-violet compound was isolated from *E. hochstetteri* and identified as an azulene derivative as described in **Section 4.4.1**. However, this compound is thought to be an artefact of the extraction and isolation process.

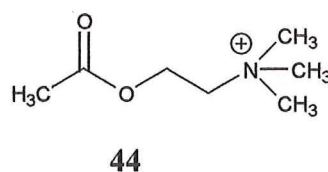
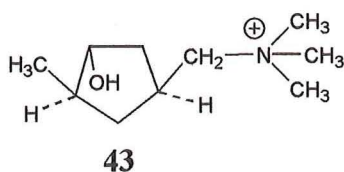


Picture 4.1 *Entoloma hochstetteri*

4.1.2 Natural products isolated from the *Entoloma* genus

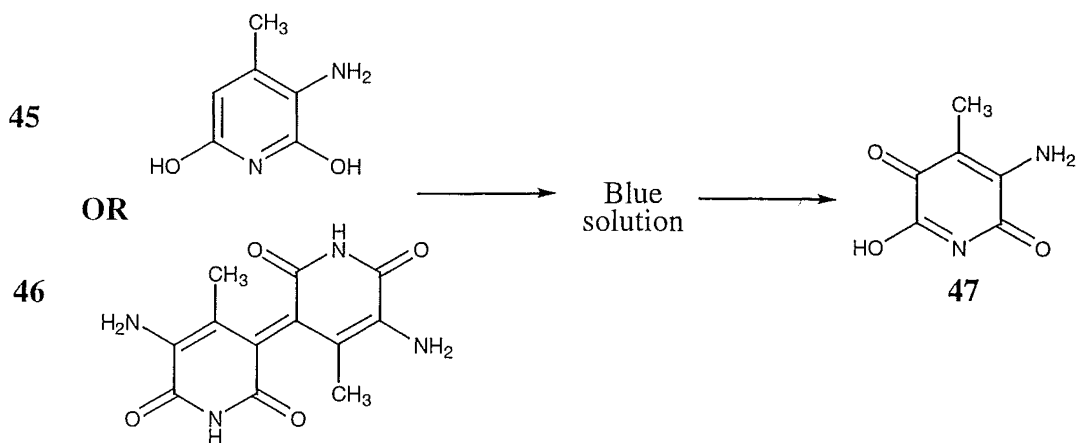
Toxic *Entoloma* species

Both *Entoloma rhodopolium* and *E. sinuatum* have been implicated in cases of poisoning. The symptoms include abdominal pains, vomiting, diarrhoea and unconsciousness. The toxic component(s) of *E. sinuatum* is(are) still unknown. Muscarine (43) has been isolated from *E. rhodopolium* and is thought to be the toxic component. *L*-(+)-Muscarine is also a minor component of *Amanita muscaria* (Fig. 1.1, Fly Agaric). The toxic properties of muscarine (43) are consistent with those observed with *E. rhodopolium* poisonings and are probably due to structural similarities of muscarine with the neurotransmitter acetylcholine (44).⁶¹



Pigments isolated from *Entoloma incanum*

Entoloma incanum is a yellow-green mushroom that turns blue-green on bruising. This colour change has been attributed to the presence of the substituted pyridine 45 or its dimer, 46. This compound readily oxidises to a blue pigment and then, after further oxidation, to the yellow compound incaflavin (47). Synthesis of 45 followed by oxidation allowed the isolation of incaflavin (47).¹⁶

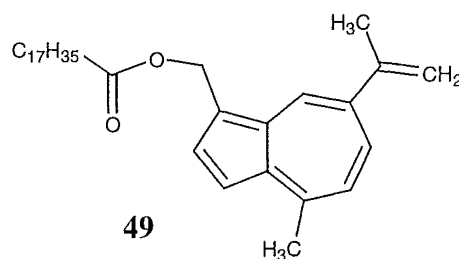
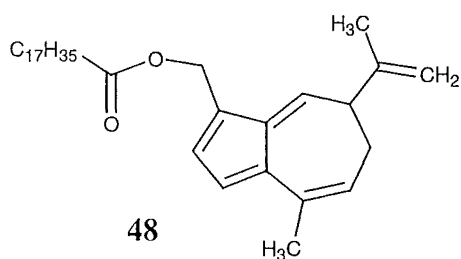


4.1.3 Guaiane pigments from *Lactarius* species

A variety of sesquiterpene pigments of the guaiane type have been isolated from a number of species in the *Lactarius* genus and are included in reviews by Gill and Steglich.^{16,17} Many species of *Lactarius* produce characteristic milky latex when the fruiting body is cut or damaged. In certain species, this latex is pigmented.

Lactarius deterrimus and *L. deliciosus*

The isolation of the orange-yellow pigment of *L. deterrimus* and *L. deliciosus* has been reported. Isolation at low temperature and under an inert atmosphere yielded the stearate ester (48) of 14-hydroxyguai-1,3,5,9,11-pentaene. Many earlier attempts to isolate the pigments of these species gave azulene derivatives that are now regarded as artefacts of *in vivo* enzymatic secondary processes, which result from damage to the fruiting body. Typically, attempted isolation under standard conditions from undamaged fruiting bodies resulted in green polymeric material.¹⁶

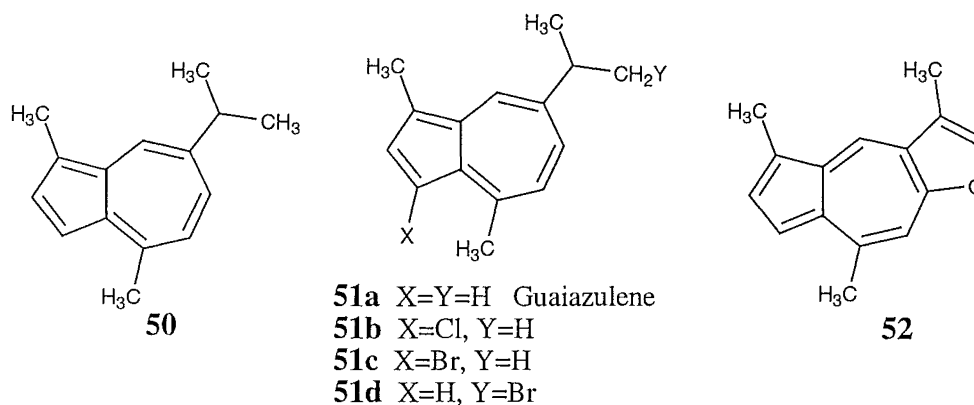


Lactarius indigo

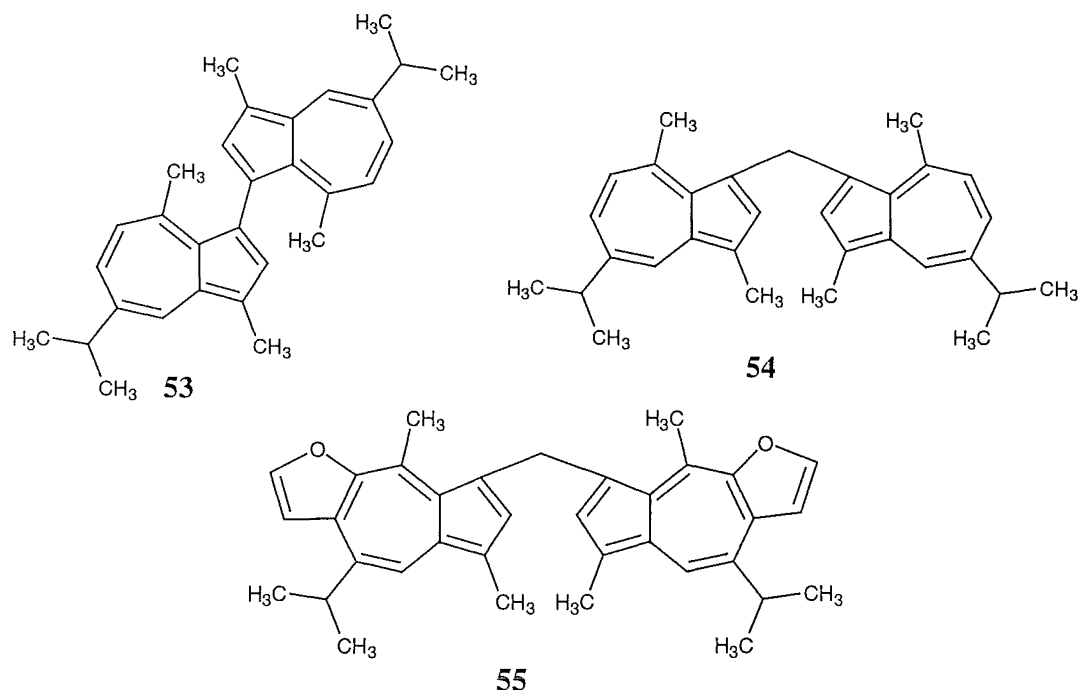
A genuine natural azulene, 1-stearoyloxymethylene-4-methyl-7-ispropenylazulene (**49**), has been reported as the pigment in the blue latex of *Lactarius indigo*. Addition of methanol to an acetone solution of the crude extract yielded green polymeric material. Isolation of the pigment was achieved using mild extraction and chromatographic techniques on silica in acetone/hexane 1:9 (using straight hexane also gave a colour change to dark green).⁶²

4.1.4 Guaiane pigments from marine sources

Sesquiterpenes possessing the guaiane skeleton have been reported from a number of purple and blue pigmented gorgonians (soft corals). These include guaiazulene (**50**),⁶³ other halogenated derivatives (**51a-d**)⁶⁴ and an azulenefuran, linderazulene (**52**).⁶⁵ These azulene derivatives were isolated under mild conditions, often at low temperature.



The bis-guaiazulenyl compound **53** was isolated from the same gorgonian as compounds **51a-d**, and was thought to be an artefact of the latter. Compounds **53** and **54** were later isolated from the gorgonian *Calicogorgia granulosa* reported as genuine natural products.⁶⁶ Gorgiabisazulene (**55**) has also been reported as a genuine natural product because it was detected by HPLC early in an extraction protocol.⁶⁷



The joining of two azulene units, as in **53**, **54** and **55**, has been seen in the auto-oxidation products of guaiazulene. Compounds **53** and **54** are in fact the major products. The additional methylene carbon in **54** and **55** is thought to arise from an intermolecular one-carbon transfer in an unstable oxidation product.⁶⁸ This would therefore strongly suggest all the dimeric compounds are oxidation artefacts, as during the reported isolation no special attempts were made to maintain a low temperature, or exclude oxygen.

4.1.5 Biological activity of guaiane pigments

No biological activity was reported for the pigments isolated from either *L. deliciosus* or *L. deterrimus*. In comparison, various biological activities have been reported for guaiazulene and the derivatives isolated from marine sources. These activities have included inhibition of cell division of fertilised ascidian eggs for **51a**, **52**, **55**,⁶⁷ and antimicrobial activity for **53**, **54**⁶⁶ and guaiazulene (**50**).⁶³

4.2 Extraction of *E. hochstetteri*

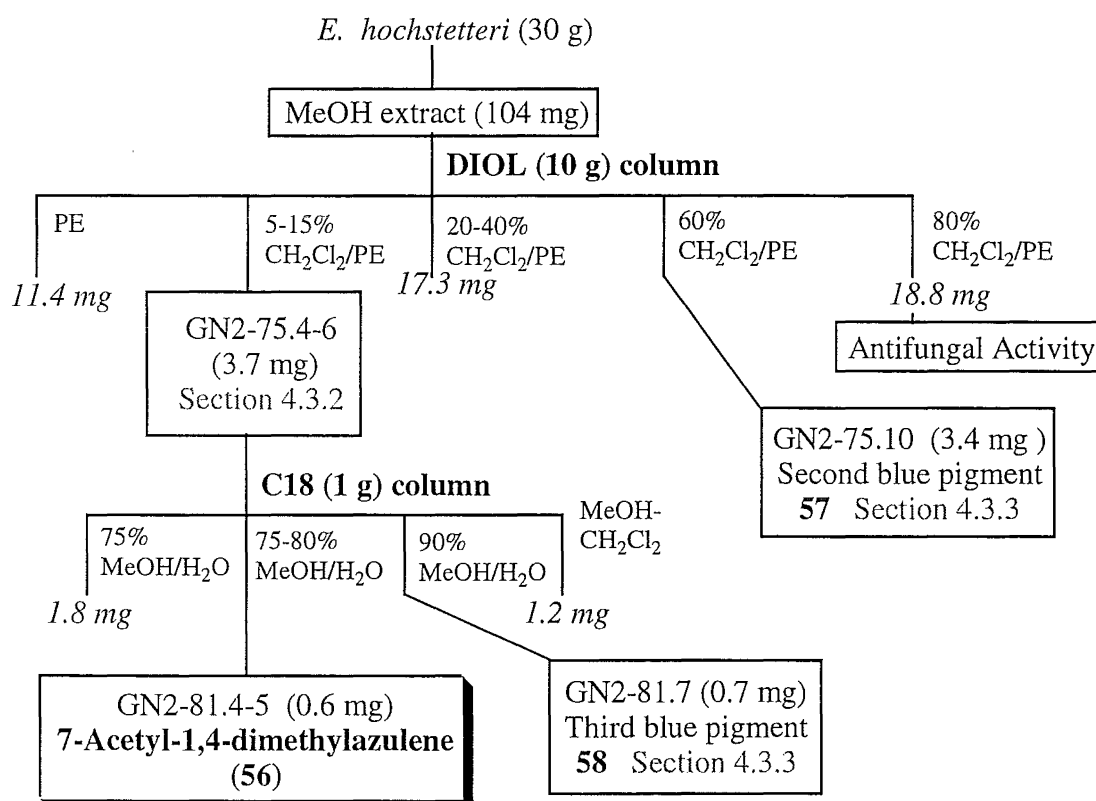
The fruit bodies of *E. hochstetteri* extracted in this investigation were collected on the Charming Creek Walkway, North Westland, New Zealand. Repeated extraction of the fruit bodies (30 g) with MeOH followed by evaporation of the solvent under vacuum gave a dark green oil (104 mg, 96CC1-1, *Trichophyton mentagrophytes* (5 mm, 0.3 mg/disk)). TLC on silica of the crude extract gave a number of coloured spots ranging in colour from blue to green. After approximately half an hour, most of the spots on the TLC plate had turned green. Some of these subsequently turned red. This colour change occurred on silica, DIOL and CN plates, and so oxidation was thought to be occurring.

4.3 Chromatography of the *E. hochstetteri* extract

4.3.1 General

An outline of the chromatography required to isolate **56** is outlined in **Scheme 4.1**.

Scheme 4.1



4.3.2 Isolation of **56**

Purification of the pigments was attempted by normal-phase (DIOL) chromatography with elution by petroleum ether through to CH₂Cl₂. Fourteen fractions were collected, and combinations were made by TLC on silica. The fractions (GN2-75.4-6, 3.7 mg) that eluted in 5-15% CH₂Cl₂ contained two high R_f blue spots by TLC on silica (CH₂Cl₂/1% MeOH). The fractions (GN2-75.12-14) that eluted in 80% CH₂Cl₂/PE were found to exhibit mild antifungal activity.

The combined fraction of GN2-75.4-6 was separated on a small reverse-phase (C18) column eluted with a stepped gradient from 75% MeOH/H₂O to MeOH and then CH₂Cl₂. Combinations were made by TLC on silica, resulting in eight fractions. Fractions were analysed by ¹H NMR spectroscopy, with fractions GN2-81.4-5 (0.6 mg) containing a blue pigment **56**. The structural elucidation of compound **56** is discussed in **Section 4.4.1**.

4.3.3 Other Pigments

Two other blue compounds were detected at different stages during the chromatography of **56**. Neither of these two compounds was ever obtained in high enough purity to enable identification, but both contained similar aromatic signals in their ¹H NMR spectra consistent with a guaiane skeleton.

The second compound eluted from the first column (DIOL) in 60% CH₂Cl₂/petroleum ether (*R_f* = 0.4, 20% MeOH/CH₂Cl₂). The ¹H NMR spectrum of this fraction (GN2-75.10, 3.4 mg) revealed signals with similar splitting patterns to those of **56**. Unfortunately, this sample also contained a significant amount of long alkyl-chain material. Attempts to purify this compound using reverse-phase (C18) chromatography gave only polar green material by TLC on silica. ¹H NMR spectra run in a variety of solvents showed little soluble material present. The signals observed in the ¹H NMR spectrum of GN2-75.10 and the partial structure of compound **57** before attempted purification, are discussed in **Section 4.4.2**.

The third blue compound **58** was found in a fraction (GN2-81.7, 0.7 mg) that eluted from the C18 column used to purify **56**. This compound had almost identical ¹H NMR signals to **57**. The fraction GN2-81.7 was still relatively impure and contained alkyl-

chain material. The signals observed in the ^1H NMR spectrum of GN2-81.7 are discussed in **Section 4.4.2**, which leads to a possible partial structure for compound **58**.

4.4 Structure elucidation

4.4.1 Structure elucidation of **56**

The molecular formula of **56** was determined by HREIMS as $\text{C}_{14}\text{H}_{14}\text{O}$ (eight double bond equivalents). IR spectroscopy indicated the presence of a carbonyl resonance at 1672 cm^{-1} . The ^1H NMR spectrum (**Fig. 4.1**) revealed three methyl singlets (δ_{H} 2.74, 2.75 and 2.88) and five olefinic or aromatic signals between δ_{H} 7.0–9.0. Unusual coupling constants were observed for the five olefinic or aromatic signals. The protons at δ_{H} 7.06 and 8.20 were split by $11.0 (\pm 0.1)$ Hz while the protons at δ_{H} 7.52 and 7.68 were split by 3.9 Hz. A small coupling constant of 1.8 Hz was also observed between δ_{H} 8.20 and 9.00, suggesting a 1,3 relationship. Two-dimensional NMR experiments, including HSMQC and HMBC, along with NOE experiments enabled the structure to be determined.

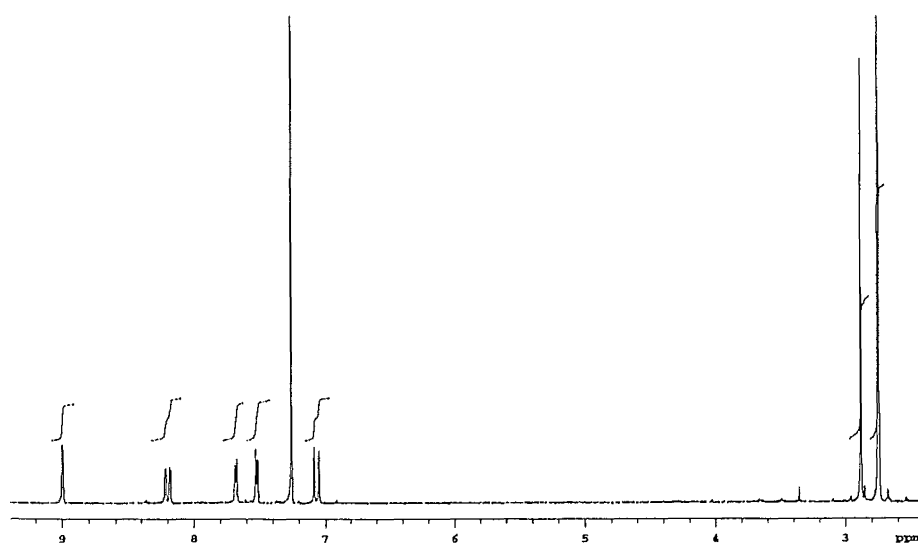


Figure 4.1 ^1H NMR spectrum of **56** (in CDCl_3)

^{13}C NMR resonances were obtained from either the HMBC or the HSMQC NMR experiments. All one-bond C-H connectivities were obtained from correlations in the HSMQC spectrum. HMBC and HSMQC NMR experiments were originally run in CDCl_3 and subsequently d_6 -benzene, which allowed separation of the overlapping methyl signals. The protons at δ_{H} 7.06 and 8.20 were obviously adjacent, due to the mutual splitting of 11.0 (± 0.1) Hz. The proton at δ_{H} 7.06 showed HMBC correlations to the aromatic methyl carbon at δ_{C} 24.8 (δ_{H} 2.88) and a quaternary carbon at δ_{C} 137.1. An NOE was observed for the proton at δ_{H} 7.06 when the protons of the methyl at δ_{H} 2.88 were irradiated. An HMBC correlation was also observed from the methyl at δ_{H} 2.88 to the carbon (δ_{C} 124.2) to which the proton at δ_{H} 7.06 was attached. This methyl was also correlated to two quaternary carbons at δ_{C} 137.1 and δ_{C} 149.4. Hence, the fragment illustrated in **Fig 4.2** was determined.

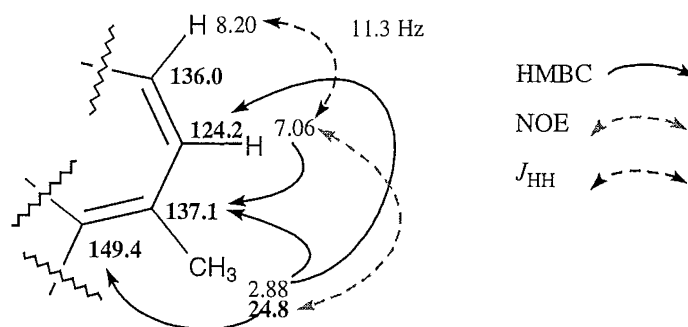


Figure 4.2 HMBC correlations, NOE effects and J_{HH} coupling constants for **56**

Further connectivity was established with the proton at δ_{H} 8.20, which showed a small coupling constant of 1.8 Hz with a proton at δ_{H} 9.00. The magnitude of this coupling is consistent with a 1,3 relationship. An HMBC correlation from the proton at δ_{H} 7.06 to a carbon at δ_{C} 127.7 (C7) allowed the assignment of this carbon as the quaternary carbon between δ_{H} 8.20 (H6) and δ_{H} 9.00 (H8). The acetyl substituent at C7 was established with HMBC correlations from the methyl at δ_{H} 2.75 and the proton at δ_{H} 9.00 to a carbonyl at δ_{C} 196.7. An NOE was also observed for the methyl at δ_{H} 2.75 when either the proton at δ_{H} 9.00 or 8.20 was irradiated, as illustrated in **Fig. 4.3**. In CDCl_3 , this acetyl methyl at δ_{H} 2.75 is overlapping with the aromatic methyl at δ_{H}

2.74. To confirm our assignment HMQC, HMBC and NOE experiments were also run in d_6 -benzene. The three methyl signals were more resolved (δ_{H} 2.61, 2.57 and 2.38) in this solvent, with the acetyl methyl at δ_{H} 2.38. The NOEs observed in d_6 -benzene confirmed the assignment of the fragment illustrated in **Fig. 4.3**.

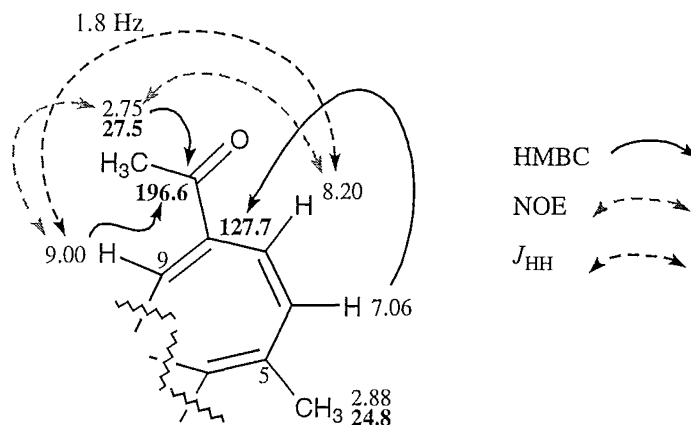


Figure 4.3 HMBC correlations, NOE effects and J_{HH} coupling constants for **56**

At this point, four of the eight double bond equivalents had been accounted for. The final pair of methine protons yet to be assigned were split with a J_{HH} of 3.9 Hz. From the HSMQC spectrum one proton (δ_{H} 7.68) was attached to a carbon at δ_{C} 136.8 while the other (δ_{H} 7.52) was attached to a carbon at δ_{C} 118.9. An HMBC correlation from the proton at δ_{H} 7.52 to the quaternary carbon at δ_{C} 137.1 led to the establishment of further connectivity through the molecule, as illustrated in **Fig. 4.4**. An NOE for the proton at δ_{H} 7.52 was observed when the methyl at δ_{H} 2.88 was irradiated (and *vice versa*), confirming the assignment.

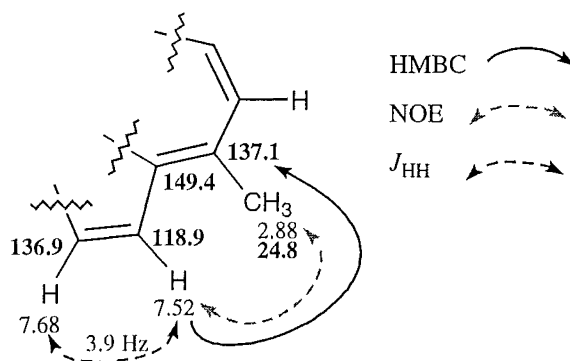


Figure 4.4 HMBC correlations, NOE effects and J_{HH} coupling constants for **56**

Further connections were made with NOEs observed for the methyl at δ_{H} 2.74 (δ_{H} 2.61 in d_6 -benzene) when either of the proton at δ_{H} 9.00 or δ_{H} 7.68 was irradiated. Again, this assignment was confirmed when HMBC, HSMQC and NOE spectra were run in d_6 -benzene. An HMBC correlation was also observed from the methyl protons at δ_{H} 2.74 to the methine at δ_{C} 136.9, as illustrated in **Fig. 4.5**. The assignment of the quaternary carbons C1 and C8a was ambiguous due to the lack of unique HMBC correlations. These carbons could therefore be at either δ_{C} 133.8 or δ_{C} 134.0.

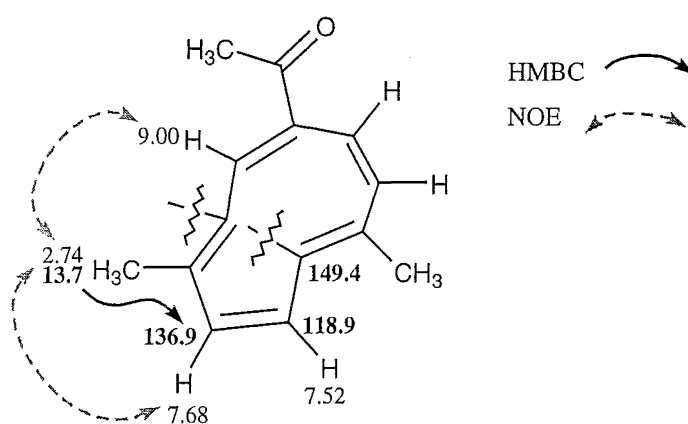
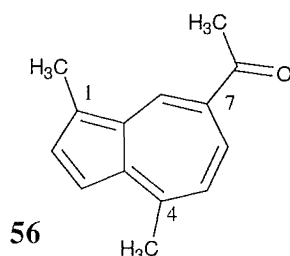


Figure 4.5 HMBC correlations and NOE effects for **56**

At this point, all the atoms from the molecular formula ($\text{C}_{14}\text{H}_{14}\text{O}$) had been assigned, but only six out of eight double bond equivalents had been accounted for. The final two must therefore arise from a bicyclic ring with linkage between the carbons at δ_{C} 149.4 and 134.0 (or δ_{C} 138.8) to give an aromatic azulene skeleton. The structure of **56** was therefore assigned as 7-acetyl-1,4-dimethylazulene.



The coupling constants observed for **56** are consistent with other compounds with the azulene skeleton, including guaiazulene (**50**).^{63,68}

Table 4.1 ^1H and ^{13}C NMR data in CDCl_3 for **56**

Number	^1H (J_{HH} Hz)	^{13}C	HMBC	NOE
1		133.8*		
1Me	2.74	13.7	118.8	8.20, 9.00
2	7.68 (3.9)	136.9	118.9	2.74
3	7.52 (3.9)	118.9	134.0, 137.1	2.88
3a		149.9		
4		137.1		
4Me	2.88	24.8	149.5, 137.1, 124.2	7.06, 7.52
5	7.06 (11.0)	124.3	24.8, 127.7, 137.1	8.20, 2.88
6	8.20 (1.8, 11.3)	136.0		7.06, 2.74
7		127.7		
7C=O		196.7		
7Me	2.75	27.5	133.8, 136.8	As for 1Me
8	9.00 (1.8)	133.5	133.8, 196.7	2.74, 2.75
8a		134.0*		

* Could be interchanged

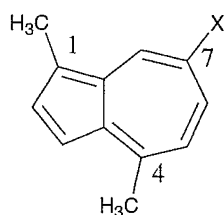
Table 4.2 ^1H and ^{13}C NMR data in d_6 -benzene for **56**

Number	^1H (J_{HH} Hz)	^{13}C	HMBC	NOE
1		132.9*		
1Me	2.61	13.3	132.9, 134.5, 136.3	7.61, 9.21
2	7.61 (3.8)	136.3		2.61
3	7.44 (3.8)	119.4		2.57
3a		148.5		
4		137.0		
4Me	2.57	24.2	123.7, 137.0, 148.5	6.75, 7.44
5	6.75 (11.1)	123.7	148.5	2.57, 8.19
6	8.19 (10.9, 1.4)	136.6		2.38, 6.75
7				
7C=O		196.6		
7Me	2.38	26.5	196.6	8.19, 9.21
8	9.21 (1.2)	134.1	132.9, 196.6	2.38, 2.61
8a		134.4*		

* Could be interchanged

4.4.2 Other Pigments

The ^1H NMR spectra of both compounds **57** and **58** contained aromatic signals with almost identical chemical shifts and coupling constants (Table 4.3). As can be seen from Table 4.3, the aromatic ^1H NMR signals of both **57** and **58** are also very similar to those of guaiazulene **50**. Two aromatic methyl singlets were observed in the ^1H NMR spectra of both compounds **57** and **58**, which is also consistent with a guaiane skeleton. Therefore, although the structures of **57** and **58** could not be assigned they must have a guaiane skeleton with only minor modification. Comparison of ^1H NMR data also ruled out the possibility of **57** and **58** being the oxidation products **53** and **54**. The question remains whether either of these compounds are in fact artefacts of oxidation or genuine natural products.



57 and **58** X = Unknown

Table 4.3 Selected ^1H NMR resonances for the unknown compounds **57** and **58** in comparison with guaiazulene (**50**) and oxidation products **53** and **54**⁶⁸

Compound	Me1	C2	C3	Me4	C5	C6	C8
57 (J_{HH} Hz)	2.65	7.61 (3.9)	7.23 (3.9)	2.82	6.97 (10.7)	7.45 (1.9, 10.7)	8.22 (1.9)
58 (J_{HH} Hz)	2.65	7.61 (3.5)	7.23 (3.5)	2.82	6.98 (10.8)	7.43 (1.9, 10.9)	8.22 (1.9)
50 (J_{HH} Hz)	2.66	7.61 (4.0)	7.20 (4.0)	2.81	6.98 (10.8)	7.42 (10.8, 2.0)	8.18 (2.0)
53 (J_{HH} Hz)	2.60	7.46	-	2.18	6.78 (10.8)	7.29 (10.8, 2.0)	8.18 (2.0)
54 (J_{HH} Hz)	2.52	7.10	5.21 (CH ₂)	2.93	6.78 (11.0)	7.24 (11.0, 2.0)	8.05 (2.0)

4.5 Discussion

A number of pigments with the guaiane skeleton have been isolated from marine and terrestrial sources as discussed in the introduction to this chapter. Many of the compounds isolated have in fact been artefacts, resulting from auto-oxidation during the isolation procedure. 7-Acetyl-1,4-dimethylazulene (**56**) has been found as a minor component of auto-oxidation of guaiazulene.⁶⁸ It is therefore most probable that the isolation of 7-acetyl-1,4-dimethylazulene (**56**) from *E. hochstetteri* was due to oxidation during the extraction and chromatography. The colour changes observed - from blue to green and then to red - are consistent with the auto-oxidation of guaiazulene (**50**)⁶⁸ and also the observations reported during the isolation of 1-stearoyloxymethylene-4-methyl-7-isopropenylazulene (**49**) from *Lactarius indigo*.⁶²

7-acetyl-1,4-dimethylazulene (**56**) did not account for the antifungal activity of the crude extract of *E. hochstetteri* but other oxidation products of guaiazulene (**50**) (see **Sections 4.1.3-4**) have been found to have antimicrobial activity. The mild antifungal activity observed for the crude extract is therefore probably due to one of these products. Further work to isolate the antifungal component or on the remainder of the pigments (**57** and **58**), whether oxidation products or not, was hindered due to the small amount of material. Taking into account the development of green polymeric material with exposure to MeOH during the investigation of *Lactarius indigo*,⁶² extraction of *E. hochstetteri* in MeOH was in hindsight an unfortunate decision. Recollection with immediate low temperature extraction and chromatography (excluding MeOH) under a nitrogen atmosphere could possibly solve the problem of auto-oxidation products and allow the isolation of the true bright blue pigment of *E. hochstetteri*.

After this work was completed, we were made aware that a group at Industrial Research Limited (Wellington, New Zealand) was investigating *E. hochstetteri* as a source of

pigments for use in the food industry. Great difficulties were encountered during their attempted isolation of pigments from fruiting bodies. An azulene derivative of some kind was isolated from the fruiting bodies but was not **56**.⁶⁹ The fungus was successfully grown in liquid culture but no pigment production was observed under the conditions used.

CHAPTER FIVE

CORTINARIUS SPECIES (CATLINS)

5.1 Introduction

Extracts of *Cortinarius* sp. collected in the Catlins Forest Park, Southland were found to be significantly biologically active. They showed cytotoxicity against the P388 cell line and broad spectrum antimicrobial activity. This mushroom was targeted for further investigation due to this activity and because a large amount could be recollected. Three related compounds were isolated from this mushroom, with the chromatography discussed in **Sections 5.2-3** of this chapter. The structure elucidation of these three compounds is described in **Section 5.4** of this chapter. All three of these compounds (**59**, **60** and **61**) were assigned as disulfides, with two (**59** and **61**) being symmetrical disulfides and the third an unsymmetrical disulfide (**60**). All three of these compounds were assigned as containing *N*-oxide functionality.

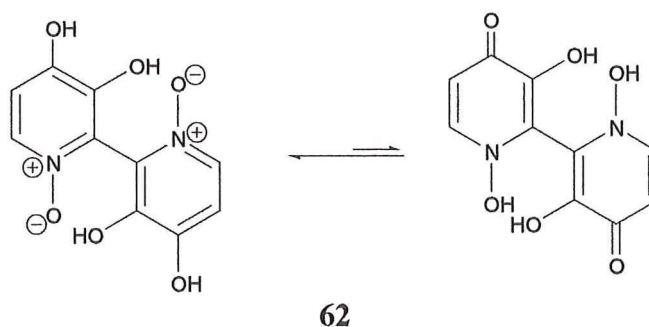
5.1.1 Chemistry of the *Cortinarius* genus

The *Cortinarius* genus displays great variety and is certainly the largest in New Zealand and also in Europe.^{70,71} A characteristic of this genus is the partial veil or cortina that is usually very conspicuous on immature specimens as fine cobweb-like material covering the gills.

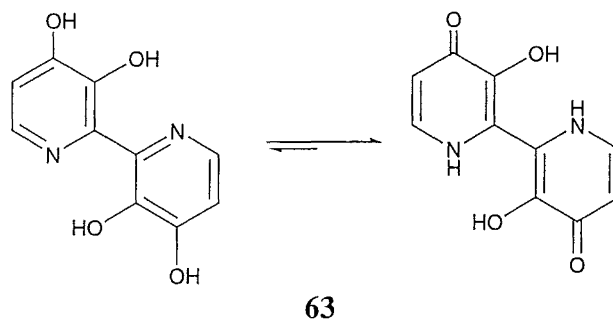


Picture 5.1 The cortina of a typical species in the *Cortinarius* genus

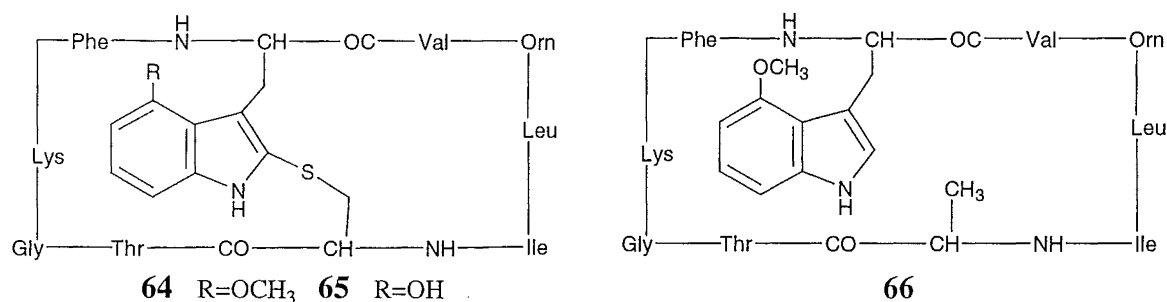
An interesting variety of natural products have been isolated from this genus in other parts of the world. Many species in the Northern Hemisphere are known to be very toxic including *Cortinarius orellanus* Fr., *Cortinarius speciosissimus* Kuhn. & Romagn.⁷¹ The nature of the toxic component(s) of these mushrooms has been an area of dispute since the first isolation of a toxic component of *C. orellanus*. This first component was isolated and called orellanine and later assigned the bipyridyl *N*-oxide structure **62**.⁷² Subsequently, an X-ray crystal structure was obtained for the natural product and synthesis of the proposed structure provided conclusive evidence that the assigned structure **62** was indeed correct. Orellanine (**62**) has also been found in *C. orellanoides* Hry., *C. raineriensis* Smith & Stuntz, *C. fluorescens* Horak and *C. speciosissimus* Kühn & Romagn.⁷³



Orellanine (**62**) is relatively unstable and decomposes with loss of oxygen to form orelline (**63**), which is yellow and non-toxic.⁷²

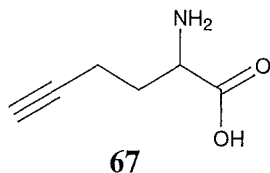


A series of cyclic polypeptide toxins isolated from *Cortinarius speciosissimus* were structurally characterised as cortinarin A (**64**), B (**65**) and C (**66**). In this report, 60 different species of *Cortinarius* were also screened by TLC to determine the presence of the cortinarins. Relatively high concentrations of cortinarin A (**64**) were found in *C. orellanus*, *C. orellanoides* and *C. speciosissimus*, while only these three species contained cortinarin B (**65**). Cortinarin A (**64**) is thought to be non-toxic.⁷¹



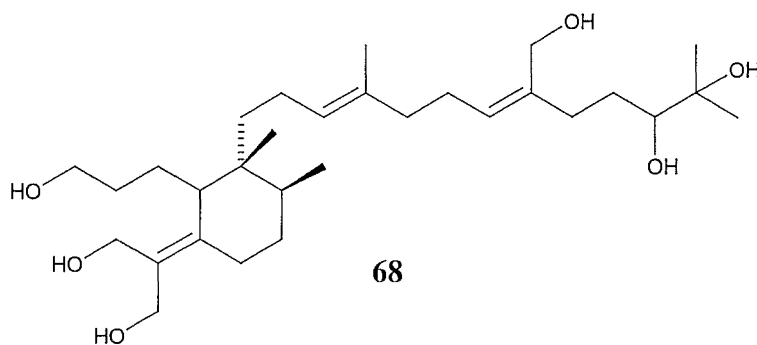
Toxicity studies on cortinarin B (**65**) have shown a relatively low mouse mortality rate (5 mg i.p. administration) after four days. However, after 2 weeks, when the mice were killed, mild to severe kidney damage was observed.⁷¹ The toxic action of synthetic and natural orellanine (**62**), and other dipyrrolyl compounds, on renal epithelial cells has been reported.⁷³ Damage was noted after 24 hours at concentrations of 10⁻³ M and was more pronounced after 48 hours. This suggests that orellanine (**62**) is the significantly toxic component of the majority of toxic species of *Cortinarius* where both orellanine (**62**) and the cortinarin cyclic peptides (**64-66**) have been isolated.

An investigation of *C. claricolor* var. *tenuipes* has been reported with the isolation and identification of the non-proteinaceous amino acid 2-(*S*)-aminohex-5-ynoic acid (**67**). This amino acid was isolated because it showed strong growth inhibition against *Bacillus subtilis*.⁷⁴



An enormous number of pigments have been identified from mushrooms in the *Cortinarius* genus, which are covered thoroughly in the reviews by Gill and Steglich.^{16,17}

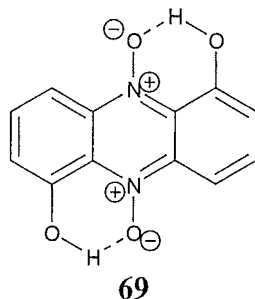
A number of bitter compounds have been isolated from a variety of *Cortinarius* species. *Cortinarius crystallinus*, *C. croceo-coeruleus* and *C. vibratilis* produce the strongly bitter triterpene crystallopicrin **68**.²⁰



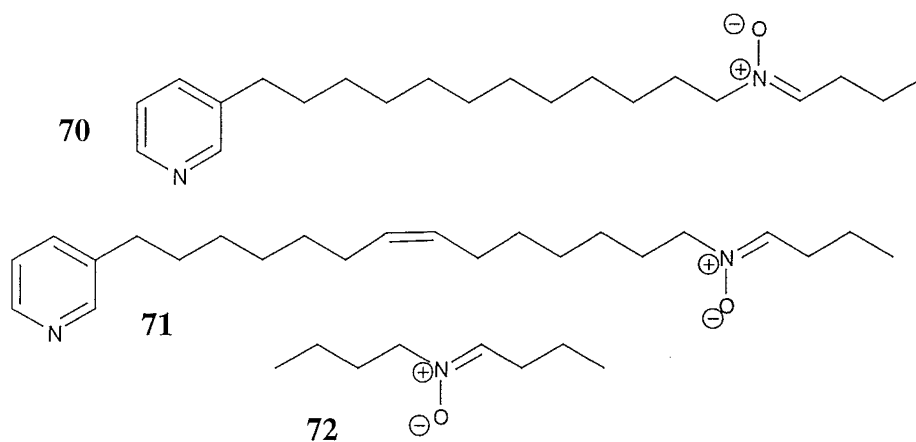
5.1.2 *N*-Oxide and *N*-hydroxy containing natural products

Several *N*-oxide and *N*-hydroxy containing natural products have been isolated from a variety of sources, many with interesting biological activity. Iodinin (**69**), a potent *N*-oxide-containing antibiotic, was isolated from *Chrombacterium iodinum* in 1938⁷⁵ and

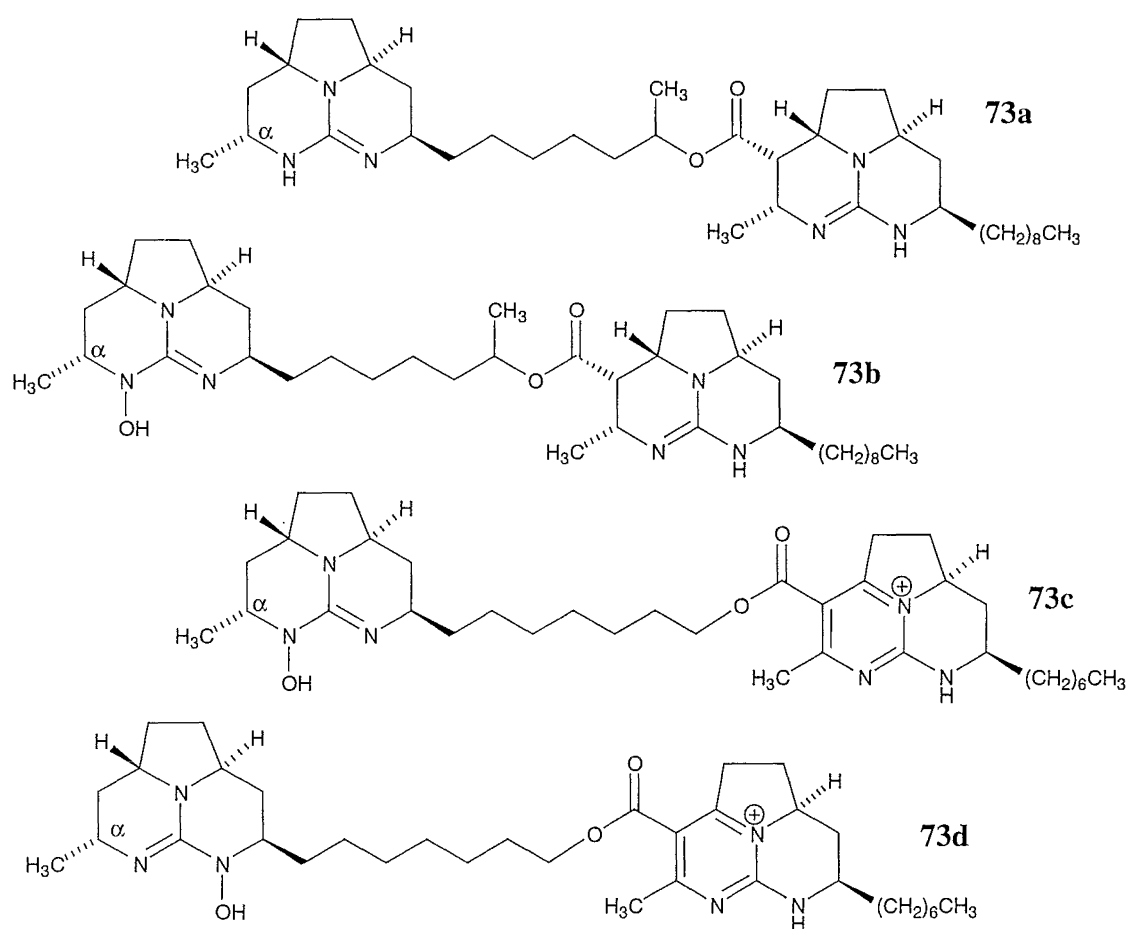
later was identified as 1,6-dihydroxyphenazine 5,10-dioxide.⁷⁶ There is also orellanine (bipyridyl *N*-oxide, **62**), which was discussed in **Section 5.1.1** of this chapter.



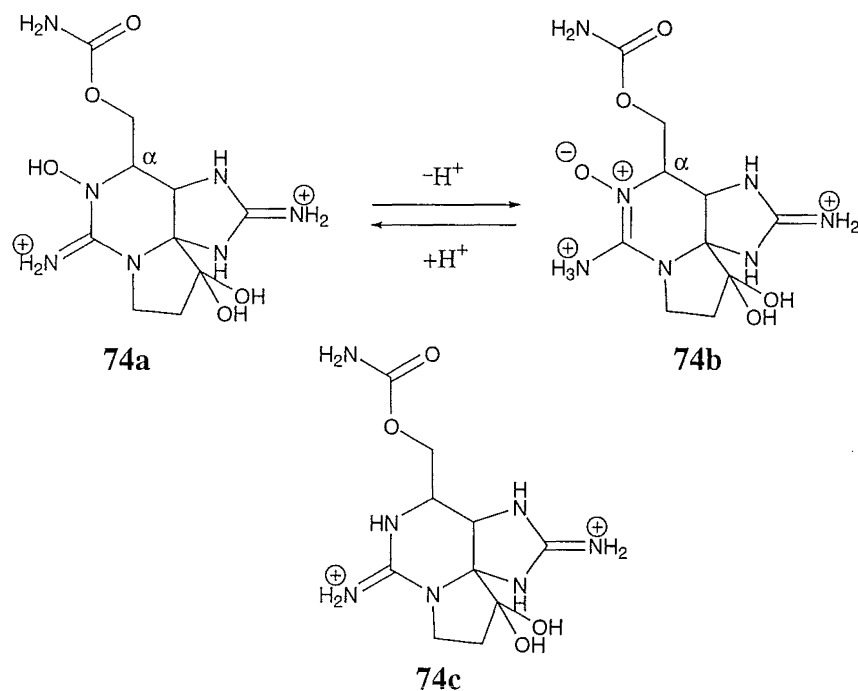
A series of *N*-oxide compounds have been isolated from marine sources and identified as the nitrones **70** and **71**. Synthesis of compound **72** and comparison of ¹H and ¹³C NMR data with those for the natural products confirmed the assignment. The chemical shift of the methylene carbon and protons in **72** were δ_C 65.4 and δ_H 3.81 respectively.⁷⁷



Batzellandines F-I have been isolated from the marine sponge *Batzella* sp. and the structures determined as **73a-d**. The position of the *N*-hydroxy group in compounds **73b-d** was each determined by the downfield change in chemical shift of the adjacent carbon and proton. The α -methine to the *N*-hydroxy functionality changed by $\Delta\delta_C$ 8.6 from **73a** to **73c** and $\Delta\delta_C$ 8.1 from **73a** to **73d**. The downfield change in chemical shift of the α -proton with addition of the *N*-hydroxy functionality was less significant at approximately $\Delta\delta_H$ 0.2 in each example.⁷⁸



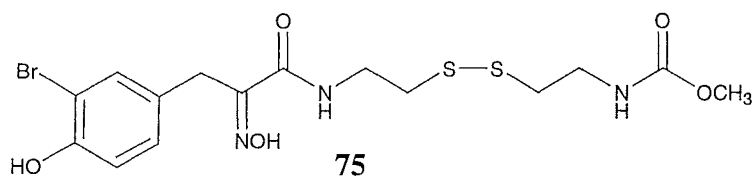
Neosaxitoxin (**74a**) is an *N*-hydroxy containing marine biotoxin produced by the dinoflagellate *Gonyaulax tamarensis* and has been isolated from a variety of shellfish.⁷⁹ The structure of neosaxitoxin was determined by comparison of ^1H and ^{13}C NMR data with those for saxitoxin (**74c**), which does not have the *N*-hydroxy group. The position of the oxygen was based on the observed downfield shift of the α -carbon and proton. The chemical shift of the α -proton moved downfield by $\Delta\delta_{\text{H}}$ 0.3 and the carbon by $\Delta\delta_{\text{C}}$ 11.2. The chemical shift of the ^1H NMR signals were found to be pH dependent. This was most prominent for the α -proton, which moved upfield at basic pH. This change was attributed to the *N*-oxide form predominating at basic pH (**74b**).⁷⁹



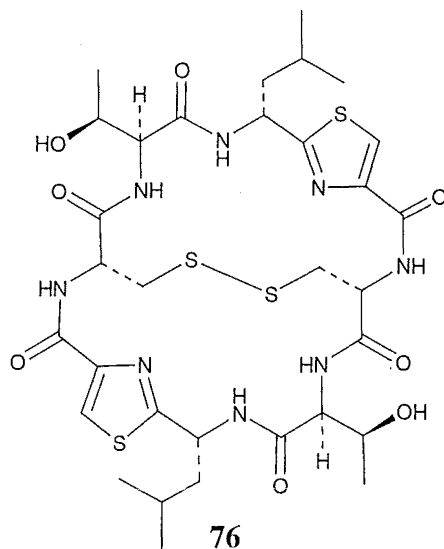
5.1.3 Disulfide natural products

The disulfide bond is an important chemical functional group for living organisms. The thiol-containing amino acid cysteine is one of the twenty amino acids that are incorporated into proteins and peptides. Two free thiol groups can then be oxidised to form a disulfide bond. These disulfide bonds help fix the tertiary structure of the amino acid backbone and thus play an important role in protein structure.

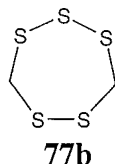
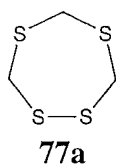
Several disulfide containing secondary metabolites have been isolated from both marine, plant and fungal sources. These include the bromotyrosine-cysteine derivatives that have been isolated from soft-bodied marine sponges and assigned as psammaplin D (75), and the corresponding dimers, which form through disulfide exchange.⁸⁰



A number of cyclic peptides have been isolated that contain an intramolecular disulfide bond across the macrocycle. An example of these cyclic peptides is preulithiacyclamide (**76**).⁸¹



A series of sulfur-rich natural products have been reported as antibiotic flavorants from the shiitake mushroom, *Lentinus edodes*. These include the cyclic polysulfides **77a-b**.²⁵



5.2 Extraction of *Cortinarius* sp.

5.2.1 Original Biological Screening results

The collection of fungal fruiting bodies from the Catlins Forest Park in May 1995 gave a number of specimens that yielded significantly biologically active extracts. The *Cortinarius* species 95CA1-26 gave extracts that were both significantly cytotoxic

(IC₅₀ 144 ng/mL (aqueous extract) and 1948 ng/mL (organic extract)) and antimicrobial.



Picture 5.2 *Cortinarius* species (Catlins)

5.2.2 Recollection

Recollection of a large amount of this species of *Cortinarius* was attempted the following autumn (May 1996). In total 230 g of fruiting bodies were collected and frozen. A small sample (2 g) of this collection was extracted with MeOH and screened in the biological assays. The results for this sample (96CA1-1) were the same as for 95CA1-26.

Chemical Screening

A small sample of a MeOH extract of *Cortinarius* sp. (Catlins) was examined using “chemical screening.”[‡] A MeOH solution (2 mg/mL) was prepared and aliquots were chromatographed on C18, CBA, LH20 and DIOL cartridges.

[‡] A procedure developed in the Marine Group for the rapid evaluation of chemical and physical properties of bioactive extracts.

Chromatography with C18 returned the greatest mass with the cytotoxicity concentrated in the MeOH fraction. This suggested that the cytotoxic components were of medium polarity. The most cytotoxic fraction that eluted from the LH20 cartridge was the last one. This result suggested that the active components were of small to medium size. The mass returned from the DIOL cartridge was low and the activity appeared to be spread over a number of fractions. The mass returned and the level of cytotoxicity of the fractions collected from the CBA cartridge was very low. This result suggested the active components contained strong basic functionality. Reverse-phase (C18) was therefore chosen as the first step of chromatography on the extract of *Cortinarius* species.

Large Scale Extraction

A sample (200 g) of *Cortinarius* species (Catlins) fruiting bodies was soaked overnight in 60:40 MeOH/H₂O then repeatedly extracted with MeOH. The MeOH was removed under vacuum and then the H₂O removed by freeze-drying. A brown, cytotoxic extract (4.09 g, IC₅₀ 925 ng/mL) was obtained, which also showed significant antimicrobial activity (10-15 mm, 10 mg/disk).

5.3 Chromatography of *Cortinarius* sp. extracts

5.3.1 Chromatography of the first extract

A general outline of the chromatography of the first extract of *Cortinarius* species is given in **Scheme 5.1**. A detailed description of the isolation can be found in the **Experimental**.

Preliminary chromatography of the MeOH/H₂O extract of *Cortinarius* sp.

Initially a small sample (50 mg) of the large scale extract was purified by reverse-phase chromatography. The solvent system was based on a stepped gradient from H₂O through to MeOH. The fractions (1.4 mg) that eluted in 40-60% MeOH/H₂O were the most active with IC₅₀ values of 43 ng/mL. The ¹H NMR spectra of these active fractions were very simple with only four aromatic signals, each integrating for one proton. HPLC analysis using reverse-phase (C18) also showed a single compound. Compound **59** was identified as 2,2'-dithiobis(pyridine *N*-oxide) - also known as dipyrithione and omadine disulfide.⁸² The structure determination of **59** is discussed in **Section 5.4.1**.

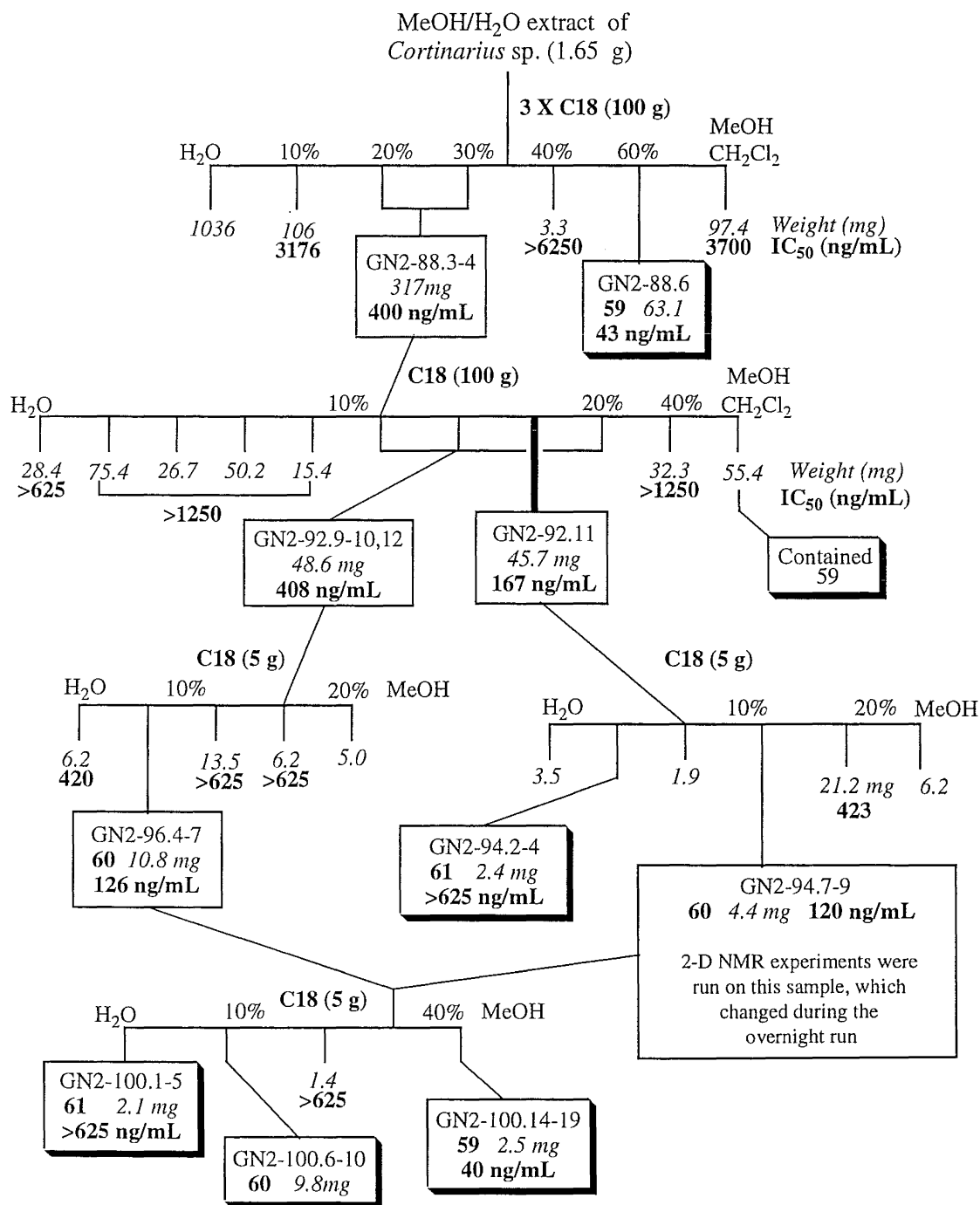
The combined fraction (1.3 mg) that eluted in 10-30% MeOH/H₂O from the initial column showed moderate cytotoxicity (the individual fractions had IC₅₀ values ranging from 700-3000 ng/mL). Analysis of this fraction by reverse-phase HPLC (C18) revealed a number of components. The ¹H NMR spectrum of this fraction showed aromatic signals similar to **59**. Chromatography of the full extract was then undertaken so that the more polar cytotoxic component could be isolated and identified.

Chromatography of the remainder of the first extract (Scheme 5.1)

The remainder of the extract was divided into three with each portion separated by a reverse-phase (C18) chromatography. Elution with a gradual stepped gradient from H₂O through to MeOH gave twenty fractions from each of the three columns that were combined by TLC (C18) and assay results for the P388 cell line. Of these combined fractions the most cytotoxic was GN2-88.6 (63.1 mg, IC₅₀ 43 ng/mL), which eluted in 60-80% MeOH/H₂O. By ¹H NMR spectroscopy, this fraction was shown to contain the previously identified 2,2'-dithiobis(pyridine *N*-oxide) (**59**). The more polar band of cytotoxicity eluted in H₂O to 20% MeOH/H₂O (GN2-88.3-4, 317.4 mg, IC₅₀ 400 ng/mL). The ¹H NMR spectrum of this combined fraction contained aromatic signals

similar to those of identified as **59**. This fraction was therefore further purified to isolate the unknown cytotoxic component.

Scheme 5.1



This combined fraction (GN2-88.3-4, 317.4 mg) was subjected to further reverse-phase (C18) chromatography with twenty fractions being collected and submitted for assay against the P388 cell line. Again, the ^1H NMR spectra of the late eluting fractions (GN2-92.16-20, 17.4 mg) showed the previously identified **59**. The more polar band of cytotoxicity was concentrated in one fraction (GN2-92.11, 45.7 mg, IC_{50} 169 ng/mL), which eluted in 10% MeOH/ H_2O . The ^1H NMR spectrum of this fraction contained the aromatic signals similar to those of **59**, along with a number of other signals between δ_{H} 1.5-4.5.

The first purification of compounds **60** and **61**

Further chromatography of GN2-92.11 (45.7 mg) by reverse-phase (C18) was carried out, eluting with a gradual stepped gradient from H_2O through 10% MeOH/ H_2O and then to MeOH. Fractions that eluted in 10% MeOH/ H_2O (GN2-94.6-11) were analysed by ^1H NMR spectroscopy and were all found to contain the same aromatic (δ_{H} 7.2-8.2) and aliphatic signals (δ_{H} 1.5-4.5). Fractions GN2-94.7-9 (4.4 mg) were found to be the cleanest so they were combined and 2-D NMR experiments were run on this sample. A number of fragments were assigned for compound **60**, but full connectivity could not be confirmed by correlations in the HMBC experiment. The structure elucidation of **60** is described in **Section 5.4.2**.

During the overnight run of NMR experiments on compound **60** a number of signals arose from the base line. Each new signal appeared to correspond to an equivalent in the original compound. The new aromatic signals corresponded to that of compound **59**. The new non-aromatic signals were subsequently found to correspond to those of fractions GN2-94.2-4 (2.4 mg) that eluted from the same column in H_2O . 2-D NMR experiments were subsequently run on this sample. The structure of this compound has been assigned as the symmetrical disulfide **61**. The structural elucidation of **61** is described **Section 5.4.3**.

Further chromatography to obtain pure samples of compounds **60** and **61**

Although 2-D NMR experiments had been run on these two compounds the initial data obtained did not give conclusive evidence for the proposed structures. Problems of decomposition added to difficulties with samples quickly becoming impure. Clean material was required for further spectroscopic analysis, including ^1H NMR spectra in alternative solvents (e.g. d_6 -DMSO) and for mass spectrometry.

Further chromatography of combined fractions that surrounded those previous purified above and the now impure samples of **60** gave a fraction containing **61** (GN2-100.1-5, 2.1 mg) and **60** (GN2-100.6-10, 9.8 mg). HRFABMS (Canterbury) was obtained on compound **60**, but was unsuccessful on **61**.

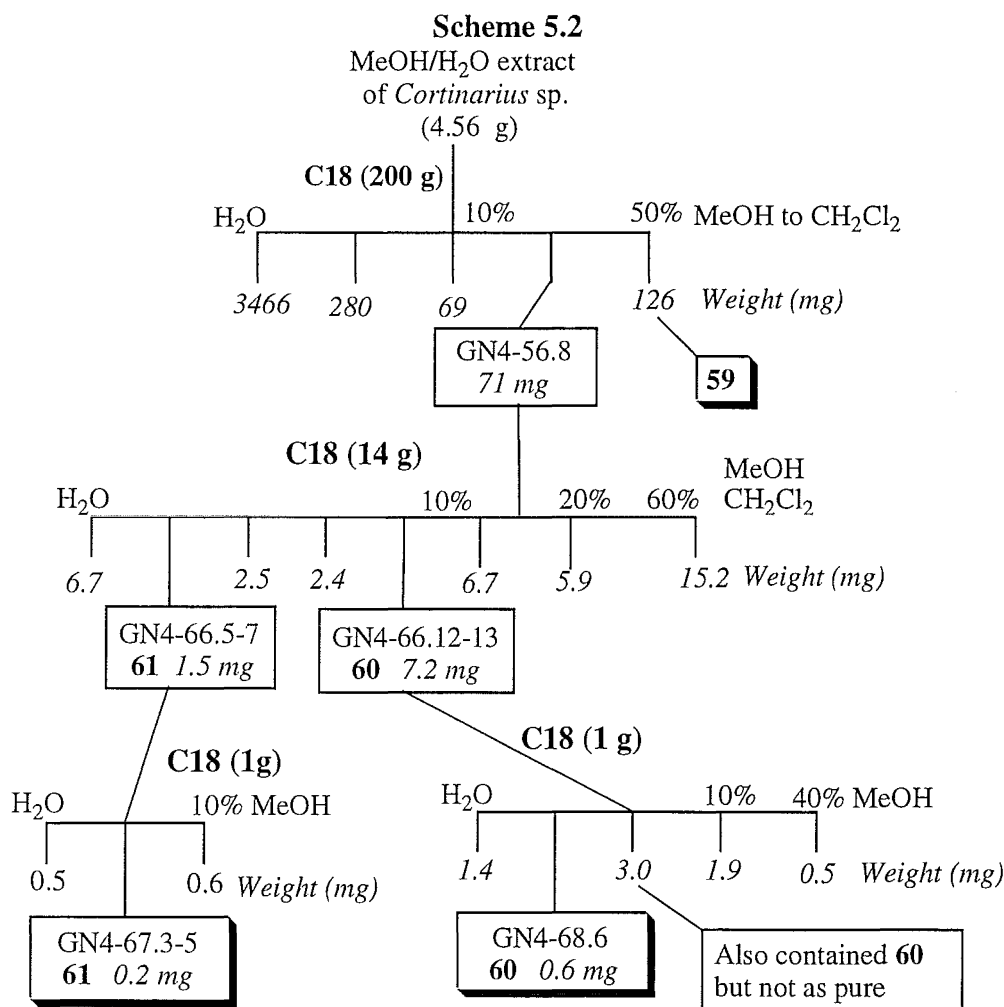
5.3.2 Second collection, extraction and chromatography of *Cortinarius* sp. (Catlins)

Extraction

A second extraction of *Cortinarius* sp. (Catlins) fruiting bodies (125 g) with H_2O gave a brown, moderately cytotoxic extract (4.56 g, IC_{50} 1115 ng/mL), which also showed antimicrobial activity. The level and spectrum of activity was consistent with the first collection and extraction of *Cortinarius* sp. (Catlins).

Chromatography of this second extract

An outline of the isolation is illustrated in **Scheme 5.2**.



Initial chromatography of this second extract of *Cortinarius* sp. (Catlins) by reverse-phase (C18) chromatography yielded fractions (GN4-56.5-8, 163 mg (in total), 10-20% MeOH/H₂O) that contained visible amounts of the compound **60**. A number of attempts were made to purify a small amount of this combined fraction by reverse-phase (C18) HPLC. A number of solvent systems were tried including the addition of TFA, but these were unsuccessful. The peak that corresponded to compound **60** was always very broad and overlapped with impurities. Chromatography on LH20 with elution in 70% H₂O/MeOH was also tried in an attempt to purify **60**. However, only poor separation was obtained. Therefore, the strategy for purification of **60** and **61**

reverted to reverse-phase (C18) bench columns as pure material had already been obtained by this method.

Purification of fraction GN4-56.8

Fraction GN4-56.8 (71 mg) was separated by reverse-phase (C18) chromatography with elution using a stepped gradient from H₂O through 10-20% MeOH/H₂O. The fractions that eluted in H₂O (GN4-66.5-7, 0.9 mg) contained **61**. This was further purified to yield fractions GN4-67.3-5 (0.2 mg) that were shown to contain pure homodimer **61**. These samples were sent to Dr L.K. Pannell for mass spectrometry analysis including ESIMS and HRFABMS.

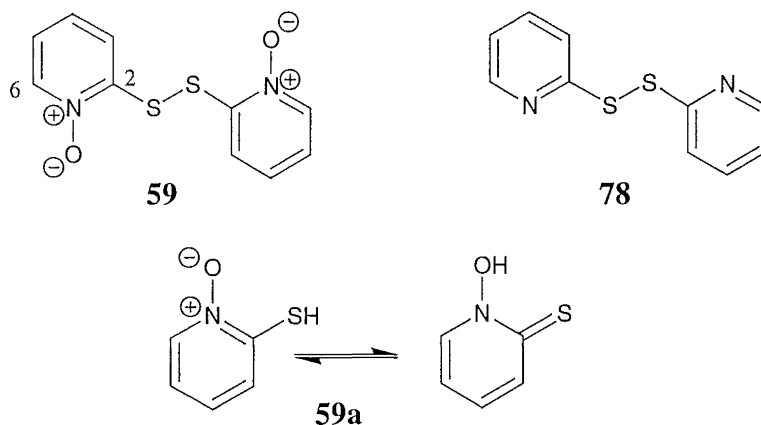
The fractions that eluted in 10% MeOH/H₂O (GN4-66.11-14) all contained the parent compound **60**. Fractions GN4-66.12-13 (7.2 mg) were further purified by reverse-phase chromatography. This gave fraction GN4-68.6 (0.6 mg), which by ¹H NMR spectroscopy contained pure parent compound **60**. This sample was also sent to Dr L.K. Pannell for mass spectrometry analysis. Fractions GN4-68.7-10 were not as pure but were used to obtain NMR spectra in alternative solvents such as *d*₆-DMSO and *d*-TFA. The sample that was run in *d*-TFA was subsequently dried under high vacuum and then re-examined in D₂O.

5.4 Structure elucidation

5.4.1 Structure elucidation of 2,2'-dithiobis(pyridine *N*-oxide) (**59**)

The ^1H NMR spectrum (**Fig. 5.1**) of **59** was very simple, with only four aromatic signals each integrating for one proton. A series of simple irradiation experiments determined the order in which the protons were situated around the ring. The IR spectrum of **59** contained two very broad peaks centred on 3361 and 1400-1600 cm^{-1} . High resolution mass spectrometry by electron impact ionisation (EI) gave an apparent molecular ion at m/z 220.0128 corresponding to the formula of $\text{C}_{10}\text{H}_8\text{N}_2\text{S}_2$ (requires 220.0128).

The ^1H and ^{13}C NMR data (**Table 5.1**) for **59** were inconsistent with those for 2,2'-dithiobispyridine (**78**).⁸³ However, the ^1H NMR data for **59** were more consistent with those of 2-thiopyridine *N*-oxide **59a**.⁸⁴ The chemical shifts of the carbons and protons on pyridine *N*-oxides are found upfield of the equivalent pyridine compounds. The mass spectrum of compound **59** was consistent with that of 2,2'-dithiobis(pyridine *N*-oxide) from the MBS/NIST mass spectral library, where the two oxygen atoms are not observed. Subsequent analysis by FABMS gave a molecular ion at m/z 253 (MH^+), which is consistent with retention of both the *N*-oxides. The structure of **59** was therefore assigned as 2,2'-dithiobis(pyridine *N*-oxide).



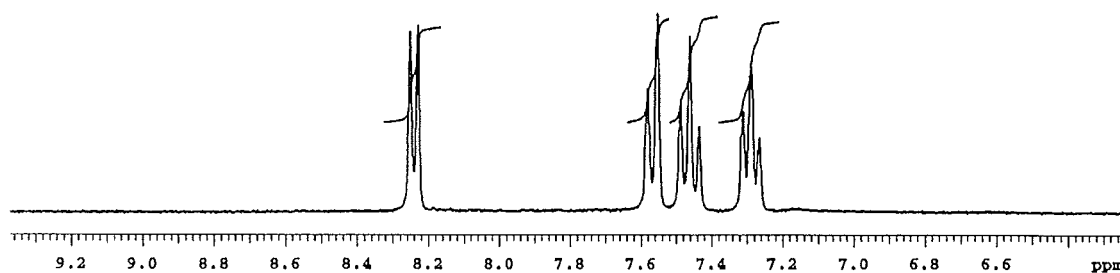


Figure 5.1 ^1H NMR spectrum of **59** (D_2O)

Table 5.1 ^1H and ^{13}C NMR data for 2,2'-dithiobis(pyridine *N*-oxide) (**59**)

Number	δ_{H} (J_{HH} Hz) ($\text{CDCl}_3 + d_5\text{-Pyr}$)	δ_{H} (J_{HH} Hz) (D_2O)	δ_{C} (D_2O)
2			150.5
3	7.57 dd (1.7, 8.0)	7.56 d (8.3)	124.6*
4	7.25 m	7.46 d (8.3)	133.6
5	7.16 m	7.29 m	125.7*
6	8.29 dd (1.0, 6.3)	8.24 d (6.3)	141.1

* These assignments could be reversed

5.4.2 Structure elucidation of cortamidine oxide (**60**)

The ^1H NMR spectrum of **60** (Fig. 5.2) showed aromatic signals (δ_{H} 7.26, 7.56, 7.96, 8.16) similar to those of 2,2'-dithiobis(pyridine *N*-oxide) (**59**) and a number of other signals between δ_{H} 3.95 and 1.50. The ^{13}C NMR spectrum of **60** showed a carbonyl signal at δ_{C} 177.7, six carbons from δ_{C} 124-154 and six more in the aliphatic region (δ_{C} 19.4-57.1). Five of the carbons in the aromatic region were consistent with those observed for **59**.

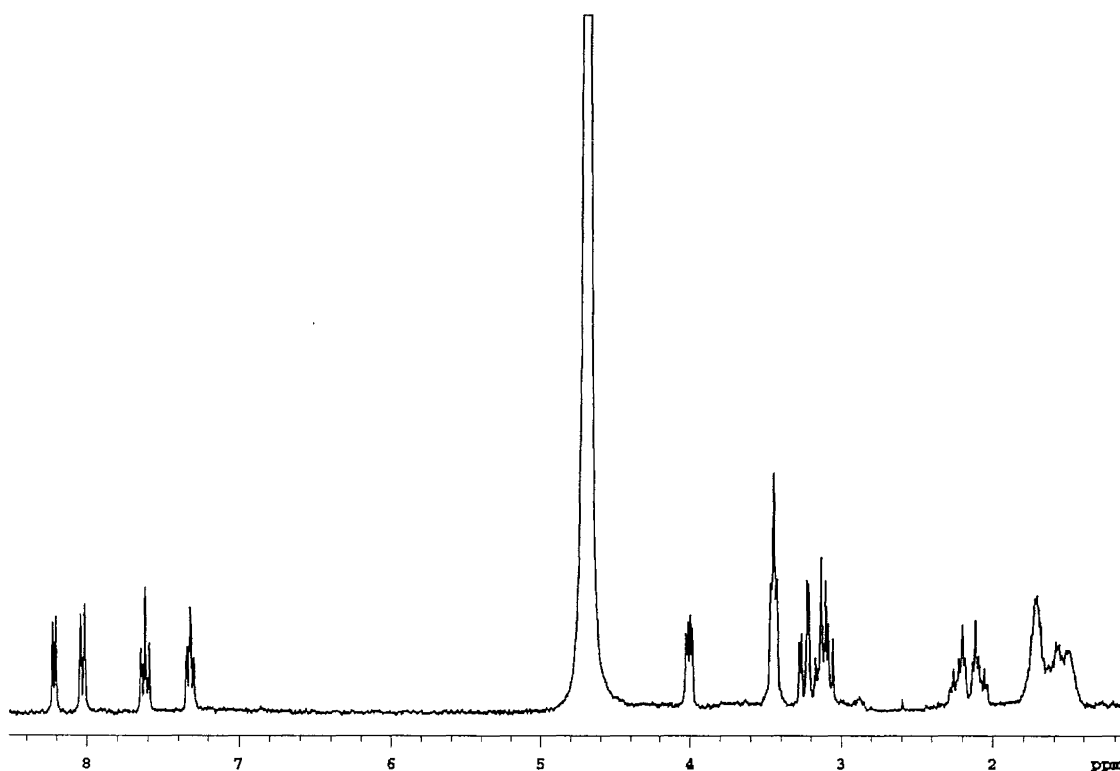
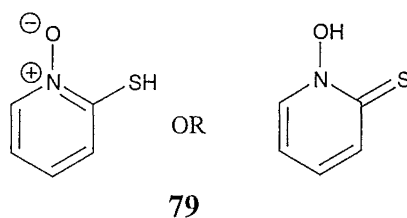


Figure 5.2 ^1H NMR spectrum of cortamidine oxide (**60**) (in D_2O)

Mass spectrometry in EI gave no parent ion but fragment ions (m/z 127, 110, 78, 67) were observed similar to those for 2,2'-dithiobis(pyridine *N*-oxide) (**59**). HREIMS on these fragment ions allowed assignment of the m/z 127.0115 as **79** ($\text{C}_5\text{H}_5\text{NOS}$ requires 127.0091), as also seen in the spectrum of 2,2'-dithiobis(pyridine *N*-oxide) (**59**). FABMS in a NOBA matrix gave an MH^+ ion at m/z 344, MNa^+ at 366 and MK^+ at 382.

At high resolution the MH^+ ion was observed at m/z 344.07102, which gave the formula as $\text{C}_{13}\text{H}_{17}\text{O}_4\text{N}_3\text{S}_2$ (requires 344.0738).



HMBC and COSY correlations allowed the full assignment of the 2-thiopyridine *N*-oxide fragment, as illustrated in **Fig. 5.3**. The proton at δ_{H} 8.16 showed a COSY correlation to the proton at δ_{H} 7.26, which in turn showed a further correlation to the proton at δ_{H} 7.56. The proton at δ_{H} 7.96 also showed a COSY correlation to this proton at δ_{H} 7.56. The assignment of the aromatic carbons was achieved from correlations in an HSQC experiment. The proton at δ_{H} 8.16 was attached to a carbon at δ_{C} 140.9, which is consistent with it being adjacent to the nitrogen of the pyridine *N*-oxide. The chemical shift of the quaternary aromatic carbon at δ_{C} 153.4 was consistent with a sulfur substituent.

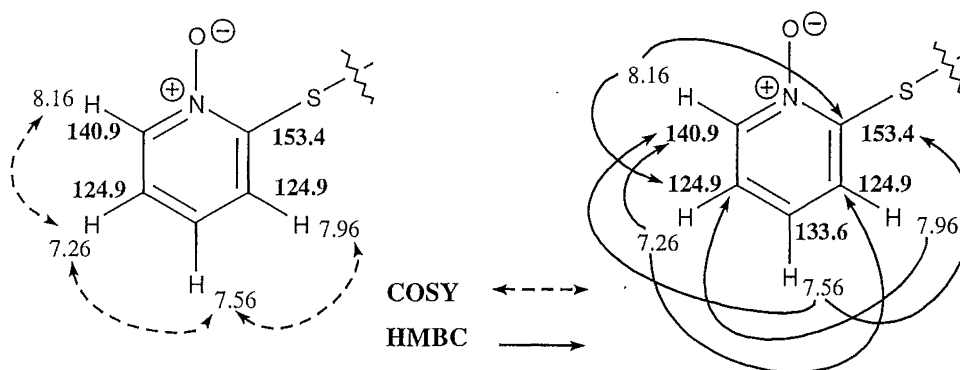


Figure 5.3 COSY and HMBC correlations for **60**

The second fragment to be assigned was an isolated spin system that consisted of the methine proton at δ_{H} 3.95 and the pair of diastereotopic protons at δ_{H} 3.15 and 3.29 (**Fig. 5.4**). COSY correlations that were observed between these three protons allowed the assignment. The methylene carbon to which the protons at δ_{H} 3.15 and 3.29 were attached was assigned from HSQC correlations as δ_{C} 42.3. The chemical shift of this

carbon is consistent with that of a methylene adjacent to a disulfide bond. The chemical shift of the equivalent methylene in cystine is δ_{C} 39.0, in comparison to cysteine, which is δ_{C} 27.4.⁸⁵ HMBC correlations were observed from the methine at δ_{H} 3.95 to the carbonyl at δ_{C} 177.7 and to the methylene at δ_{C} 42.3. This fragment was therefore assigned as a substituted cysteine linked to the pyridine *N*-oxide through a disulfide bond, as illustrated in **Fig. 5.4**. This would be consistent with disulfide exchange to form 2,2'-dithiobis(pyridine *N*-oxide) (**59**).

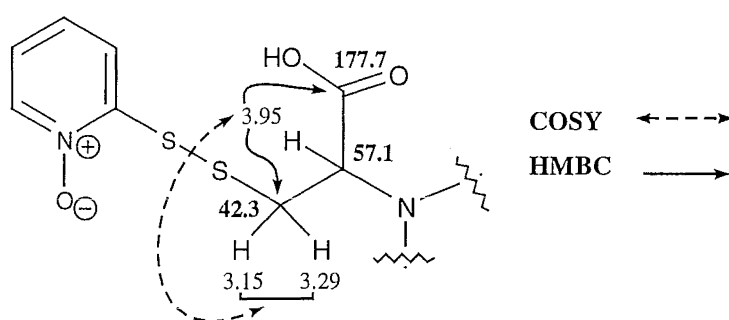


Figure 5.4 HMBC and COSY correlations for **60**

The third fragment was assigned from HMBC and COSY correlations (**Fig. 5.5**). Four contiguous methylenes could be assigned from a succession of COSY correlations (from δ_{H} 3.39 to δ_{H} 1.66, then to δ_{H} 1.50, and finally to δ_{H} 2.16/2.25). The carbons to which these protons were attached were assigned from the HSQC spectrum as δ_{C} 54.2 (δ_{H} 3.39), 23.5 (δ_{H} 1.66), 19.5 (δ_{H} 1.50) and 24.9 (δ_{H} 2.16/2.25). The chemical shift of the protons at δ_{H} 3.39 (δ_{C} 54.2) was consistent with them being adjacent to nitrogen, even if the carbon was slightly downfield from that expected for the proposed amidine structure. A six-membered ring could then be constructed with the observed HMBC correlations from the protons at δ_{H} 1.50, 2.16/2.25 and 3.39 to the quaternary carbon at δ_{C} 153.3, as illustrated in **Fig. 5.5**. These HMBC correlations around the ring ruled out the possibility of a urea carbonyl, which would have been consistent with the carbon at δ_{C} 153.3.

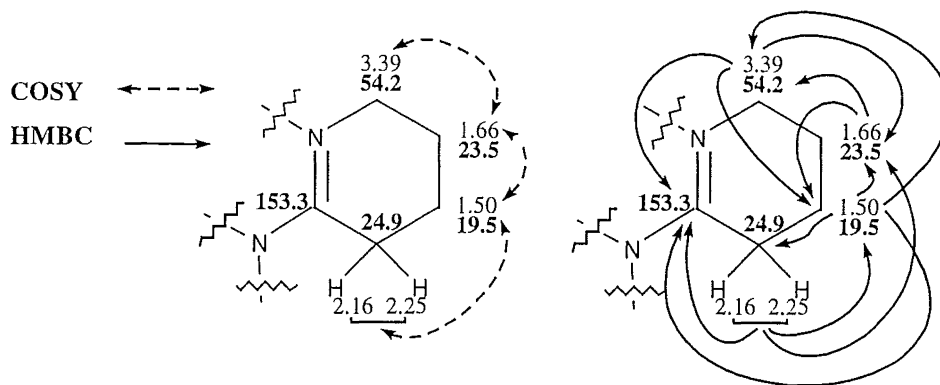


Figure 5.5 HMBC and COSY correlations for **60**

At this point there were three fragments that could be assigned by NMR experiments and limited mass spectrometry. A weak correlation in the HMBC spectrum from the proton at δ_{H} 3.95 to a quaternary carbon at δ_{C} 153.3 suggested that the cysteine residue might be connected to the six-membered tetrahydropyridine through nitrogen. Unfortunately, the closeness in chemical shift of the quaternary carbon of the tetrahydropyridine ring (δ_{C} 153.3) to that of the pyridine *N*-oxide (δ_{C} 153.4) did not allow a definitive assignment. This connection was later confirmed during the structure elucidation of the related compound **61** (see **Section 5.4.3**). A correlation was observed in the HMBC spectrum of **61** from the equivalent α -proton (now at δ_{H} 4.16) to the quaternary carbon now at δ_{C} 152.9. The connection between the tetrahydropyridine and the cysteine fragment of **61** was assigned as illustrated in **Fig. 5.6**.

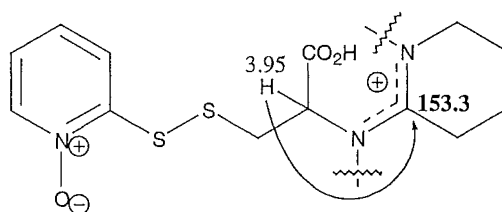
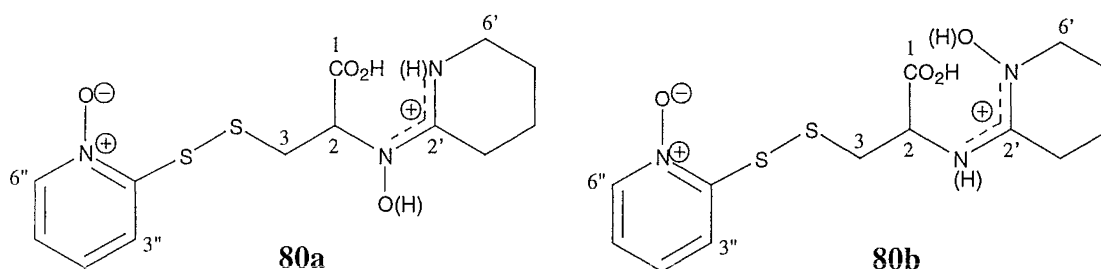


Figure 5.6 An HMBC correlation for **60**

At this point, all the carbons and protons from the NMR spectra of **60** had been assigned. Of the heteroatoms available, only one oxygen was unassigned. Therefore, oxygenation of a heteroatom was required. Of those heteroatoms available, the sulfur atoms could not be involved because the chemical shifts of the carbons adjacent to the

sulfur were not consistent with oxidation.⁸⁵ The isolation of 2,2'-dithiobis(pyridine *N*-oxide) (**59**) and compound **61**, presumably from disulfide exchange, supported this conclusion. The nitrogen atoms of the tetrahydropyridine and the cysteine fragment were the only positions left. Therefore, the two possibilities are oxygen on one of these nitrogens. Each of these two possibilities then has a number of tautomeric forms represented as either **80a** or **80b**.



Oxidation of Nitrogen

There were no fragments in the mass spectra obtained that could be used to discriminate between the two possible positions of oxygenation. Oxidised nitrogen is known to move the adjacent quaternary imine or amidine ¹³C NMR resonance upfield and the other adjacent protons and carbon downfield.⁸⁶ This downfield shift for the protons on adjacent carbons is usually between $\Delta\delta_{\text{H}}$ 0.2-0.4. Examples include the nitron of cribrochalinamine oxide A (**70**) and B (**71**) where the methylene adjacent to the *N*-oxide was reported at δ_{C} 65.4 and the nitron carbon at δ_{C} 146.0 (for **70**).⁷⁷ The addition of an *N*-hydroxy function to the guanidinium group of saxitoxin (**74c**) to form neosaxitoxin (**74a**) moved the methine adjacent to nitrogen downfield by $\Delta\delta_{\text{C}}$ 11.2.⁷⁹ ¹³C NMR data were found for 2,3-dihydroisoquinoline (**81a**), the protonated form **81b**, 2,3-dihydroisoquinoline *N*-oxide (**81c**), and the corresponding protonated form **81d**. The ¹³C NMR data for **60** were closest to those of **81d** (Fig. 5.7).

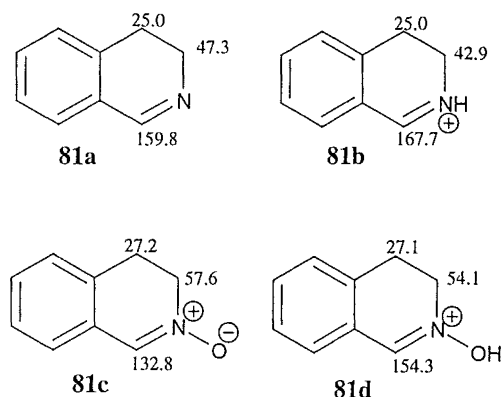


Figure 5.7 ^{13}C NMR data for **81a-81d**

Unfortunately, the functional group proposed for **60** is not a guanidinium group or a nitron, but rather an amidine *N*-oxide, so the downfield chemical shift observed in these examples could only be used as a guide. The only example of an amidine *N*-oxide in the literature with assigned carbon and proton data was for 2-amino-5,5-dimethylpyrroline *N*-oxide (**82**).⁸⁷ However, the ^{13}C NMR data were not complete as the signal for the quaternary carbon adjacent to the *N*-oxide was assigned by default as under the solvent signal somewhere between δ_{C} 47.5-48.5 (Fig. 5.8).

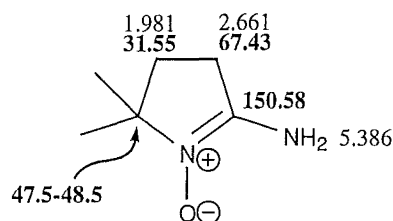
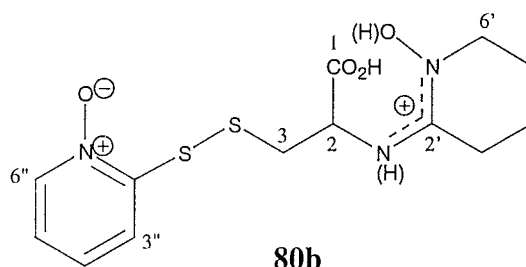


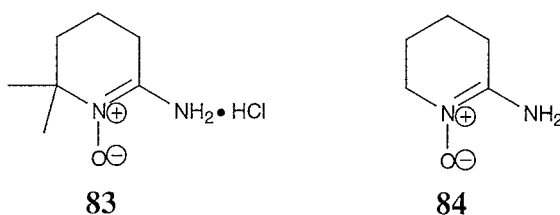
Figure 5.8 ^1H and ^{13}C NMR data for **82**

The chemical shift of the cysteine α -carbon and proton were slightly downfield compared to that of cystine but only by approximately $\Delta\delta_{\text{C}}$ 2.4 and this could be accounted for by the *N*-substitution. The chemical shifts of the protons designated as H6' were compared to those of 2-(methylamino)-3,4,5,6-tetrahydropyridine and were found to be similar. The chemical shift of C6' in **60** would have been expected at around δ_{C} 45, if no oxygen were present on the adjacent nitrogen. From the trends

reported in the literature, the oxygen was therefore assigned as being on the tetrahydropyridine ring (**80b**).



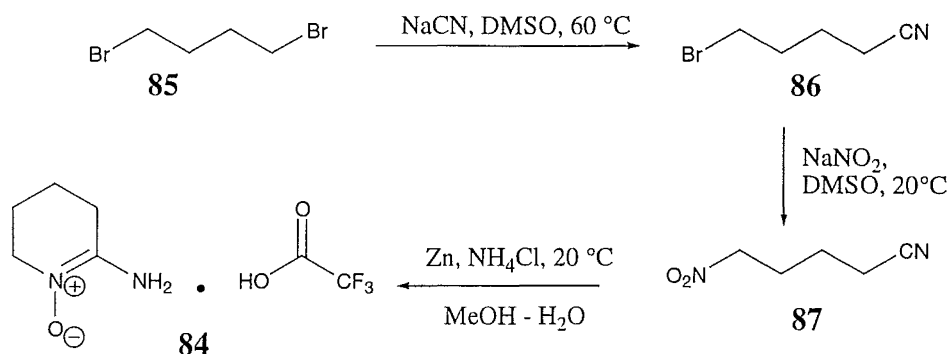
2-Amino-6,6-dimethyl-3,4,5,6-tetrahydropyridine-*N*-oxide (**83**) was also found in the literature but no NMR data were reported.⁸⁸ To confirm the assignment of **60** the synthesis of 2-amino-3,4,5,6-tetrahydropyridine-*N*-oxide (**84**) was undertaken. The method of ring closure used was the same as that previously reported for 5-methyl-5-nitro-valeronitrile, which used zinc and ammonium chloride to provide compound **83** (as the hydrochloride salt).⁸⁸



Synthesis of 2-amino-3,4,5,6-tetrahydropyridine-*N*-oxide (**84**)[†]

5-Bromovaleronitrile (**86**) was prepared from 1,4-dibromobutane (**85**) (Scheme 5.3). Thus, to a solution of 1,4-dibromobutane (**85**) in warm DMSO (60 °C) was added sodium cyanide in small portions over 30 min. After stirring for a further 30 min the reaction was cooled to room temperature. After a standard work-up procedure and fractional distillation 5-bromovaleronitrile (**86**) was obtained.

[†] The author acknowledges the assistance of Mr Andrew Phillips with the preparation of the compounds in this sequence.

Scheme 5.3 Synthesis of 2-amino-3,4,5,6-tetrahydropyridine-*N*-oxide (**84**)

5-Nitrovaleronitrile (**87**) was prepared from 5-bromovaleronitrile (**86**) obtained above. To a suspension of sodium nitrite in DMSO at room temperature was added the nitrile **86** in DMSO over a period of ca. 10 min. The reaction became homogenous and was stirred for 4 hr at room temperature. After a standard workup and flash chromatography 5-nitrovaleronitrile (**87**) was obtained as a light yellow oil.

Cyclisation of 5-nitrovaleronitrile (**87**) to the amidine *N*-oxide **84** was achieved using a mild reductant in mildly acidic conditions (**Scheme 5.3**). Thus, to 5-nitrovaleronitrile and solid ammonium chloride in MeOH/H₂O at 0 °C was added zinc dust. The reaction was allowed to warm to room temperature and stirred for 16 hr. The solution was then filtered and acidified with trifluoroacetic acid. The solvent was removed *in vacuo* to yield after purification 2-amino-3,4,5,6-tetrahydropyridine-*N*-oxide (**84**) as a light orange oil. A plausible mechanism for this reduction and subsequent cyclisation is illustrated in **Appendix II**. The mechanism of these types of reductions has not been extensively studied although it is thought to proceed via a number of one-electron transfers followed by protonation.^{89,90}

The ¹H and ¹³C NMR data for 2-amino-3,4,5,6-tetrahydropyridine-*N*-oxide (**84** as the TFA salt) were consistent with those of the relevant fragment in compound **60** (as the TFA salt) (**Fig. 5.9**). The position of oxygenation was therefore assigned to the nitrogen of the tetrahydropyridine ring.

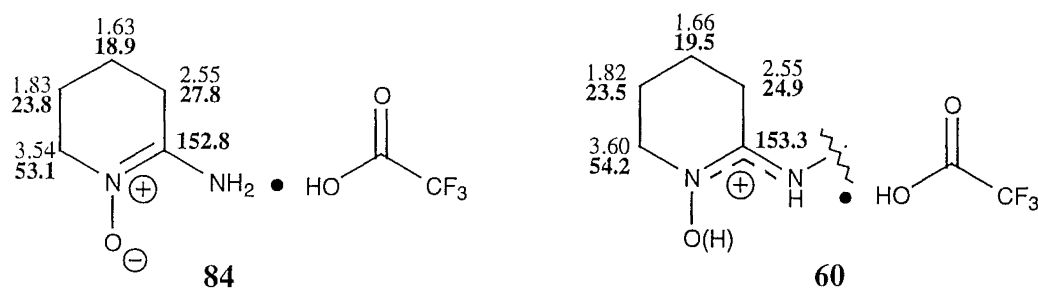
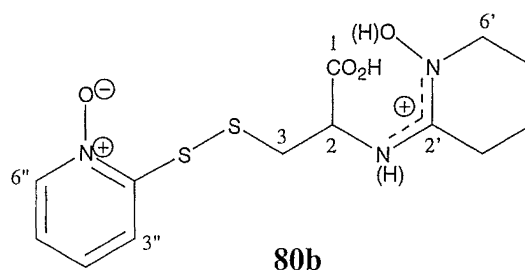


Figure 5.9 ^1H and ^{13}C NMR data for **84** (as TFA salt) and ^1H NMR data for **60** (as TFA salt) and ^{13}C NMR data for **60** (not as TFA salt)

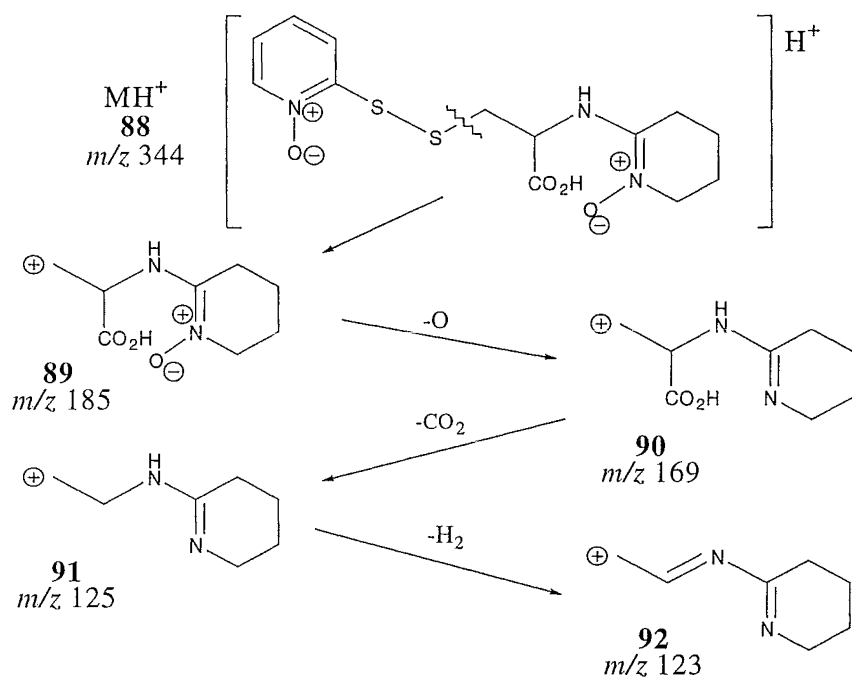


N-oxide or *N*-hydroxy functionality

The tautomeric behaviour of 2-amino-5,5-dimethyl-1-pyrroline and its corresponding *N*-oxide has been reported using IR spectroscopy in chloroform. It was concluded that both these compounds are aminopyrroline derivatives and not the tautomeric iminopyrrolidines, at least in chloroform solution.⁹¹

The *N*-hydroxy proton was observed for batzellandines G-I in d_6 -DMSO as a sharp singlet at δ_{H} 10.51.⁷⁸ No *N*-hydroxy proton was observed by ^1H NMR spectroscopy for the natural product **60** or the synthesised compound **84**, even when d_6 -DMSO was used as the solvent. This would therefore suggest that compound **60** exists in the *N*-oxide form. The ions observed by electrospray ionisation mass spectrometry were consistent with the *N*-oxide tautomer for compound **60**. The parent ion (MH^+) was observed at m/z 344 (**88**) when the fragmentation voltage was under 50 V. This ion decreased as the applied voltage was increased to 150 V to give ions at m/z 217, 185 (**89**), 169 (**90**), 125 (**91**) and 123 (**92**). Examination of the fragment ions showed no loss of OH (17) but loss of oxygen (16) from the fragment ion at m/z 185 to 169, which

would indicate that the *N*-oxide tautomer was the form in which this compound exists. Structures **88-92** were drawn as the *N*-oxide tautomer and the charges were arbitrarily drawn at point of cleavage for simplification. A loss of oxygen (16) was also observed in the FAB mass spectrum of the synthetic compound **84**.



Negative NOEs

All of the NOEs observed for compound **60** were negative. This would indicate a molecular formula of greater than 1000 Da even though the molecular mass of **60** was determined as 343 Da. An explanation for the negative NOEs could be that two molecules of **60** are in fact forming an ion pair in solution and therefore the relaxation of the individual protons is as for a larger molecule. By ESI mass spectrometry, the dimeric ions M_2H^+ , M_2Na^+ and M_2K^+ were observed at m/z 687, 709 and 725 respectively. The appearance of these ions was concentration dependent so is not conclusive evidence for dimer formation in solution. However, the ion pairing explanation is supported by the positive NOEs observed for compound **61**, even though the molecular mass is greater. A possible explanation for this could be intramolecular ion pairing in compound **61**. No evidence for dimer formation was observed for **61** by

ESI mass spectrometry at the same concentrations at which there was for **60**, which supports the ion pairing explanation.

Final conclusions on the structure of cortamidine oxide (**60**)

The structure of cortamidine oxide was assigned as the mixed disulfide **60**. The oxygen substituent on the tetrahydropyridine was unambiguously assigned by comparison of NMR data with those of the synthetic 2-amino-3,4,5,6-tetrahydropyridine-*N*-oxide (**84**).

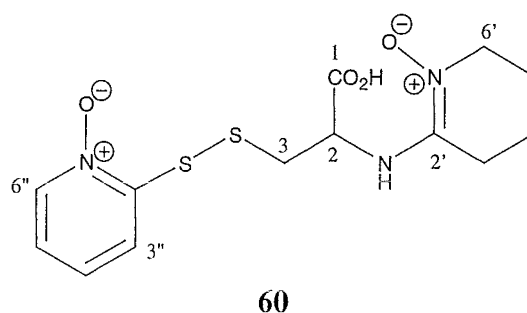


Table 5.2 NMR data for compound **60** (in D₂O)

H/C	δ_{H} (J_{HH} Hz)	δ_{C} #	HMBC	COSY	NOE (all negative)*
1		177.7			
2	3.95 dd (3.9, 8.7)	57.1	177.7, 42.3	3.05/3.19	7.96, 3.39, 3.05/3.19, 2.06/2.15
3a	3.05 dd (8.9, 14.2)	42.3		3.95, 3.19	7.96, 3.95
3b	3.19 dd (3.9, 14.2)		153.3	3.95, 3.05	
2'		153.3			
3'a	2.06 m	24.9	153.3, 23.5, 19.5	2.15, 1.50	3.95
3'b	2.15 m		153.3, 23.5, 19.5	2.06, 1.50	3.95
4'	1.50 m	19.5	153.3, 54.2, 24.9, 23.5	2.06/2.15, 1.66	
5'	1.66 m	23.5	54.2, 24.9, 19.5	3.39, 1.50	3.39
6'	3.39 m	54.2	153.3, 23.5, 19.5	1.66	3.05/3.19, 1.66
2''		153.4			
3''	7.96 d (8.3)	124.9	124.9	7.56	7.56
4''	7.56 m	133.6	153.4, 140.9, 124.9	7.96, 7.26	
5''	7.26 m	124.9	153.4, 140.9, 124.9	8.16, 7.56	
6''	8.16 d (6.4)	140.9	153.4, 133.6, 124.9	7.26	7.26

The carbon chemical shifts are from a ¹³C spectrum run in D₂O with a drop of *d*₆-DMSO for referencing.

* see Section 5.4.2 - *Negative NOEs* p101

5.4.3 Structural assignment of **61**

The first disulfide compound (**59**) to be isolated in this series was the dimer of 2-thiopyridine *N*-oxide. The second was a mixed disulfide and was assigned the name cortamidine oxide and the structure **60**. During the isolation of **60** a third disulfide compound (**61**) was isolated and characterised as the symmetrical dimer of the non-aromatic half of compound **60**.

HRFABMS using a NOBA matrix gave a molecular ion for the sodium salt (MNa^+) of **61** at m/z 457.1193 giving a molecular formula of $\text{C}_{16}\text{H}_{26}\text{O}_6\text{N}_4\text{S}_2\text{Na}$ (requires 457.1192). This is consistent with **61** being a symmetrical dimer of the non-aromatic half of the mixed disulfide **60**. Electrospray ionisation mass spectrometry confirmed this proposed structure with a doubly charged parent ion (MH_2^{++}) observed at m/z 218 when no fragmentation voltage was applied. This ion decreased as the applied voltage was increased to give ions at m/z 434 (M^+) with 50 V and then m/z 251, 185 (**89**), 169 (**90**), 125 (**91**) and 123 (**92**) as the voltage was increased to 150 V. Most of these ions had also been observed for the mixed disulfide **60** (see page 26).

The ^{13}C NMR data for **61** were almost identical ($<\Delta\delta_{\text{C}}$ 0.0-1.2) to those of the relevant part of **60**. The largest difference of $\Delta\delta_{\text{C}}$ 1.2 was an upfield shift for the methylene α to the disulfide bond. This shift brought the resonance closer to that of the equivalent methylene in cystine (δ_{C} 39.0). The differences in the ^1H NMR spectrum (**Fig. 5.10**) were greater than those observed for the carbon resonances. The largest differences were for the methylene protons $\text{H3a'}/\text{H3b'}$ and the methine protons H2 . These three protons shifted upfield by up to $\Delta\delta_{\text{H}}$ 0.24.

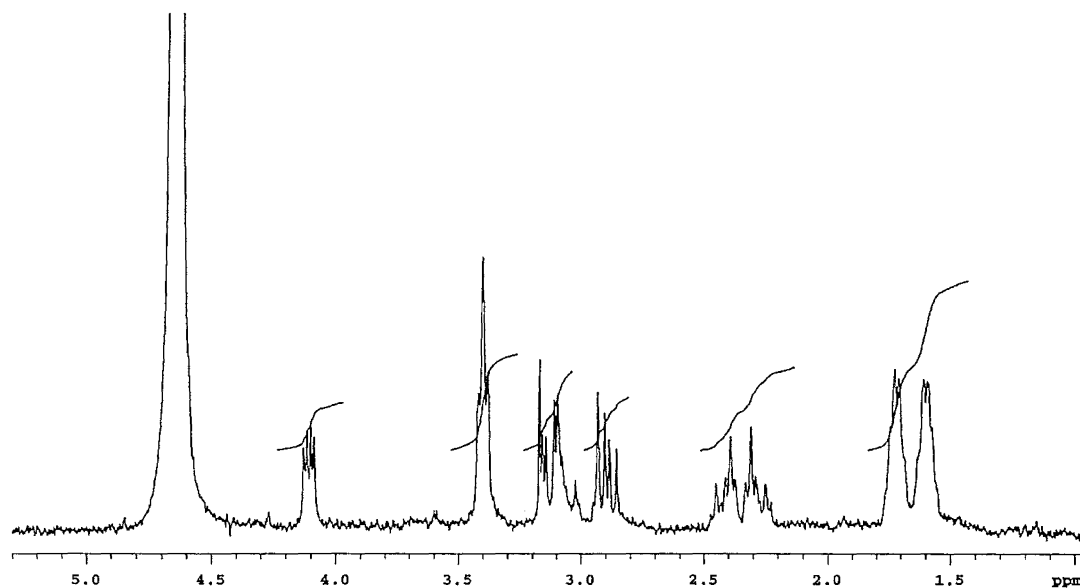


Figure 5.10 ^1H NMR spectrum of **61** (in D_2O)

2-D NMR experiments confirmed the connectivity through the molecule as for **60**. The crucial HMBC correlation from the methine proton at δ_{H} 4.16 to the quaternary carbon at δ_{C} 152.9 was observed in an HMBC experiment when optimisation for long-range coupling constants (J_{nxh}) was set at 4 Hz (**Fig. 5.11**).

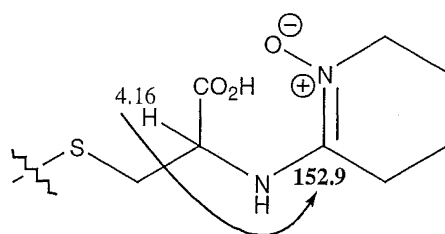


Figure 5.11 HMBC correlation for **61**

The structure of the third disulfide compound was therefore assigned as the symmetric dimer **61**.

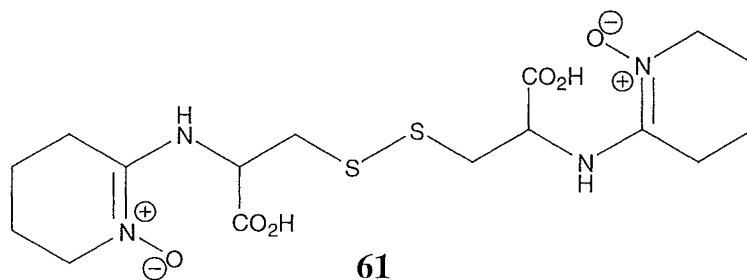


Table 5.3 NMR data for compound **61** (in D₂O)

H/C	δ_{H} (J_{HH} Hz)	δ_{C} #	HMBC	NOE (all positive)*
1		178.5		
2	4.16 dd (8.7, 4.2)	57.3	178.5, 42.1 (153.5 jnxh=4)	2.90/3.12, 2.31/2.39
3a	2.90 dd (14.7, 8.8)	42.1	178.5, 57.3	4.16
3b	3.12 dd (14.6, 4.3)		178.5, 57.3	4.16
2'		152.9		
3'a	2.31 m	25.0	152.9, 23.5, 19.6	4.16, 1.59
3'b	2.39 m			4.16, 1.59
4'	1.59 m	19.6	152.9, 25.0, 23.5	2.31/2.39
5'	1.71 m	23.5	54.1, 25.0, 19.6	3.40
6'	3.40 m	54.1	152.9, 23.5, 19.6	1.71

The carbon chemical shifts are from a ¹³C spectrum run in D₂O with a drop of *d*₆-DMSO for referencing.

* see Section 5.4.2 - *Negative NOEs* p101

The upfield shift of some ¹H NMR resonances between compounds **60** to **61**

The observed upfield shift of the proton resonances for H2 and H3a'/H3b' from compound **60** to **61** could be explained with the loss of an aromatic ring that was shielding these protons in compound **60**. Such anisotropic affects are the principle behind the Mosher's method for the determination of absolute stereochemistry.⁴⁶ An NOE effect was observed between the H3a'/H3b' and the H2 methine protons in both compounds **60** and **61** confirming their close proximity in space. An NOE was also observed between the H2 methine proton of compound **60** and the aromatic proton at δ_{H} 7.96 (H3'') indicating their close proximity in space. The loss of the 2-thiopyridine *N*-oxide ring from the mixed disulfide **60**, via disulfide exchange, removes the shielding effect from many of the protons in the dimer **61**. The protons that were shielded by this aromatic ring in compound **60** would therefore move downfield in the dimer **61** as was observed. Molecular modelling of the mixed disulfide **60** was attempted using Macromodel to see if this was the case but difficulties arose with lack of parameters for

the *N*-oxide functionality. Basic AM1 minimisation of a number of conformers using Spartan gave a low energy conformer with the aromatic ring residing back towards the tetrahydropyridine ring as illustrated in Fig. 5.12. This would be consistent with the NOE between the H3a'/H3b' and the H2 methine protons in both compounds **60** and **61** and between the H2 methine proton of compound **60** and the aromatic proton at δ_{H} 7.96 (H3'').

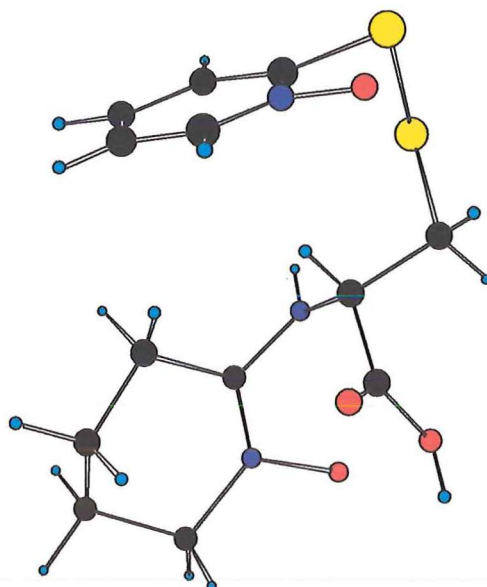


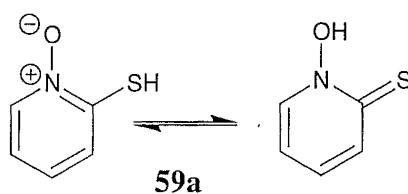
Figure 5.12 Spartan modelling of compound **60**

5.5 Biological activity of 2,2'-dithiobis(pyridine *N*-oxide) (**59**), cortamidine oxide (**60**) and **61**

5.5.1 2,2'-Dithiobis(pyridine *N*-oxide) (**59**)

Compound **59** was isolated as the most biologically active component of the *Cortinarius* species extract and was identified as 2,2'-dithiobis(pyridine *N*-oxide). This compound is commercially available from Aldrich Chemical Company, Inc. The significant antibacterial and antifungal activity observed for compound **59** against all

the micro-organisms screened was consistent with that reported. Compound **59** was also found to be cytotoxic against the P388 cell line with an IC_{50} value of 40 ng/mL. Compounds containing 2-thiopyridine functionality are known to exhibit significant biological activity. 2-Thiopyridine *N*-oxide or *N*-hydroxypyridine-2-thione (**59a**) is reported to have antimicrobial³ and anticancer activity⁹² and the zinc salt is the active ingredient in several antidandruff shampoos.⁹³ This biological activity has been attributed to both their chelating properties with metal ions (Fe^{3+} and Zn^{2+}) and their ability to produce photogenerated radical species.⁹⁴



5.5.2 Cortamidine oxide (**60**) and compound **61**

The second compound isolated and assigned as cortamidine oxide (**60**) was found to have the same spectrum of antifungal and antibacterial activity and cytotoxicity to that of **59**, but approximately 2-fold less active. Compound **61** (the symmetrical dimeric disulfide of the non-aromatic part of **60**) was found to have no biological activity in the assays screened. It would therefore seem clear that the biological activity of cortamidine oxide (**60**) arises from the 2-thiopyridine *N*-oxide group.

5.6 Conclusions

Three compounds were isolated from the *Cortinarius* species collected in the Catlins and structurally assigned as 2,2-dithiobispyridine *N*-oxide (**59**), cortamidine oxide (**60**) and a second symmetrical disulfide **61**. The two symmetrical dimers (**59** and **61**) arise via disulfide exchange from the unsymmetrical cortamidine oxide (**60**). This type of exchange has been reported during the isolation of compounds that contain disulfide bonds.⁸⁰ All three compounds contain *N*-oxide functionality. Compounds **59** and **60** both contained 2-thiopyridine *N*-oxide functionality. This functionality is consistent with the biological activity (cytotoxicity and antimicrobial activity) observed for compounds **59** and **60**. The zinc salt of 2-thiopyridine *N*-oxide is in fact the active ingredient in many antidandruff shampoos.⁹³ Compounds containing pyridine *N*-oxide functionality have been reported from species in the *Cortinarius* genus before, namely the toxin orellanine (**62**).⁷² Both cortamidine oxide (**60**) and the symmetrical disulfide **61** contained a fragment assigned as an amidine *N*-oxide. No natural products were found in the literature that contained this functionality, although a number of synthetic compounds have been reported, including 2-amino-6,6-dimethyl-3,4,5,6-tetrahydropyridine-*N*-oxide (**83**)⁸⁸ and 2-amino-5,5-dimethylpyrroline *N*-oxide (**82**).⁸⁷

CHAPTER SIX

CORTINARIUS ROTUNDISPORUS

6.1 Introduction

Organic extracts of *Cortinarius rotundisporus* Cleland & Cheel[#] showed significant cytotoxicity in the screening programme of Australian fungi. This mushroom was targeted for further investigation due to this observed activity and because a large amount was available from Dr Melvyn Gill (Department of Chemistry, University of Melbourne). Two related compounds were isolated and identified as the malabaricane derivatives rotundisine A (**94**) and B (**95**). The extraction and chromatography of these compounds is described in **Section 6.2** and **6.3**. The structural elucidation of compounds **94** and **95** is described in **Section 6.4** of this chapter.

[#]May, T.M.; Wood, A.E., *Fungi of Australia Volume 2A, Catalogue and Bibliography of Australian*

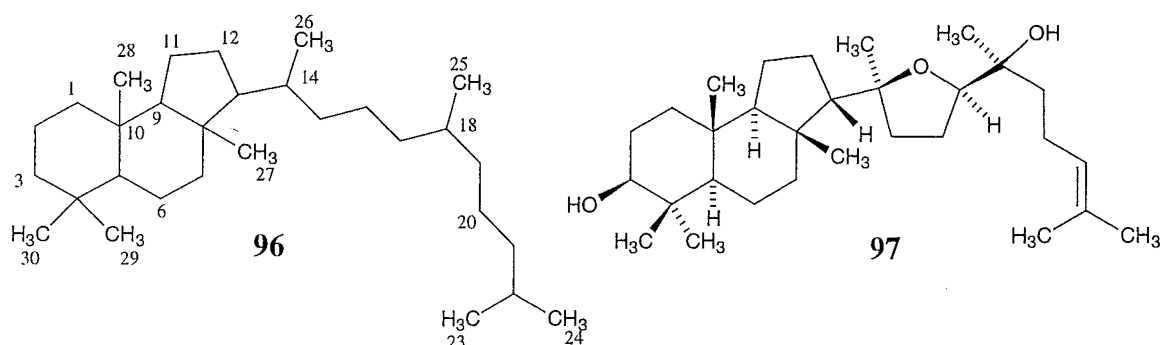
Macrofungi I. Basidiomycota p.p. , 1997, Australian Biological Resources Study, Canberra.

6.1.1 Natural products isolated from the *Cortinarius* genus

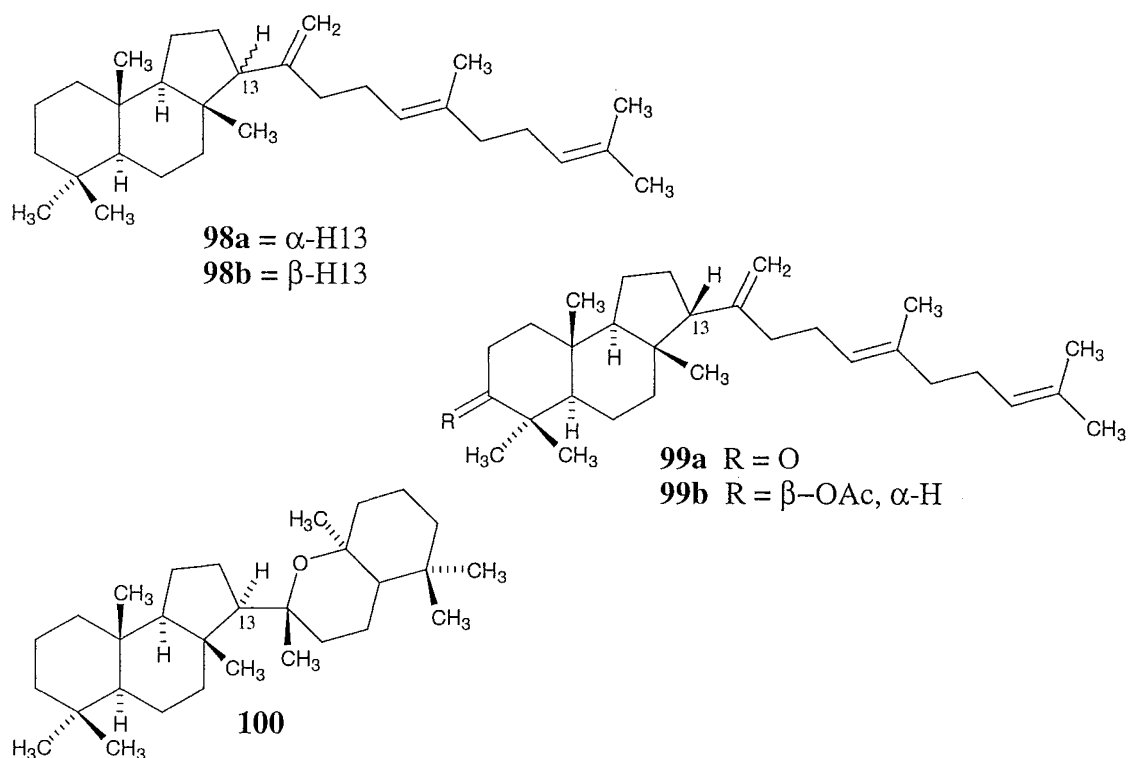
A description of the biologically active natural products that have been isolated from mushrooms in the *Cortinarius* genus can be found in the **Introduction to Chapter Five**.

6.1.2 Malabaricane triterpenes isolated from plants

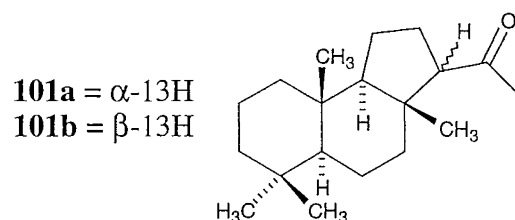
The malabaricane skeleton (**96**) was first proposed when the triterpene malabaricol (**97**) was isolated from the bark of the plant *Ailanthus malabarica* DC (Kannaka, *Hal-maddi*; Malayalam, Mattipal).⁹⁵ The absolute stereochemistry of malabaricol (**97**) was established by X-ray crystallographic analysis.⁹⁶



A number of malabaricane derivatives have been isolated from other plants including the fern *Lemmaphyllem microphyllum* var. *obovatum* (**98a** and **98b**),⁹⁷ the flowering plant *Pyrethrum santolinoides* DC (= *Tanacetum sinaicum* Del. Ex DC) (**99a** and **99b**)⁹⁸ and *Colysis elliptica* Ching (**100**).⁹⁹ The skeleton of compounds **99a** and **99b** is thought to be the biosynthetic precursor to the original malabaricol (**97**).⁹⁸



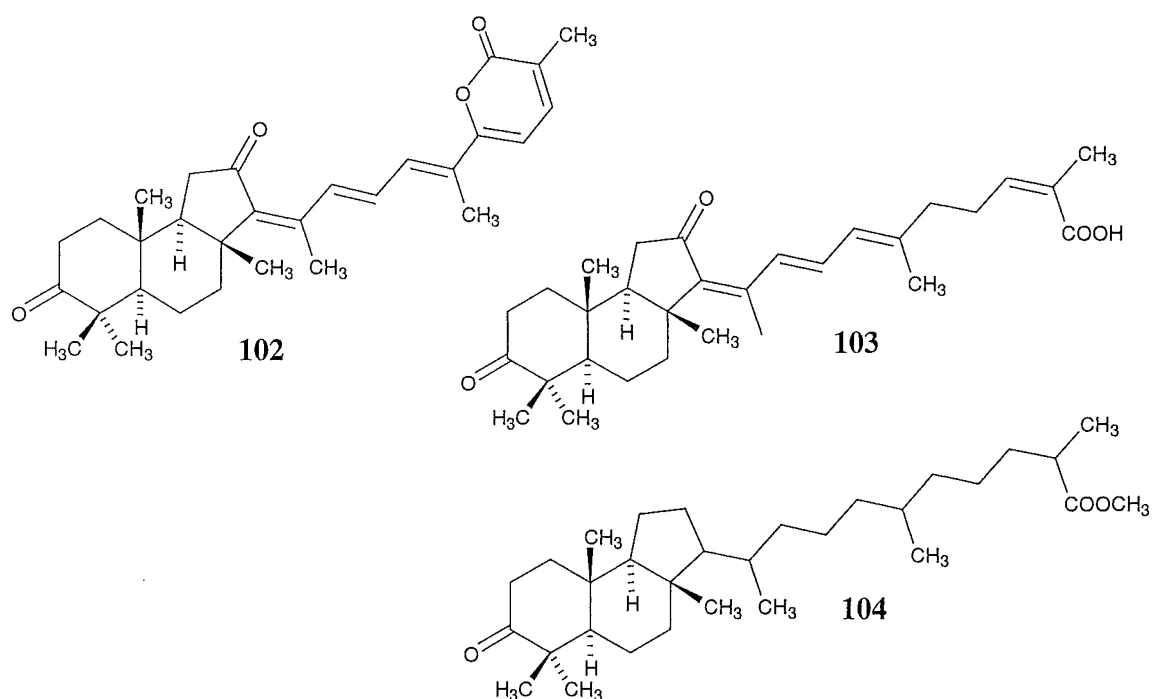
Natural products have been isolated that have both the α -H and β -H stereochemistry at C13. Compound **98b** (β -H13) was degraded to the ketone **101b** and compared with the analogous ketone derived from malabaricol (**97**) (also the β -H ketone, **101b**) by their respective CD and ORD spectra and were found to be identical in all aspects. Since the absolute stereochemistry of malabaricol was known, the absolute stereochemistry of compounds **98b** (β -H13) could be determined.⁹⁷ For compounds **99a** and **99b**, the relative stereochemistry was obtained from NMR data using NOE experiments.



6.1.3 Malabaricane/Isomalabaricane triterpenes from marine sources

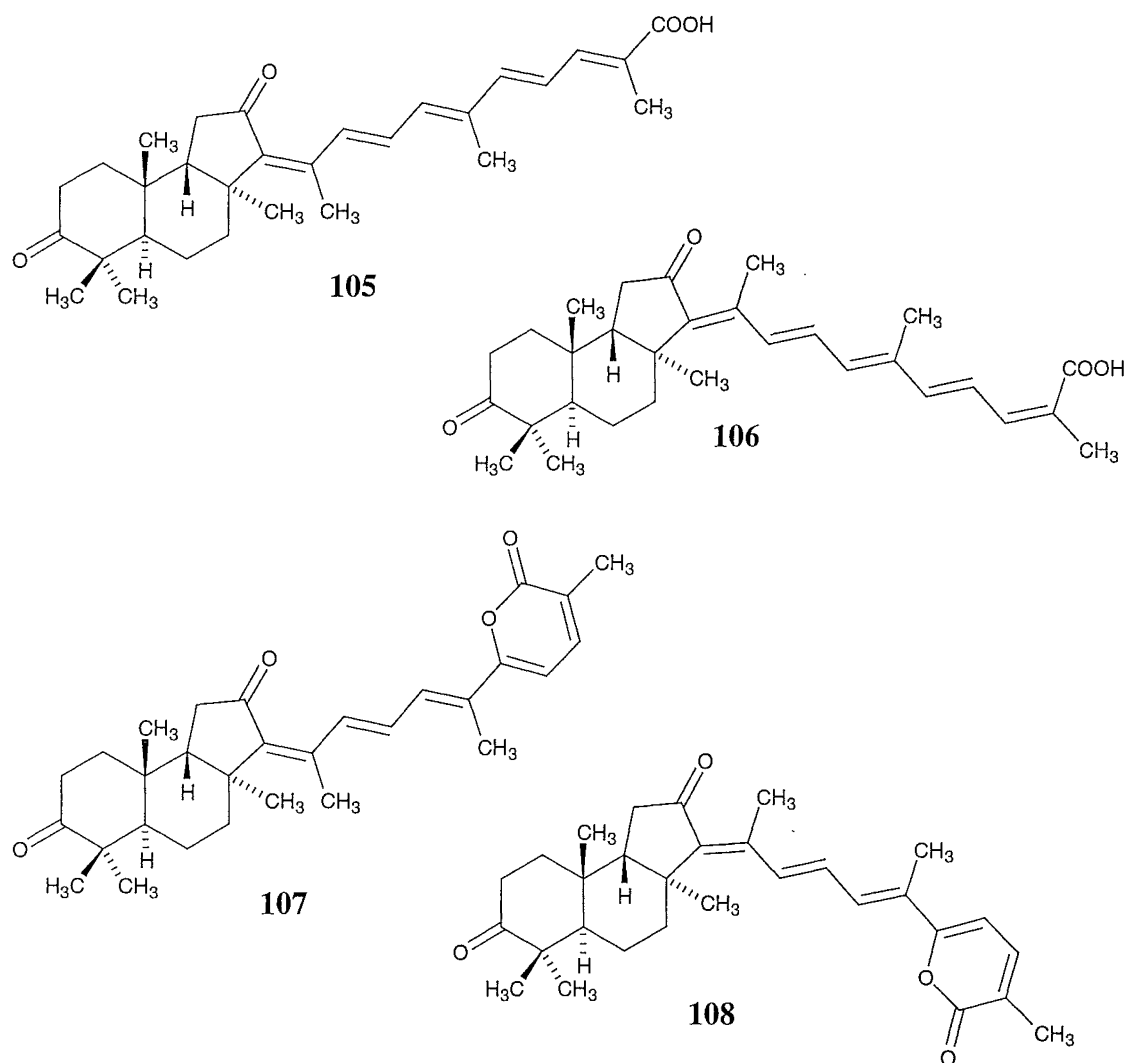
Stellettin

The first reported isolation of a triterpene with the malabaricane skeleton from a marine organism was from the Fijian sponge *Jaspis stellifera*. Three compounds were isolated and structurally assigned including compounds **102** and **103**. The relative configuration of compound **102** was originally misassigned from a CD study of the hydrogenation product **104** as *trans-anti-trans*, the same as the original plant-derived malabaricol (**97**).¹⁰⁰



Subsequently, other groups have isolated compounds including stellettin E (**105**), stellettin F (**106**), stellettin B (**107**) and stellettin A (**108**) from a variety of *Stelletta* sponges.^{101,102,103} The ¹H and ¹³C NMR data for stellettin B (**107**) were identical to those reported for **102**. The absolute stereochemistry for stellettin B (**107**) was elucidated by X-ray crystallographic analysis with the ring stereochemistry for these triterpenes, isolated from marine organisms, being correctly assigned as *trans-syn-trans*, as shown in compounds **105-108**. The carbon skeleton with the *trans-syn-trans* ring

junctions is now known as isomalabaricane.¹⁰¹ The relative stereochemistry of compounds **105**, **106** and **108** was assigned by using NOE experiments.



Globostellatic acids

Further triterpenes with the isomalabaricane skeleton have been isolated from a Japanese marine sponge *Stelletta globostellata* Carter, 1883 (Stellettidae). Bioassay guided isolation yielded four compounds, the globostellatic acids A-D.¹⁰⁴

Biological activity of the stellettins and globostellatic acids

All of these marine derived isomalabaricanes have shown cytotoxicity in a variety of assays. Stellettins A-F are all cytotoxic and have been assessed against the NCI 60-cell line screen with GI₅₀ values of 0.28 μ M (stellettins A/B (**107/108**)), 0.09 μ M (stellettins C/D) and 0.98 μ M (stellettins E/F (**105/106**)).¹⁰⁵ The globostellatic acids A-D are cytotoxic against the P388 murine leukaemia cell line, with IC₅₀ values of 0.1, 0.1, 0.45 and 0.1 μ g/mL, respectively.¹⁰⁴

6.2 Extraction of *Cortinarius rotundisporus*

Original screening result

The original sample (2 g) of *Cortinarius rotundisporus* (95MG1-222) was extracted with 3:1 MeOH/CH₂Cl₂. This crude extract showed cytotoxicity against both the P388 cell line (IC₅₀ 4752 ng/mL) and the BSC-1 cell line (host cell line in the antiviral assay). A visual description of the BSC-1 cells after incubation with this sample was 12 (large scruffy cells), which is often observed for compounds that show inhibition against protein phosphatase.¹⁰⁶ *C. rotundisporus* was considered a good target for further investigation because no chemistry was known and a good supply of the fruiting bodies was available.

Extraction

A sample (634 g - including ice) of *C. rotundisporus* fruiting bodies was extracted twice with ethanol (Dr Malcolm Buchanan, Melbourne), yielding two brown extracts (1.95 g and 880 mg). Both extracts were separately partitioned between H₂O and EtOAc (Dr Malcolm Buchanan, Melbourne - first extract). All four residues were submitted for biological assay against the P388 cell line. Both of the EtOAc residues showed

cytotoxicity against the P388 cell line, with IC₅₀ values of 3400 ng/mL (1st extraction) and 4200 ng/mL (2nd extraction).

Chemical Screening

A small sample of the EtOAc residue of the *C. rotundisporus* extract was examined using “chemical screening.”[‡] All samples that eluted from the cartridges were submitted for assay against the P388 cell line. The cytotoxicity eluted in the MeOH fraction from reverse-phase (C18), the third MeOH fraction from gel permeation (LH20) and the CH₂Cl₂ and EtOAc fractions from normal-phase (DIOL).

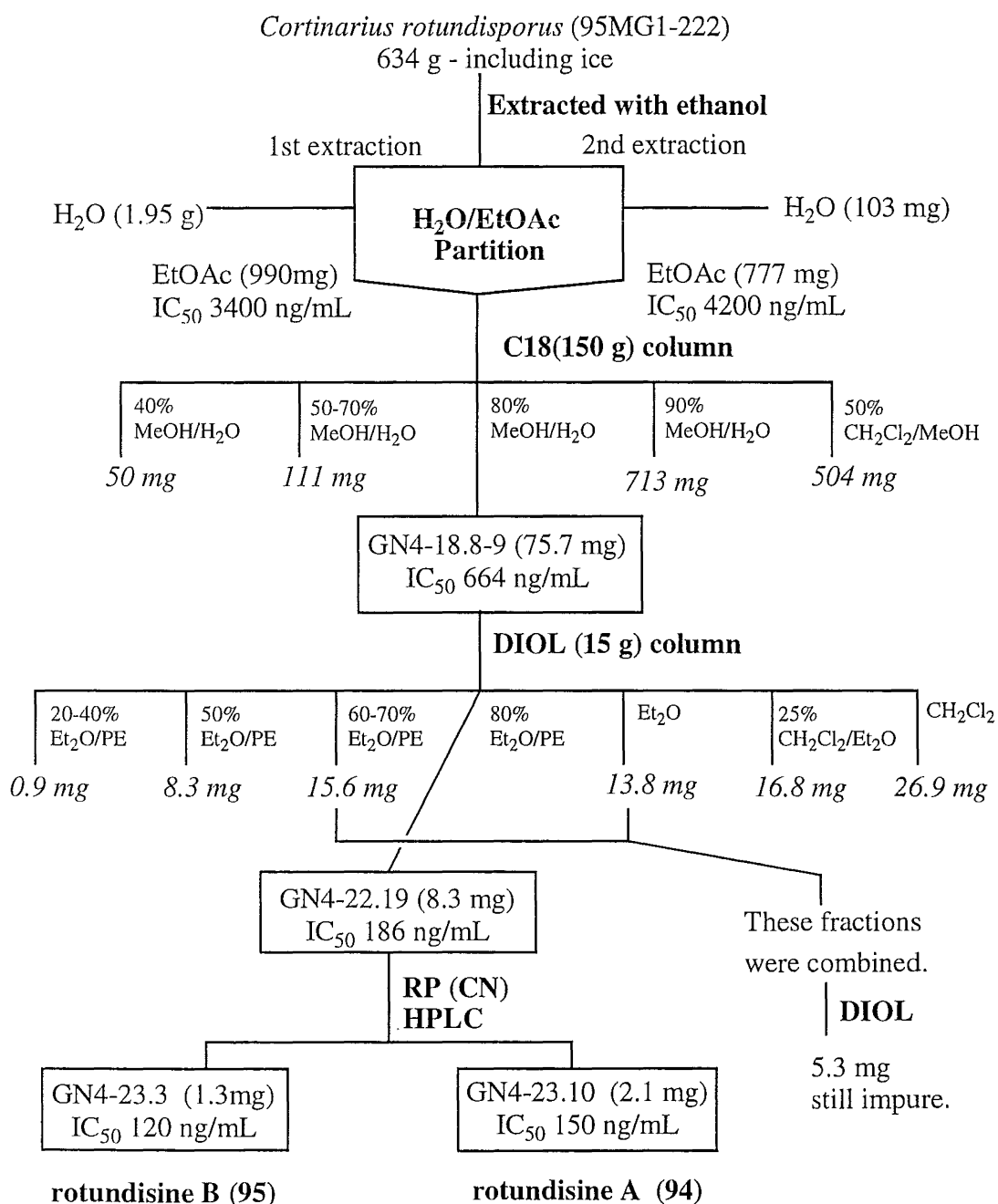
The choice of phase for the initial chromatography was therefore reverse-phase (C18), as the activity eluted cleanly in the MeOH fraction. This good separation is in contrast to the normal-phase (DIOL), where the activity eluted in both the CH₂Cl₂ and EtOAc fractions.

[‡] A procedure developed in the Marine Group for the rapid evaluation of chemical and physical properties of bioactive extracts.

6.3 Chromatography of *Cortinarius rotundisporus* extract

A general outline of the chromatography that was used to isolate compounds **94** and **95** is given in Scheme 6.1.

Scheme 6.1



Chromatography of residues from the EtOAc partition

The combined EtOAc residues GN4-11.1 (990 mg) and GN4-11.3 (777 mg) were loaded onto a reverse-phase (C18) column and eluted with a stepped gradient from H₂O through MeOH, and finally stripped with CH₂Cl₂. Fractions were collected and assayed for cytotoxicity against the P388 cell line. The activity was centred on fraction GN4-18.8 (39.6 mg) with an IC₅₀ value of 488 ng/mL. Fractions GN4-18.8-9 were combined due to their similar ¹H NMR spectra and assay results.

The combined sample of GN4-18.8-9 (75.7 mg) was loaded onto a normal-phase (DIOL) column, eluted with a stepped gradient from petroleum ether through ether, CH₂Cl₂, and finally stripped with MeOH. Fractions were collected, and combinations made by TLC (DIOL). Combined fractions were submitted for assay against the P388 cell line and examined by ¹H NMR spectroscopy. The cytotoxicity centred on fraction GN2-22.19 (8.3 mg) with an IC₅₀ value of 186 ng/mL. The ¹H NMR spectrum of this fraction was very crowded and appeared to contain at least two main components. Surrounding fractions also showed some cytotoxicity, and the ¹H NMR spectra of these fractions were similar to those of GN2-22.19. Although the ¹H NMR spectra of these fractions were crowded, two signals consistent with aldehyde protons (δ_{H} 9.43 and 10.28) were present in all the cytotoxic samples. A selection of chromatographic phases were tested by TLC to optimise separation of these remaining components. Reverse-phase on C18 and CN gave poor separation (1:1 to 4:1 MeOH/H₂O) while normal-phase on CN (IPA/hexanes) gave excellent separation.

Purification of cytotoxic fraction GN4-22.19

Analytical HPLC on CN with a normal-phase solvent (3% IPA/hexanes) gave well-separated peaks. Fraction GN4-22.19 (8.3 mg) was then separated by semi-preparative CN HPLC (3% IPA/hexanes), with two main peaks being collected. The first was GN4-23.3 (RT 51 min, 1.3 mg, IC₅₀ 120 ng/mL) and the second GN4-23.10 (RT 104

min, 2.1 mg, IC₅₀ 150 ng/mL). Both these samples were shown to be homogenous by TLC and ¹H NMR spectroscopy. Subsequent structural elucidation using a combination of mass spectrometry and NMR experiments enabled their assignment as rotundisine A (**94**) and B (**95**).

Purification of fractions surrounding GN4-22.19

To obtain more of **94** and **95** the surrounding fractions from the last column (GN22.17-18 and 22.20-22) that by ¹H NMR spectroscopy contained these aldehydes (δ_{H} 9.43 and 10.28) were combined and further chromatographed. However, this was unsuccessful, as the compounds appeared to be decomposing. A drop in specific activity (mass/IC₅₀) as the attempted purification proceeded also suggested decomposition may have been occurring.

6.4 Structural elucidation of compounds **94** and **95**

The ¹H NMR spectra of **94** (Fig. 6.1) and **95** (Fig. 6.17) were very similar. More of compound **94** was available, so the structural elucidation was attempted on this compound first.

6.4.1 Structural elucidation of compound **94**

General features of compound **94**

The molecular formula of **94** was determined as C₃₂H₄₈O₇ from HREIMS. FABMS (*d*-glycerol matrix) run after MeOD exchange showed two exchangeable protons due to the MD⁺ at 548 (from a MH⁺ of 545). Three carbonyl resonances were observed in the IR spectrum (1666, 1720 and 1737 cm⁻¹).

One of the carbonyl absorption bands was consistent with an acetate, which was supported by the characteristic methyl signal in the ^1H NMR spectrum (**Fig. 6.1**) at δ_{H} 2.08. The ^1H NMR spectrum also showed an aldehyde signal at δ_{H} 10.28, three olefinic or aromatic methine protons (δ_{H} 6.22, 6.89 and 7.25) and three methines possibly attached to oxygenated carbons. In the aliphatic region of the ^1H NMR spectrum (**Fig. 6.1**) there were six methyl singlets (δ_{H} 0.91, 0.98, 1.14, 1.25, 1.26 and 1.38) and a number of methylene signals. This large number of aliphatic methyl signals is characteristic of a terpenoid-type skeleton.

All one-bond C-H connectivities were obtained from correlations in the HSQC spectrum. HMBC and HSQC NMR experiments were originally run in CDCl_3 and subsequently in d_6 -benzene, which allowed separation of some overlapping signals. HMBC and HSQC NMR experiments were also run in d_6 -DMSO so the exchangeable hydroxy protons could be observed and assigned.

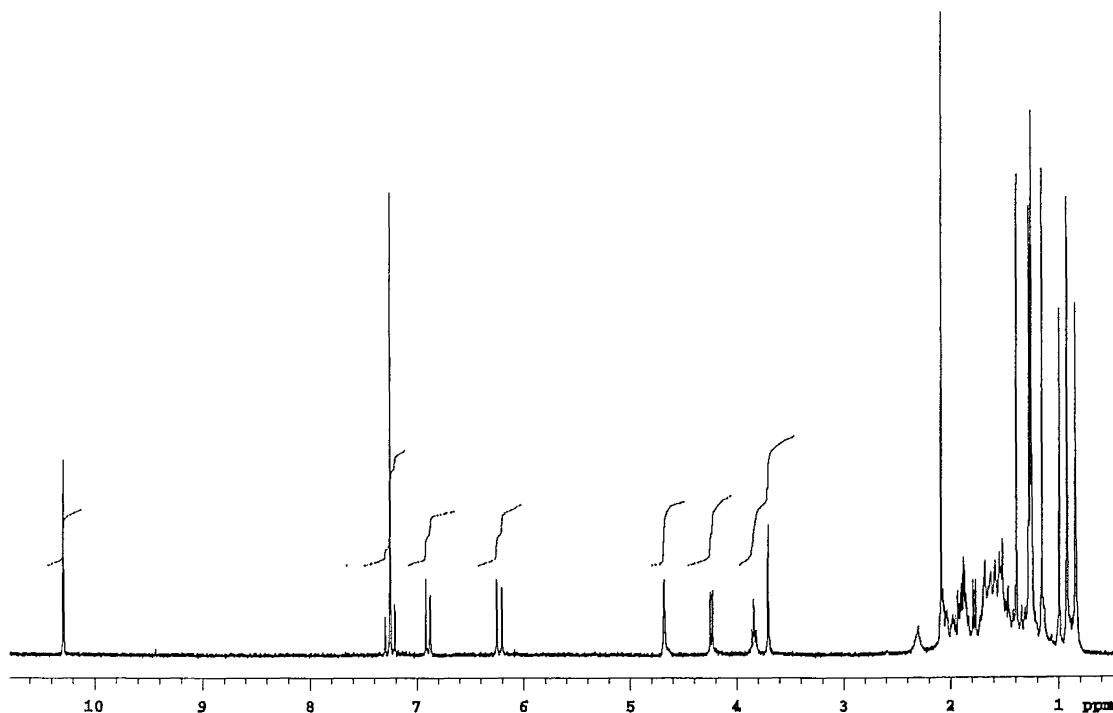


Figure 6.1 ^1H NMR spectrum of **94** (in CDCl_3)

Connectivity through the tricyclic system

The methyl protons at δ_{H} 2.08 (δ_{C} 21.3) were assigned as an acetate due to an HMBC correlation to the carbonyl at δ_{C} 170.6. The methine at δ_{H} 4.68 (δ_{C} 78.2) also showed a correlation to this carbonyl. Each of the methyl groups at δ_{H} 0.83 (δ_{C} 27.9) and δ_{H} 0.91 (δ_{C} 21.2) showed HMBC correlations to each other's carbon, and then both to three other carbon resonances (δ_{C} 78.2, 51.5 and 36.6). The methine at δ_{H} 4.68 (δ_{C} 78.2) also showed an HMBC correlation to the methine at δ_{C} 51.5 (δ_{H} 1.52). The assignment of this fragment is illustrated in **Fig. 6.2**.

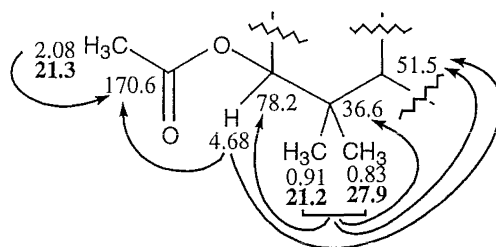


Figure 6.2 HMBC correlations for **94**

The assignment of a second fragment (**Fig. 6.3**) started with 1-D TOCSY correlations (in CDCl₃) from the methine at δ_{H} 4.24 (δ_{C} 72.1) to the methine at δ_{H} 1.78 (δ_{C} 60.9). The oxygenated substituent at the δ_{H} 4.24 methine was assigned from ¹H, HMBC and HSQC NMR spectra run in *d*₆-DMSO as a hydroxy group (δ_{H} 5.82). HMBC correlations were observed from this hydroxy proton at δ_{H} 5.82 to the carbons at δ_{C} 60.9 and δ_{C} 72.1. A 1-D TOCSY experiment (in *d*₆-DMSO) where the proton at δ_{H} 5.82 was irradiated showed a sequential increase in intensity of the signals at δ_{H} 4.24 and then δ_{H} 1.78, as the mixing time was increased from 0.01 to 0.08 s. The methine at δ_{C} 60.9 is relatively downfield for one that is only attached to carbons, but it does have two β -methyl groups, which would account for the observed chemical shift.

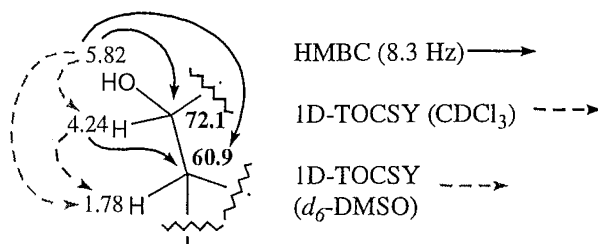


Figure 6.3 HMBC and 1-D TOCSY correlations for **94**

The fragment illustrated in **Fig. 6.3** was further extended to form a five-membered ring with correlations from the methine at δ_{H} 1.78 to a quaternary carbon at δ_{C} 45.9 and to a methyl carbon at δ_{C} 18.9. The corresponding methyl protons at δ_{H} 0.98 (δ_{C} 18.9) showed correlations to the same quaternary carbon at δ_{C} 45.9, to the methine at δ_{C} 60.9 and to the methylene at δ_{C} 40.1. The protons of this methylene (δ_{H} 1.44/1.60, δ_{C} 40.1) showed an HMBC correlation to a methine at δ_{C} 61.1. The protons (δ_{H} 3.71) of this methine (δ_{C} 61.1) showed HMBC correlations to the quaternary carbon at δ_{C} 45.9, the methylene at δ_{C} 40.1, the methyl at δ_{C} 18.9, and to the ketone at δ_{C} 216.7. In an HMBC experiment where the optimisation for long-range coupling constants was set at 2 Hz, a correlation was observed from the methine at δ_{H} 4.24 to the ketone at δ_{C} 216.7, therefore confirming the fragment as illustrated in **Fig. 6.4**. The chemical shifts of the C^{13} carbon (δ_{C} 61.1) and proton (δ_{H} 3.71) are relatively downfield for a methine with no oxygen atom directly attached. However, this carbon is both α to an olefin and a ketone, which would account for the observed chemical shifts.

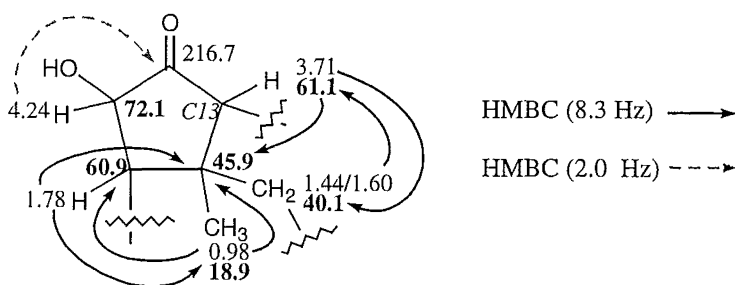


Figure 6.4 HMBC (J_{nxh} 8.3 and 2.0 Hz) correlations for **94**

The fragments illustrated in **Fig. 6.2** and **6.4** were joined to give that shown in **Fig. 6.5** due to HMBC correlations from the methyl protons at δ_{H} 1.26 to the quaternary carbon

to the methine carbons at δ_C 60.9 and 51.5. The methine at δ_H 1.78 showed an HMBC correlation to the methyl at δ_C 17.5 in addition to those mentioned above. In an HMBC experiment where the optimisation for long-range coupling constants was set at 4.0 Hz (in comparison to the usual 8.3 Hz), a correlation was observed from the methine at δ_H 1.78 to the methine carbon at δ_C 51.5 (see **Fig. 6.5**).

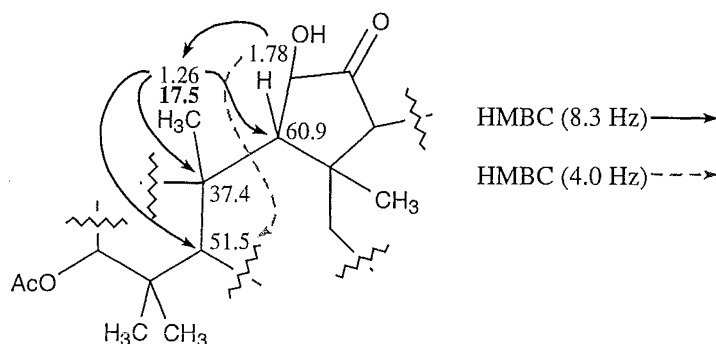


Figure 6.5 HMBC (J_{nh} 8.3 and 4.0 Hz) correlations for **94**

The tricyclic structure illustrated in **Fig. 6.6** was assigned using a combination of HMBC and HSQC-TOCSY correlations. The methine at δ_H 4.68 showed an HSQC-TOCSY correlation to a methylene at δ_C 22.4 when the mixing time was 0.02 s, and then a correlation to a second methylene at δ_C 33.1 with a mixing time of 0.08 s. The methyl at δ_H 1.26 showed an HMBC correlation to the methylene at δ_C 33.1, confirming the assignment. The second ring was established with HMBC and HSQC-TOCSY correlations from the methylene protons at δ_H 1.44/1.60 to another methylene at δ_C 18.6 and to the methine at δ_C 51.5. These correlations are illustrated in **Fig. 6.6**.

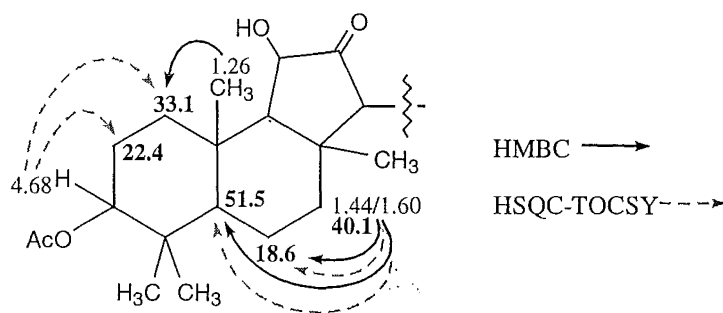


Figure 6.6 HMBC and HSQC-TOCSY correlations for **94**

Assignment of the substituted diene system

Further connectivity through the molecule was achieved with HMBC correlations from the methine at δ_{H} 3.71 to the quaternary olefinic carbon at δ_{C} 130.2, the aldehyde carbon at δ_{C} 189.3 and to the olefinic methine at δ_{C} 150.2. The aldehyde proton also showed an HMBC correlation to the quaternary olefinic carbon at δ_{C} 130.2 and to the methine at δ_{C} 61.1. Connectivity through the olefinic system was achieved using a combination of HMBC and HSQC-TOCSY correlations, and coupling constants, with a selection illustrated in **Fig. 6.7**. A NOESY correlation was observed between the aldehyde proton (δ_{H} 10.28) and the olefinic proton at δ_{H} 7.25. The spatial proximity of these two protons allowed the assignment of the olefin between the carbons at δ_{C} 130.2 and 150.2 as having the *Z* stereochemistry. The second olefin was assigned as the *E* stereochemistry from the magnitude of the coupling constant ($J_{\text{HH}} = 14.7$ Hz) between the protons at δ_{H} 7.25 and 6.22.

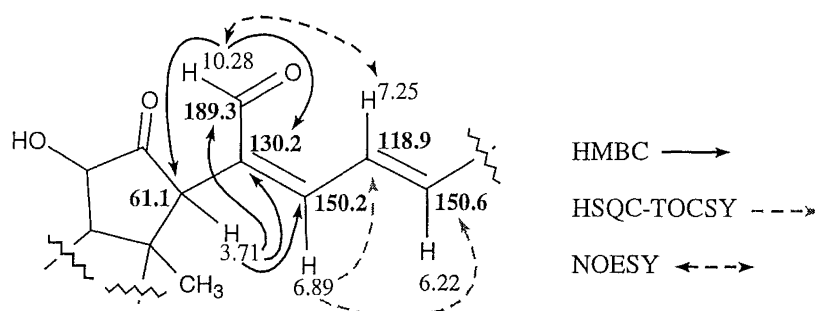


Figure 6.7 HMBC, HSQC-TOCSY and NOESY correlations for **94**

Assignment of the substituted tetrahydrofuran system

At this point, there was one double bond equivalent and two oxygen atoms from the molecular formula unassigned. Connectivity from the diene system was achieved with HMBC correlations from the methine protons at δ_{H} 6.22 and 7.25 to an oxygenated quaternary carbon at δ_{C} 82.7. The methyl at δ_{H} 1.38 showed correlations to this same carbon (δ_{C} 82.7), the olefinic carbon at δ_{C} 150.6 and the methylene at δ_{C} 38.1. The proton at δ_{H} 3.84 showed HSQC-TOCSY correlations to the methylene at δ_{C} 26.3 when the mixing time was 0.02 s, and then to δ_{C} 38.1 when the mixing time was increased to

0.08 s. The assignment of these methylene protons was achieved with correlations in the HSQC spectrum from δ_{H} 1.88 to the carbon at δ_{C} 26.3, and from δ_{H} 1.86 and 1.92 to the carbon at δ_{C} 38.1. The final three carbons were assigned from HMBC correlations from the methyl protons at δ_{H} 1.14 and 1.25 to the methine carbon at δ_{C} 86.1 (δ_{H} 3.84), a quaternary oxygenated carbon at δ_{C} 70.9 and to the other's carbon. The oxygen substituent of the quaternary carbon at δ_{C} 70.9 was assigned from the HMBC spectrum, run in d_6 -DMSO, as the hydroxyl proton at δ_{H} 4.26. HMBC correlations were observed from this proton (δ_{H} 4.26) to the quaternary carbon at δ_{C} 70.9 and to the two methyl groups at δ_{C} 24.2 and 27.3 (as illustrated in **Fig. 6.8**).

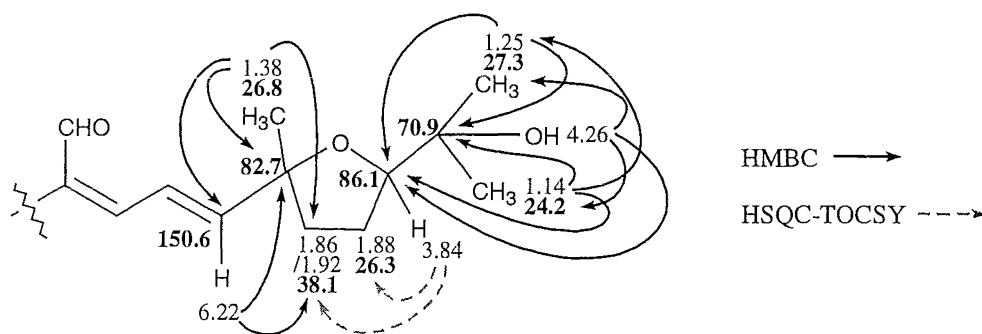
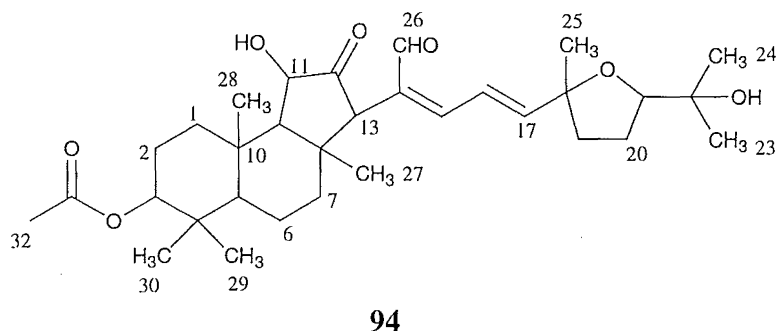


Figure 6.8 HMBC and HSQC-TOCSY correlations for **94**

The two exchangeable protons, initially detected by MS, had therefore been assigned. Consequently, the final double bond equivalent must arise from an ether bond between the carbons at δ_{C} 82.7 and δ_{C} 86.1, to form the five-membered ring as illustrated in **Fig. 6.8**. The structure was therefore assigned as **94**.



Assignment of relative stereochemistry of **94**

The relative stereochemistry of **94** was assigned from correlations in the NOESY spectrum and analysis of coupling constants from the ^1H NMR spectrum. NOESY correlations from the proton at δ_{H} 4.68 (H3) to both of the geminal methyls at δ_{H} 0.91 (Me30) and δ_{H} 0.83 (Me29) allowed the assignment of the H3 proton (δ_{H} 4.68) as equatorial (**Fig. 6.9**). From the ^1H NMR spectrum, the $^3J_{\text{HH}}$ coupling constants for the H3 proton were measured as 2.6 Hz. This is consistent with the H3 proton being equatorial. The acetate group (C31-32) was therefore assigned as being axial. Further NOESY correlations between the methyl at δ_{H} 0.91 (Me30), the methyl at δ_{H} 1.26 (Me28) and the proton at δ_{H} 2.03 (H2a) allowed the assignment of all three as axial (**Fig. 6.9**). The H2b proton at δ_{H} 1.66 was therefore assigned as equatorial.

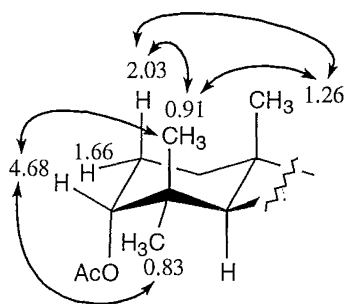


Figure 6.9 NOESY correlations for **94**

A NOESY correlation from the methyl at δ_{H} 1.26 (Me28) to the methyl at δ_{H} 0.98 (Me27) established both as axial. NOESY correlations from the methine proton at δ_{H} 1.52 to the equatorial Me29 at δ_{H} 0.83 and to H9 at δ_{H} 1.78 allowed the assignment of the ring junctions as *trans-anti-trans*. This stereochemistry of the ring junctions is the same as that assigned to malabaricol (**97**).⁹⁶ The H9 proton was also correlated to the proton at δ_{H} 3.71 (H13) in the NOESY spectrum, which allowed the assignment of H13 as axial. These correlations are illustrated in **Fig. 6.10**.

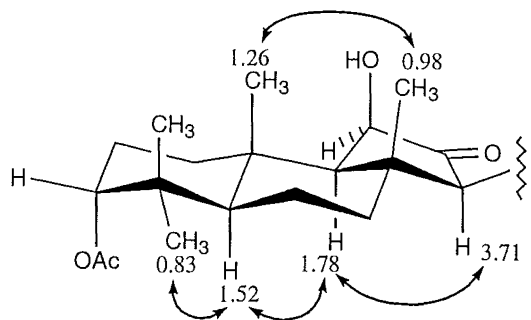


Figure 6.10 NOESY correlations for **94**

Of the two protons on the C7 methylene (δ_{H} 1.44/1.60), the one at δ_{H} 1.60 was assigned as axial due to a NOESY correlation with the H13 proton (δ_{H} 3.71). When the proton at δ_{H} 4.24 (H11) was irradiated in a 1-D NOESY experiment, an enhancement was observed for H9 (δ_{H} 1.78). H9 had been assigned as axial due to a number of NOESY correlations as detailed above so H11 (δ_{H} 4.24) must therefore be equatorial as illustrated in **Fig. 6.11**.

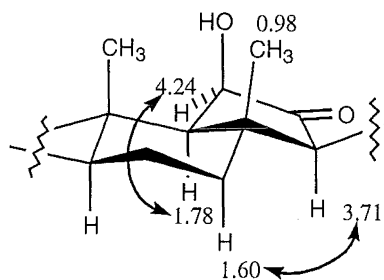


Figure 6.11 NOESY correlations for **94**

NOESY correlations were observed between the Me27 (0.98) and the olefinic proton at δ_{H} 6.89 (H16), suggesting a conformation with the aldehyde pointing away from the ketone of the tricyclic structure. The aldehyde proton at δ_{H} 10.28 (H26) was correlated to the olefinic proton at δ_{H} 7.25 in the NOESY spectrum, confirming their proximity in space (as seen in **Fig. 6.12**).

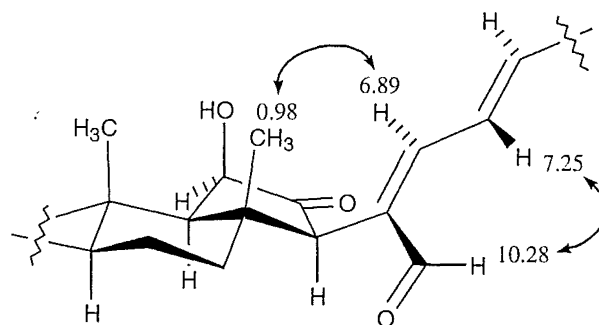


Figure 6.12 NOESY correlations for **94**

The relative stereochemistry of the substituted tetrahydrofuran fragment was established with NOESY correlations, and was supported by molecular modelling. The methyl protons at δ_{H} 1.38 (Me25) were correlated in the NOESY spectrum to both the olefinic protons at δ_{H} 6.22 (H17) and 7.25 (H16). The methine proton at δ_{H} 3.84 (H22) was correlated to the H16 olefinic proton. For H22 and H16 to be close in proximity, *anti* relative stereochemistry across the ring is required. The methine proton at δ_{H} 3.84 (H22) was also correlated to both the methyl groups at δ_{H} 1.14 (Me23) and δ_{H} 1.25 (Me24) of the isopropanol fragment. The methyl at δ_{H} 1.38 (Me25) was also correlated in the NOESY spectrum to the H19b (δ_{H} 1.86) methylene proton on the ring.

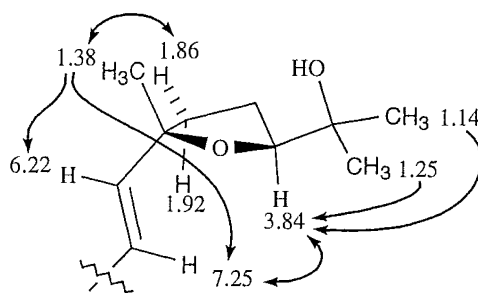


Figure 6.13 NOESY correlations for **94**

Conformational analysis using the Monte Carlo method on a simplified model (**Fig. 6.14**) revealed two conformations of comparable energy that by the Boltzman distribution made up approximately 75% of the population.¹⁰⁷ All the NOESY correlations could be accounted for by examination of the distances between the protons in these conformers (**Fig. 6.14**).

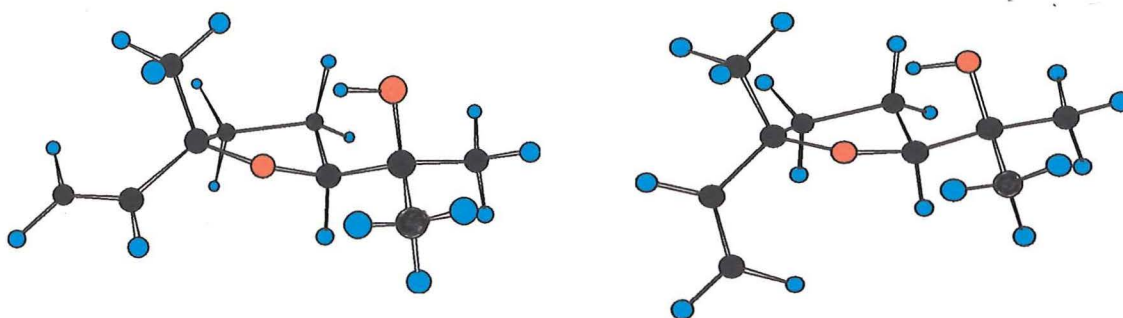


Figure 6.14 The two conformers generated from the Monte Carlo conformational analysis of the of *anti* substituted tetrahydrofuran model

Further molecular modelling supported the assignment as *anti*. A Monte Carlo search of conformational space for the *syn* substituted tetrahydrofuran model (**Fig. 6.15**) revealed only one significant conformer. The observed NOESY correlations were inconsistent with this conformer.

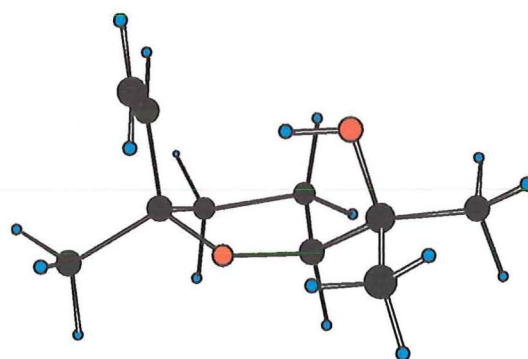


Figure 6.15 The conformer generated from the Monte Carlo conformational analysis of the *syn* substituted tetrahydrofuran

The assigned substituted tetrahydrofuran system has been found in a number of other natural products. The relative stereochemistry of several of these compounds was assigned by the comparison of their ^1H and ^{13}C NMR data with similar compounds where X-ray crystal structures had been obtained.^{108,109,110,111,112,113} Comparison of the ^1H and ^{13}C NMR data for the reported compounds showed differences of approximately $\Delta\delta_{\text{H}}$ 0.1 between the H21 protons for the *syn* and *anti* relative stereochemistries, in compounds with similar overall structure. However, the absolute chemical shift values differed depending on the substituent at the C18 carbon.

Therefore, no conclusions could be drawn from the comparison of just ^1H and ^{13}C NMR chemical shift data for the relevant fragment in **94** with those reported. The splitting observed for H21 in the ^1H NMR spectra of the reported compounds did appear to be characteristic for the *syn* or *anti* relative stereochemistries irrespective of the substituent at C18. The splitting observed for H21 in the ^1H NMR spectrum of **94** was not of first order. Simulation using approximated coupling constants (J_{HH} for H21/H20a=4.2 Hz, H21/H20b=10.6 Hz, H20a/H20b=14.0 Hz, H20a/H19a=7.0 Hz, H20b/H19b=7.0 Hz, H19a/20b=13 Hz and 19a/19b=14.0 Hz) and the known chemical shift data gave a multiplet consistent with that observed (Fig.6.16). The coupling constants of 4.2 Hz ($J_{\text{H21/H20a}}$) and 10.6 Hz ($J_{\text{H21/H20b}}$) are consistent with those reported for the *anti* stereochemistry of the substituted tetrahydrofuran system. The relative stereochemistry of the substituted tetrahydrofuran fragment was therefore assigned on the NOESY spectral data obtained and the coupling constants approximated for H21 in compound **94**.

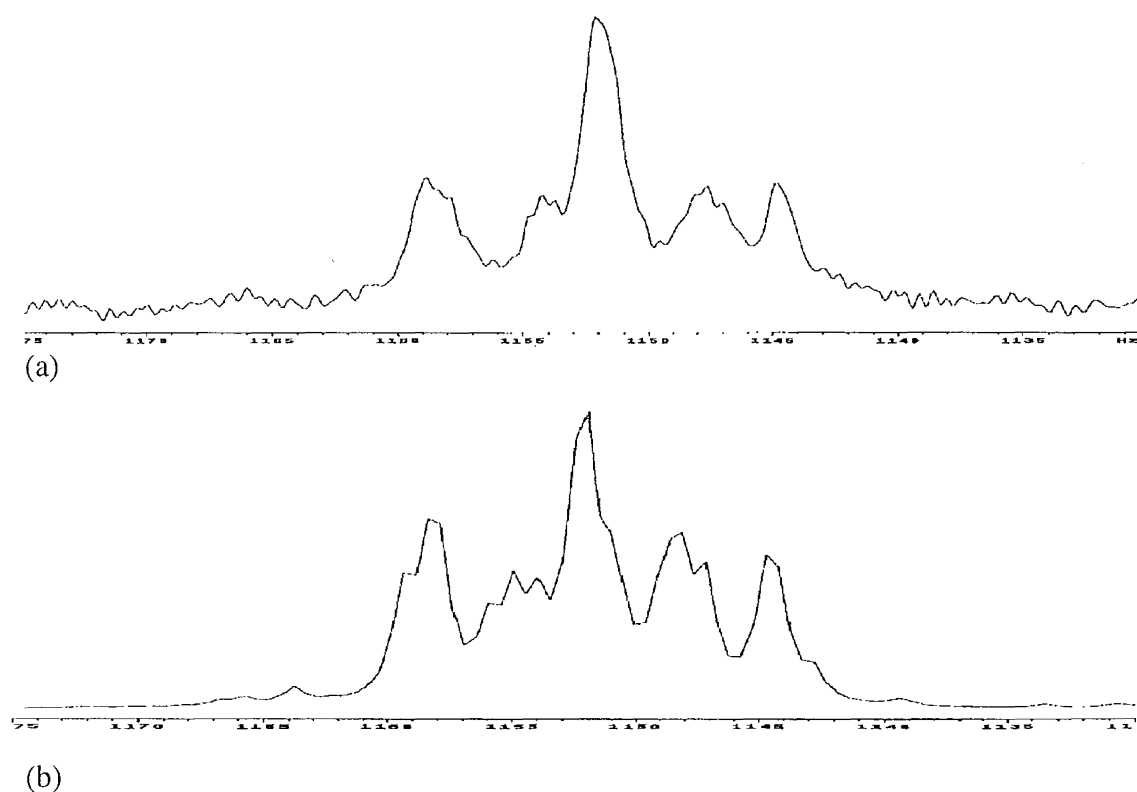


Figure 6.16 a) Observed multiplet for H21, b) Simulated multiplet for H21

The relative stereochemistry between the tricyclic system and the substituted tetrahydrofuran ring was not determined as no NOESY correlations were observed that would support an assignment. Therefore, the structure of this cytotoxic triterpene was assigned as either **94a** or **94b**.

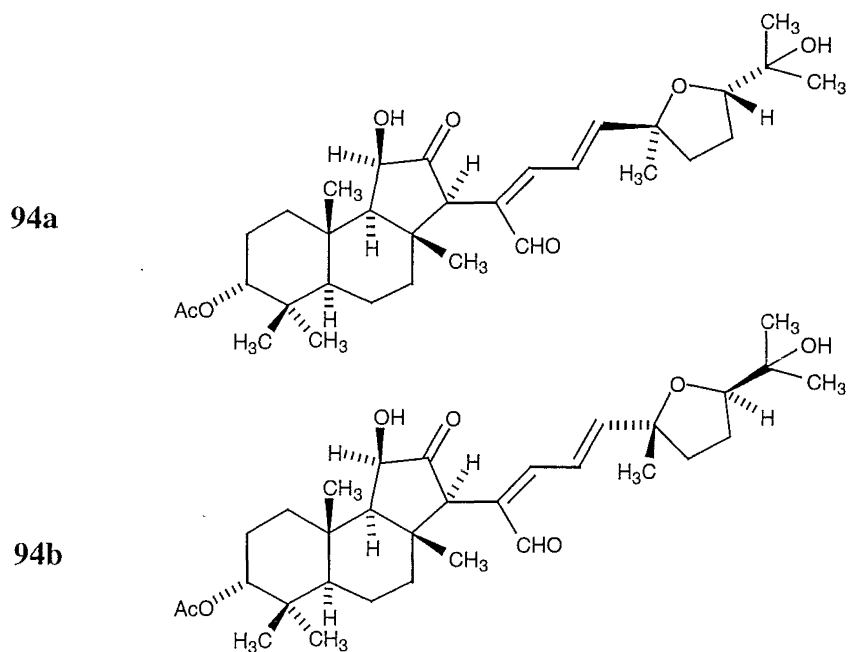


Table 6.1 NMR data for **94** (in CDCl₃)

#	δ_{C}	δ_{H} (J_{HH} Hz)	HMBC 8.3 Hz	HSQC- TOCSY mix=0.02 (0.08)	NOESY
1a	33.1	1.56 m		22.4	
1b		1.68 m		22.4	
2a	22.4	2.03 m		33.1 (78.2)	1.26, 1.66, 0.91
2b		1.66 m		33.1 (78.2)	2.03
3	78.2	4.68 t (2.6)	170.6, 51.5, 33.1	22.4 (33.1)	0.91, 0.83
4	36.6				
5	51.5	1.52 m	21.2, 17.5		1.78, 0.83
6	18.7	1.54 m	51.5		
7a	40.1	1.60 m	61.1, 51.5, 18.7	18.6 (18.6, 51.5)	3.71
7b		1.44 m	61.1, 51.5, 18.7	18.6 (18.6, 51.5)	
8	45.9				
9	60.9	1.78 d (7.2)	72.1, 45.9, 37.4, 18.9, 17.5	72.1 (72.1 larger)	3.71, 1.52
10	37.4				
11	72.1	4.24 d (7.1)	45.9	60.9 (60.9 larger)	3.71, 2.30
12	216.7				
13	61.1	3.71 s	216.7, 189.3, 150.2, 130.2, 45.9, 18.9		1.78, 1.60
14	130.2				
15	150.2	6.89 d (12.0)	150.6, 118.9, 61.1, 189.1	150.6, 118.9	7.25, 6.22, 0.98
16	118.9	7.25 dd (12.1, 14.8)	150.2, 82.7	150.6, 150.2	10.28, 1.38
17	150.6	6.22 d (14.9)	150.2, 82.7	150.2, 118.9	1.92, 1.38
18	82.7				
19a	38.1	1.92 m	26.2		
19b		1.86 m	26.2		
20	26.2	1.88 m	86.1, 38.1		
21	86.1	3.84 m		26.3, 38.1 (38.1)	1.88, 1.25, 1.14
22	70.9				
23	24.2	1.14 s	86.1, 70.9, 27.3		
24	27.3	1.25 s	86.1, 70.9, 24.2		3.84
25	26.8	1.38 s	150.6, 82.7, 38.1		7.25, 6.22, 1.86
26	189.3	10.28 s	130.2, 61.1		7.25
27	18.9	0.98 s	60.9, 45.9, 40.1		1.26, 1.44
28	17.5	1.26 s	60.9, 51.5, 37.4, 33.1		2.03, 1.56, 0.98, 0.91
29	21.2	0.91 s	78.2, 51.5, 36.6, 27.9		2.03, 1.26
30	27.9	0.83 s	78.2, 51.5, 36.6, 21.2		1.52
31	170.6				
32	21.3	2.08 s	170.6		

6.4.2 Structural elucidation of compound **95**

General features of compound **95**

HREIMS gave the molecular formula of compound **95** as $C_{32}H_{48}O_7$, the same as for compound **94**. Comparison of the 1H NMR data for compounds **94** and **95** showed only a small area where there were differences. From the 1H NMR spectrum of compound **95** (Fig. 6.17), the chemical shift of the olefinic protons (H15-17) were different and the H13 proton had moved. This corresponded to the diene fragment and the point of its attachment to the tricyclic system. The olefinic proton β to the aldehyde moved downfield from δ_H 6.22 in compound **94** to δ_H 7.19 in **95**. The central olefinic proton moved upfield from δ_H 7.25 in compound **94** to δ_H 6.59 in **95**. The chemical shift of the aldehyde proton had also shifted upfield, from δ_H 10.28 in compound **94** to δ_H 9.43 in **95**. The other major difference was in the chemical shift of the H13 proton, which moved upfield from δ_H 3.71 (**94**) to δ_H 3.57 in compound **95**.

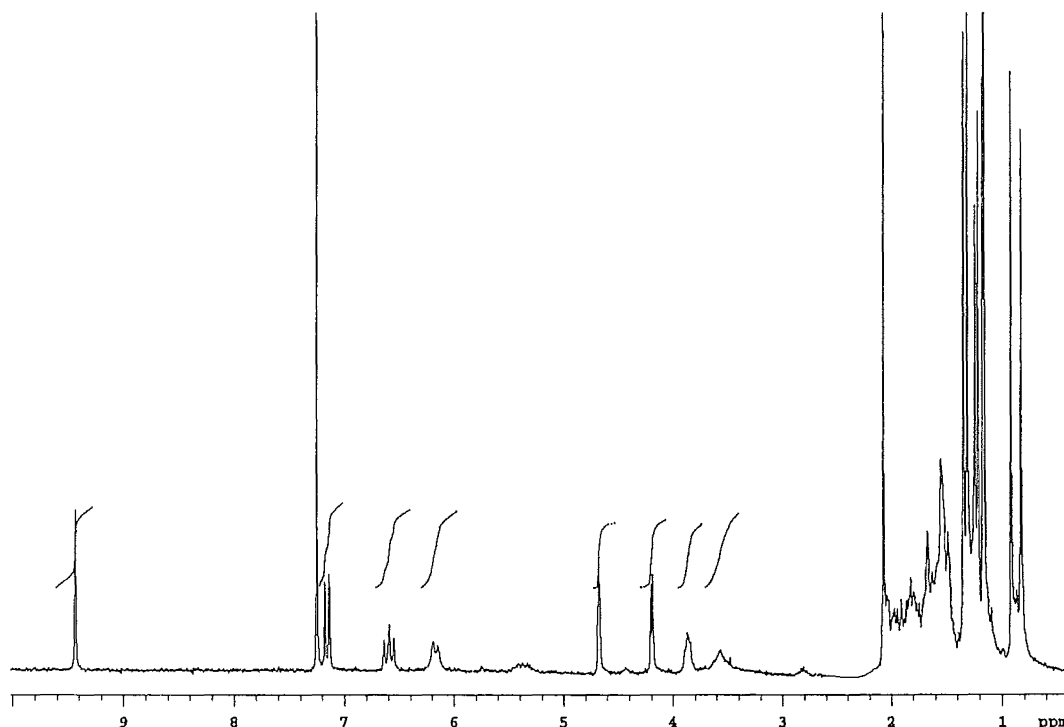


Figure 6.17 1H NMR spectrum of **95**

Assignment of the structure of compound **95**

Assignment of the ^1H and ^{13}C NMR data for compound **95** was accomplished using HMBC and HSQC-TOCSY experiments as for compound **94** (discussed in detail in **Section 6.4.1**). The carbon backbone of **95** was confirmed as being the same as **94**.

The only other possible differences could be epimerisation of a stereocentre or isomerisation of one of the double bonds. The magnitude of the coupling constant (15.1 Hz) for the disubstituted olefin, between δ_{H} 6.59 (H16) and 6.16 (H17), was still consistent with *E* stereochemistry. From the chemical shifts of the olefinic protons and the NOESY correlation observed in that region, it was clear that the stereochemistry of the second olefin of compound **95** was different to that of **94**. A NOESY correlation was observed between the aldehyde proton (δ_{H} 9.43, H26) and the H15 (δ_{H} 7.19) olefinic proton. A second NOESY correlation was observed between the central olefinic proton at δ_{H} 6.59 (H16) and the methine proton at δ_{H} 3.57 (H13). These correlations allowed the assignment of the stereochemistry of the C14/C15 olefin as *E* and the conformation of the diene relative to the tricyclic system as illustrated in **Fig.6.18**.

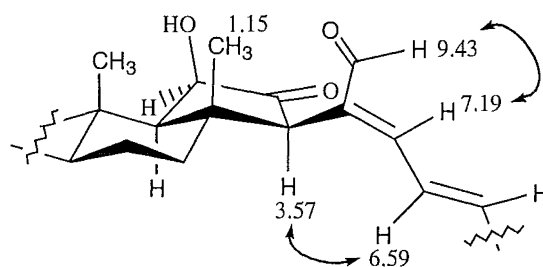


Figure 6.18 NOESY correlations for **95**

The relative stereochemistry of the substituted tetrahydrofuran system of **95** was assigned as *anti*, the same as **94** (**Fig. 6.19**). The chemical shift of H21 (δ_{H} 3.86) and the NOESY correlation observed between H21 and H16 (δ_{H} 6.59) were consistent with modelling discussed in **Section 6.4.1**.

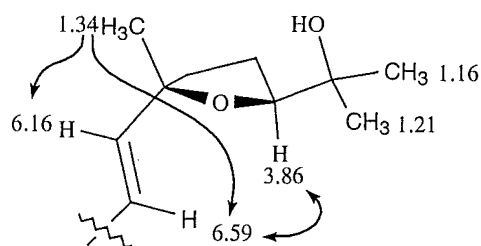


Figure 6.19 NOESY correlations for **95**

As with compound **94**, the relative stereochemistry of the tricyclic system and the substituted tetrahydrofuran ring in compound **95** was not determined, as no NOESY correlations were observed that would support an assignment. Therefore, the structure of the second cytotoxic triterpene was assigned as either **95a** or **95b**.

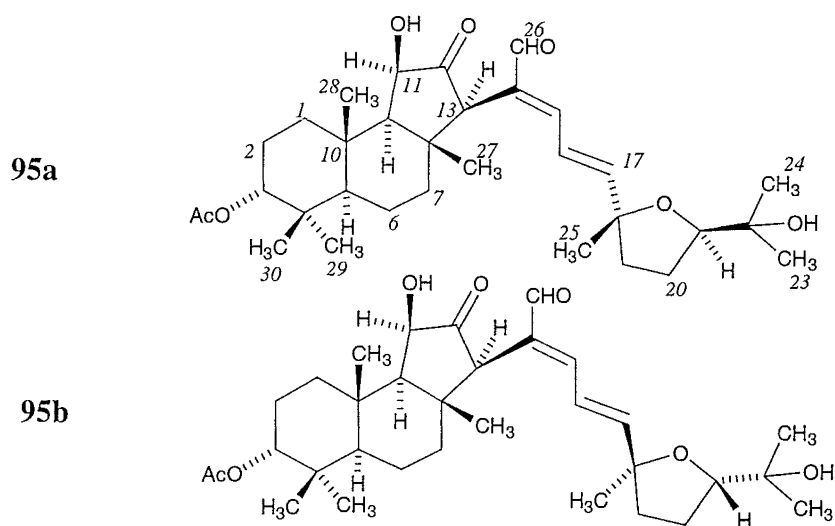


Table 6.2 NMR data for **95** (in CDCl₃)

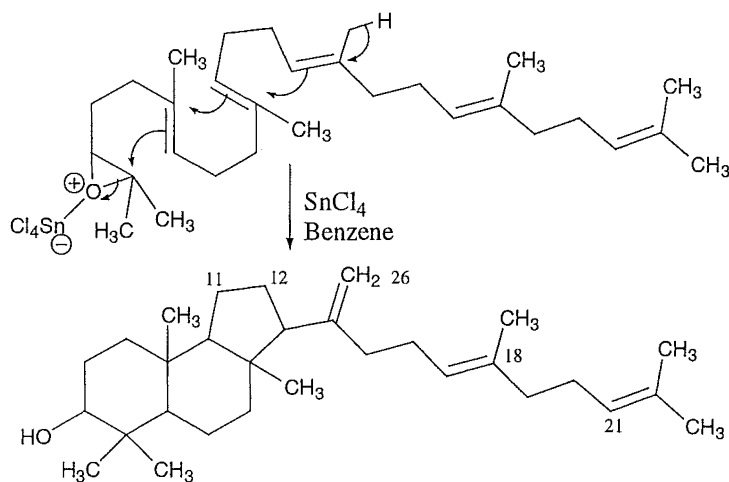
#	δ_C	δ_H (J_{HH} Hz)	HMBC 8.3 Hz	NOESY
1	33.0	1.48 m	78.3, 37.3	
		1.68 m	78.3, 37.3	
2a	22.1	2.04 m		4.68, 1.64, 1.31, 0.91
2b		1.63 m		
3	78.3	4.68 t (2.5)	33.0, 51.4, 170.6	0.83, 0.92, 1.65, 2.04
4	36.1			
5	51.4	1.47 m		1.68
6	18.6	1.54/1.52 m	51.4	
7	41.4	1.53 m	51.4	
8	46.3			
9	62.2	1.58 m	46.3	
10	37.3			
11	72.6	4.19 d (5.6)	46.3, 60.6	3.57, 1.65, 1.58
11OH		2.30 m		
12	216.7			
13	60.6	3.57 br m	152.7, 62.2	6.59, 4.19, 1.58
14	134.6			
15	152.7	7.19 d (12.2)	194.7, 150.0, 60.6	9.43, 6.59, 6.16
16	115.6	6.59 m (11.6, 14.6)	82.6	7.19, 6.16, 3.86, 1.53
17	150.0	6.16 br d (14.7)	37.7	1.92, 1.34
18	82.6			
19a/b	37.7	1.92/1.78 m	26.8	
20	26.8	1.80 m		
21	85.3	3.86		6.59, 1.80, 1.21
22	72.3			
23	22.0	1.16 s	85.3, 72.3, 26.7	
24	26.7	1.21 s	85.3, 72.3, 22.0	3.86
25	27.0	1.34 s	150.0, 82.6, 37.7	6.59, 6.16
26	194.7	9.43 s	134.6, 60.6	7.19
27	20.0	1.15 s	62.2, 41.3	1.55
28	17.3	1.31 s	62.2, 51.4, 37.3, 33.0	2.04, 1.15, 0.92
29	21.3	0.92 s	78.3, 51.4, 36.1, 27.6	4.68, 1.31
30	27.6	0.83 s	78.3, 51.4, 36.1, 21.3	4.68
31	170.6			
32	21.0	2.07 m	170.6	

6.4.3 Isomerisation of the C14-C15 olefin

The slow interconversion of compounds **94** and **95** was observed by ^1H NMR spectroscopy over a period of months. For a sample that contained pure **94**, a slow increase of the aldehyde signal (δ_{H} 9.43) for compound **95** was observed, and *vice versa* for compound **95**.

6.5 Proposed biosynthesis of rotundisine A (**94**) and B (**95**)

It is known that non-enzymatic cyclisation of 2,3-epoxysqualene produces a number of products, including the tricyclic malabaricane skeleton.¹¹⁴ It wouldExtensive oxidation would then be required to give the aldehyde (C26), the ketone (C12) and α -hydroxy group (C11) and also the substituted tetrahydrofuran ring between C18 and C21.



6.6 Biological activity of rotundisine A (**94**) and B (**95**)

The crude extract of *Cortinarius rotundisporus* showed cytotoxicity against the P388 cell line and against the host cells (BSC-1) in the antiviral assay, with a visual

description of type 12. This visual interpretation of how the cells change, when compared to the control cells, is due to the toxic effects of the test compounds. These changes may be related to the mode of action. For example, the visual description of type 12 is often observed for compounds that show inhibition against protein phosphatase.¹⁰⁶

The pure samples of **94** and **95** were assayed against the P388 cell line and were found to have moderate cytotoxicity, with IC₅₀ values of 150 and 120 ng/mL respectively. Compounds **94** and **95** also showed cytotoxicity against the host cells of the antiviral assay, with a visual description of type 12 (large scruffy cells).

6.7 Discussion

An extract of *Cortinarius rotundisporus* was found to be cytotoxic against the P388 cell line during a screening programme of Australian basidiomycetes. The cytotoxic components were isolated and structurally assigned as rotundisine A (**94**) and B (**95**). At the time this work was completed, there were no reports in the literature of malabaricane triterpenes being isolated from fungi. Subsequently, through personal communication with Professor Steglich, we have been made aware that his group has recently isolated a malabaricane triterpene (but not compounds **94** and **95**) from a rare European species of *Cortinarius*.¹¹⁵

Future work could entail extraction on a larger scale and re-isolations of these components so that the absolute stereochemistry could be determined. The aldehyde or the secondary alcohol could be derivatised if required.

CHAPTER SEVEN

EXPERIMENTAL

7.1 General methods

7.1.1 Nuclear magnetic resonance (NMR)¹²⁰

Proton detected NMR spectra were recorded on a Varian Unity 300 spectrometer at 23°C, operating at 300 MHz. Carbon detected NMR spectra were recorded on a Varian XL300 spectrometer at 23°C, operating at 75 MHz. Other NMR experiments described in this thesis *viz.* 1D-TOCSY, 2D-TOCSY, COSY, NOE, NOESY and the reverse-detected HSMQC, HSQC and HMBC experiments were all recorded on the Unity spectrometer, at 300 MHz. For the work detailed in **Chapters Two-Four** and **Six** this instrument was fitted with a Nalorac Z.spec MID300 3 mm Indirect Detection Probe. For the work detailed in **Chapter Five** the instrument was fitted with a Pulsed Field Gradient MLD driver with a 5mm Indirect Detection Probe. Chemical shifts in this thesis are described in parts per million (ppm), on the δ scale, and were referenced to

the appropriate solvent peaks: CDCl_3 referenced to CHCl_3 at δ_{H} 7.25 ppm (^1H) and CHCl_3 at δ_{C} 77.0 ppm (^{13}C); CD_3OD referenced to CHD_2OD at δ_{H} 3.30 ppm (^1H) and CD_3OD at δ_{C} 49.3 ppm (^{13}C); DMSO-d_6 referenced to $(\text{CD}_3)(\text{CHD}_2)\text{SO}$ δ_{H} 2.50 (^1H) and $(\text{CD}_3)_2\text{SO}$ δ_{C} 39.6 (^{13}C); for D_2O 5% DMSO was added and referenced to $(\text{CD}_3)(\text{CHD}_2)\text{SO}$ δ_{H} 2.5 (^1H) and $(\text{CD}_3)_2\text{SO}$ δ_{C} 39.6 (^{13}C). ^1H NMR spectra were recorded using an acquisition time (AT) of 2.0 s. ^{13}C NMR spectra were recorded using an AT of 0.878 s and a delay (D1) of 1.0 s. APT experiments were recorded using an AT of 0.878 s. All difference NOE experiments were recorded in undegassed solutions, with an AT of 1.0 s and an irradiation time (D2) of 2.0 s. The decoupler was offset 10,000 Hz for the control experiment. Percentage enhancements reported in this thesis represent the observed increase in the intensity of a specific resonance relative to the corresponding signal in the control spectrum. NOESY experiments were run using an AT of 0.468 s and a mixing time of 0.30 s. With the Pulse Field Gradient system, 1D-NOESY experiments were run with an AT of 1.0 s, and D2 of 2.0 s. COSY experiments were recorded using an AT of 0.216 s and a relaxation delay (D1) of 1.0 s. 1D-TOCSY spectra were recorded using an AT of 2.0 s, a D1 of 1.0 s and mixing times as indicated in the discussion. HSMQC experiments were recorded with an AT of 0.2 s with D1 set for individual samples when selecting the null value and $J_{\text{C-H}}=145$ Hz. HSMQC-TOCSY experiments were run with the same parameters as the HSMQC experiment, with the addition of an arrayed mixing time of 0.02 and 0.08 s. HSQC experiments with the Pulsed Field Gradient system were run with an AT of 0.137 s, a D1 of 1.0 s and $J_{\text{X-H}} = 140$ Hz. HMBC experiments were recorded with an AT of 0.21 s (0.137 with the Pulsed Field Gradient system), a relaxation delay of 0.3 s, $J = 140$ Hz and $^nJ_{\text{CH}} = 8.3$ Hz, unless otherwise stated.

7.1.2 Mass spectrometry

Mass spectrometry at the University of Canterbury was performed on a Kratos MS80 Mass Spectrometer operated at 4 kV. Various ionisation techniques were used including electron impact, (EI)¹²¹ at 70eV and chemical ionisation (CI; C₄H₁₀). The softer ionisation technique of fast atom bombardment (FAB)¹²² was used where necessary. FAB was performed with an Ion Tech ZN11FN ion gun using Xe as the reagent gas, operating at 8 kV and 2 mA, with either *m*-nitrobenzyl alcohol (NOBA), magic bullet (m-b, 50% thioerythritol/thiothreitol), or glycerol as the matrix.

Some samples required further mass spectrometry analysis at other institutions. Where this occurred the following acronym with proceed the data: NIH (Dr Lewis K. Pannell, NIDDK, NIH, USA); ANU (Professor Rodney Rickards, ANU, Australia).

Samples analysed by electrospray ionisation mass spectrometry (ESIMS) were dissolved in a solution of 1:1 CH₃CN/H₂O which was acidified with acetic acid for the positive ion mode basified with sodium hydroxide for negative ion mode, unless otherwise stated.

7.1.3 Infra-red (IR) spectroscopy and Optical Dispersion Rotation Measurements¹²¹

IR spectra were recorded using a Shimadzu 8201PC series FTIR interfaced with a PC General computer with Shimadzu Hyper IR software (based on Spectacle). Spectra were run neat on either a KBr or CaF₂ disc, or in a solution of chloroform.

Optical Rotatory Dispersion (ORD) measurements were performed on a Jasco model J-20 Recording Spectropolarimeter ($S=2\text{ m}^{\circ}/\text{cm}$; $l=1\text{ cm}$;) in MeOH (spectranorm grade) at the stated concentration.

7.1.4 High Performance Liquid Chromatography

Analytical high performance liquid chromatography (HPLC) was performed on a Philips PU4100 Liquid Chromatograph equipped with a Philips PU4120 Diode Array Detector interfaced to a PC General 486 computer running Philips PU6003 Diode Array Detector System Software (V3.0) and a Hewlett Packard 7475A Plotter. Solvents used were degassed by using helium.

Semi-preparative HPLC was performed on a Shimadzu LC-4A with a Shimadzu SPD-2A S single wavelength UV detector and a Sekonic SS-250F recorder. Solvents used were degassed with helium being bubbled through them.

Water was purified using a MilliQ deionising system. The methanol (MeOH) (J.T. Baker, HPLC reagent grade) used was undistilled. All other solvents were of technical grade and were purified and re-distilled before use. "Hexanes" was prepared from petroleum ether (10 L, b.p. 50-70°C) by nitration with a mixture of concentrated HNO_3 (1 L) and concentrated H_2SO_4 (1 L) with mechanical stirring for two days. The organic layer was separated from the nitrating mixture and washed with water (*ca.* 20 L) until colourless. The solution was left to dry over CaCl_2 overnight, filtered through a column of alumina (Laporte, 100 mesh) and finally distilled. All solvents (with the exception of MilliQ water) were filtered through a Millipore filter apparatus, equipped with a Rainin Nylon-66 filter (0.45 μm) prior to use. All samples were filtered through a syringe filter (Alltech, 0.45 μm) prior to injection.

Analytical HPLC on reverse-phase (C18) was carried out using either a Microsorb-MV (5 μm , 100 Å, 4.6 x 250 mm), Rainin (3 μm , 100Å, 4.6 x 100 mm) or Brownlee Labs (5 μm , 60 Å, 4.6 x 250 mm) column, as stated. The analytical cyano (CN) column used for normal-phase HPLC was an Altech (Spherisorb CN, 5 μm , 250 x 4.6 mm).

Semi-preparative normal-phase HPLC on CN was carried out on an Altech/Applied Science (Econosil CN, 10 μm , 10 x 250 mm) column.

Medium pressure chromatography was performed on a Lobar chromatography set up, with a variable speed electric pump (Mill-Royal D pump), to achieve a typical flow rate of 10 mL/min. The system was equipped with a LKB Broma 2238 UVICORD SII detector and a LKB Broma 2210 recorder. Reverse-phase chromatography was performed on a Lobar Lichroprep[®] RP-18 column (40-63 μm , 25 x 310 mm, E. Merck, Darmstadt, Germany). Normal-phase chromatography was performed using a Lobar LiChroprep[®] CN column (40-63 μm , 25 x 310 mm, E. Merck, Darmstadt, Germany).

7.1.5 Column chromatography

All column chromatography was performed with glass columns of stated dimensions. Solvents used were all of commercial grade, distilled once in glass distillation apparatus, except MeOH, which was distilled twice. "Flash" columns were run under N₂ gas (oxygen free) pressure (0.5 kPa).

Silica flash chromatography was performed on Merck silica gel 60 (230-400 mesh).¹¹⁶ Bakerbond DIOL (40 μm APD) was used for chromatography carried out in **Chapters Two** and **Four**, while Merck DIOL (40 μm APD) was used for work carried out in **Chapter Six**. Pre-swelled Sephadex LH20 (Pharmacia Biotech AB) was used for gel permeation chromatography.

Octadecyl (C18) reverse-phase packing used for preparative and flash column chromatography in **Chapters Two** and **Four** had been prepared from silica gel (Davisil, 35-70 μm) using a solution of octadecyltrichlorosilane (2% v/v, EGA-Chemie) in carbon tetrachloride. The silica gel was stirred gently with a teflon-coated magnetic follower overnight before washing twice with carbon tetrachloride. Unreacted chloro groups were substituted by washing with dry MeOH. A carbon tetrachloride solution of chlorotrimethylsilane (2% v/v, Aldrich) was used to end-cap any unreacted hydroxyl groups. The reverse-phase material was finally washed twice with dichloromethane (CH_2Cl_2) and MeOH to remove the reagents. The C18 reverse-phase material was extensively washed with MeOH immediately before use.

Octadecyl (C18) reverse-phase packing used for preparative and flash column chromatography in **Chapters Five** and **Six** was Bakerbond (40 μm Prep LC Packing). Small scale preparative C18 reverse-phase column chromatography was performed using Alltech disposable cartridges (200 mg).

7.1.5 Thin Layer Chromatography

The analytical thin layer chromatography (TLC) on silica described in this thesis was performed using Merck silica gel 60 F₂₅₄ aluminium-backed sheets (0.2 mm in thickness). DIOL analytical TLC was performed using Merck F₂₅₄ glass-backed plates (0.2 mm thickness). C18 analytical TLC was performed on Whatman MKC 18F TLC plates (0.2 mm thickness). When TLC plates on C18 were eluted with greater than 20% $\text{H}_2\text{O}/\text{MeOH}$ (or CH_3CN) it was necessary to bake the plates in an oven ($\sim 70^\circ\text{C}$) for approximately half an hour to stop the C18 lifting off the glass.

All TLC plates were initially visualised under short-wavelength (λ 254 nm) light and subsequently with either phosphomolybdic acid in ethanol spray (10% w/v) or with potassium permanganate in ethanol/H₂O dip (1:1, 10% w/v).

7.1.6 Dry solvents

Dry tetrahydrofuran (THF) and diethyl ether (ether) were distilled from sodium-benzophenone ketyl. Dry dichloromethane (CH₂Cl₂) and *N,N*-dimethylformamide (DMF) were distilled from calcium hydride. Dry methanol was distilled from magnesium metal and iodine. All dry solvents were distilled immediately prior to use with the exception of DMF and MeOH, which were previously distilled and then stored over molecular sieves (3Å).

The trichloroacetimidate of 2-methylbut-3-yn-2-ol was prepared by the method of Overman.¹¹⁷ All other reagents and solvents were used as received. All reactions were conducted under an atmosphere of nitrogen in oven or flame dried glassware, except hydrogenation reactions that were conducted under an atmosphere of hydrogen.

7.2 Work described in Chapter Two

7.2.1 Extraction and chromatography of *Favolaschia calocera*

Work done during a Masters degree involved the purification of a CH₂Cl₂ extract of *F. calocera* fruiting bodies.²⁹ A sample (80 g) of the fruiting bodies was freeze-dried, crushed to a coarse powder and extracted with CH₂Cl₂. Removal of the solvent *in vacuo* gave a thick dark-orange oil (3.70 g). This extract was divided into thirds and purified using Bakerbond DIOL (60 g, 2.5 x 22 cm) column chromatography with a

stepped gradient from petroleum ether through CH_2Cl_2 , EtOAc and finally MeOH. Twenty fractions (GN2-117.1-23) were collected with combinations made based on TLC (DIOL).

Chromatography of fraction GN2-117.22

Research conducted towards this thesis included chromatography of fraction GN2-117.22 by normal phase (DIOL) column chromatography (12 g; 2 x 8 cm), eluted with a stepped gradient from petroleum ether through CH_2Cl_2 , EtOAc, and finally MeOH. Twenty-eight fractions (GN2-118.1-28) were collected, with combinations made based on TLC (DIOL). Fractions GN2-118.17-25 (50.1 mg) were loaded onto a reverse-phase column (C18; 8 g; 1 x 10 cm) and eluted with a stepped gradient system from H_2O through to MeOH and then to CH_2Cl_2 . This gave fraction GN2-15.20 that was identified by NMR spectroscopy and mass spectrometry as a mixture of two fatty acid esters, at the 5- position, of (2*E*,6*E*)-1-(2-hydroxy-4-methoxyphenyl)-5-hydroxy-3,7,11-trimethyldodeca-2,6,10-triene (**30a-b**) (Section 2.2, Chapter Two).

LRFABMS (NOBA) MH^+ 583 (palmitate ester), MH^+ 611 (stearate ester).

HREIMS m/z 326.2246 ($\text{C}_{22}\text{H}_{30}\text{O}_2$ requires 326.2245), 284.2738 ($\text{C}_{18}\text{H}_{36}\text{O}_2$ requires 284.2715, stearic acid), 256.2402 ($\text{C}_{16}\text{H}_{32}\text{O}_2$ requires 256.2402, palmitic acid).

^1H NMR (CDCl_3) δ 6.74 (d, $J_{\text{HH}} = 8.8$ Hz, 1H, H17), 6.66 (s, 1H, H14), 6.63 (m, 1H, H16), 5.68 (m, 1H, H5), 5.34 (m, 1H, H2), 5.18 (m, 1H, H6), 5.13 (m, 1H, H10), 3.74 (s, 3H, H22), 3.30 (m, 2H, H1), 2.39 (dd, $J_{\text{HH}} = 7.8, 13.4$ Hz, 1H, H4a), 2.28 (m, 1H, H4b), 2.26 (m, 2H, H24), 2.03 (m, 2H, H9), 1.97 (m, 2H, H8), 1.81 (s, 3H, H21), 1.72 (s, 3H, H20), 1.67 (s, 3H, H12), 1.60 (s, 3H, H19), 1.60 (m, 2H, H25), 1.38 (m, 2H, H26), 1.38 (m, 2H, H27), 1.20 (m, 2H, H28), 1.20 (7 resonances, remainder of saturated FA chain), 0.88 (t, $J_{\text{HH}} = 6.8$ Hz, 3H, H29).

^{13}C NMR (CDCl_3) δ 173.8 (C23), 153.7 (C15), 147.9 (C18), 140.5 (C7), 133.7 (C3), 131.4 (C11), 128.2 (C13), 125.1 (C2), 123.7 (C10), 123.3 (C6), 116.4 (C17), 115.6

(C14), 111.7 (C16), 69.4 (C5), 55.6 (C22), 45.2 (C4), 39.0 (C8), 34.3 (C24), 31.6 (C27), 29.6 (C1), 29.1-29.9 (remainder of saturated FA chain), 26.3 (C9), 25.6 (C12), 25.0 (C25), 22.3 (C28), 17.7 (C19), 16.9 (C20), 16.6 (C21), 14.1 (C29). IR (CDCl₃, cm⁻¹) 3590, 3400-3550, 2927, 2854, 1720, 1498, 1465, 1232, 1195, 1176, 1043.

Methanolysis of 30a-b mixture.

Sodium methoxide (80 μ L, 5 mg/mL) in MeOH was added to compounds **30a-b** (2.0 mg) in dry MeOH (0.5 mL), and was allowed to stir for 12 hours. At this point, TLC (silica) showed no starting material to be present. The reaction was then quenched with saturated aqueous ammonium chloride (3 mL) and extracted with ether/EtOAc. The organic layer was washed with brine, dried (MgSO₄) and then the solvent removed *in vacuo* to yield a mixture of the alcohol and the desired fatty acid methyl esters (FAMES). The ¹H NMR spectrum of this mixture confirmed there had been methanolysis of the ester bond, due to the appearance of a new methoxy signal (δ_{H} 3.66). The sample was then analysed by GCMS using a DB-WAX column and standard conditions for analysis of FAMES. Two peaks eluted in the GC trace. The first (RT=18:13 min) was assigned as methyl palmitate (C16:O, hexadecanoic acid, methyl ester) and the second peak (RT=20:26 min) as methyl stearate (C18:O, octadecanoic acid, methyl ester).

Chromatography of fraction GN2-117.25

Fraction GN2-117.25 (182 mg) was purified with normal-phase (DIOL) column chromatography (5 g, 2 x 120 cm). Elution with a gradient solvent system from petroleum ether through to CH₂Cl₂, then EtOAc and finally stripped with MeOH gave twenty-one fractions, which were combined by TLC (DIOL).

The ¹H NMR spectrum of the fractions that eluted with 80% petroleum ether/CH₂Cl₂ (GN2-2.7-8, 69 mg) indicated a compound possibly structurally related to the major

component (**28a**) of the CH_2Cl_2 extract. Further purification using Lobar chromatography on normal phase CN (2% IPA/Hexane) followed by semi-preparative HPLC on CN (4% IPA/Hexane, 2.5 mL/min) yielded (*E*)-6-Phenylhex-5-en-2-ol (**32**, 3.0 mg).⁴⁴ ^1H NMR (CDCl_3) δ 7.4-7.2 (m, ArH, 5H, H7-11), 6.4 (d, $J_{\text{HH}} = 11.1$, 15.9 Hz, 1H, H1), 6.2 (m, 1H, H2), 3.9 (m, 1H, H5), 2.3 (m, 2H, H3), 1.6 (m, 2H, H4), 1.2 (d, $J_{\text{HH}} = 6.0$ Hz, 3H, H6). ^{13}C NMR (CDCl_3) δ 137.6 (ArCH=), 130.2 (CH=), 130.2 (CH=), 128.3 (ArH), 126.8 (ArH), 126.0 (ArH), 67.6 (OCH), 38.5 (CH_2), 29.0 ($\text{CH}_2\text{CH=}$), 23.2 (CH_3).

The fraction that eluted with 20% petroleum ether/ CH_2Cl_2 (GN2-2.9, 18.3 mg) was further purified by reverse-phase (C18) column chromatography (2 g; 0.5 x 5 cm) using a gradient solvent system from H_2O through to MeOH. The fraction that eluted in 80% MeOH/ H_2O (GN2-11.17, 3.0 mg) contained methyl (4*E*,6*E*)-3-hydroxy-7-phenylhepta-4,6-dienoate (**28b**).⁴² ^1H NMR (CDCl_3) δ 7.41 (m, 2H, H9/13), 7.33 (m, 2H, H10/12), 7.24 (m, 1H, H11), 6.76 (dd, $J_{\text{HH}} = 10.2$, 15.6 Hz, 1H, H6), 6.55 (d, $J_{\text{HH}} = 15.4$ Hz, 1H, H7), 6.47 (d, $J_{\text{HH}} = 10.2$, 15.6 Hz, 1H, H5), 5.83 (dd, $J_{\text{HH}} = 0.9$, 6.2, 15.1 Hz, 1H, H4), 4.66 (m, 1H, H3), 3.73 (s, 3H, H14), 2.63 (m, 1H, H2a), 2.60 (m, 1H, H2b). IR (CDCl_3 , cm^{-1}) 3695, 3606, 2926, 1728, 1603, 1439.

7.2.2 Absolute stereochemistry of methyl 4,6-(*E,E*)-3-benzoyloxy-7-phenylhepta-4,6-dienoate (**28a**)

Methanolysis of **28a**.

Sodium methoxide in MeOH (200 μL of a 0.2 mM stock solution) was added to a solution of benzoyl ester **28a** (10.0 mg, $[\alpha]_{\text{D}}^{25} = +0.97^\circ$) in methanol (200 μL). The reaction was allowed to stir for one hour, then quenched with saturated aqueous ammonium chloride, and loaded onto a reverse-phase chromatographic cartridge (C18, 200 mg). Elution of the cartridge with H_2O /MeOH (1:1) then elution with MeOH gave

a mixture of the desired alcohol **28b** and an elimination by-product. Chromatography on DIOL (1 g, 0.5 x 5 cm) yielded methyl, (4*E*,6*E*)-3-hydroxy-7-phenylhepta-4,6-dienoate (**28b**) (2.5 mg, 40%). ¹H NMR data for this product was consistent both with that in the literature and that obtained for the isolated alcohol from the extract.⁴² ¹H NMR (CDCl₃) δ 7.41 (m, 2H, H9/13), 7.33 (m, 2H, H10/12), 7.24 (m, 1H, H11), 6.76 (dd, *J*_{HH} = 10.2, 15.6 Hz, 1H, H6), 6.57 (d, *J*_{HH} = 15.4 Hz 1H, H7), 6.46 (d, *J*_{HH} = 10.2, 15.6 Hz, 1H, H5), 5.85 (dd, *J*_{HH} = 0.9, 6.2, 15.1 Hz, 1H, H4), 4.65 (m, 1H, H3), 3.73 (s, 3H, H14), 2.63 (m, 1H, H2a), 2.60 (m, 1H, H2b). IR (CDCl₃, cm⁻¹) 3695, 3606, 2926, 1728, 1603, 1439.

Methoxytrifluorophenylacetic acid (MTPA) esters

The method reported by Ward *et al* for the preparation of MTPA esters was modified slightly in our preparation of (*R*)- and (*S*)-MTPA esters **28c** and **28d**.⁴⁵ Approximately six equivalents of the respective MTPACl was required to form the desired esters.

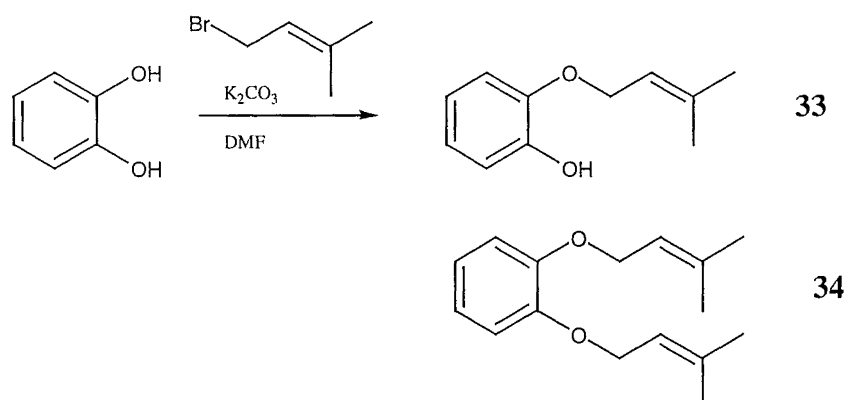
Alcohol **28b** (1.0 mg, 4.3 μmol) in CH₂Cl₂ (50 μL) was added to (*S*)-(-)-MTPACl (7.0 mg, 27.7 μmol). DMAP (1.0 mg, 8.1 μmol) in CH₂Cl₂ (50 μL) and triethylamine (10 μL, 0.07 μmol) were then added, and the reaction allowed to stir for one hour. The solvent was evaporated and chromatography on DIOL (1 g, 0.5 x 5 cm) gave methyl (4*E*,6*E*)-3-((*R*)-MTPA)-7-phenylhepta-4,6-dienoate (**28c**, 0.9 mg, 41%). HREIMS M⁺ 448.1492 (C₂₄H₂₃O₅F₃ requires 448.1497). ¹H NMR (CDCl₃) δ 7.28-7.50 (m, 10H, ArH), 6.67 (dd, *J*_{HH} = 10.2, 15.1 Hz, 1H, H6), 6.56 (d, *J*_{HH} = 15.1, 1H, H7), 6.45 (dd, *J*_{HH} = 10.2, 15.1 Hz, 1H, H5), 5.96 (m, 1H, H3), 5.67 (dd, *J*_{HH} = 7.6, 15.0 Hz, 1H, H4), 3.67 (s, 3H, H14), 3.42 (br s, 3H, H2a), 2.83 (dd, *J*_{HH} = 8.9, 16.1 Hz, 1H, H2a), 2.70 (dd, *J*_{HH} = 4.6, 16.1 Hz, 1H, H2b).

Alcohol **28b** (0.7 mg, 3.0 μmol) in CH₂Cl₂ (50 μL) was added to (*R*)-(+)-MTPACl (3.7 mg, 14.9 μmol). DMAP (1.0 mg, 8.1 μmol) in CH₂Cl₂ (50 μL) and triethylamine (10

μL , 71 μmol) were then added, and the reaction stirred for one hour. The solvent was then evaporated and chromatography on DIOL (1 g, 0.5 x 5 cm) gave methyl (4*E*,6*E*)-3-((*S*)-MTPA)-7-phenylhepta-4,6-dienoate (**28d**, 0.3 mg, 23%). HREIMS M^+ 448.1498 ($\text{C}_{24}\text{H}_{23}\text{O}_5\text{F}_3$ requires 448.1497). ^1H NMR (CDCl_3) δ 7.26-7.55 (m, 10H, ArH), 6.63 (dd, 1H, H6), 6.57 (m, 1H, H5), 5.99 (m, 1H, H3), 5.79 (dd, $J_{\text{HH}} = 7.8, 15.0$ Hz, 1H, H4), 3.60 (s, 3H, H14), 3.53 (br s, 3H, H24), 2.81 (dd, $J_{\text{HH}} = 8.1, 15.6$ Hz, 1H, H2a), 2.67 (dd, $J_{\text{HH}} = 4.8, 15.6$ Hz, 1H, H2b).

7.2.3 Synthetic details for model compounds 33-40

2-Hydroxyphenyl-1-(3-methylbut-2-en-1-yloxy) ether (33)

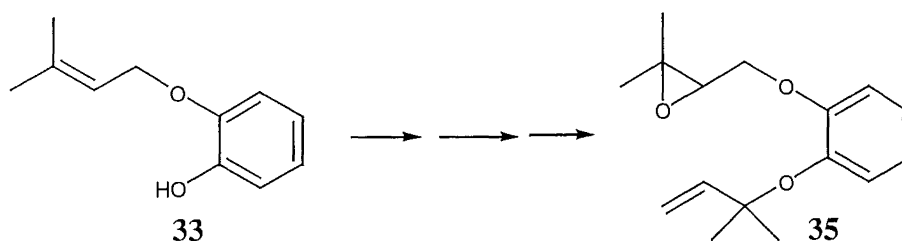


Catechol (20.7 g, 188 mmol) was added to potassium carbonate (5.2 g, 37.6 mmol) in dry DMF (650 mL) and cooled to 0 °C. 1-Bromo-3-methylbut-2-ene (4.4 mL, 37.6 mmol) was added dropwise over 10 minutes. The reaction was allowed to warm to room temperature and stirred for 18 hours. The reaction mixture was diluted with water (150 mL) and extracted with diethyl ether/ethyl acetate (1:1, 4 x 150 mL). The combined organic phases were washed with 5% aqueous hydrochloric acid, brine, dried (MgSO_4) and then evaporated. Dry flash column chromatography¹¹⁸ on silica with ether/petroleum ether (1:9) gave the title compound **33** (5.65 g; 84%) as a colourless oil.

HREIMS M^+ 178.0997 ($C_{11}H_{14}O_2$ requires 178.0993). 1H NMR ($CDCl_3$) δ 6.82-6.93 (m, 4H, ArH), 5.72 (d, $J_{HH} = 2.0$ Hz, 1H, OH), 5.49 (m, 1H, =CH), 4.57 (d, $J_{HH} = 6.9$ Hz, 2H, OCH_2), 1.80 (s, 3H, CH_3), 1.74 (s, 3H, CH_3). ^{13}C NMR ($CDCl_3$) δ 145.5, 145.3, 138.2, 120.9, 119.5, 118.8, 114.0, 111.6, 65.2, 25.2, 17.6. IR ($CDCl_3$, cm^{-1}) 3521-3445, 2975, 2933, 2915, 1612, 1596, 1501, 1466, 1385, 1259, 1220, 1199, 1106, 997, 742.

1,2-Di-(3-methylbut-2-en-1-yloxy) benzene (**34**) (130 mg, 5%) was also isolated as a colourless oil. HREIMS M^+ 246.1618 ($C_{16}H_{22}O_2$ requires 246.1619). 1H NMR ($CDCl_3$) δ 6.89 (m, 4H, ArH), 5.52 (m, 2H, =CH), 4.58 (d, $J_{HH} = 6.4$ Hz, 4H, OCH_2), 1.76 (s, 3H, CH_3), 1.72 (s, 3H, CH_3). ^{13}C NMR ($CDCl_3$) δ 148.9, 136.9, 120.9, 120.4, 114.1, 65.9, 25.7, 18.1. IR ($CDCl_3$, cm^{-1}) 2979, 2918, 2867, 1591, 1502, 1452, 1245, 1215, 1120. Microanalysis calcd for $C_{16}H_{22}O_2$: C, 78.01; H, 9.00. Found: C, 77.54; H, 9.29.

1-(2,3-Epoxy-3-methylbut-1-yloxy)-2-(2-methylbut-3-en-2-yloxy) benzene (35**)**



(i) Ether **33** (68 mg, 0.38 mmol), potassium carbonate (500 mg, 3.8 mmol), potassium iodide (370 mg, 2.3 mmol), 18-crown-6 (10 mg, 0.03 mmol) and 3-chloro-3-methylbutyne (720 μ L, 7.6 mmol) in dry acetone (3 mL) were refluxed under nitrogen for 22 hours.⁵⁰ After cooling to room temperature, 5% aqueous hydrochloric acid was added, followed by extraction with ether. The ether layer was washed with brine, dried ($MgSO_4$) and evaporated. Flash chromatography on silica with ether/petroleum ether (1:9) gave 1-(2-methylbut-3-yn-2-yloxy)-2-(3-methylbut-2-en-1-yloxy) benzene (55 mg, 60 %) as a colourless oil. HREIMS M^+ 244.1470 ($C_{16}H_{20}O_2$ requires 244.1463).

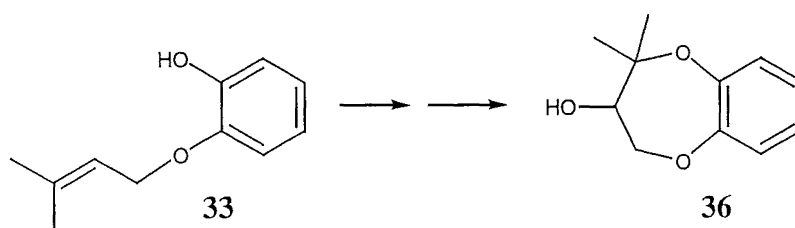
^1H NMR (CDCl_3) δ 7.41 (m, 1H, ArH), 7.01(m, 1H, ArH), 6.90 (m, 1H, ArH), 6.87(m, 1H, ArH), 5.49 (m, 1H, =CH), 4.51 (d, $J_{\text{HH}} = 6.3$ Hz, 2H, ArOCH_2), 2.49 (s, 1H, $\equiv\text{CH}$), 1.76 (s, 3H, CH_3), 1.70 (s, 3H, CH_3), 1.64 (s, 6H, CH_3). ^{13}C NMR (CDCl_3) δ 152.1 (ArO), 145.0 (ArO), 136.7 ($=\text{C}$), 124.1 (ArH), 123.8 (ArH), 120.6 (ArH), 120.3 ($=\text{CH}$), 114.5 (ArH), 86.1 ($\equiv\text{C}$), 74.0 (O-C), 73.1 ($\equiv\text{CH}$), 65.8 (OCH_2), 29.1 (2CH_3), 25.4 (CH_3), 18.0 (CH_3). IR (CDCl_3 , cm^{-1}) 3292, 2985, 2935, 2916, 1593, 1496, 1452, 1380, 1253, 1205, 1110, 1043. Microanalysis calcd for $\text{C}_{16}\text{H}_{20}\text{O}_2$ C,78.65; H,8.25. Found: C,78.87; H,8.08.

(ii) The alkyne product obtained above (47 mg) was partially hydrogenated over 5% palladium on barium sulfate (16 mg, 33% w/w) with quinoline (16 mg, 33% w/w) in ethyl acetate (50 mL) at 20 °C and atmospheric pressure. After 2 hours the solution was filtered through Celite and the solvent evaporated. The residue was dissolved in ether, washed with 5% aqueous hydrochloric acid, brine, then dried (MgSO_4) and finally evaporated. The ^1H NMR spectrum indicated that the product was essentially pure 1-(3-methylbut-2-en-1-yloxy)-2-(2-methylbut-3-en-2-yloxy) benzene (44 mg, 92%) as a colourless oil. HREIMS M^+ 246.1614 ($\text{C}_{16}\text{H}_{22}\text{O}_2$ requires 246.1619). ^1H NMR (CDCl_3) δ 6.80-7.02 (m, 4H, ArH), 6.17 (dd, $J_{\text{HH}} = 10.7, 17.4$ Hz, 1H, =CH), 5.49 (m, 1H, =CH), 5.11 (dd, $J_{\text{HH}} = 0.9, 17.5$ Hz, 1H, =CH₂), 5.05 (dd, $J_{\text{HH}} = 0.9, 10.4$ Hz, 1H, =CH₂), 4.52 (d, $J_{\text{HH}} = 6.2$ Hz, 2H, OCH_2), 1.76 (s, 3H, CH_3), 1.71 (s, 3H, CH_3), 1.42 (s, 6H, CH_3). ^{13}C NMR (CDCl_3) δ 152.5 (ArO), 145.7 (ArO), 144.3, 136.7, 124.2, 123.4, 120.4, 120.4, 114.7, 112.9, 80.6, 65.9, 26.5, 25.7, 18.1. IR (CDCl_3 , cm^{-1}) 2976, 2931, 1591, 1496, 1450, 1379, 1255, 1206, 1110.

(iii) The partial hydrogenation product (42 mg, 0.17 mmol) obtained from (ii) was added to a solution of *m*-CPBA (46 mg, 0.18 mmol, 70 % purity) in CH_2Cl_2 (50 mL) at 0 °C. The solution was allowed to warm to room temperature and stirred for 15 hours. The reaction was then poured into a solution of ice-cold saturated aqueous sodium

bicarbonate and extracted with CH_2Cl_2 . The organic phase was washed with brine, dried (MgSO_4) and then evaporated. Chromatography on silica with ether/petroleum ether (1:9) gave 1-(2,3-epoxy-3-methylbut-1-yloxy)-2-(2-methylbut-3-en-2-yloxy) benzene (**35**) (28 mg, 61%) as a colourless oil. HREIMS M^+ 262.1568 ($\text{C}_{16}\text{H}_{22}\text{O}_3$ requires 262.1568). ^1H NMR (CDCl_3) δ 6.85-7.04 (m, 4H, ArH), 6.16 (dd, 1H, $J_{\text{HH}} = 10.8, 17.6$ Hz, =CH), 5.14 (dd, 1H, $J_{\text{HH}} = 1.0, 17.6$ Hz, =CH₂), 5.07 (dd, 1H, $J_{\text{HH}} = 1.1, 10.7$ Hz, =CH₂), 4.12 (m, 1H, OCH₂), 4.09 (m, 1H, OCH₂), 3.17 (m, 1H, OCH), 1.44 (s, 6H, OCH₃), 1.33 (s, 3H, =CCH₃), 1.37 (s, 3H, =CCH₃). ^{13}C NMR (CDCl_3) δ 152.2 (ArO), 145.7(ArO), 144.1 (=C), 124.4 (ArH), 123.6 (ArH), 121.3 (ArH), 115.2 (=CH₂), 113.2 (ArH), 80.9 (ArOC), 68.1 (OCH₂), 61.5 (OCH), 58.2 (epoxide-C), 26.6 (CH₃), 26.5 (CH₃), 24.6 (CH₃), 18.9 (CH₃). IR (CH_2Cl_2 , cm^{-1}) 2979, 2929, 1591, 1498, 1450, 1379, 1255, 1209, 1132, 1112. Microanalysis calcd for $\text{C}_{16}\text{H}_{22}\text{O}_3$ C,73.25; H,8.45. Found: C,72.98; H,8.65.

2,2-Dimethyl-3-hydroxy-3,4-dihydro-2H-1,5-benzodioxepin (**36**)⁴⁷



(i) Ether **33** (1.80 g, 10 mmol) in CH_2Cl_2 (10 mL) was added to a solution of *m*-CPBA (4.9 g, 20 mmol, 70% purity) in CH_2Cl_2 (40 mL) at 0 °C. The solution was allowed to warm to room temperature and stirred for 16 hours. The reaction was poured into an ice-cold solution of saturated aqueous sodium bicarbonate and extracted with CH_2Cl_2 . The organic phase was washed with brine, dried (MgSO_4) and evaporated. The ^1H NMR spectrum indicated the product was almost pure 2-hydroxyphenyl-1-(2,3-epoxy-3-methylbut-1-yloxy) ether (1.65 g, 85%). HREIMS M^+ 194.0941 ($\text{C}_{11}\text{H}_{14}\text{O}_3$ requires 194.0942). ^1H NMR (CDCl_3) δ 6.84-6.94 (m, 4H, ArH), 4.27 (dd, $J_{\text{HH}} = 4.1, 11.0$ Hz,

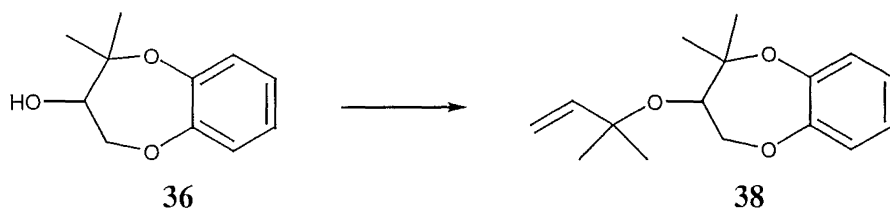
1H, ArOCH₂), 4.08 (dd, $J_{\text{HH}} = 6.3, 10.9$ Hz, 1H, ArOCH₂), 3.17 (dd, $J_{\text{HH}} = 4.2, 6.2$ Hz, 1H, OCH), 1.40 (br s, 3H, CCH₃), 1.37 (br s, 3H, CCH₃). IR (CDCl₃, cm⁻¹) 3450.4, 2977, 2929, 1583, 1492, 1456, 1257, 1068.

(ii) Tin (IV) chloride (990 μL , 8.4 mmol) was added to a solution of the epoxide (1.65 g, 8.4 mmol) generated in (ii), in THF (115 mL) at 0 °C. The reaction was allowed to stir for 20 minutes then quenched by pouring into a solution of saturated sodium bicarbonate and extracted with ether. The organic phase was washed with brine, dried (MgSO₄) and evaporated. Chromatography on silica with ether/petroleum ether (2:8) gave the title compound **36** (426 mg, 22% from **33**). ¹H and ¹³C NMR data were consistent with those in the literature.⁴⁷ Microanalysis calcd for C₁₁H₁₄O₃ C,68.02; H,7.27. Found: C,68.02; H,7.27.

Also isolated was the major side product of this reaction (177 mg, 9%) a six-membered ring hemiacetal (**37a**) in equilibrium with the ketone (**37b**). Spectral data collected on the mixture included HREIMS M⁺ 194.0943 (C₁₁H₁₄O₃ requires 194.0942). IR (CDCl₃, cm⁻¹) 3562, 2974, 2939, 2881, 2252, 1722, 1596, 1494, 1463, 1390, 1305, 1265, 1191.

37a (assigned from the mixture) ¹H NMR (CDCl₃) δ 6.87-6.91 (m, ArH), 4.12 (d, $J_{\text{HH}} = 10.1$ Hz, 1H, OCH₂), 3.88 12 (d, $J_{\text{HH}} = 10.1$ Hz, 1H, OCH₂), 3.19 (br s, 1H, OH), 2.08 (sept, $J_{\text{HH}} = 6.9$ Hz, 1H, CH), 1.11 (d, $J_{\text{HH}} = 6.9$ Hz, 3H, CH₃), 1.08 (d, $J_{\text{HH}} = 6.9$ Hz, 3H, CH). ¹³C NMR (CDCl₃) δ 142.3 (ArO), 141.7 (ArO), 122.4 (ArH), 121.4 (ArH), 117.8 (ArH), 116.9 (ArH) 96.0 (OCOH), 67.8 (OCH₂), 34.2 (CH), 16.4 (CH₃), 15.7 (CH₃).

37b (assigned from the mixture) ¹H NMR (CDCl₃) δ 6.87-6.91 (m, ArH), 4.76 (s, 2H, OCH₂), 2.68 (sept, $J_{\text{HH}} = 6.8$ Hz, 1H, CH), 1.14 (CH₃). ¹³C NMR (CDCl₃) δ 222.2 (C=O), 147.8 (ArO), 142.3 (ArO), 116.4-124.1 (ArH), 74.7 (O CH₂), 37.2 (CH), 17.9 (CH₃).

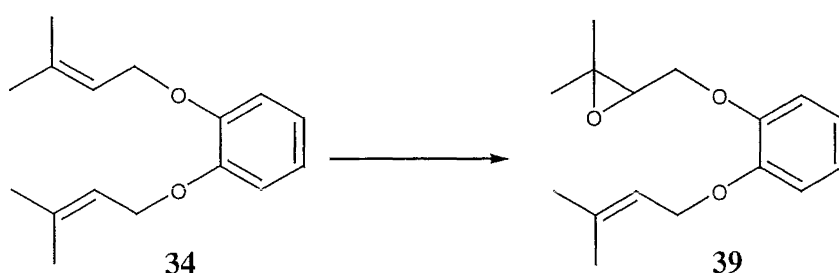
2,2-Dimethyl-3-(2-methylbut-3-en-2-yloxy)-3,4-dihydro-2H-1,5-benzodioxepin (38)

(i) Alcohol **36** (86 mg, 0.44 mmol) in CH_2Cl_2 (200 μL) was added to the trichloroacetimidate⁵² of 3-methylbut-1-yn-3-ol (1.0 g, 4.4 mmol) in cyclohexane (880 μL) at room temperature under nitrogen. Boron trifluoride etherate (9 μL) was subsequently added to the reaction and then allowed to stir overnight.^{53,54} The reaction was then quenched with solid sodium bicarbonate and filtered through a plug of silica. Chromatography on silica (30:1 petroleum ether/EtOAc) removed the excess trichloroacetimidate and yielded a crude sample of 2,2-dimethyl-3-(2-methylbut-3-en-2-yloxy)-3,4-dihydro-2H-1,5-benzodioxepin (33 mg, 28%). HREIMS 260.1404 ($\text{C}_{16}\text{H}_{20}\text{O}_3$ requires 260.1412). ^1H NMR (CDCl_3) 6.90-6.93 (m, 2H, ArH), 4.41 (m, 1H, OCH_2), 4.07 (m, 1H, OCH_2), 4.04 (m, 1H, OCH), 2.49 (s, 1H, $\equiv\text{CH}$), 1.50 (s, 6H, CH_3), 1.44 (s, 3H, CH_3), 1.23 (s, 3H, CH_3).

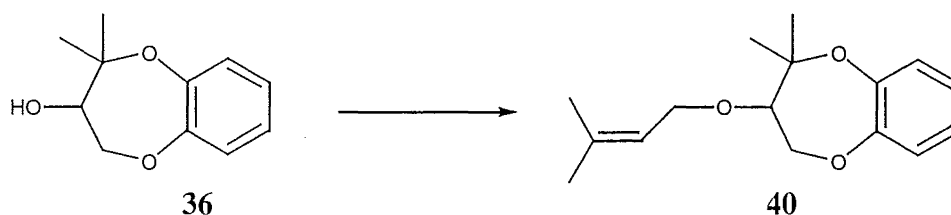
(ii) Partial hydrogenation of this alkyne (10 mg, 0.04 mmol) was carried out with 5% palladium on barium sulfate (3 mg, 33% w/w) with quinoline (3 mg, 33% w/w) in EtOAc (3 mL) at 20 °C and atmospheric pressure for 16 hours. The reaction was then filtered through Celite and the solvent evaporated. The residue was dissolved in ether, washed with 5% aqueous hydrochloric acid, brine, then dried (MgSO_4) and finally evaporated to yield 2,2-dimethyl-3-(2-methylbut-3-en-2-yloxy)-3,4-dihydro-2H-1,5-benzodioxepin (8 mg, 75%). HREIMS M^+ 262.1565 ($\text{C}_{16}\text{H}_{22}\text{O}_3$ requires 262.1568). ^1H NMR (CDCl_3) δ_{H} 6.88-6.90 (m, 4H, ArH), 5.87 (dd, 1H, $J_{\text{HH}} = 10.7, 17.5$ Hz, $\text{CH}=\text{CH}_2$), 5.16 (br d, 1H, $J_{\text{HH}} = 17.6$ Hz, $\text{CH}_2=\text{CH}$), 5.14 (br d, 1H, $J_{\text{HH}} = 10.7$ Hz, $\text{CH}_2=\text{CH}$), 4.20 (dd, 1H, $J_{\text{HH}} = 3.4, 12.2$ Hz, OCH_2), 3.96 (dd, 1H, $J_{\text{HH}} = 3.4, 8.0$ Hz, OCH_2), 3.68 (dd, 1H, $J_{\text{HH}} = 3.4, 7.8$ Hz, OCH), 1.40 (s, 3H, CH_3), 1.30 (s, 6H, CH_3), 1.19 (s, 3H, CH_3).

CH₃). ¹³C NMR (CDCl₃) δ 151.3 (ArO), 146.6 (ArO), 143.6 (=CH), 124.0 (ArH), 123.8 (ArH), 123.0 (ArH), 120.1 (ArH), 114.3 (=CH₂), 81.3 (ArOC), 76.1 (OCCH=), 75.5 (OCH), 71.6 (OCH₂), 28.1(CH₃), 26.7 (=CCH₃), 26.3 (=CCH₃), 21.6 (CH₃). IR (CDCl₃, cm⁻¹) 2981, 2975, 1491, 1262, 1143, 1065, 934, 886. Microanalysis calcd for C₁₆H₂₂O₃ C,73.25; H,8.45. Found: C,73.54; H,8.15.

1-(2,3-Epoxy-3-methylbut-1-yloxy)-2-(3-methylbut-2-en-1-yloxy) benzene (39)



Diether **34** (100 mg, 0.4 mmol) was added to a solution of *m*-CPBA (100 mg, 0.4 mmol, 70% pure) in CH₂Cl₂ (10 mL) at 0 °C. The solution was allowed to warm to room temperature and stirred for two hours. The reaction was then poured into a saturated solution of ice-cold aqueous sodium bicarbonate and extracted with ether/petroleum ether (1:1). The organic phase was washed with brine, dried (MgSO₄) and evaporated. Chromatography on silica with ether/petroleum ether (1:9) gave the diepoxide product (8 mg) and the title compound **39** (52 mg, 68% based on returned starting material). HREIMS M⁺ 262.1562 (C₁₆H₂₂O₃ requires 262.1568). ¹H NMR (CDCl₃) δ 6.89-6.98 (m, ArH, 4H), 5.52 (m, 1H, =CH), 4.57 (d, *J*_{HH} = 6.5 Hz, 2H, OCH₂C=), 4.20 (dd, *J*_{HH} = 5.0, 11.7 Hz, 1H, ArOCH₂), 4.13 (dd, *J*_{HH} = 5.4, 11.4 Hz, 1H, ArOCH₂), 3.18 (m, 1H, CH-epoxide), 1.77 (s, 3H, =CCH₃), 1.73 (s, 3H, =CCH₃), 1.36 (s, 3H, epoxide-CH₃), 1.31 (s, 3H, epoxide-CH₃). ¹³C NMR (CDCl₃) δ 149.2 (ArO), 148.9 (ArO), 137.5 (=C), 121.8 (ArH), 121.1 (ArH), 120.0 (=CH), 115.0 (ArH), 114.2 (ArH), 68.2 (OCH₂), 65.9 (OCH₂CH=), 61.5 (OCH), 58.3 (OC(CH₃)₂), 25.7 (CH₃), 24.4 (CH₃), 18.8 (CH₃), 18.0 (CH₃). IR (CDCl₃, cm⁻¹) 2966, 2931, 2879, 1595, 1504, 1450, 1380, 1249, 1213, 1120.

2,2-Dimethyl-3-(3-methylbut-2-en-1-yloxy)-3,4-dihydro-2H-1,5-benzodioxepin (40)

Dioxepin alcohol **36** (30 mg, 1.5 mmol) in dry THF (1 mL) was added to sodium hydride (7 mg, 0.3 mmol) in THF (3 mL) at 0 °C. 1-Bromo-3-methylbut-2-ene (350 μ L, 3 mmol) was added with the reaction allowed to warm to room temperature and stirred for 12 hours. The reaction mixture was then poured into a solution of saturated aqueous ammonium chloride and extracted with ether/ethyl acetate (1:1). The organic phase was washed with brine, dried (MgSO_4) and then evaporated. Chromatography on silica with ether/petroleum ether (1:9) gave the title compound **40** (20 mg, 50%) as a colourless oil and recovered starting alcohol **36** (8 mg). HREIMS M^+ 262.1572 ($\text{C}_{16}\text{H}_{22}\text{O}_3$ requires 262.1568). ^1H NMR (CDCl_3) δ 6.91-6.96 (m, 4H, ArH), 5.34 (m, 1H, =CH), 4.22 (dd, $J_{\text{HH}} = 3.0, 12.5$ Hz, 1H, ArOCH₂), 4.11 (dd, $J_{\text{HH}} = 6.7, 11.7$ Hz, 1H, OCH₂CH=), 4.08 (dd, $J_{\text{HH}} = 7.3, 11.7$ Hz, 1H, OCH₂CH=), 3.95 (dd, $J_{\text{HH}} = 7.4, 12.7$ Hz, 1H, ArOCH₂), 3.52 (dd, $J_{\text{HH}} = 3.1, 7.4$ Hz, 1H, OCH), 1.78 (br s, 3H, =CCH₃), 1.68 (br s, 3H, =CCH₃), 1.45 (s, 3H, CH₃), 1.19 (s, 3H, CH₃). ^{13}C (CDCl_3) δ 151.5 (ArO), 147.1 (ArO), 137.4 (=C), 124.0 (ArH), 123.8 (ArH), 123.4 (ArH), 120.6 (ArH), 120.9 (=CH), 81.9 (OCH), 80.2 (OC), 68.6 (OCH₂), 67.2 (OCH₂CH=), 27.5 (CH₃), 25.6 (=CCH₃), 20.5 (CH₃), 17.9 (=CCH₃). IR (CDCl_3 , cm^{-1}) 2977, 2937, 1598, 1409, 1456, 1261, 1074. Microanalysis calcd for $\text{C}_{16}\text{H}_{22}\text{O}_3$ C, 73.25; H, 8.45. Found: C, 73.34; H, 8.65.

7.2.4 Culturing of *Favolaschia calocera*

General techniques and procedures

All culturing work was carried out in a laminar flow cabinet using standard aseptic techniques. Solid phase cultures of *F. calocera* were grown on Potato Dextrose Agar (PDA) plates. The agar was made up to one-fifth normal strength (5 g/L) with distilled H₂O, autoclaved, cooled, poured into sterile petrie dishes that were allowed to set and then stored at -4 °C until required. Subcultures were taken approximately every six weeks. A plug from the outer regions of an old plate was placed upside down on a fresh plate. These plates were incubated for 2 weeks at 25 °C and then left at room temperature. Liquid broth cultures of *F. calocera* were grown using Potato Dextrose Broth (PDB) also at one-fifth the normal strength (5 g/L). Distilled H₂O (2 L) was added to PDB powder (10 g) and allowed to stir until all the material had dissolved. PDB (approx. 150 mL) was poured into a series of Fernback flasks (3 x 300 mL), autoclaved, cooled, then inoculated with 40-50 plugs of *F. calocera* grown on PDA plates. These cultures were incubated for 21 days at 25°C. The broth was combined and filtered through a bed of Celite to remove the mycelial mat.

Chromatography of the liquid broth of *F. calocera*

The filtered liquid broth was directly loaded onto a reverse-phase (C18) column (15 g, 2 x 8 cm) and eluted with a stepped gradient from H₂O through to MeOH and 1:1 MeOH/CH₂Cl₂. Seven fractions were collected and submitted for assay against the P388 cell line. The fraction that eluted with MeOH (GN2-18.5) showed significant cytotoxicity (IC₅₀ 18.5 ng/mL) against the P388 assay. Four batches were cultured and chromatographed in the same manner. All the fractions that eluted in MeOH showed significant cytotoxicity. All the active fractions were analysed by analytical reverse-phase (C18) HPLC and by ¹H NMR spectroscopy. A number of peaks in the chromatograph had UV spectra consistent with that for the strobilurin skeleton.

Characteristic signals in the ^1H NMR spectra were also visible, including a cluster of methoxy signals (δ_{H} 3.6-3.8).

Chromatography of fraction eluting in MeOH.

The active fractions that eluted in MeOH, were combined (51.0 mg) and further purified by normal-phase (DIOL) column chromatography (10 g, 2 x 10 cm), with a stepped gradient from petroleum ether through CH_2Cl_2 , EtOAc and a final MeOH strip. Twenty-seven fractions were collected and combinations were made by TLC (silica). All the combined fractions were analysed by analytical reverse-phase (C18) HPLC, ^1H NMR spectroscopy and submitted for assay against the P388 cell line and for antimicrobial assays. Only fractions GN2-23.7-8 (1.3 mg, IC_{50} 10 ng/mL) showed significant cytotoxicity, while fractions GN2-23.5 through to 23.15 showed significant antifungal (but no antibacterial) activity (2 $\mu\text{g}/\text{disk}$). The ^1H NMR spectrum of the combined fraction GN2-23.7-8 showed it to be a mixture, but the characteristic signals for 9-methoxystrobilurin K (**16**) were visible. Discussion of these results is detailed in **Section 2.5.3**.

7.3 Work described in Chapter Three

7.3.1 Collection, extraction and screening

Collection

Each fungal sample that was collected was given a unique number. This number included the year of collection (e.g. 96), a two letter acronym to represent the site of collection (e.g. CV – Craigieburn Visitors Centre), a number for the collection from that site that year (usually 1-2) and finally a specimen number for that particular collection trip (e.g. 1-60). A collection data sheet was completed for each specimen, which included identification (if possible), morphological and collection site details. Samples were frozen as soon as possible with voucher specimens freeze-dried.

Extraction and screening

A sample (2 g) of each collected specimen was extracted with 3:1 MeOH/CH₂Cl₂ (20 mL) by blending in a Vertis blender for 5 minutes. After centrifugation, the supernatant was decanted to give the organic extract. Another sample (2 g) was extracted with distilled H₂O (20 mL) by the same method. Both extracts of each collected specimen were submitted for the full array of biological assays as detailed in **Section 3.3**.

Results

The screening results from this collection are detailed in **Section 3.4** and discussed in **Section 3.5**.

7.4 Work described in Chapter Four

7.4.1 Extraction and chromatography of *Entoloma hochstetteri*

Extraction

The bright blue fruiting bodies (30 g) of *Entoloma hochstetteri* were extracted with MeOH repeatedly until no pigmentation remained. Evaporation of the solvent under vacuum gave a dark green oil (104 mg, 96CC1-1). This extract was screened in our in-house assays and showed mildly antifungal activity against *Trichophyton mentagrophytes* (5mm, 0.3 mg/disk).

Chromatography of the *E. hochstetteri* extract

Purification of the pigments observed by TLC was attempted by normal-phase (DIOL) column chromatography (10 g, 2 x 10 cm) with a stepped gradient from petroleum ether through to CH₂Cl₂. Fourteen fractions were collected and combinations made after TLC analysis (silica). The combined fraction (GN2-75.4-6, 3.7 mg) that eluted in 5% CH₂Cl₂ contained two high running blue spots by TLC (silica) (CH₂Cl₂/1% MeOH).

Fraction GN2-75.4-6 was separated on small reverse-phase (C18) column (1 g, 0.5 x 5 cm) eluted with a stepped gradient from 1:3 H₂O/MeOH through 1:9 H₂O/MeOH, MeOH and then stripped with CH₂Cl₂. Eight fractions were collected and combinations were by TLC (silica) and comparison of ¹H NMR spectra.

The combined fraction GN2-81.4-5 (0.6 mg) contained a blue pigment and was shown to be homogeneous by TLC (silica) and ¹H NMR spectroscopy. Using 2-D NMR experiments and mass spectrometry this blue compound was identified as 7-acetyl-1,4-dimethyl azulene (**56**). The structural elucidation of this compound is discussed in **Chapter Four**. HREIMS M⁺ 198.1044 (C₁₄H₁₄O requires 198,1044); *m/z* 183 (M-

CH₃) 155, 128, 115, 77. IR (neat, cm⁻¹) 3143, 2343, 1816, 1795, 1672 (C=O), 1598, 1471, 1469, 1386, 1097.

7.5 Work described in Chapter Five

7.5.1 First extraction of *Cortinarius* species (Catlins)

Chemical screening

The extract of *Cortinarius* sp. (Catlins) was examined using “chemical screening.”[‡] A MeOH solution (2 mg/mL) was prepared from a small sample of the extract. An aliquot (200 µL) of this solution was loaded onto a C18 cartridge followed by an aliquot of H₂O (200 µL). Three fractions were collected from a steep stepped gradient (solvent, IC₅₀: 1:1 MeOH/H₂O, 1120 ng/mL; MeOH, 556 ng/mL; 1:1 MeOH/CH₂Cl₂, 1540 ng/mL). The same aliquot (200 mL) was loaded on to a cartridge packed with LH20 (1.5 g). Four fractions were collected from elution with MeOH (volume, IC₅₀: 3.3 mL, >6250 ng/mL; 1 mL, 10143 ng/mL; 4 mL, 1120 ng/mL; 4 mL, 590 ng/mL). A third aliquot was coated onto a small amount of Celite and dry packed onto a DIOL cartridge. Three fractions were collected from a steep stepped gradient (solvent, IC₅₀: petroleum ether, 312 ng/mL; CH₂Cl₂; 97 ng/mL; EtOAc, 6407 ng/mL; MeOH, 1890). A fourth aliquot was loaded onto a CBA cartridge. Three fractions were collected (solvent, IC₅₀: MeOH/NH₄OAc, 2186 ng/mL; MeOH/NH₃, 4791 ng/mL; MeOH/TFA, 8568 ng/mL).

[‡] A procedure developed in the Marine Group for the rapid evaluation of chemical and physical properties of bioactive extracts.

Large scale extraction

A sample (200 g) of *Cortinarius* species (Catlins) fruiting bodies was soaked overnight in MeOH/H₂O (60:40, 600 mL). The solvent was then decanted and the residue blended with a measure of MeOH (300 mL) and filtered. This was repeated three times. The MeOH was removed under vacuum and then the H₂O removed by freeze-drying. A brown, moderately cytotoxic extract (4.09 g IC₅₀ 925 ng/mL) was obtained, which also showed significant antimicrobial activity (5-15 mm, 0.15 mg/disk).

7.5.2 Chromatography of the first extract of *Cortinarius* sp. (Catlins)

Preliminary chromatography of the *Cortinarius* sp. extract

Initially, a small sample (50 mg) of the extract was loaded onto a reverse-phase (C18) column (10 g, 2 x 8 cm) and eluted with a stepped gradient from H₂O through to MeOH. Twenty fractions were collected, analysed by TLC (C18) and submitted for assay against the P388 cell line. Combinations were made using both the TLC and assay results. The fractions (GN2-77.17-18, 1.4 mg) that eluted in 40-60% MeOH/H₂O were the most active, both having an IC₅₀ value of 60 ng/mL. The ¹H NMR spectrum of the most active fraction (GN2-77.18) was very simple, containing only four aromatic signals. HPLC analysis using reverse-phase (C18) showed a single compound. This compound was later identified as 2,2'-dithiobis(pyridine *N*-oxide) - also known as dipyrithione - (**59**) and is discussed in Section 5.4.1.

Compound (**59**)

HREIMS (M-32)⁺ 220.0128 (C₁₀H₈N₂S₂ requires 220.0128). EIMS *m/z* 67, 78 (100%), 79, 80, 82, 110 (84%), 111, 126, 127, 128, 129, 142, 155, 156 (14%), 220 (20%), 221, 222.

FABMS (glycerol matrix) MH^+ 253. (MBS/NIST Library - Dipyrithione MW 252 $C_{10}H_8N_2O_2S_2$ EIMS m/z 48, 52, 67, 78 (100%), 83, 110(50%), 111, 128, 129, 130, 142, 155, 156(95%), 157, 187, 188, 189, 220(95%), 221, 222, M^+ not observed).

IR (CaF_2 plate, cm^{-1}) 3361 (broad), 1660 (broad), 1461, 1417.

The fractions (GN2-77.8-14, 1.3 mg) that eluted in 10-30% MeOH/ H_2O all showed moderate cytotoxicity with IC_{50} values ranging from 700-3000 ng/mL. Analysis of this combined fraction by reverse-phase (C18) HPLC revealed a number of components. Chromatography of the full extract was then undertaken so that the more polar cytotoxic component could be isolated and identified.

Chromatography of the remainder of the first extract

The remainder of the extract (3.7 g) was divided into three portions for purification (1.15, 0.70 and 1.8 g). These portions were each loaded onto a reverse-phase (C18) column (100 g, 3 x 600 cm) and eluted with a gradual stepped gradient from H_2O through to MeOH. Twenty fractions were collected from each of the three columns, with fractions analysed by TLC (C18) and submitted for assay against the P388 cell line. Combinations were made by comparison of the TLC and assay results. The most cytotoxic combined fraction (GN2-88.6, 97.4 mg, IC_{50} <19.5-98 ng/mL), which eluted in 60-80% MeOH/ H_2O , was analysed by 1H NMR spectroscopy and was shown to contain the previously identified 2,2'-dithiobis(pyridine *N*-oxide) (**59**). The more polar band of cytotoxicity (GN2-88.3, 317.4 mg, IC_{50} 174-626 ng/mL) eluted in H_2O to 20% MeOH/ H_2O . The 1H NMR spectrum of this sample contained aromatic signals similar to those identified as compound **59**. This fraction was therefore further purified to isolate this polar unknown component.

The combined fraction (GN2-88.3, 317.4 mg) was loaded onto a reverse-phase (C18) column (100 g, 3 x 600 cm) and eluted with a gradual stepped gradient from H_2O

through 40% MeOH and then quickly through to MeOH. Twenty fractions were collected and submitted for assay against the P388 cell line. Combination of these fractions was made on the assay results and the ^1H NMR spectra of the active fractions. The ^1H NMR spectrum of the combined fraction (GN2-93.9, 17.4 mg) that eluted in 60% MeOH showed the previously identified 2,2'-dithiobis(pyridine *N*-oxide) (**59**). The more polar cytotoxic band was concentrated in one fraction (GN2-93.7, 45.7 mg, IC_{50} 169 ng/mL), which eluted in 10% MeOH/ H_2O . The ^1H NMR spectrum of this fraction contained similar aromatic signals to those compound **59**, along with a number of other signals between δ_{H} 1.5-4.5.

The first purification of compounds 60 and 61

The polar cytotoxic fraction (GN2-93.7, 45.7 mg) was further purified by loading onto another reverse-phase (C18) column (8 g, 1 x 10 cm), which was eluted with a gradual stepped gradient from H_2O through 10% MeOH/ H_2O and then to MeOH. Seventeen fractions were collected and submitted for assay against the P388 cell line. Fractions (GN2-94.6-94.11) that eluted in 10% MeOH/ H_2O were analysed by ^1H NMR spectroscopy and were all found to contain the same aromatic (δ_{H} 7.2-8.2) and aliphatic signals. Fractions GN2-94.7-9 (4.4 mg) were found to be the cleanest and were combined so 2-D NMR experiments could be run on this sample. From these NMR experiments three structural fragments were assigned for compound **60** (Section 5.4.2).

During the overnight-run of NMR experiments on compound **60** a number of new signals arose from the base line. Each new signal appeared to correspond to an equivalent in the original compound, with the aromatic signals corresponding to that of **59**. A pure sample with the new signals (corresponding to the non-aromatic fragment) was found on examination of fractions GN2-94.2-4 (2.4 mg), which eluted from the same column in H_2O . 2-D NMR experiments were subsequently run on this sample

(GN2-94.2-4). The two non-aromatic fragments assigned to compound **60** could also be assigned for compound **61** and is described in detail in **Section 5.4.3**.

Further chromatography to obtain pure samples of compounds 60 and 61

Although 2-D NMR experiments had been run on these two compounds the initial data obtained did not give conclusive evidence for the proposed structures. Problems of decomposition added to difficulties with samples quickly becoming impure. Clean material was required for further spectroscopic analysis, including ^1H NMR spectra in alternative solvents (e.g. DMSO), ORD measurements and for mass spectrometry. Therefore, fractions that eluted from the second reverse-phase (C18) column (GN2-92.1-) either side of the most active fraction (GN2-92.11, already purified) were combined. This combined sample was loaded onto a reverse-phase (C18) column (5 g, 1 x 15 cm) and eluted with a stepped gradient from H_2O through 10-40% $\text{MeOH}/\text{H}_2\text{O}$. Fifteen fractions were collected and analysed by TLC (C18) and ^1H NMR spectroscopy. The ^1H NMR spectra of fractions that contained the parent compound **60** revealed they were still not pure. At this point, a number of fractions (GN2-94.7-9, -94.12-16; -96.4-7, 23.1 mg) from previous columns that contained the parent compound **60** were combined along with the fraction where decomposition had occurred during overnight NMR experiments. This combined sample was loaded onto another reverse-phase (C18) column and eluted with H_2O then 10% $\text{MeOH}/\text{H}_2\text{O}$. The first fraction that eluted was the homodimer **61** (2.1 mg). Fractions that eluted in 10% $\text{MeOH}/\text{H}_2\text{O}$ (100.6-10, 9.8 mg) contained the parent compound **60**. HRFABMS was obtained on the parent compound **60** but was unsuccessful on the homodimer **61**.

7.5.3 Second collection, extraction and chromatography of *Cortinarius* sp. (Catlins)

Extraction

A sample of frozen *Cortinarius* sp. (Catlins) fruit bodies (125 g) was repeatedly extracted with H₂O. A brown, moderately cytotoxic extract (4.56 g, IC₅₀ 1115 ng/mL) was obtained, which also showed antimicrobial activity. The level and spectrum of activity was consistent with the first collection and extraction of *Cortinarius* sp. (Catlins).

Chromatography of this second extract

The aqueous extract of *Cortinarius* sp. (Catlins) was loaded on to a reverse-phase (C18) column (200 g, 4.5 x 17 cm) and eluted with a stepped gradient from H₂O through 10-50% MeOH/H₂O. Twelve fractions were collected and analysed by ¹H NMR spectroscopy. Fractions that eluted in 10-20% MeOH/H₂O (GN4-56.5-8, 163 mg) all contained visible amounts of the parent compound **60**. A number of attempts were made to purify a small amount of these fractions by reverse-phase (C18) HPLC, including a number of solvent systems and the addition of TFA, but were unsuccessful. Chromatography on LH20 with elution in 70% H₂O/MeOH was also tried in an attempt to purify compound **60**. Only poor separation was obtained so the strategy for purification of compounds **60** and **61** therefore reverted to reverse-phase (C18) columns with elution in a gradual stepped gradient, as pure material had already been obtained by this method.

Purification of fraction GN4-56.8

Fraction GN4-56.8 (71 mg) was loaded onto a reverse-phase (C18) column (14 g, 2 x 12 cm) and eluted with a stepped gradient from H₂O through 10-20% MeOH/H₂O. Twenty fractions were collected analysed by ¹H NMR spectroscopy.

The fractions that eluted in H₂O (GN4-66.5-66.7, 0.9 mg) contained the compound **61**. Fractions GN4-66.5-7 were combined and loaded onto a small reverse-phase (C18) column (1 g, 0.5 x 5 cm), which was eluted in H₂O, with ten fractions (0.5 mL each) being collected. Fractions GN4-67.3-5 (0.2 mg) were shown to contain pure compound **61**, so were combined and sent to Dr L.K. Pannell for mass spectrometric analysis, including ESIMS and HRFABMS.

The fractions that eluted in 10% MeOH/H₂O (GN4-66.11-14, 11.8 mg) all contained the parent compound **60**. Fractions GN4-66.12-13 were combined and loaded onto a small reverse-phase (C18) column (1 g, 0.5 x 5 cm) and eluted with a stepped gradient from H₂O through 10-20% MeOH. Eighteen fractions were collected and analysed by ¹H NMR spectroscopy. Fraction GN4-68.6 (0.6 mg) contained pure parent compound **60**, which was also sent to Dr L.K. Pannell for mass spectrometric analysis.

Cortamidine oxide (**60**)

HREIMS - No molecular ion was observed - m/z 127.0115 (C₅H₅NOS requires 127.0091). EIMS m/z 52, 67, 78, 79, 111, 127, 149, 156.

FABMS (Canterbury and ANU) MH⁺ 344.0710 (C₁₃H₁₈O₄N₃S₂ requires 344.0738). m/z 366 (MNa⁺), 382 (MK⁺), 398 (MN_{a2}⁺), 404 (MNaK⁺), 420 (MK₂⁺).

ESIMS (NIH) (positive ion mode) 50V – m/z 709 (2MNa⁺), 687 (2MH⁺), 344 (MH⁺), 217, 169; 150V - m/z 251, 217, 123, 82.

ESIMS (NIH) (negative ion mode) 50V – m/z 364 [(MNa-2H)-], 215, 158; 60V - 364, 267, 215, 158, 123; 120V - 364, 274, 215, 158, 126, 123.

ESIMS (NIH) (positive, not acidified) – same as that for the acidified runs.

¹H NMR (DMSO) δ (very poor spectrum due to small sample and large water signal) 8.34 (d, J_{HH} = 6.4 Hz, H1), 7.96 (d, J_{HH} = 7.4 Hz, H1), 7.48 (d, J_{HH} = 7.8 Hz, H1), 7.31 (d, J_{HH} = 6.3 Hz, H1), 1.72 (m, 2H), 1.60 (m, 2H).

IR (on CaF₂ disk, cm⁻¹) 3263 (broad), 2927, 2856, 1666, 1660, 1651, 1645, 1614, 1573, 1558, 1539, 1504, 1463, 1456, 1417, 1379, 1326, 1265, 1188, 1083, 1026.

$[\alpha]_{\text{D}}^{25} = -10.0^{\circ}$ (0.3 mg/mL, MeOH).

Compound **60** as the TFA salt

¹H NMR (D₂O) δ 8.23 (d, $J_{\text{HH}} = 6.5$ Hz, 1H, H6''), 8.01 (d, $J_{\text{HH}} = 8.3$ Hz, 1H, H3''), 7.66 (t, $J_{\text{HH}} = 8.1$ Hz, 1H, H4''), 7.34 (t, $J_{\text{HH}} = 6.6$ Hz, 1H, H5''), 4.56 (dd, $J_{\text{HH}} = 3.9$, 9.7 Hz, 1H), 3.60 (m, 2H), 3.42 (dd, $J_{\text{HH}} = 4.0$, 14.8 Hz, 1H), 3.18 (dd, $J_{\text{HH}} = 9.3$, 14.8 Hz, 1H), 2.55 (m, 2H), 1.82 (m, 2H), 1.66 (m, 2H).

Compound **61**

HRFABMS (NIH) (NOBA) 457.1193 (35.7%) (C₁₆H₂₆O₆N₄S₂Na requires 457.1192).

EIMS (compound decomposes on the probe).

ESIMS (NIH) (positive ion mode): 50V – m/z 435 (MH⁺), 218 (MH₂⁺⁺); 100V – m/z 435 (MH⁺), 251, 217, 185 (**89**), 169 (**90**), (starting to appear – m/z 141, 125 (**91**), 123 (**92**), 82); 200V – m/z 435, 251, 229, 185, 169, 141, 125, 123, 115, 82.

ESIMS (NIH) (negative ion mode) 50V – m/z 455 ((MNa-2H)⁻), 433 ((M-H)⁻), 216; 75V – m/z 455, 433, 249, 183; 125V – m/z 455, 433, 271, 249, 183; 153, 139, 123; 200V – m/z 455, 433, 271, 249, 183; 153, 139, 123 (**92**).

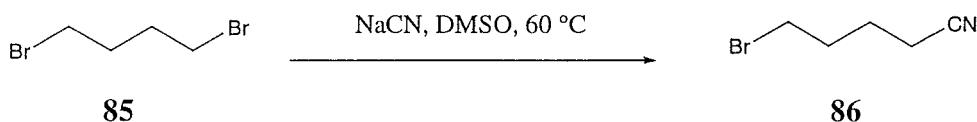
¹H NMR (DMSO) δ (3.84 (m), 3.43 (m, H₂), 3.12 (dd, $J_{\text{HH}} = 3.5$, 13.7 Hz, H₁), 2.92 (dd, $J_{\text{HH}} = 8.3$, 13.2 Hz, H₁), 2.42 (m), 1.74(m, 2H), 1.64 (m, 2H).

Compound **61** as the TFA salt

¹H NMR (D₂O) δ 4.43 (dd, $J_{\text{HH}} = 3.4$, 9.0Hz, 1H), 3.64 (m, 2H), 3.32 (dd, $J_{\text{HH}} = 3.9$, 14.5 Hz, 1H), 3.00 (dd, $J_{\text{HH}} = 9.1$, 14.9, 1H), 2.64 (m, 1H), 2.60 (m, 1H), 1.71 (m, 2H), 1.85(m, 2H).

7.5.4 Synthesis of 2-amino-3,4,5,6-tetrahydropyridine-*N*-oxide (84)

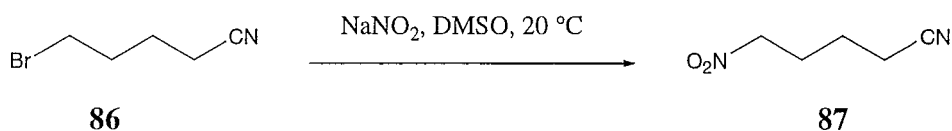
5-Bromopentan-1-nitrile



To a solution of 1,4-dibromobutane (**85**) (15 mL, 0.125 mol) in DMSO (100 mL) at 60 °C was added NaCN (6.13 g, 0.125 mol) in 10 approximately equal portions over 30 min. After stirring for a further 30 min the reaction was cooled to room temperature and diluted with Et₂O/hexane (1:1, 400 mL) then washed with saturated aqueous NaHCO₃, 10% aqueous HCl (*CARE!*), H₂O, and saturated brine (200 mL each). The organic phase was dried (MgSO₄), filtered and the solvent removed *in vacuo* to yield a yellow oil. Fractional distillation through a 10 cm Vigreux column gave 1,4-dibromobutane (**86**) (4.08 g) and the title compound **86** (9.41 g, 55% based on returned starting material). Bp 90 °C @ 2 mmHg.

HREIMS M⁺ 160.9836 (C₅H₈BrN requires 160.9840). ¹H NMR (CDCl₃) δ 3.42 (t, *J*_{HH} = 6.3 Hz, 2H), 2.39 (t, *J*_{HH} = 6.8 Hz, 2H), 2.01 (m, 2H), 1.84 (m, 2H). ¹³C NMR (CDCl₃) δ 119.0 (CN), 31.9, 31.0, 23.8, 16.3. FTIR (KBr, film, cm⁻¹) 2943, 2249, 1553, 1435, 1387, 1375.

5-Nitropentan-1-nitrile

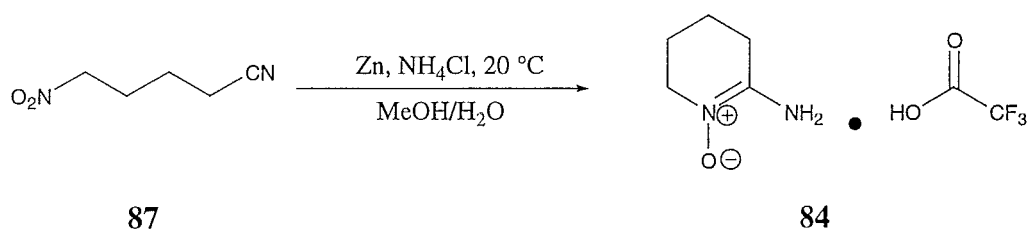


To a suspension of NaNO₂ (690 mg, 10 mmol) in DMSO (50 mL) at room temperature was added the nitrile **86** (1.62 g, 10 mmol) in DMSO (10 mL) over a period of ca. 10 min. The reaction became homogenous and was stirred for 4 hr at room temperature then diluted with Et₂O/EtOAc (1:1, 200 mL) and washed with saturated aqueous NaHCO₃, 10% aqueous HCl, H₂O, and saturated brine (200 mL each). The organic

phase was dried (MgSO_4), filtered and the solvent removed *in vacuo* to yield a light yellow oil. Flash chromatography (3:1 petroleum ether/EtOAc) gave 5-bromovaleronitrile (841 mg) and the title compound **87** (310 mg, 50% based on returned starting material).

HREIMS MH^+ 129.0663 ($\text{C}_5\text{H}_9\text{N}_2\text{O}_2$ requires 129.0664). ^1H NMR (CDCl_3) δ 4.46 (t, $J_{\text{HH}} = 6.3$ Hz, 2H), 2.44 (t, $J_{\text{HH}} = 6.8$ Hz, 2H), 2.16 (m, 2H), 1.78 (m, 2H). ^{13}C NMR (CDCl_3) δ 118.5 (CN), 74.3, 25.9, 22.2, 16.6. FTIR (KBr, film, cm^{-1}) 2943, 2872, 2247, 1454, 1292, 1251, 1238.

2-Amino-3,4,5,6-tetrahydropyridine-*N*-oxide (**84**)



To the nitrile **87** (100 mg, 0.78 mmol) and NH_4Cl (33 mg, 0.62 mmol) in $\text{MeOH}/\text{H}_2\text{O}$ (1:1, 10 mL) at 0 $^\circ\text{C}$ was added Zn dust (139 mg, 2.13 mmol). The reaction was warmed from 0 $^\circ\text{C}$ to room temperature stirred for 16hr then filtered and acidified to pH 2 with trifluoroacetic acid. The solvent was removed *in vacuo* to yield 2-amino-3,4,5,6-tetrahydropyridine-*N*-oxide (**84**) as a light orange oil.

^1H NMR (D_2O) δ 3.56 (t, $J_{\text{HH}} = 6.3$ Hz, 2H), 2.58 (t, $J_{\text{HH}} = 6.4$ Hz, 2H), 1.87 (m, 2H), 1.66 (m, 2H). ^{13}C NMR (D_2O) δ 153.0, 53.0, 27.6, 23.7, 18.8.

FTIR (KBr, film, cm^{-1}) 3500- 2800 (br), 1720-1620 (br), 1454, 1427, 1201, 1137, 1026, 1001, 839, 800, 723.

HRFABMS MH^+ 115.0867 ($\text{C}_5\text{H}_{11}\text{N}_2\text{O}$ requires 115.0871). LRFABMS m/z 229 (M_2H^+), 115 MH^+ and 99 (MH^+-16).

7.6 Work described in Chapter Six

7.6.1 Extraction of *Cortinarius rotundisporus*

Extraction

A sample (634 g - included ice) of *Cortinarius rotundisporus* (MG1-222) fruiting bodies was extracted by Dr Malcolm Buchanan (University of Melbourne, Australia). Extraction with ethanol yielded a thick brown sample that was partitioned between H₂O/EtOAc (H₂O - 19.5 g and EtOAc – 990 mg). A second extraction with ethanol gave additional material (880 mg). The second extract and the first two residues were then sent to University of Canterbury. The second extract was subsequently partitioned between H₂O/EtOAc. This gave residues after evaporation of the solvent of H₂O – 110 mg and EtOAc – 777 mg. All four samples were submitted for biological assay against the P388 cell line. The activity was concentrated in the EtOAc partitions (IC₅₀ 3400 ng/mL (1st extraction) and 4200 ng/mL (2nd extraction)).

Chemical screening

A small sample of the EtOAc residue of *C. rotundisporus* was examined using “chemical screening.”[‡] A MeOH solution (2 mg/mL) was prepared with an aliquot (200 µL) loaded onto a C18 cartridge follow by an aliquot of H₂O (200 µL). Three fractions were collected from a steep stepped gradient (solvent, IC₅₀; 1:1 MeOH/H₂O, >12500 10⁻⁶ dil.; MeOH, 574 10⁻⁶ dil.; 1:1 MeOH/CH₂Cl₂, >12500 10⁻⁶ dil.). Another aliquot (200 mL) was loaded on to a cartridge packed with LH20 (5 g). Four fractions were collected from elution with MeOH (volume, IC₅₀; 3.3 mL, >12500 10⁻⁶ dil.; 1 mL, >12500 10⁻⁶ dil.; 4 mL, 914 10⁻⁶ dil.; 4 mL, >12500 10⁻⁶ dil.). A third aliquot

[‡] A procedure developed in the Marine Group for the rapid evaluation of chemical and physical properties of bioactive extracts.

was coated onto a small amount of Celite and dry packed onto a DIOL cartridge. Three fractions were collected from a steep stepped gradient (solvent, IC₅₀; CH₂Cl₂, 914 10⁻⁶ dil.; EtOAc, 6791 10⁻⁶ dil.; MeOH, >12500 10⁻⁶ dil.).

7.6.1 Chromatography of *Cortinarius rotundisporus*

Chromatography of EtOAc partition

The combined EtOAc residues (GN4-11.1 - 990 mg and GN4-11.3 - 770 mg) were loaded onto a reverse-phase (C18) column (150 g, 4 x 20 cm), which was eluted with a stepped gradient from H₂O through MeOH, and then stripped with CH₂Cl₂. Thirteen fractions were collected and assayed for cytotoxicity against the P388 cell line. The cytotoxicity was centred on the fraction that eluted in 80%MeOH/H₂O (GN4-18.8, 75.7 mg, IC₅₀ 1000 ng/mL).

The active fraction (GN4-18.8, 76.8 mg) was loaded onto a normal-phase (DIOL) column (15 g, 2 x 10) and eluted with a stepped gradient from petroleum ether through diethyl ether, CH₂Cl₂, and finally stripped with MeOH. Twenty-seven fractions were collected and combinations were made by TLC (DIOL). These combined fractions were submitted for assay against the P388 cell line and examined by ¹H NMR spectroscopy. The cytotoxicity centred on fraction GN4-22.19 (8.3 mg, IC₅₀ 186 ng/L). Surrounding fractions also showed some cytotoxicity: GN4-22.16 (2.8 mg, IC₅₀ 648 ng/L); 22.17 (6.8 mg, IC₅₀ 1419 ng/L); 22.20 (4.0 mg, IC₅₀ 304 ng/L); 22.21 (9.8 mg, IC₅₀ 2691 ng/L). The ¹H NMR spectrum of GN4-22.19 was complex and appeared to contain at least two main components. The ¹H NMR spectra of surrounding the fractions were also complex, although two signals consistent with aldehyde protons (δ 9.43 and 10.28) were present in all the cytotoxic samples. A selection of chromatographic phases were tested by TLC to optimise separation of these remaining

components. Reverse-phase on C18 and CN gave poor separation (1:1 to 4:1 MeOH/H₂O) while normal-phase on CN (IPA/hexanes) gave excellent separation.

Purification of cytotoxic fraction (GN4-22.19)

Analytical HPLC on CN with a normal-phase solvent (3%IPA/hexanes) gave well-resolved peaks. Fraction GN4-22.19 (8.3 mg) was subsequently separated by semi-preparative CN HPLC (3%IPA/hexanes), with two main peaks being collected. The first had a retention time of 51 min (GN4-23.3, 1.3 mg, IC₅₀ 110 ng/mL) and the second 104 min (GN4-23.10, 2.1 mg, IC₅₀ 120 ng/mL). Both these samples were shown to be pure by TLC (silica) and ¹H NMR spectroscopy. Subsequent structural elucidation using 2-D NMR experiments enabled their assignment as rotundisine A (**94**) and B (**95**) (described in detail in **Section 6.4, Chapter Six**).

Purification of fractions surrounding GN4-22.19

To obtain additional amounts of compounds **94** and **95** the surrounding fractions from the last column (22.17-18 and 22.20-22) that were cytotoxic were combined and chromatographed. However, this was unsuccessful, as the compounds appeared to be decomposing. The drop in specific activity (mass/IC₅₀) as the purification proceeded also suggested decomposition could have been occurring.

Rotundisine A (94**)**

HREIMS M⁺ 544.3385 (C₃₂H₄₈O₇ requires 544.3399), HRFABMS (glycerol) MH⁺ 545.3478 (C₃₂H₄₉O₇ requires 545.3478). Fragment ions EIMS m/z 526 (544 - H₂O), 486 (M - AcOH)⁺, 485 (545 - AcO)⁺, 467 (485 - H₂O)⁺, 466, 407, 293, 281, 255, 231, 219, 217, 189, 187, 181, 175, 169, 143, 135, 133, 131, 128, 125, 121, 119, 107, 95, 93, 91, 85, 83, 81, 79, 77.

^1H NMR (d_6 -DMSO) δ 10.33 (s, 1H, H26), 7.40, 6.83, 6.39, 5.78 (d, $J_{\text{HH}} = 5.8$ Hz, 1H, OH11), 4.66 (br s, 1H, H3), 4.26 (s, 1H, OH22), 4.19 (m, 1H, H11), 3.84 (m, 1H, H21), 3.61 (s, 1H, H13), 2.13 (s, 3H, H32), 1.42, 1.33, 1.16, 1.15, 1.01, 0.97, 0.89.

^1H NMR (d_6 -benzene) δ 10.31 (s, 1H, H26), 7.25 (m, 1H, H16), 7.05 (d, $J_{\text{HH}} = 11.7$ Hz, 1H, H15), 5.78 (d, $J_{\text{HH}} = 14.6$ Hz, 1H, H17), 4.89 (m, 1H, H3), 3.69 (d, $J_{\text{HH}} = 7.3$ Hz, 1H, H11), 3.55 (m, 2H, H13 and H21), 1.88 (s, 3H, H32), 1.85/1.65 (m, 2H, H2), 1.66/1.42 (m, 2H, H20), 1.59/1.38 (m, 2H, H7), 1.49 (m, 2H, H1), 1.44 (m, 2H, H19), 1.40 (m, 1H, H5), 1.30/1.20 (m, 2H, H6), 1.28 (m, 1H, H9), 1.22 (s, 3H, Me28), 1.20 (s, 3H, Me24), 1.09 (s, 3H, Me25), 1.04 (s, 3H, Me27), 1.03 (s, 3H, Me23), 0.83 (s, 3H, Me30), 0.69 (s, 3H, Me29).

^{13}C NMR (d_6 -benzene) δ 215.7 (C12), 189.0 (C26), 169.9 (C31), 150.6 (C17), 150.1 (C15), 131.6 (C14), 118.9 (C16), 86.7 (C21), 83.1 (C18), 78.5 (C3), 72.5 (C11), 71.0 (C22), 61.9 (C13), 61.0 (C9), 52.4 (C5), 46.3 (C8), 41.2 (C7), 38.5 (C19), 38.2 (C10), 37.2 (C4), 33.5 (C1), 28.6 (C30), 27.9 (C24), 27.3 (C25), 26.7 (C20), 25.4 (C23), 23.3 (C2), 21.9 (C29), 21.5 (C32), 19.8 (C27), 19.5 (C6), 18.3 (C28).

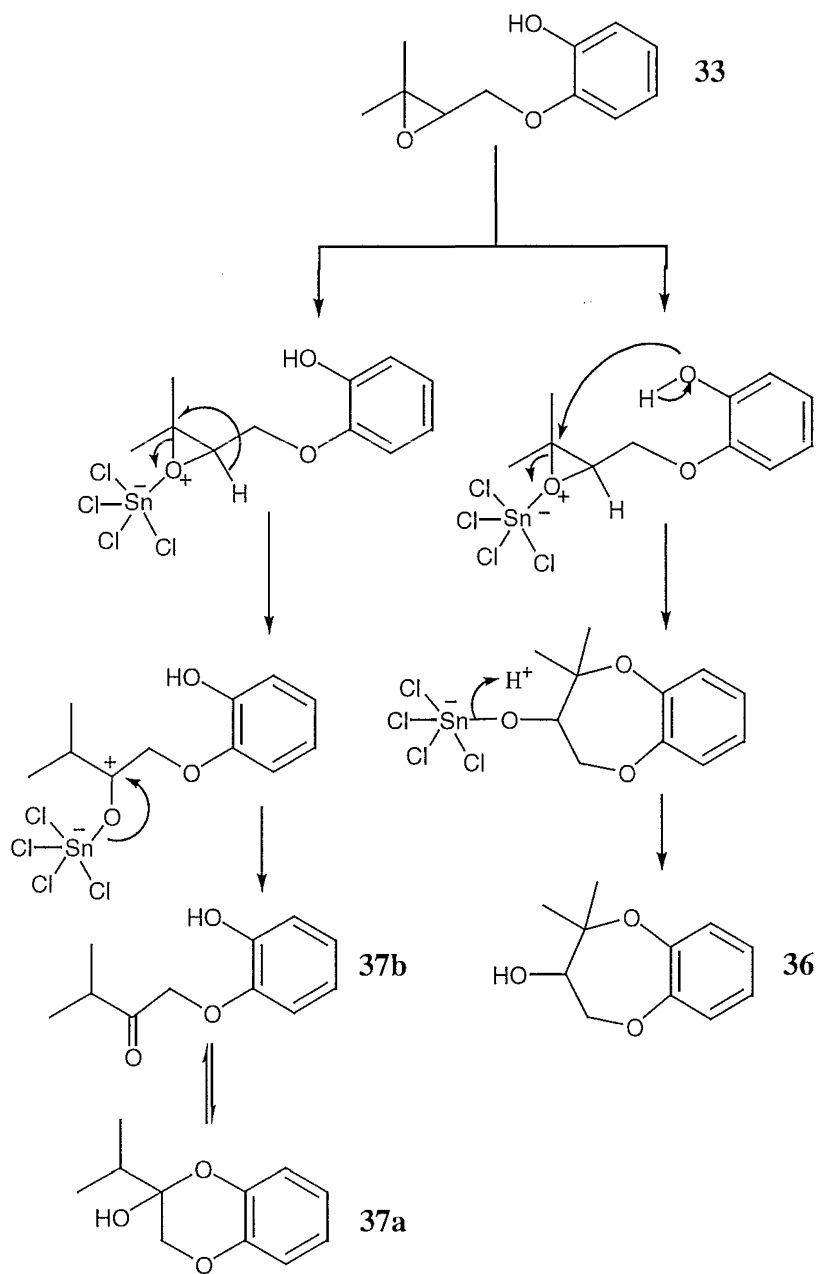
IR (CH_2Cl_2 , cm^{-1}) 3577, 2976, 2931, 2873, 2256, 1737, 1720, 1666, 1631, 1461, 1390, 1375, 1338, 1303, 1259, 1217, 1182, 1155, 1141, 1105, 1087, 1053, 1033, 1018, 975, 935, 879.

Rotundisine B (95)

Fragment ions EIMS m/z 526 (544 - H_2O), 486 ($\text{M} - \text{AcOH}$) $^+$, 485 (545 - AcO) $^+$, 467 (485 - H_2O) $^+$, 466, 407, 293, 281, 255, 231, 219, 217, 189, 187, 181, 175, 169, 143, 135, 133, 131, 128, 125, 121, 119, 107, 95, 93, 91, 85, 83, 81, 79, 77.

Appendix I

Reaction mechanism for the stannic chloride mediated epoxide opening of compound **33** that leads to the dioxepin **36**.



References

- 1 William, D.H.; Stone, M.J.; Hauck, P.R.; Rahman, S.K., *J. Nat. Prod.*, **1989**, 52, 1189-1208.
- 2 Hung, D.T.; Jamison, T.F.; Schreiber, S.L., *Chemistry and Biology*, **1996**, 3, 623-639.
- 3 Albert, A., *Selective toxicity*, 7th Ed., **1985**, Chapman Hall, London.
- 4 Levy, S.B., *Scientific American*, **1998**, 278(3), 32-39.
- 5 Ghisalberti, E.L., *Bioactive Natural Products: Detection and Isolation of Bioactive Natural Products*, **1993**, CRC Press, Inc., Boca Raton.
- 6 Buczacki, S., *Collins Guide - Mushrooms and Toadstools of Britian and Europe*, **1992**, Harper Collins Publishers, Glasgow.
- 7 Turner, W.B.; Aldridge, D.C., *Fungal Metabolites II*, **1983**, Academic Press, London.
- 8 Nisbet, L.J.; Winstanley, D.J.; Bu'lock, J.D., *Bioactive Microbial Products: Search and Discovery*, **1982**, 6, 59-61.
- 9 Monaghan, R.L.; Tkacz, J.S., *Ann. Rev. Micro.*, **1990**, 44, 271-301.
- 10 Turner, W.B., *Fungal Metabolites*, **1971**, Academic Press, London.
- 11 Ayer, W.A.; Browne, L.M., *Tetrahedron*, **1981**, 37, 2199-2248.
- 12 Weete, J.D., *Phytochemistry*, **1973**, 12, 1843-1864.
- 13 Yokoyama, S.; Natori, S.; Aoshima, K., *Phytochemistry*, **1975**, 14, 487-497.
- 14 Kasai, T.; Larsen, P.O., *Fortschr. Chem. Org. Naturst.*, **1980**, 39, 173-285.
- 15 Hatanaka, S.-I., *Fortschr. Chem. Org. Naturst.*, **1992**, 59, 1-140.
- 16 Gill, M.; Steglich, W., *Prog. Chem. Org. Nat. Prod.*, **1987**, 51, 1-317.

-
- 17 Gill, M., *Nat. Prod. Rep.*, **1994**, *11*, 67-90.
 - 18 Gill, M., *Aust. J. Chem.*, **1995**, *48*, 1-26.
 - 19 Steglich, W., *Pure Appl. Chem.*, **1981**, *53*, 1233-1240.
 - 20 Steglich, W., *Biologically Active Molecules: Some Chemical Phenomena of Mushrooms and Toadstools*, **1989**, Springer-Verlag, Berlin.
 - 21 Gloer, J.B., *Acc. Chem. Res.*, **1995**, *28*, 343-350.
 - 22 Benedict, R.G.; Brady, L.R., *J. Pharm. Sci.*, **1972**, *61*, 1820.
 - 23 Bresinsky, A.; Besl, H., *A Colour Atlas of Poisonous Fungi*, English translation, **1990**, Wolfe Publishing Ltd, London.
 - 24 Harvey, A.L., *Drugs from Natural Products*, **1993**, Ellis Horwood Ltd, England.
 - 25 Morita, K.; Kobayashi, S., *Chem. Pharm. Bull.*, **1967**, *15*, 988-993.
 - 26 Anke, T.; Steglich, W., *Biologically Active Molecules: β -Methoxyacrylate Antibiotics*, **1989**, Springer-Verlag, Berlin.
 - 27 Clough, J.M., *Nat. Prod. Rep.*, **1993**, *10*, 565-574.
 - 28 Newman, D.J., Natural Products Branch, NCI, personal communication.
 - 29 Nicholas, G.M., *Masters Thesis*, **1994**, University of Canterbury.
 - 30 Nicholas, G.M.; Blunt, J.W.; Cole, A.L.J.; Munro, M.H.G., *Tetrahedron Lett.*, **1997**, *38*(42), 7465-7468.
 - 31 Zapf, S.; Werle, A.; Anke, T.; Klostermeyer, D.; Steffan, B.; Steglich, W., *Angew. Chem. Int. Ed. Engl.*, **1995**, *43*(2), 196-198.
 - 32 Weber, W.; Anke, T.; Bross, M.; Steglich, W., *Planta Med.*, **1990**, *56*(5), 446-450.
 - 33 Backens, S.; Steglich, W.; Bauerle, J.; Anke, T., *Liebigs Ann. Chem.*, **1988**, 405-409.

-
- 34 Wood, K.A.; Kau, D.A.; Wrigley, S.K.; Beneyto, R.; Renno, D.V.; Ainsworth, A.M.; Penn, J.; Hill, D.; Killacky, J.; Depledge, P., *J. Nat. Prod.*, **1996**, *59*, 646-649.
- 35 Anke, T.; Oberwinkler, F.; Steglich, W.; Schramm, G., *J. Antibiotics*, **1977**, *30*, 806-810.
- 36 Schramm, G.; Steglich, W.; Anke, T.; Oberwinkler, F., *Chem. Ber.*, **1978**, *111*, 2779-2784.
- 37 Anke, T.; Schramm, G.; Schwalge, B.; Steffan, B.; Steglich, W., *Liebigs Ann. Chem.*, **1984**, 1616-1625.
- 38 Weber, W.; Anke, T.; Steffan, B.; Steglich, W., *J. Antibiotics*, **1990**, *43*, 207-212.
- 39 Engler, M.; Anke, T.; Klostermeyer, D.; Steglich, W., *J. Antibiotics*, **1995**, *48*, 884-885.
- 40 Miller, A., *Chemistry and Industry*, **1997**, *1*, 7.
- 41 Nicholas, G.M.; Blunt, J. W.; Cole, A. L. J.; Munro, M. H. G., *Tetrahedron*, in press.
- 42 Kashman, Y.; Isaacs, S.; Benayahu, Y., *J. Nat. Prod.*, **1994**, *57*(5), 648-649.
- 43 Arnone, A.; Cardillo, R.; Nasini, G.; Vajnade Pava, O., *J. Nat. Prod.*, **1994**, *57*, 602-606.
- 44 Takai, K.; Mori, I.; Oshima, K.; Nozaki, H., *Bull. Chem. Soc. Jpn.*, **1984**, *57*, 446-451.
- 45 Ward, D.E.; Rhee, C.K., *Tetrahedron Lett.*, **1991**, *32*, 7165-7166.
- 46 Dale, J.A.; Mosher, H.S., *J. Am. Chem. Soc.*, **1973**, *95*, 512-519.
- 47 Williams, R.M.; Cushing, T.D., *Tetrahedron Lett.*, **1990**, *31*, 6325-6328,
- Cushing, T.D.; Sanz-Cervera, J.F.; Williams, R.M., *J. Am. Chem. Soc.*, **1996**, *118*, 557-579.

-
- 48 Fredenhagen, A.; Hug, P.; Peter, H.H., *J. Antibiotics*, **1990**, 31(44), 6325-6328.
- 49 Crombie, L.; Crombie, W.M.L.; Jamieson, S.V., *Tetrahedron Lett.*, **1980**, 21, 3607-3610.
- 50 Crombie, L.; Jamieson, S.V., *J. Chem. Soc. Perkin Trans. I*, **1982**, (7), 1467-1475.
- 51 Molecular modelling used PC Spartan 1.1 (Wavefunction Inc., Irvine, CA) at the AM1 level.
- 52 Overman, L.E., *J. Am. Chem. Soc.*, **1976**, 98, 2901-2910.
- 53 Armstrong, A.; Brackenridge, I.; Jackson, R.F.W.; Kirk, J.M., *Tetrahedron Lett.*, **1988**, 29, 2483-2489.
- 54 Bourgeois, M.; Montaudn, E.; Maillard, et B., *Tetrahedron*, **1993**, 49, 2477-2484.
- 55 Steglich, W.; Steffan, B, personal communications.
- 56 Cole, A.L.J., Department of Plant and Microbial Sciences, University of Canterbury, personal communications.
- 57 Ellis, G., Bioassay Laboratory, University of Canterbury, personal communications.
- 58 Munro, M.H.G., University of Canterbury, personal communication.
- 59 Taylor, M., *Mushroom and Toadstools*, **1991**, Reed, New Zealand.
- 60 Taylor, M., personal communication.
- 61 Maki, T.; Takahashi, K.; Shibata, S., *Agr. Food Chem.*, **1985**, 33, 1204-1205.
- 62 Harmon, A.D.; Weisgraber, K.H.; Weiss, U., *Experientia*, **1980**, 36, 54-56.
- 63 Fusetani, N.; Matsunaga, S.; Konosu, S., *Experientia*, **1981**, 37, 680.
- 64 Li, M.K.W.; Scheuer, P.J., *Tetrahedron Lett.*, **1984**, 25 (6), 587-590.

-
- 65 Imre, S.; Thomson, R.H.; Yalhi, B., *Experientia*, **1981**, *37*, 442-443.
- 66 Seo, Y.; Rho, J.R.; Geum, N.; Yoon, J.B.; Shin, J., *J. Nat. Prod.*, **1996**, *59*, 985-986.
- 67 Ochi, M.; Kataoka, K.; Tatsukawa, A.; Kotsuki, H.; Shibata, K., *Chem. Lett.*, **1993**, 2003-2006.
- 68 Matsubara, Y.; Takekuma, S.; Yokoi, K.; Yamamoto, H.; Nozoe, T., *Bull. Chem. Soc. Jpn.*, **1987**, *60*, 1415-1428.
- 69 Bloor, S.J., Industrial Research Ltd, New Zealand, personal communication.
- 70 Stevenson, G., *New Zealand Fungi an Illustrated Guide*, **1994**, Canterbury University Press, Christchurch.
- 71 Tebbett, I.R.; Caddy, B., *Experientia*, **1984**, *40*, 441-446.
- 72 Antkowiak, W.Z.; Gessner, W.P., *Tetrahedron Lett.*, **1979**, *21*, 1931-1934.
- 73 Feifel, E.; Rohrmoser, M.M.; Gstraunthaler, G., *Sydowia Beihefte*, **1995**, *10*, 48-61.
- 74 Aoyagi, Y.; Sugahara, T., *Phytochemistry*, **1985**, *24*, 1835-1936.
- 75 Clemo, G.R.; McIlwain, H., *J. Chem. Soc.*, **1938**, 479-483.
- 76 Clemo, G.R.; Daglish, A.F., *J. Chem. Soc.*, **1950**, 1481-1485.
- 77 Matsunaga, S.; Shinoda, K.; Fusetani, N., *Tetrahedron Lett.*, **1993**, *34*, 5953-5954.
- 78 Patil, A.D.; Freyer, A.J.; Taylor, P.B.; Carte, B.; Zuber, G.; Johnson, R.K.; Faulkner, D.J., *J. Org. Chem.*, **1997**, *62*, 1814-1819.
- 79 Shimizu, Y.; Hsu, C.; Fallon, W.E.; Oshima, Y.; Miura, I.; Nakanishi, K., *J. Am. Chem. Soc.*, **1978**, *100*, 6791-6793.
- 80 Jimenez, C.; Crews, P., *Tetrahedron*, **1991**, *47*, 2097-2102.

-
- 81 Patil, A.D.; Freyer, A.J.; Killmer, L.; Chambers-Myers, C.; Johnson, R.K., *Nat. Prod. Lett.*, **1997**, 9, 181-187.
- 82 *Dictionary of Organic Compounds*, 5th ed, **1982**, Chapman and Hall, New York.
- 83 Pouchert, C.J.; Behnke, J., *The Aldrich Library of ¹H and ¹³C NMR Spectra*, 1st Ed., **1993**, Aldrich Chemical Company, Inc., U.S.A.
- 84 Pouchert, C.J., *The Aldrich Library of NMR Spectra*, 2nd Ed., **1983**, Aldrich Chemical Company, Inc., U.S.A.
- 85 Pretsch, E.; Seibl, J.; Simon, W.; Clerc, T., *Tables of spectral data for structure determination of organic compounds*, English translation of 2nd Ed. 1981, 1983, Springer-Verlag, Berlin.
- 86 Torssell, K.B.G., *Nitrile Oxides, Nitrones, and Nitronates in Organic Synthesis, Organic Nitro chemistry (2)*, **1988**, VCH Publishers, Inc., USA.
- 87 Bandara, B.M.B.; Hinojosa, O.; Bernfsky, C., *J. Org. Chem.*, **1992**, 57, 2652-2657.
- 88 Aurich, H.G.; Trösken, J., *Chem. Ber.*, **1972**, 105, 1216.
- 89 March, J., *Advanced Organic Chemistry – Reaction Mechanisms and Structure*, 4th Ed., **1992**, John Wiley and Sons, Inc, USA, p1216.
- 90 House, H.O., *Modern Synthetic Reactions*, 2nd Ed., **1972**, W.A. Benjamin, Inc, Philippines, p210-211.
- 91 Forrester, A.R.; Thomson, R.H., *Spectrochimica Acta*, **1963**, 19, 1481.
- 92 Lepri, E.; Castagnino, E.; Binaglia, L.; Giampietri, A.; Corsano, S.; Fioretti, M.C., *Arzneim. Forsch/Drug Res.*, **1993**, 43, 381-383.
- 93 Marks, R.; Pearse, A.D.; Walker, A.P., *Br. J. Dermatol.*, **1985**, 112, 415-422.
- 94 Krzysztof, J.R.; Chignell, C.F., *Photochemistry and Photobiology*, **1994**, 60, 442-449.
- 95 Chawla, A.; Dev, S., *Tetrahedron Lett.*, **1967**, (48), 4837-4843.

-
- 96 Paton, W.F.; Paul, I.C.; Bajaj, A.G.; Dev, S., *Tetrahedron Lett.*, 1979, (43), 4153-4154.
- 97 Masuda, K.; Shiojima, K.; Ageta, H., *Chem. Pharm. Bull.*, **1989**, 37, 1140-1142.
- 98 Jakupovic, J.; Eid, F.; Bohlmann, F.; El-Dahmy, S., *Phytochemistry*, **1987**, 25, 1536-1538.
- 99 Ageta, H.; Masuda, K.; Inoue, M.; Ishida, T., *Tetrahedron Lett.*, **1982**, 23, 4349-4352.
- 100 Ravi, B.N.; Wells, R.J.; Croft, K.D., *J. Org. Chem.*, **1981**, 46, 1998-2001.
- 101 McCabe, T.; Clardy, J.; Minale, L.; Pizza, C.; Zollo, F.; Riccio, R., *Tetrahedron Lett.*, **1982**, 23, 3307-3310.
- 102 McCormick, J.L.; McKee, T.C.; Cardellina II, J. H.; Leid, M.; Boyd, M.R., *J. Nat. Prod.*, **1996**, 59, 1047-1050.
- 103 Su, J.Y.; Meng, Y.H.; Seng, L.M.; Fu, X.; Schmitz, F.J., *J. Nat. Prod.*, **1994**, 57, 1450-1451.
- 104 Ryu, G.; Matsunaga, S.; Fusetani, N., *J. Nat. Prod.*, **1996**, 59, 512-514.
- 105 McKee, T.C.; Bokesch, H.R.; McCormick, J.L.; Rashid, M.A.; Spielvogel, D.; Gustafson, K.R.; Alavanja, M.M.; Cardellina II, J.H.; Boyd, M.R., *J. Nat. Prod.*, **1997**, 60, 431-438.
- 106 Perry, N.B.; Ellis, G.; Blunt, J.W.; Haystead, T.A.J.; Lake, R.J.; Munro, M.H.G., *Nat. Prod. Lett.*, **1998**, 11, 305-312.
- 107 Molecular modelling was performed using Spartan v.4.1.2 on a IBM RS6000, and also with PC Spartan Plus (Wavefunction Inc., Irvine, CA). For the conformational analysis 100 conformers were generated and energy minimised using the MM2 force field.
- 108 Blunt, J.W.; McCombs, J.D.; Munro, M.H.G.; Thomas, F.N., *Magnetic Resonance in Chemistry*, **1989**, 27, 792-795.

-
- 109 Norte, M.; Fernández, J.J.; Souto, M.L.; García-Grávalos, M.D., *Tetrahedron Lett.*, **1996**, 37, 2671-2674.
- 110 Norte, M.; Fernández, J.J.; Souto, M.L.; Gavín, J.A.; García-Grávalos, M.D., *Tetrahedron*, **1997**, 53, 3173-3178.
- 111 Norte, M.; Fernández, J.J.; Souto, M.L., *Tetrahedron*, **1997**, 53, 4649-4654.
- 112 Rao, M.M.; Meshulam, H.; Zelnik, R.; Lavie, D., *Phytochemistry*, **1975**, 31, 333-339.
- 113 Tanaka, O.; Yahara, S., *Phytochemistry*, **1978**, 17, 1353-1358.
- 114 Tamelen, E.E.; Willet, J.; Schwartz, M.; Nadeau, R., *J. Am. Chem. Soc.*, **1966**, 88, 5937-5938.
- 115 Steglich, W., personal communication.
- 116 Still, W.C.; Kahn, M.; Mitra, A., *J. Org. Chem.*, **1978**, 43(14), 2923-2925.
- 117 Overman, L.E., *J. Am. Chem. Soc.*, **1976**, 98, 2901-2910.
- 118 Harwood, L.M., *Aldrichimica Acta*, **1985**, 18, 5.
- 119 Gill, M., personal communication.
- 120 Friebolin, H., *Basic one- and two-dimensional spectroscopy*, **1991**, VCH, New York, NY (USA).
- 121 Kemp, W., *Organic spectroscopy*, **1992**, 3rd Ed, Macmillan Education Ltd, London.
- 122 Caprioli, R.M., in *Biologically active molecules: FAB basic concepts and practical considerations* Edited by Schlunegger, U.P., **1989**, Springer-Verlag, Berlin.